Prepared in cooperation with the Central Platte Natural Resources District and the Nebraska Natural Resources Commission

An Integrated Hydrologic Model to Support the Central Platte Natural Resources District Groundwater Management Plan, Central Nebraska

Scientific Investigations Report 2023–5024

U.S. Department of the Interior
U.S. Geological Survey

Cover. Cozad Canal near Cozad, Nebraska. Photograph by Jonathan P. Traylor, U.S. Geological Survey.

An Integrated Hydrologic Model to Support the Central Platte Natural Resources District Groundwater Management Plan, Central Nebraska

By Jonathan P. Traylor, Moussa Guira, and Steven M. Peterson

Prepared in cooperation with the Central Platte Natural Resources District and the Nebraska Natural Resources Commission

Scientific Investigations Report 2023–5024

U.S. Department of the Interior
U.S. Geological Survey

U.S. Geological Survey, Reston, Virginia: 2023

Suggested citation:
Traylor, J.P., Guira, M., and Peterson, S.M., 2023, An integrated hydrologic model to support the Central Platte Natural Resources District Groundwater Management Plan, central Nebraska: U.S. Geological Survey Scientific Investigations Report 2023–5024, 143 p., https://doi.org/10.3133/sir20235024.

Associated data for this publication:
Traylor, J.P., 2023, MODFLOW-One-Water model used to support the Central Platte Natural Resources District Groundwater Management Plan, central Nebraska: U.S. Geological Survey data release, https://doi.org/10.5066/P9G3Q5XK.

U.S. Geological Survey, 2017, USGS water data for the Nation: U.S. Geological Survey National Water Information System database, https://doi.org/10.5066/F7P55KJN.

ISSN 2328-0328 (online)

Acknowledgments

The authors express their gratitude to Brandi Flyr and Duane Woodward (retired) of the Central Platte Natural Resources District for their coordination and cooperation throughout the duration of this study that began in 2016. Their local knowledge of the study area was invaluable to the completion of the project.

The authors also recognize additional U.S. Geological Survey (USGS) scientists that contributed to the study: Benjamin Dietsch, Kellan Strauch, Brent Hall, Alec Weisser, and Chris Hobza from the USGS Nebraska Water Science Center; Mike Fienen from the USGS Upper Midwest Water Science Center for his invaluable help with the predictive uncertainty aspect of the study; and Joseph Richards from the USGS Central Midwest Water Science Center. This project would not have been possible without the Nebraska Natural Resources Commission Water Sustainability Fund and USGS Cooperative Matching Funds Program.

Contents

Figures

Tables

Conversion Factors

U.S. customary units to International System of Units

Multiply	By	To obtain
	Length	
inch (in.)	39.3701	meter (m)
foot (ft)	0.3048	meter (m)
mile (mi)	1.609	kilometer (km)
	Area	
acre	4,047	square meter (m^2)
acre	0.004047	square kilometer (km^2)
square mile (mi^2)	2.590	square kilometer (km^2)
	Volume	
acre-foot (acre-ft)	1,233	cubic meter (m^3)
	Flow rate	
acre-foot per year (acre-ft/yr)	0.000039087	cubic meter per second (m^3/s)
cubic foot per second (ft^3/s)	0.02832	cubic meter per second (m^3/s)
cubic foot per day (ft^3/d)	0.02832	cubic meter per day (m^3/d)
gallon per minute (gal/min)	0.06309	liter per second (L/s)
inch per year (in/yr)	25.4	millimeter per year (mm/yr)
mile per hour (mi/h)	1.609	kilometer per hour (km/h)
million gallons per day (Mgal/d)	0.04381	cubic meter per second (m^3/s)
	Hydraulic conductivity	
foot per day (ft/d)	0.3048	meter per day (m/d)
	Hydraulic gradient	
foot per mile (ft/mi)	0.1894	meter per kilometer (m/km)
	Transmissivity	
foot squared per day (ft^2/d)	0.09290	meter squared per day (m^2/d)

Temperature in degrees Celsius (°C) may be converted to degrees Fahrenheit (°F) as follows:

$$°F = (1.8 \times °C) + 32.$$

Temperature in degrees Fahrenheit (°F) may be converted to degrees Celsius (°C) as follows:

$$°C = (°F - 32) / 1.8.$$

Datum

Vertical coordinate information is referenced to the North American Vertical Datum of 1988 (NAVD 88).

Horizontal coordinate information is referenced to the North American Datum of 1983 (NAD 83).

Altitude, as used in this report, refers to distance above the vertical datum.

Abbreviations

AET actual evapotranspiration

baseline 1982 gwlevels baseline April 30, 1982, groundwater altitudes simulated by the development Central Platte Integrated Hydrologic Model

CIR crop irrigation requirement

CNPPID Central Nebraska Public Power and Irrigation District

COHYST Cooperative Hydrology Study

CPIHM Central Platte Integrated Hydrologic Model

CPNRD Central Platte Natural Resources District

CWD crop water demand

Eg evaporation of groundwater

Ei evaporation of irrigation water

Ep evaporation of precipitation

ET evapotranspiration

ETg evapotranspiration of groundwater

ETp evapotranspiration of precipitation

ET_{ref} reference evapotranspiration

FEI fraction of evaporation from irrigation

FIESWI fraction of inefficient losses to surface water from irrigation

FIESWP fraction of inefficient losses to surface water from precipitation

FMP Farm Process package

FTR fraction of transpiration

FutBase base scenario

Futdrought3yr 3-year drought scenario

Futdrought10yr 10-year drought scenario

Futdroughtjun2sep mid-growing season drought scenario

Futdroughtmar2may early growing season drought scenario

Futirr7in scenario limiting annual groundwater irrigation pumping to 7 inches

Futirr9in scenario limiting annual groundwater irrigation pumping to 9 inches

Futirr10in scenario limiting annual groundwater irrigation pumping to 10 inches

GHB General Head Boundary package

GMP Groundwater Management Plan

GWMA Groundwater Management Area

HU hydrostratigraphic unit

Kc crop coefficient

Kh	horizontal hydraulic conductivity
Ksb	vertical hydraulic conductivity of streambed
lidar	light detection and ranging
MAD	maximum acceptable decline
MF–OWHM	MODFLOW–One-Water Hydrologic Model
MODFLOW	modular finite-difference flow model
MODFLOW–NWT	modular finite-difference flow model with Newton solver
n	number of calibration targets
NeDNR	Nebraska Department of Natural Resources
NRD	Natural Resource District
NWIS	National Water Information System
OFE	on-farm efficiency
PEST	Parameter ESTimation
PET	potential evapotranspiration
Φ	phi, the PEST objective function
Φ_r	regularization phi, a part of the PEST objective function
PPT	precipitation
r	residual, as the difference between time and space equivalent measured and simulated values.
R^2	coefficient of determination
SFR	Streamflow Routing package
Ss	specific storage
SVDA	singular value decomposition-assist
Sy	specific yield
Tg	transpiration of groundwater
Ti	transpiration of irrigation water
Tp	transpiration of precipitation
USGS	U.S. Geological Survey
UZF	Unsaturated Zone Flow package
w	weight applied to the observation
WBS	water-balance subregion

An Integrated Hydrologic Model to Support the Central Platte Natural Resources District Groundwater Management Plan, Central Nebraska

By Jonathan P. Traylor, Moussa Guira, and Steven M. Peterson

Abstract

The groundwater and surface-water supply of the Central Platte Natural Resources District supports a large agricultural economy from the High Plains aquifer and Platte River, respectively. This study provided the Central Platte Natural Resources District with an advanced numerical modeling tool to assist with the update of their Groundwater Management Plan.

An integrated hydrologic model, called the Central Platte Integrated Hydrologic Model, was constructed using the MODFLOW-One-Water Hydrologic Model code with the Newton solver. This code integrates climate, landscape, surface water, and groundwater-flow processes in a fully coupled approach. Model framework included 163 rows; 327 columns; 2,640 feet cell sides; and 3 vertical layers. A predevelopment model simulated steady-state hydrologic conditions prior to April 30, 1895, and a development period model discretized into 610 stress periods simulated transient hydrologic conditions from May 1, 1895, to December 31, 2016, using 170 biannual stress periods from 1895 to 1980, and monthly stress periods from May 1, 1980, to December 31, 2016.

Calibration of the Central Platte Integrated Hydrologic Model involved two phases: a manual adjustment of parameters, followed by the automated calibration completed using BeoPEST that was facilitated by the employment of the singular value decomposition-assist features of PEST that specified 50 super parameters assembled from the 435 adjustable parameters and Tikhonov regularization. The average absolute groundwater-level residuals for model layers one, two, and three were 6.1, 12.4, and 7.4 feet, respectively. Calibrated horizontal hydraulic conductivity was about 70, 32, and 35 feet per day for layers 1, 2, and 3, respectively. The largest development period inflow to groundwater was recharge from deep percolation past the root zone, averaging 1,122,257 acre-feet per year (2.7 inches per year), and the largest outflow was to irrigation wells, averaging 693,171 acre-feet per year (10.2 inches per year for the Central Platte Natural Resources District). Other substantial groundwater outflows included evapotranspiration and base flow. For the total development period, there was a net change in storage of −122,393 acre-feet per year (−0.3 inch per year).

The calibrated Central Platte Integrated Hydrologic Model was used to simulate eight different potential future climate and irrigation pumping conditions from January 1, 2017, to December 31, 2049. Simulated future groundwater levels within the Central Platte Natural Resources District varied significantly between scenarios and locally, from 13.8 feet below to 7.6 feet above baseline 1982 groundwater levels. Most areas exhibited groundwater-level declines for the drought scenarios and rises for the alternate irrigation scenarios. Changes in scenario groundwater levels correlated with the relations between farm net recharge and irrigation pumping. Linear “first order second moment” techniques indicated that the uncertainty in projected groundwater altitudes was reduced by 15.33 feet through model calibration.

Introduction

The Central Platte Natural Resources District (CPNRD; fig. 1*A*) is 1 of 23 Natural Resources Districts (NRDs) throughout Nebraska created by Nebraska Legislature (Nebraska Legislature, 1969) in 1969 with the goal of protecting its natural resources (Nebraska Association of Resources Districts, 2020). The NRDs are responsible for regulating groundwater use (University of Nebraska-Lincoln, 2020); the Nebraska Department of Natural Resources regulates surface-water use. The groundwater and surface-water supply of the CPNRD is one of its most valuable natural resources. Current beneficial water uses within the CPNRD include domestic and industrial water supply for a population of about 112,000; irrigation water supply for about 1 million acres; and minimum annual flows of more than 1 million acre-feet (acre-ft) of water in the Platte River for recreational and wildlife habitat use. The groundwater and surface-water supply supports an agricultural economy that generates more than $2 billion per year (U.S. Department of Agriculture, 2019). The CPNRD’s main groundwater management goal is “to assure an

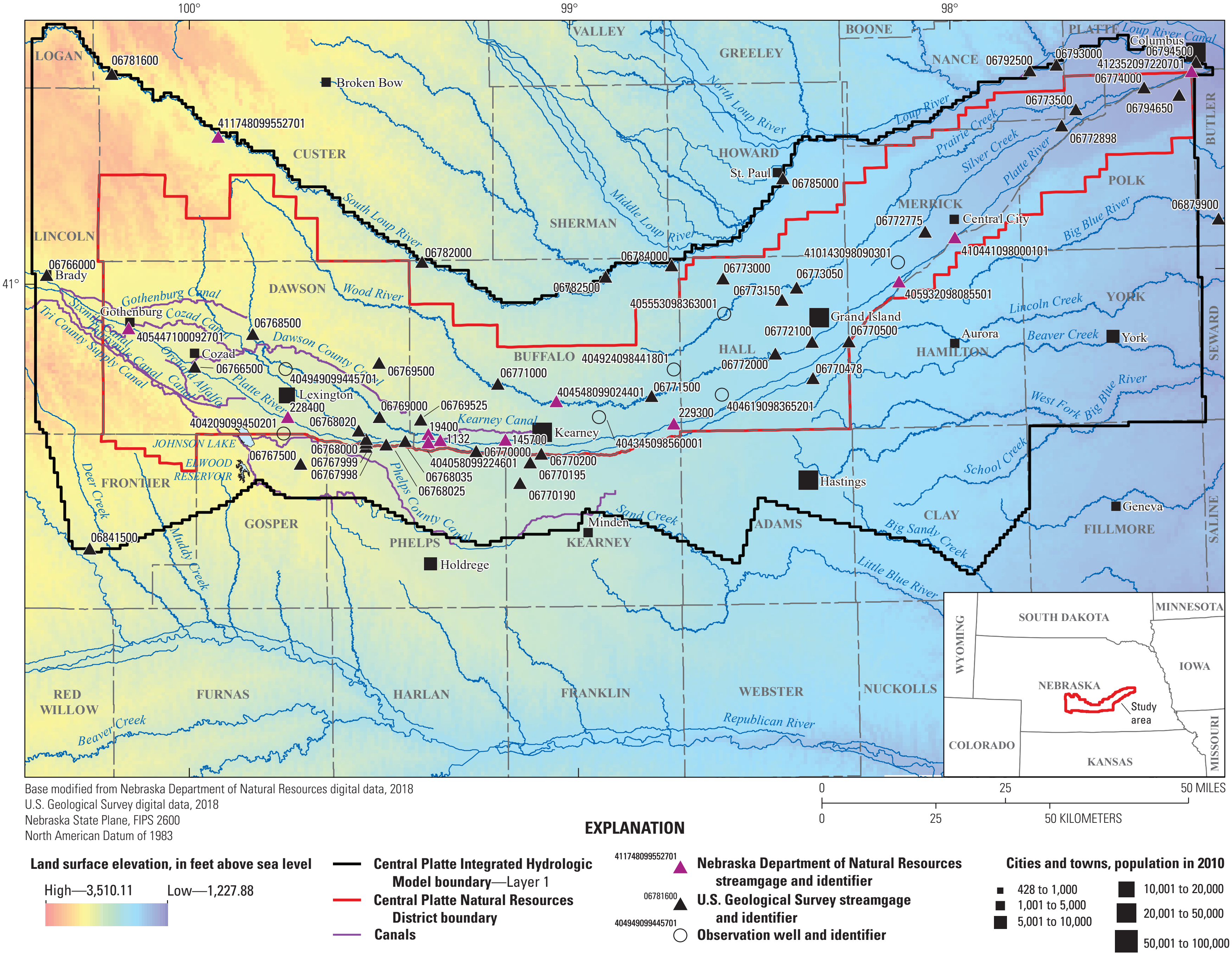

Figure 1. Map of the study area, the Central Platte Natural Resources District, central Nebraska. *A*, Central Platte Natural Resources District boundary, county boundaries, cities and towns by population, and major surface-water bodies. *B*, Central Platte Natural Resources District Groundwater Management Area boundaries, streams and canals simulated with the Streamflow Routing package, and soil classification used in the Central Platte Integrated Hydrologic Model. *C*, Subregional watersheds in the study area.

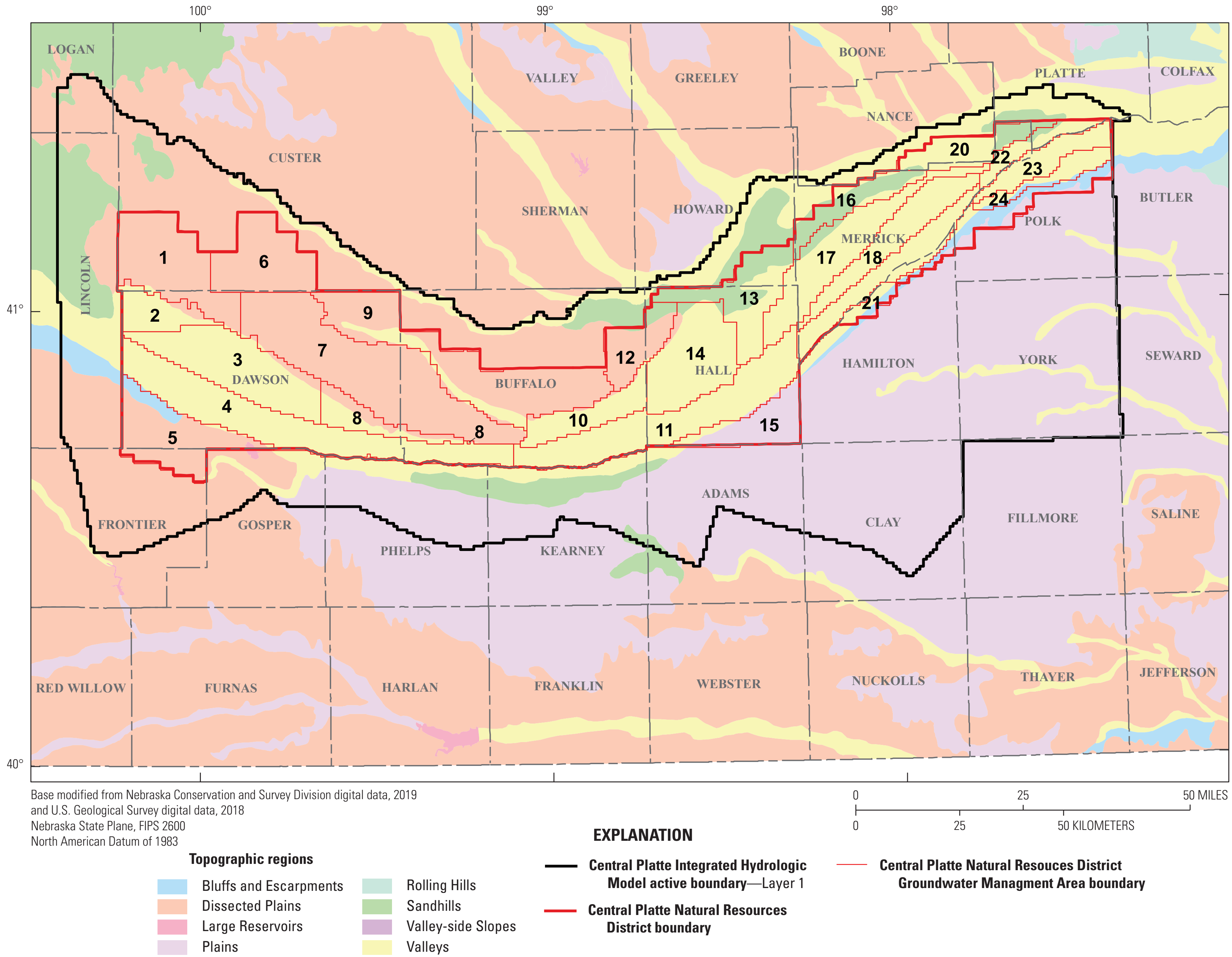

Figure 1.—Continued

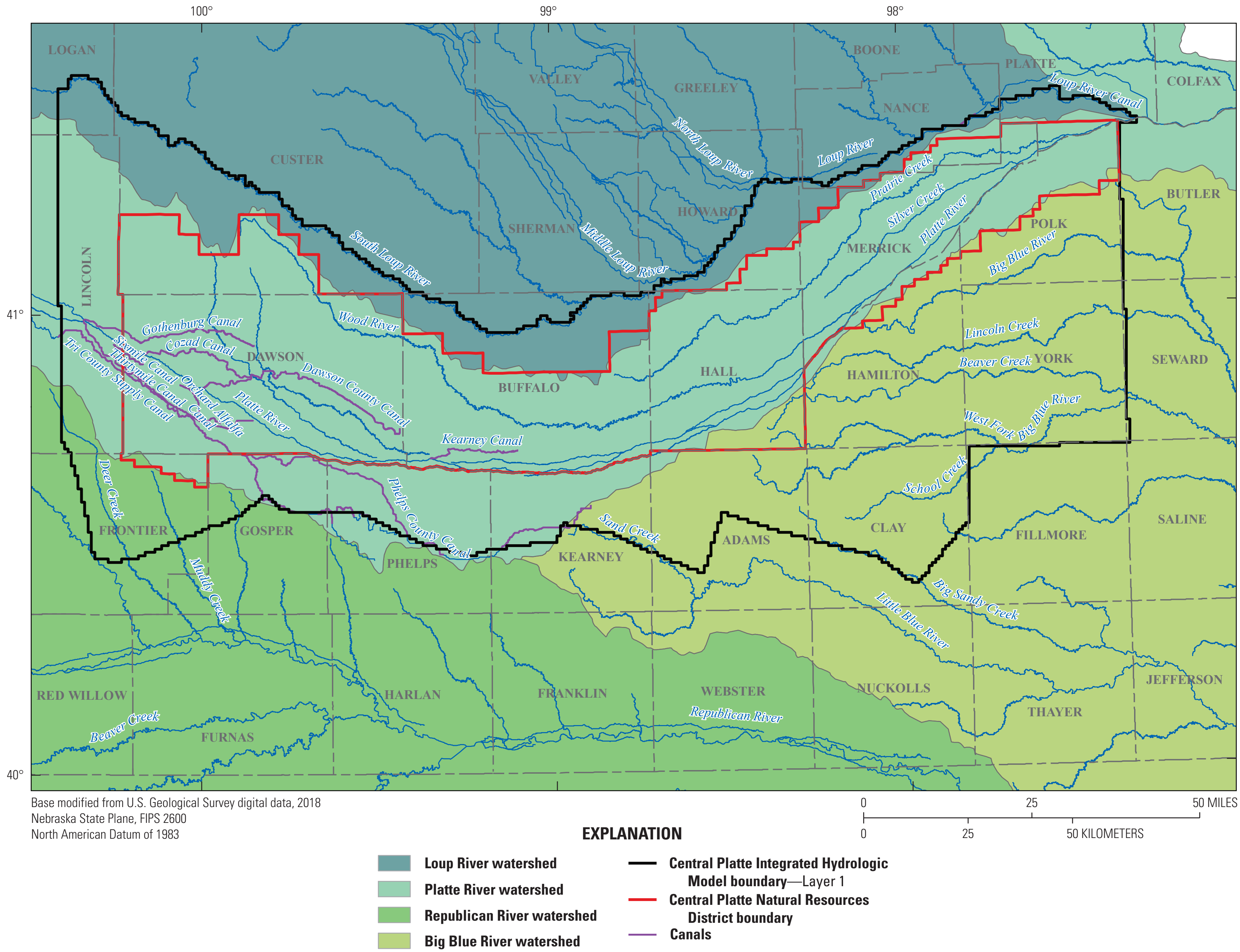

Figure 1.—Continued

adequate supply of water for feasible and beneficial uses through proper management, conservation, development and utilization of the District's water resources" (Central Platte Natural Resources District, 2019, p. 1).

Proper regulation of groundwater resources is necessary because during a normal growing season in the CPNRD, effective precipitation (the portion that does not immediately run off to a surface-water body) is usually less than the amount crops need to produce a robust harvest. For example, corn is estimated to need about 25 inches of water from May through September (Kranz and others, 2008), whereas effective precipitation in that time period is normally only about 10 to 15 inches, which leaves a net deficit of about 10 to 15 inches that generally must be met through irrigation. The CPNRD's groundwater management strategy, which includes irrigation, is set in their Groundwater Management Plan (GMP), a requirement for each NRD determined by the Nebraska Groundwater Management and Protection Act (Nebraska Legislature, 2004) in 1982. The CPNRD's GMP, initially adopted in 1987, specifies maximum acceptable declines (MADs) of 10 to 30 feet (ft) for 24 Groundwater Management Areas (GWMAs) across the CPNRD (fig. 1*B*), with the declines based on spring 1982 (approximately April 30, 1982) groundwater levels (Central Platte Natural Resources District, 2020a). The CPNRD monitors the groundwater-level declines and recovery across the 24 GWMAs each year to assess how the irrigation and climate stresses affect the groundwater resources. As specified in their GMP, if the groundwater levels decline to 50 percent of the MADs (5 and 15 ft, respectively, for each GWMA), phase II management would take effect, which triggers mandatory reductions in irrigated acres and establishment of spacing limits for new irrigation wells. Declines in groundwater levels to 70, 90, and 100 percent of the MADs for each GWMA would trigger phase III, IV, and V management, respectively, which include mandates of additional cutbacks in irrigated acreage and increased spacing limits for new wells (Central Platte Natural Resources District, 2020a).

To improve groundwater management and to better understand the effects of specific groundwater-management decisions on groundwater levels and streamflow, the CPNRD has been involved with ongoing groundwater-flow modeling efforts. The CPNRD's initial and revised GMP rules and regulations were set using groundwater-flow models developed in the 1980s (Peckenpaugh and Dugan, 1983; Peckenpaugh and others, 1987). In 1998, the Platte River Cooperative Hydrology Study (COHYST; https://cohyst.nebraska.gov/) was initiated as a major component of a three-State (Colorado, Nebraska, and Wyoming) cooperative agreement with the U.S. Department of the Interior. COHYST was tasked to collect additional data and to create numerical groundwater-flow models for use in support of regulatory and management decisions. COHYST is a cooperative effort to improve the understanding of hydrological conditions of the Platte River upstream from Columbus, Nebraska, and to evaluate changes to current and proposed water uses in the Platte River Basin, including the part of the watershed within the CPNRD (fig. 1*C*). Three overlapping groundwater-flow models were originally developed for the eastern, central, western COHYST regions and are described in Peterson (2009), Carney (2008), and Luckey and Cannia (2006), respectively. Later groundwater-flow model updates combined the eastern and central model units into a single model as described in Cooperative Hydrology Study (2017). The CPNRD (and other NRDs with the Platte River) used the COHYST groundwater models to determine depletions to the Platte River from increases in groundwater use; these depletions were implemented as offset goals in their management plans.

The latest revision to the CPNRD's GMP was the addition of the Integrated Management Plan in July 2009 (Central Platte Natural Resources District, 2020b). Recent updates to the CPNRD's Integrated Management Plan were made using a groundwater-flow model developed for the COHYST (Cooperative Hydrology Study, 2017). The next planned revision to the CPNRD's GMP and related rules and regulations is to use a groundwater-flow model with the latest and most comprehensive science available to support hydrologic water-budget management. An update of the GMP regulations will improve the CPNRD's ability to protect and maintain sustainable groundwater resources in the area now and for future generations and will improve the phased management implementation used to specify when management or regulation of groundwater resources is necessary.

To update past numerical modeling efforts in the area, the U.S. Geological Survey (USGS), in cooperation with the CPNRD, developed a fully integrated hydrologic model. The model used the USGS modular finite difference flow model (MODFLOW)-based software called MODFLOW–One-Water Hydrologic Model (MF–OWHM; Boyce and others, 2020). The fully integrated hydrologic model of the Central Platte region of Nebraska, described in this report, will be referred to hereafter as the "Central Platte Integrated Hydrologic Model" (CPIHM).

MODFLOW–One-Water Hydrologic Model Theory and Approach

The MF–OWHM was developed to improve the simulation of the landscape, surface-water, and groundwater-flow processes in a fully integrated way to account for "all of the water everywhere and all of the time" (Hanson and others, 2014a, p. 1). The integration of climate, landscape, surface-water, and groundwater-flow processes in a fully coupled approach to hydrologic modeling simulates the natural feedbacks of a system within one numerical model. The MF–OWHM also includes specific features to simulate supply and demand driven agricultural processes, such as irrigation from canals or groundwater pumped from irrigation wells (Hanson and others, 2014a; Boyce and others, 2020). The MF–OWHM landscape processes integrate with the surface-water network through the routing of runoff to nearby streams and routing of canal diversions for irrigation to surface-water irrigated crops; the Farm process package (FMP) simulates the landscape features within the MF–OWHM (Hanson and others, 2014a; Boyce and others, 2020) (fig. 2). The MF–OWHM landscape

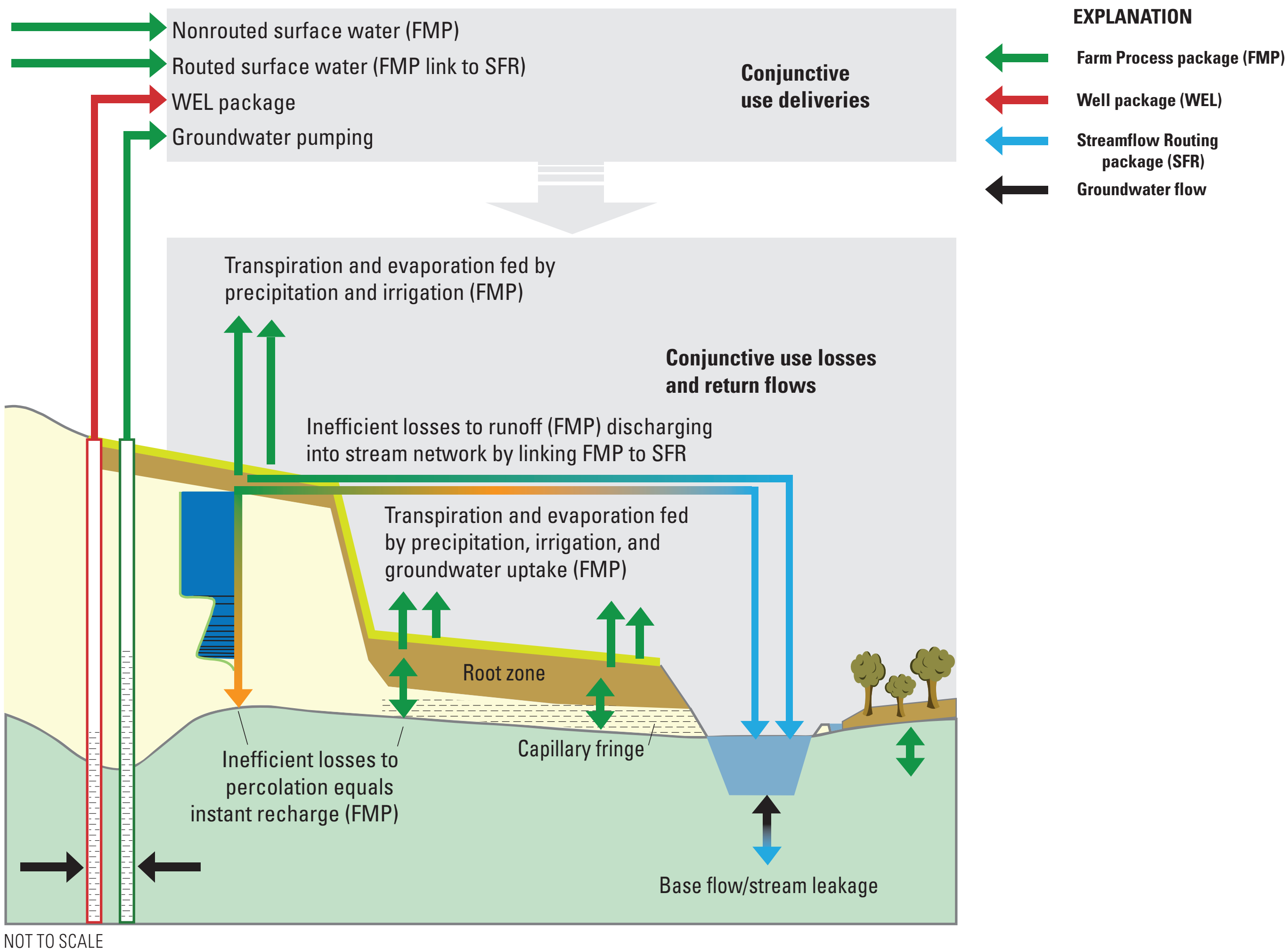

Figure 2. Schematic representation of components simulated by the Farm Process package in the modular finite difference flow model (MODFLOW) One-Water Hydrologic Model for the Central Platte Integrated Hydrologic Model (modified from Schmid and Hanson, 2009).

processes connect to the groundwater through passing of the deep percolation as recharge to the water table and evapotranspiration of groundwater (ETg) via root uptake (fig. 2).

Landscape processes simulated by the FMP within the MF–OWHM include evaporation and transpiration of precipitation (Ep and Tp), evaporation and transpiration of irrigation water (Ei and Ti), surface water applied to the landscape as irrigation, groundwater applied to the landscape as irrigation, deep percolation past the root zone, and runoff (or overland flow). Within the supply and demand framework of the MF–OWHM, the supply refers to the sources of water to the landscape such as precipitation and groundwater withdrawals or surface-water deliveries for irrigation; demand refers to components of the landscape that require a water supply such as crop consumptive use or evapotranspiration (ET). The MF–OWHM also tracks the hybrid components of evaporation and transpiration of groundwater (Eg and Tg) within FMP because the Eg and Tg occur as a result of crop types specified in FMP, but Eg and Tg are not included in the calculation of the landscape budget because the water source is groundwater. A comprehensive mathematical and theoretical description of the MF–OWHM and FMP underpinnings is in the MF–OWHM and FMP documentation (Hanson and others, 2014a; Boyce and others, 2020). The key inputs to the FMP are discussed in the “Landscape Inputs and Configuration (Farm Process)” section of this report.

The MF–OWHM first calculates the crop water demand (CWD) as the product of input reference evapotranspiration (ET_{ref}) and crop coefficients (Kc); therefore, water demand on the landscape is driven by the requirements for ET. After calculation of the CWD, the MF–OWHM finds a water supply to meet the demand. The MF–OWHM determines the supply of water based on availability at a specific location. Potential water supply to meet CWD can include natural supply such as precipitation and or root uptake of groundwater for nonirrigated land uses or crops, anthropogenic supply such as surface-water deliveries from irrigation canals or groundwater pumping from irrigation wells for irrigated crops, or a combination of all four (fig. 2). For nonirrigated crops and land uses, the actual evapotranspiration (AET) is a function of the naturally available water supply and the CWD in which AET is curtailed if CWD is greater than the naturally available water supply. Additionally, any surplus naturally available water supply not used to meet the CWD either becomes runoff to a nearby stream or deep percolation past the root zone and is passed to the unsaturated zone, if present in the simulation, or becomes recharge to the groundwater system. Surface-water deliveries from irrigation canals or groundwater pumping from irrigation wells are only selected as water supply options within the MF–OWHM if crops are user-designated to receive irrigation water supply. For irrigated crops, the MF–OWHM calculates a crop irrigation requirement (CIR) based on the supply deficit between the CWD and the natural water supply available to the crop. The final irrigation amount applied to the crop accounts for irrigation efficiencies in addition to the CIR. The AET for irrigated crops is then the function of the final irrigation amount applied and the CWD (Hanson and others, 2014a; Boyce and others, 2020).

Previous Studies

The CPNRD area has been the subject of many hydrologic studies that include investigations of numerical models, recharge, geology and hydrogeology, land use, and crop water use since the late 1890s, as outlined in Peterson (2009). The earliest studies were a comprehensive description of the Great Plains geology and groundwater, including the CPNRD region of Nebraska (Darton, 1898, 1905). Numerical groundwater-flow models have been a part of several studies in the region within the CPNRD since the 1970s (Lappala and others, 1979; Peckenpaugh and Dugan, 1983; Peckenpaugh and others, 1987). Additionally, the development of groundwater-flow models has been the focus of COHYST since its inception in 1998 (Cooperative Hydrology Study, 2017). The first three COHYST groundwater-flow models were developed for three geographic regions, called model units, within COHYST—the eastern model unit, which contains the CPNRD (Peterson, 2009); the central model unit (Carney, 2008); and the western model unit (Luckey and Cannia, 2006). COHYST–2010 is the latest model developed as a part of COHYST and is a combined soil-water balance, surface water, and groundwater-flow model of the eastern and central model units (Cooperative Hydrology Study, 2017). In support of the COHYST groundwater-flow models, a COHYST study by Cannia and others (2006) included a detailed hydrogeologic study of the surface-water and groundwater resources in the Platte River Basin. Recent studies within the CPNRD include the collection of geophysical logs to delineate stratigraphic units by Anderson and others (2009) and an assessment by Exner and others (2010) of the response of nitrate in groundwater to management practices in the CPNRD. Irons and others (2012) compared surface nuclear magnetic resonance data to results from aquifer tests completed in the CPNRD, Steele and others (2014) used several methods to determine recharge and water movement through the unsaturated zone underlying several land-use types in the CPNRD, and Lauffenburger and others (2018) used a model to forecast recharge under different future climate scenarios. An airborne electromagnetic survey was completed in the CPNRD and adjacent Twin Platte Natural Resources District to develop a 3-dimensional hydrogeologic framework of the area (Cannia and others, 2017). A groundwater-flow model of the Northern High Plains aquifer, which included the CPNRD, was developed by Peterson and others (2016), and was used to simulate the effects of alternate climate and land use on groundwater conditions from 2009 through 2049 (Peterson and others, 2020).

Purpose and Scope

The purpose of this report is to document and describe the construction, calibration, and results of the CPIHM, a numerical fully integrated hydrologic model used to simulate the CPNRD hydrologic system. The scope of the study included the development of the numerical model to simulate all important hydrologic processes from the onset of surface-water irrigation in 1895 to the end of 2016 and forecasted groundwater conditions based on eight future scenarios with varying climate and limits on irrigation from 2017 through 2049. This study builds upon previous work to provide a current (2023) hydrologic model as a tool to support science-based integrated water management in the CPNRD. To meet the objective of this study, the analyses provided information about potential future water availability and changes in groundwater levels for each scenario with respect to the baseline 1982 groundwater levels and MADs that can be used by the CPNRD to update their GMP, as described in this report. Because of extensive use of groundwater and surface water for irrigation in the study area and the lack of metered irrigation pumping data for most wells throughout the development period (1895 to 2016), the MF–OWHM was selected as the best modeling code for simulating the entire hydrologic system.

Study Area Description

The study area is focused around the CPNRD, which includes parts of 10 counties in central Nebraska and a total area of 2,136,304 acres (fig. 1*A*). The total population of the CPNRD is 137,966, with Grand Island and Kearney being the most populous cities with 48,520 and 30,787 people, respectively (U.S. Census Bureau, 2012). The city of Columbus, with a population of about 21,000, is just outside the northeastern border of the study area (fig. 1*A*). The main hydrologic features are the Platte River (fig. 1*A*), which flows from west to east for about 205 miles, and the High Plains aquifer, which underlies the entire study area with saturated thicknesses ranging from about 50 to 550 ft (McGuire and others, 2012).

Crop production drives the local economy; from 2015 to 2017, the study area contained parts or all of four of the five counties with the highest corn production in the State (U.S. Department of Agriculture, 2019). As of 2005, the study area (Central Platte Integrated Hydrologic Model boundary-layer 1; fig. 1*A*) contained about 2.17 million acres of irrigated cropland, of which about 1 million irrigated acres were in the CPNRD (Center for Advanced Land Management Information Technologies, 2010). An extensive network of canals diverts water from the Platte River to surface-water irrigators in Buffalo, Dawson, Kearney, and Phelps Counties (fig. 1*A*). The remaining 936,000 acres are supplied by groundwater irrigation from the underlying High Plains aquifer. In addition, in some areas the water table is near enough to the crop root zone for crops to actively transpire groundwater, which reduces the net irrigation requirement in that area because less irrigation water would need to be supplied. As the water table continues to rise, actual crop ET may be reduced and eventually approach zero owing to anoxia conditions in crops that are not tolerant to waterlogging.

Physiography

The entire study area lies within the Great Plains physiographic province (Fenneman, 1931). Several subdivisions of the Great Plains province are present within the study area and can be differentiated by topographic regions that include the Bluffs and Escarpments, Dissected Plains, Plains, Sandhills, and Valleys (fig. 1*B*; Conservation and Survey Division, 2019). The Dissected Plains (also known as the Dissected Loess Plains) is present in portions of Buffalo, Custer, Dawson, Frontier, Gosper, Lincoln, and Logan Counties (fig. 1*B*) and are characterized by level to rolling hills and loess bluffs that grade into the Platte River valley to the south and east (Weaver and Bruner, 1948). Areas of considerable relief with hills of 100 ft or more were created by wind and stream erosion and produced the dissected nature of the loess deposits (Weaver and Bruner, 1948). The Dissected Plains in Frontier and Gosper counties feature deeply incised canyons and flat uplands known as “tablelands.” The dominant soil type is silt that includes the Holdrege Silt Loam and Colby Silt Loam (Weaver and Bruner, 1948; University of Nebraska-Lincoln, 2018). The Plains region located in portions of Adams, Clay, Gosper, Hall, Hamilton, Howard, Kearney, Phelps, Polk, and York counties is characterized by gently rolling hills with less relief than the Dissected Plains. The Sandhills region is present primarily in outlying portions of the main Sandhills region in portions of Buffalo, Hall, Howard, Kearney, Lincoln, Merrick, and Phelps counties (fig. 1*B*). The Valleys region is primarily located along the Platte River valley lowlands in portions of Buffalo, Hall, Howard, Kearney, Lincoln, Merrick, and Phelps counties (fig. 1*B*). The Valley lowlands are typically flood-plain areas and have minimal topographic relief with an eastward slope of 6 to 8 ft per mile (Peterson, 2009; fig. 1*A*–*B*).

Climate

The climate in the study area transitions from subhumid continental classification in the east, specified in Köppen (1936), to dry subhumid continental classification in the western part of the study area (Conservation and Survey Division, 1998); that is, annual precipitation decreases westward throughout the study area. The climate is characterized by warm and humid summers and cold and windy winters. The 30-year (1981 to 2010) average annual climate normal for precipitation is 29.12 inches at Columbus; 25.23 inches at Kearney; and 23.71 inches at Gothenburg (fig. 1*A*) (National Climatic Data Center, 2019). The 30-year (1981 to 2010) average climate normal for summer minimum and maximum temperatures is 63.5 and 74.3 degrees Fahrenheit (°F) at Columbus; 60.3 and 72.4 °F at Kearney; and 60.4 and 72.9 °F at Gothenburg (National Climatic Data Center, 2019). The 30-year (1981 to 2010) average climate normal for winter minimum and maximum temperature is 15.7 and 25.1 °F at Columbus; 14.9 and 26.2 °F at Kearney; and 16.0 and 27.9 °F at Gothenburg (National Climatic Data Center, 2019).

Reference ET (ET_{ref}) was measured at University of Nebraska-Lincoln Extension field sites at Clay Center, Nebr. (not shown) located in the center of Clay County and in North Platte, Nebr. (not shown), about 25 miles west of Brady from 1983 through 2003 (fig. 1*A*; Irmak and Skaggs, 2011). Average annual ET_{ref} at Clay Center was 61.7 inches and 62.4 inches for North Platte, which is substantially higher in the study area than average annual precipitation (24.3 inches) and is typical for the subhumid climate classifications. Average monthly ET_{ref} rates exceed precipitation rates throughout the year measured at locations near Clay Center and North Platte (Irmak and Skaggs, 2011; National Climatic Data Center, 2019). Average annual AET rates for a period between 2000 and 2009 are about 24.8 inches in the study area (Szilágyi and Kovacs, 2010). However, local AET values generally exceed precipitation by as much as 130 percent for areas with widespread irrigation of crops, whereas areas with natural vegetation generally exhibit less AET compared to precipitation (Szilágyi and Kovacs, 2010). Further, AET is generally lower in the eastern part of the study area than the western area for natural vegetation while irrigated crops exhibit similar AET values across the study area (Szilágyi and Kovacs, 2010).

Land Use, Crop Coefficients, and Water Use

Land use and water use in the study area are linked and are important characteristics of the supply and demand driven hydrologic system. Prior to the Civil War (1861 to 1865), the primary land uses in Nebraska were range, pasture, and grass (Hiller and others, 2009). The adoption of the Homestead Act in 1862, the end of the Civil War in 1865, and Nebraska's statehood in 1867 encouraged settlers to move westward into the study area. In 1895, total cropland area was about 90 percent of 2005 total cropland area (Hiller and others, 2009). Since the mid-1960s, crop diversity in Nebraska decreased, and cropland is now dominated by corn and soybeans (Hiller and others, 2009).

The primary land use since the 1890s has been cultivated crops such as corn, soybeans, and winter wheat. By 1895, canals were developed to deliver surface water for crop irrigation to areas in Buffalo, Dawson, Phelps, and Kearney counties (Hiller and others, 2009; Peterson, 2009). The first irrigation wells were drilled and began pumping groundwater from the alluvial aquifer along the Platte River around 1900 (Nebraska Department of Natural Resources, 2017). Most irrigated land prior to 1940 was irrigated with surface water from canals diverted onto fields using flood irrigation techniques, but after 1940, with improvements in well-drilling technology and later the invention of the more efficient center-pivot irrigation systems, groundwater-irrigated land increased as dryland crops were converted to irrigated cropland. Since 1940, about 29,000 irrigation wells have been drilled in the study area, with most drilled between 1955 and 1990 (fig. 3; Nebraska Department of Natural Resources, 2017). In 2016, the density of irrigation wells in the study area was 3.8 wells per square mile; because of this high density, the CPNRD does not allow the drilling of new irrigation wells or development of new irrigated acres unless other irrigation wells or acres are retired (Central Platte Natural Resources District, 2019). Some irrigators have surface-water rights and groundwater wells for irrigation; the irrigated land that receives water from surface water and groundwater is described as “commingled.” Irrigators with commingled land primarily use their surface-water right and may supplement with groundwater from wells when necessary.

Within the study area, long-term land use data were available from the Cooperative Hydrology Study (2017). These data indicate that by 1950, land use in the study area was about 53 percent pasture (2,632,858 acres), 29 percent dry cropland (1,658,659 acres), 13 percent other uses (406,679 acres), and 5 percent irrigated cropland (227,884 acres; Cooperative Hydrology Study, 2017). The other land uses include open

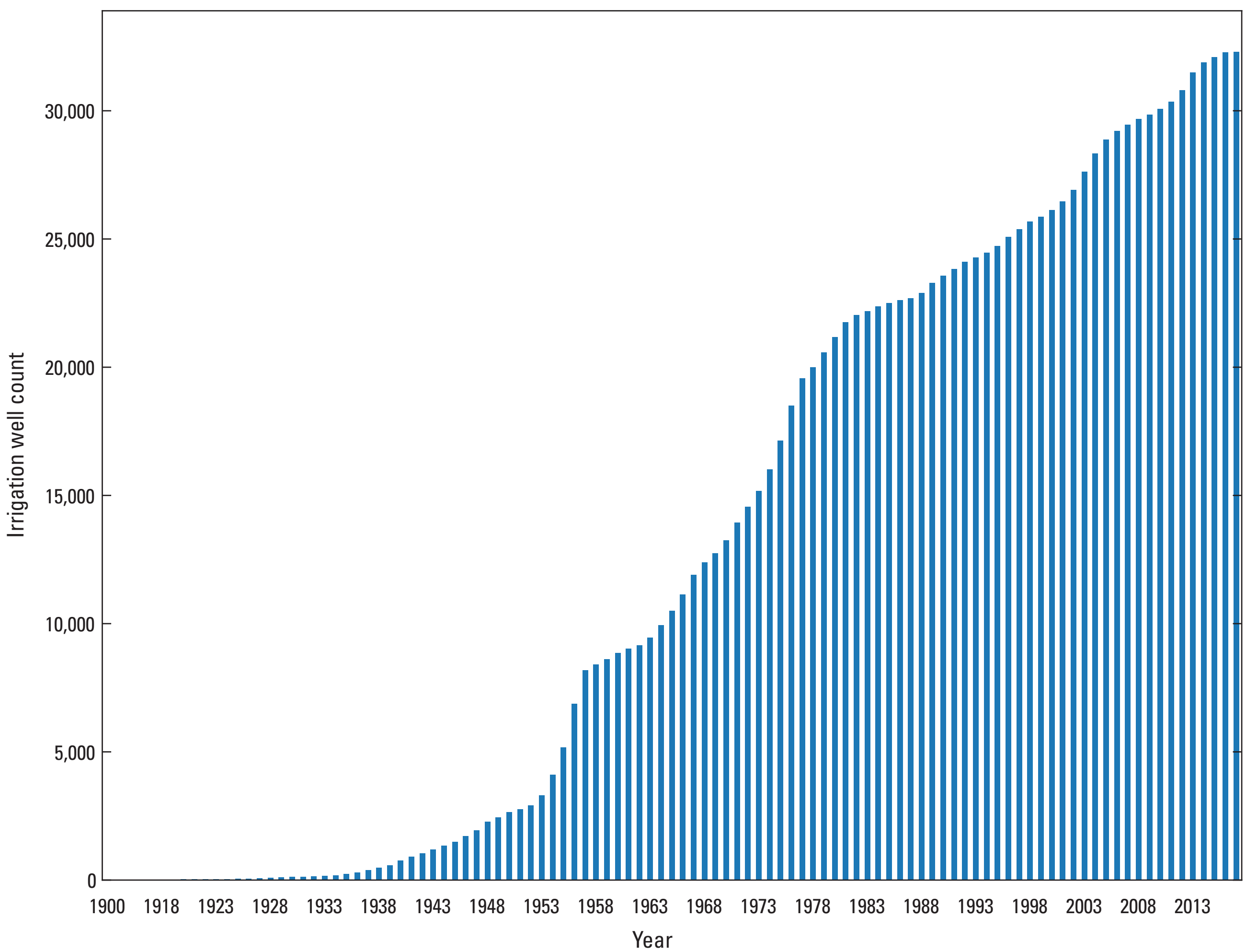

Figure 3. Irrigation well development in the study area from 1900 to 2016 (Nebraska Department of Natural Resources, 2017).

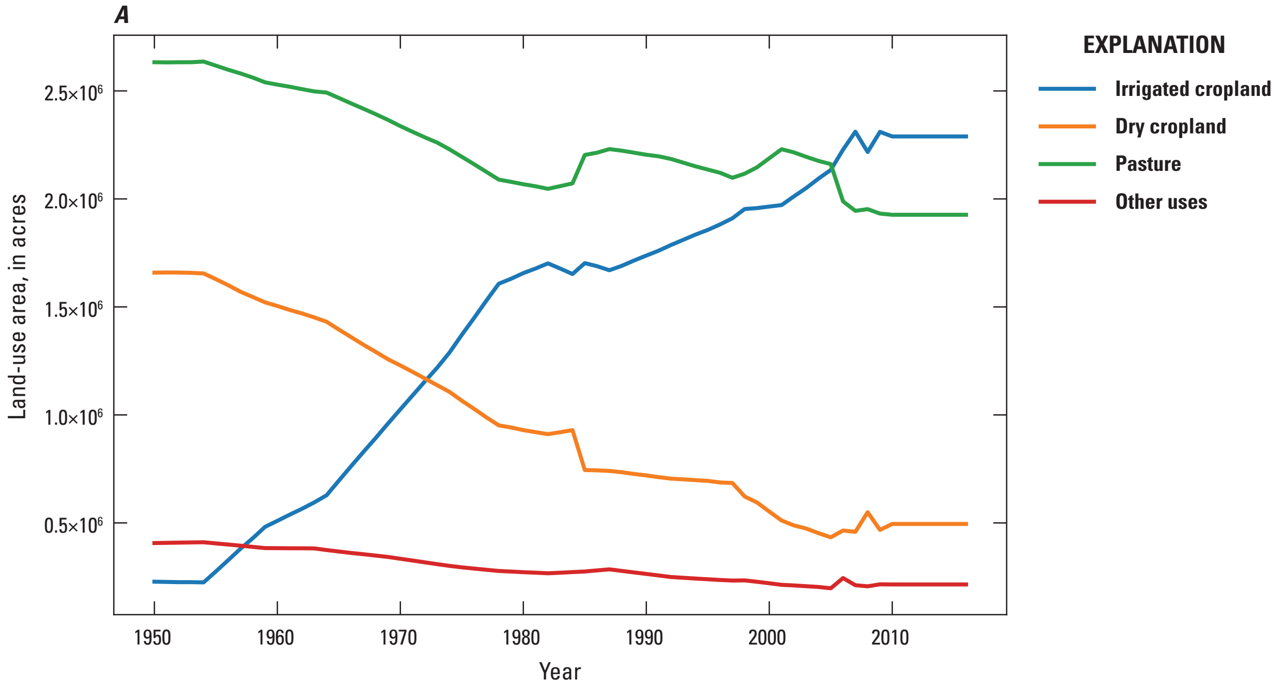

Figure 4. Land-use distribution within the study area, central Nebraska. *A*, Trends of irrigated cropland, dry cropland, pasture, and other uses, from 1950 through 2016. *B*, Groundwater irrigated cropland, dry cropland and pasture, and surface water irrigated cropland from 1950, 1985, and 2005 (this is a layered .pdf; download at https://doi.org/10.3133/sir20235024).

water, urban, riparian forest and wetlands, and roads. Between 1950 and 2016, dry cropland and pasture were converted to irrigated land supplied by groundwater wells. In 2016, the distribution was 47 percent irrigated land with 43 percent irrigated by groundwater (2,289,189 acres), 39 percent pasture (1,926,600 acres), 10 percent dry cropland (495,197 acres), and 4 percent other uses (215,094 acres; Cooperative Hydrology Study, 2017; fig. 4*A*, *B*). The development of irrigated cropland from 1950 to 2005 has taken place primarily from Buffalo County in the central part of the study area to Polk and York Counties in the eastern part of the study area (fig. 4*B*).

Crop coefficients (Kc), which are properties ascribed to plants and used to estimate AET, vary depending on land use or crop type. Allen and others (1998) reported Kc values for the two most common land uses, rangeland and corn, that vary from 0.15 to 1.05 and 0.15 to 1.20 for different parts of the growing season cycle. Crops typically are irrigated between May and September each year based on planting dates and harvesting dates from the U.S. Department of Agriculture (1997 and 2016). Further, the largest amounts of irrigation typically occur in July and August when there is the most difference between ET_{ref} and precipitation. The fraction of AET that comes from plant transpiration also varies across a single year, much like Kc values. For example, AET during the nongrowing season is predominantly from the evaporation because plants are absent or dormant. Alternately, AET is predominantly transpiration during the middle of the growing season when leaf area index is largest, and more plant surface area is available to transpire.

The primary water use has evolved since the late 1800s from surface-water irrigation to groundwater irrigation. In the late 1890s, surface water for irrigation was the primary water use by way of several canals (Peterson, 2009; fig. 1*A*). Groundwater irrigation development prior to 1940 was limited to about 760 wells (fig. 3) that irrigated about 158,000 acres. Based on 5-year water use survey data, groundwater irrigation became the primary water use after 1950, and from 1985 to 2015 the total groundwater withdrawals for irrigation were 480 to 840 million gallons per day (Mgal/d) or about 75 to 93 percent of the total water use in the Buffalo, Dawson, Hall, and Merrick counties (U.S. Geological Survey, 2017; fig. 5). Prior to the development of center-pivot irrigation systems in the early 1950s, groundwater pumped for irrigation was applied using less efficient flood irrigation methods. Flood irrigation efficiency prior to 1940 was assumed to be 50 percent (Irmak and others, 2011).

Groundwater use for irrigation within the study area is affected by precipitation; irrigation withdrawals are generally higher during years of lower-than-average precipitation and less in years of higher-than-average precipitation. For example, the reduction in groundwater use for irrigation in 2010 can be attributed to an increase in precipitation compared to other

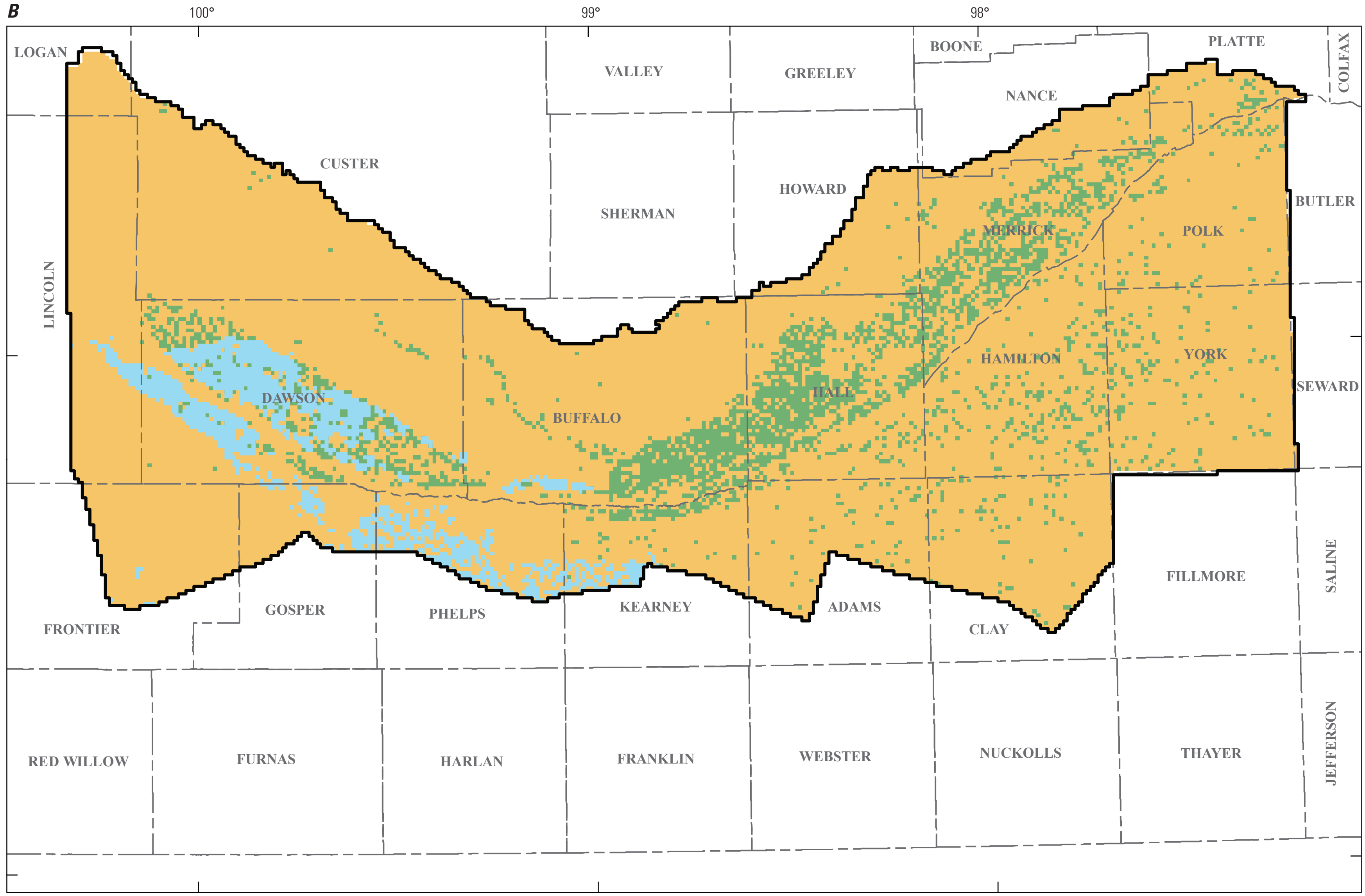

Base modified from U.S. Geological Survey digital data, 2018
Nebraska State Plane, FIPS 2600
North American Datum of 1983

0 25 50 MILES
0 25 50 KILOMETERS

EXPLANATION

- Surface water irrigated cropland in 1950
- Groundwater irrigated cropland in 1950
- Dry cropland and pasture in 1950
- Central Platte Integrated Hydrologic Model active boundary—Layer 1

Figure 4.—Continued

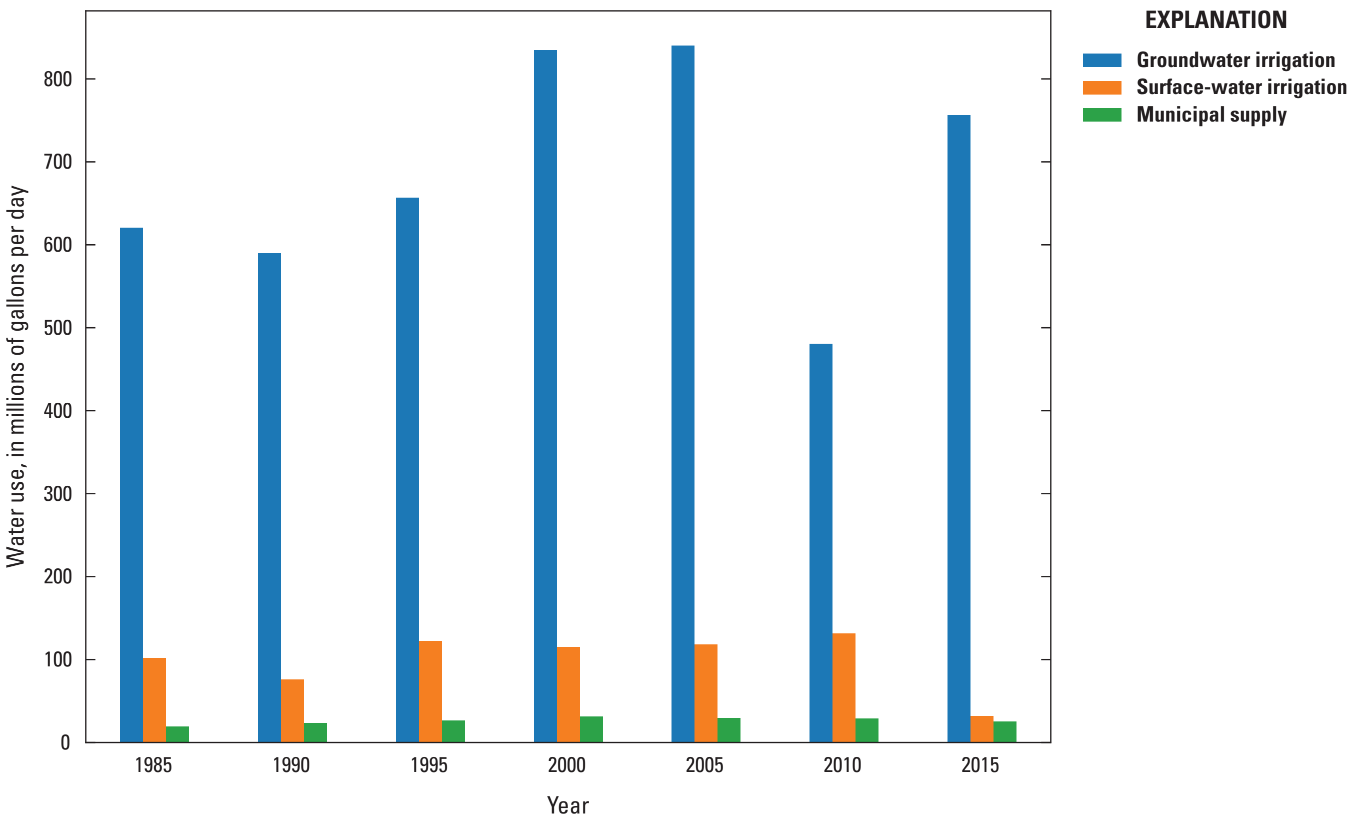

Figure 5. Primary annual water uses in Buffalo, Dawson, Hall, Merrick counties (U.S. Geological Survey, 2017).

years. Surface water used for irrigation accounted for about 32 to 132 Mgal/d or about 2 to 20 percent of total use (fig. 5). All public supply is from groundwater, and those withdrawals accounted for about 19 to 31 Mgal/d or about 3 to 5 percent of total withdrawals (fig. 5). In 2016, the primary water use in the study area was groundwater for irrigation and the secondary water use was groundwater used for public supply (Dieter and others, 2018).

Surface Water

The surface-water network consists of man-made irrigation canals and natural streams generally flowing west to east for five subregional watersheds: the Big Blue, Little Blue, Loup, Platte, and Republican Rivers (fig. 1*C*). The Platte River watershed is the primary watershed that constitutes the central region and includes the major streams such as the Platte River, Wood River, and Prairie Creek (fig. 1*C*). The Platte River flows eastward through the study area from Brady, Nebr., in the west through Kearney, Nebr., and Grand Island, Nebr., in the central region, before flowing out of the study area a few miles east of Duncan, Nebr. (not shown) (fig. 1*A*). The Platte River has the largest average annual flows in the study area. The mean annual streamflow at the Platte River near Duncan, Nebr. (USGS streamgage 06774000) is 1,420 cubic feet per second (ft^3/s) for the period of record from 1895 to 2016 (U.S. Geological Survey, 2017). The Platte River is a braided stream often with two or three main channels for much if its path through the study area (Alexander and others, 2013). The South Loup and Loup Rivers flow along the northern boundary of the study area and have more tributaries draining from the north than in the study area (fig. 1*C*). The CPNRD boundary is approximately coincident with the Platte River watershed between Gothenburg, Nebr., and Columbus, Nebr. (fig. 1*A*). The Big Blue watershed is in the eastern part of the study area and includes Big Blue River and minor streams such as the Lincoln Creek and the West Fork of the Big Blue River (fig. 1*C*). The southern part of the study area includes the Little Blue River watershed in the east, which is drained by minor streams such as Cottonwood Creek (not shown) and Big Sandy Creek, and the Republican River watershed in the southwest, which includes minor streams such as Deer Creek and Muddy Creek (fig. 1*C*). Streams that flow out of the study area include the Platte River near Columbus, Nebr.; the Big Blue River in eastern Polk County; and Lincoln Creek and Beaver Creek in eastern York County (fig. 1*C*). Muddy Creek and Deer Creek flow out of the study area in Frontier County (fig. 1*C*). The spatial location of each stream was derived from the National Hydrography Dataset (McKay and others, 2012).

Some reaches of streams leak stream water into the groundwater system, primarily in the central and eastern region (Peterson and Carney, 2002). Stream leakage depends on stream physical properties such as vertical hydraulic conductivity of the streambed, streambed thickness, channel width, and the hydraulic gradient between the stream stage and the groundwater. Calibrated vertical streambed hydraulic conductivity from groundwater-flow models developed in Peterson (2009) and Peterson and others (2016) ranged from 0.1 to 10 feet per day (ft/d). Data were unavailable to define streambed thickness; therefore, streambed thickness was assumed to be a uniform constant value of 3 ft for all streams. Stream channel widths were defined using recent areal satellite imagery from Google Earth (Google, 2018). Streambed hydraulic conductivity was also assumed to be related to the predominant soil type in that location because streams in the study area are shallow and generally do not cut into bedrock, except in the southwestern part of the study area (fig. 1*B*).

A network of eight canals divert surface water from the Platte River for irrigation. The earliest canals began diverting water in 1895 and include Cozad Canal, Dawson County Canal, Gothenburg Canal, Kearney Canal, Orchard-Alfalfa Canal, and Sixmile Canal (fig. 1*C*). Elm Creek Canal (not shown) and Thirtymile Canal began diverting water from the Platte River in 1932 and 1928, respectively (fig. 1*C*). By 1940, the eight canals (Cozad Canal, Dawson County Canal, Orchard-Alfalfa Canal, Gothenburg Canal, Sixmile Canal, Kearney Canal, Thirtymile Canal, and Elm Creek Canal) were operating in the CPNRD with the water rights to divert an estimated 200,000 acre-feet per year (acre-ft/yr) (Peckenpaugh and others, 1987; Nebraska Department of Natural Resources, 2019), which is similar to the estimated annual diversion of 193,000 acre-feet in recent years; diversion amounts can vary slightly from year to year (Peterson, 2009). After 1940, the Central Nebraska Public Power and Irrigation District (CNPPID) constructed the Tri-County and Phelps Canals, which diverted surface water from the Platte River west of the study area but had about 130,000 acre-feet leakage through the canal and lateral beds within the study area each year (Peterson, 2009). An estimated 40 percent of the diverted water to the CPNRD canals, about 80,000 acre-ft/yr, leaks through the canal and lateral beds and recharges the aquifer (Peterson, 2009; Peterson and others, 2016). The annual leakage has contributed to increases in base flow of the Platte River and some tributaries in the area (Peckenpaugh and others, 1987). Two reservoirs, Johnson Lake and Elwood Reservoir, built in 1941 and 1974, respectively, exhibit stages above the water table in the area and leak water to the underlying aquifer (Central Nebraska Public Power and Irrigation District, 2019). Hydraulic head values for Johnson Lake and Elwood Reservoir were determined using the mean lake/reservoir stage for each stress period after construction (Central Nebraska Public Power and Irrigation District, 2019).

Hydrogeology and Groundwater

The Northern High Plains aquifer is a part of the High Plains aquifer (Peterson and others, 2016) and constitutes the primary groundwater aquifer in the study area. The geologic units in the study area consist of Quaternary-age valley-fill deposits, dune sand, loess, and alluvium, and Tertiary-age Ogallala Formation silt and sandstone (Gutentag and others, 1984). The most recent units are the Holocene-age valley-fill deposits located in stream valleys that consist of coarser materials such as sands and gravels, and the wind-blown dune sand deposits present in isolated parts of the study area (fig. 6). The wind-blown Pleistocene loess deposits are present throughout the study area and contain silt and fine-grained sands and clays. Pleistocene alluvial deposits, commonly referred to as “Paleo-channels,” also are present throughout the study area as stream deposits that consist of sands and gravels. The geologic units with similar hydraulic properties such as water storage and permeability were grouped into hydrostratigraphic units (HUs) and described in Cannia and others (2006) for incorporation into groundwater-flow models developed in Luckey and Cannia (2006), Carney (2008), and Peterson (2009). The spatial distribution of HUs in the study area is presented as a fence diagram in figure 36 of Cannia and others (2006).

The Ogallala Formation is the principal geologic unit that forms the Northern High Plains aquifer (Gutentag and others, 1984). The Northern High Plains aquifer is the primary aquifer in the study area, is hydrologically connected to the Quaternary-age alluvial aquifers, and includes the Quaternary-age deposits and Tertiary-age Ogallala Formation (Cannia and others, 2006). The study area contains HUs 1–6 from Cannia and others (2006), where HUs 1 and 2 consist of Quaternary-age valley-fill, loess deposits, and alluvial aquifers; HUs 3 and 4 consist of the finer grained and less permeable Quaternary-age loess deposits and Upper-Tertiary-age portions of the Ogallala Formation; and HUs 5 and 6 consist of the sands, sandstones, silts, and gravels of the Ogallala Formation. Although HUs 3 and 4 are less permeable deposits, they are not confining units between coarser HUs 1 and 2 and HUs 5 and 6; therefore, each of the six HUs are hydrologically connected within the study area. The base of the Northern High Plains aquifer in the study area is the Cretaceous-age Pierre Shale, which is HU 10 (fig. 6). The Nebraska portion of the Northern High Plains aquifer has exhibited a loss of 6 million acre-feet of recoverable storage from predevelopment to 2015 (McGuire, 2017). The Northern High Plains aquifer serves as the source for all groundwater irrigation and public supply wells in the study area.

The groundwater is characterized by west to east regional groundwater flow (Peterson and others, 2016). Within each watershed in the study area, consistent with the regional flow system, groundwater typically flows west to east and either flows out of the study area on the eastern edge or discharges as base flow to streams. Locally, groundwater flows toward streams in the western portion of the study area where steams are gaining flow from groundwater, and groundwater flows away from streams in the central and eastern portions of the study area where streams are losing flow to groundwater. Groundwater discharge to streams, referred to as “base flow,” is a component of flow in most streams but not all reaches. Base flow is affected by pumping of wells near streams (Kollet and Zlotnik, 2003).

System	Series	Geologic unit	Hydrostratigraphic unit	Aquifer	Description	CPIHM layer
Quaternary	Holocene	Valley-fill deposits	HU 2	Alluvial aquifer	Gravels, sands, silts, and clays with coarser materials more common. Generally stream deposits. Upper fine material, if present, is assigned to Hydrostratigraphic Unit 1. Lower fine material, if present, is assigned to Unit 3. Occurs in major river valleys where it can be over 180 feet thick.	1
		Dune sand	HU 1	High Plains aquifer	Wind-deposited fine to medium sand with small amounts of clay, silt, and coarse sand. Occurs in only a few locations in Hall, Howard, Phelps, and Kearney Counties, where it can be a few tens of feet thick.	1
	Pleistocene and Holocene	Loess deposits	HU 1 when above HU 2, otherwise HU 3	High Plains aquifer	Silt with small amounts of very fine sand and clay. Deposited as wind blown dust. Occurs almost everywhere in the Eastern Model Unit from Peterson (2009), and is generally thinnest in valleys of large, active rivers. Can be over 370 feet thick in bluffs and plains adjacent to the Platte River valley, but generally only the lowest 100 feet is beneath the water table.	1 if HU 1 or 2, 2 if HU 3
	Pleistocene	Alluvial deposits	HU 1	High Plains aquifer	Gravels, sands, silts, and clays with coarser materials more common. Generally stream deposits. Upper fine material, if present, is assigned to Hydrostratigraphic Unit 1. Lower fine material, if present, is assigned to Unit 3. Occurs throughout most of the Eastern Model Unit, except where underlying bedrock is topographically higher than surrounding areas, and can be over 300 feet thick.	1 if HU 1 or 2, 2 if HU 3
Tertiary	Upper and Middle Miocene	Ogallala group	HU 4-6	High Plains aquifer	Generally unconsolidated heterogeneous mixture of gravels, sands, silts, and clays. Generally stream deposits but also contains wind-blown deposits. Upper fine material, if present, is assigned to Unit 4. Center coarse material, if present, is assigned to Unit 5. Lower fine material, if present, is assigned to Unit 6. Occurs throughout the western half of the Eastern Model Unit, where the mean thickness is around 160 feet, though it can be over 500 feet thick. Thins eastward and is absent from the eastern part of the Eastern Model Unit.	2 if HU 4, 3 if HU 5 or 6
Cretaceous	Upper Cretaceous Series	Montana group	HU 10	Pierre Shale confining unit	Pierre Shale. Shale, chalk, limestone, siltstone, and sandstone. Except for a few minor units in the Dakota Sandstone in the extreme eastern part of the area, below the High Plains aquifer, generally forms an impermeable base of High Plains aquifer. Deep marine deposits to beach deposits.	na

[CPIHM, Central Platte Integrated Hydrologic Model; HU, hydrostratigraphic unit (Cannia and others, 2006); na, not applicable because the layer is not in the CPIHM]

Figure 6. Generalized section of geologic units, hydrostratigraphic units delineated by Cannia and others (2006) (modified from Peterson, 2009), aquifers present in the study area, and the model layers for the Central Platte Integrated Hydrologic Model.

Aquifer properties, particularly horizontal hydraulic conductivity (Kh) and specific yield (Sy) have been evaluated in previous studies. Houston and others (2013) estimated Kh and Sy at test holes in the Northern High Plains aquifer, using lithologic logs to interpret Kh and Sy for vertical intervals of the aquifer. Peterson (2009) included the calibrated Kh for HUs 1 through 6; HUs 1 and 2 had Kh values of about 10 and 155 ft/d, respectively (table 1; table 3 in Peterson, 2009). The intervals representing HUs 3 and 4 consisted of predominantly silt. These two HUs had similar Kh of about 8 ft/d and acted as a semiconfining unit for most of the study area (Peterson, 2009). The average Kh for the interval representing HUs 5 and 6 was about 33 and 10 ft/d, respectively (Peterson, 2009).

Mean Kh estimates for test holes were highest for the interval representing HUs 1 and 2 at 66.6 ft/d (table 1; Houston and others, 2013). Mean Kh for the intervals representing HUs 3–6 were similar; however, the range in Kh for the upper of these intervals was from less than 1 to 325 ft/d and for the lower interval from about 5.6 to 67.7 ft/d, indicating that the lower interval sediments are much more homogeneous than the interval representing HUs 3 and 4 (table 1). Sy values were similar to the average Sy for the Northern High Plains aquifer of about 0.15 (table 1; Houston and others, 2013; McGuire, 2017).

Additionally, recharge rates to groundwater through the unsaturated zone ranged from 0.2 to 10 inches per year (in/yr) based on values measured across the CPNRD on irrigated land, dryland, and rangeland (Steele and others, 2014). Calibrated recharge simulated in Peterson (2009) had a range of about 1 to 7 in/yr (see fig. 16 and table 9 from Peterson, 2009). Calibrated recharge simulated in Peterson and others (2016) had a range of about 2 to 5 in/yr (see fig. 20B from Peterson and others, 2016).

Integrated Hydrologic Model

This section of the report describes the conceptual model of the hydrologic system, construction, and calibration of the CPIHM; results of the calibration; and scenario results of the CPIHM. The CPIHM is a numerical integrated hydrologic model developed for the CPNRD using a MODFLOW-based groundwater modeling software called MF–OWHM (Boyce and others, 2020). The MF–OWHM is a fully coupled (or fully integrated) landscape, surface water, and groundwater-flow model, which makes it a hydrologic-flow model in addition to a groundwater-flow model.

Conceptual Model of the Hydrologic System

The conceptual model of a hydrologic system is a schematic of the water cycle for a given study area that identifies and describes sources, sinks, and reservoirs of water in that system. The three main hydrologic subsystems represented in the conceptual model were the landscape water, surface water, and groundwater. The interface of each subsystem is a hydrologic boundary. Each subsystem consists of components that represent sources, sinks, and reservoirs of water. A source of water is the addition of water to a subsystem (hereafter referred to as “inflows”). A sink of water is the discharge or removal of water from a sub-system (hereafter referred to as “outflows”). Reservoirs represent water stored in a subsystem that is not an inflow or outflow. This conceptual model, to the extent possible, also describes the approximate magnitude of the reservoirs and fluxes of water for each component of the hydrologic system (referred to as “water budgets”), which creates a blueprint for construction of the numerically based computer model. After characterization of the inflows and outflows, the conceptual model becomes the framework for the accurate construction and development of the numerical hydrologic-flow model. The three subsystem components of the numeric model (climate and landscape, surface water, and groundwater) are conceptualized and described below. Conceptual descriptions include calculated fluxes representing the interaction between the subsystems and internal flows within the subsystems.

The conceptual flux estimates presented in this section of the report are based on previous studies in or near the area as described in this section and the "Previous Studies" section of this report, adapted to the 4,926,071-acre CPIHM active domain (fig. 1*A*). Conceptual flux estimates are presented for two time periods to represent the major periods

Table 1. Horizontal hydraulic conductivity and specific yield estimates for the Central Platte Integrated Hydrologic Model by hydrostratigraphic unit and model layer/group and derived from Peterson (2009) and Houston and others (2013).

[HU, hydrostratigraphic unit; <, less than]

Model layer/group	HU	Horizontal hydraulic conductivity (feet per day)			Specific yield (unitless)		
		Minimum	Average	Maximum	Minimum	Average	Maximum
1	1, 2	2.6	66.6, [1]82.5	297.3	0.026	0.165	0.255
2	3, 4	<1	29.1, [1]8	325	0.001	0.127	0.27
3	5, 6	5.6	26.24, [1]21.5	67.7	0.058	0.166	0.235

[1]Value from Peterson (2009) are averages across coincident hydrostratigraphic units of the calibrated model.

of groundwater development: the period prior to widespread groundwater irrigation development (approximately 1940), and a recent period (approximately 2011 to 2016; tables 2 and 3). There was a wide range of values for ET and groundwater irrigation pumping because of the lack of available data to accurately characterize component values or a large uncertainty in the available published data or studies. The understanding of uncertainty and error in the conceptual estimates was applied in the development and calibration of the CPIHM.

Climate and Landscape Components

The landscape in the study area includes land-use characteristics such as crop type, ET characteristics for each crop type, soil types, and surface-water characteristics. The landscape is characterized by an extensive surface-water network that includes major streams as described in the "Surface Water" section of this report. The climate and landscape water subsystems include inflows from precipitation; root uptake; inflows from surface-water deliveries or groundwater used for irrigation, runoff, and deep percolation past the root zone; and outflows of ET (broken down by source of water).

Precipitation is the largest inflow to the landscape, although locally the inflows from irrigation can exceed precipitation, particularly in drought conditions. Most surface-water deliveries occur to meet irrigation demands between May and September (table 1.1). Outflows from the landscape subsystem include ETp, ET of irrigation water, ETg that passes through the landscape, deep percolation past the root zone, and runoff of precipitation to streams. ET of irrigation water is generally the largest outflow from the landscape subsystem. Measured annual AET rates varied based on land cover and precipitation. Rangeland had the highest rates of AET that range from 22 to 36 in/yr depending on precipitation and location (Irmak, 2014). Regional irrigated and dry cropland annual AET rates were about 21.6 and 16.8 in/yr, respectively (Irmak, 2014). The AET of irrigated corn, the predominant crop in the study area, was 25.9 in/yr based on nearby measurements (Kranz and others, 2008). Based on average AET rates and land use reported by the Cooperative Hydrology Study (2017), the estimated annual volume of total AET of precipitation and irrigation was about −8,600,000 acre-feet for pre-1940 and about −9,500,000 acre-feet for the recent development period (2011–16; table 2). The uncertainty associated with these estimates was difficult to quantify owing to the lack of AET rates available for all land uses within the study area and the lack of an uncertainty assessment in the mentioned studies. The range of AET for the recent development period (2011–16), was about −8,800,000 to −11,000,000 acre-ft/yr based on the range of irrigated corn AET and rangeland AET in Kranz and others (2008), Irmak (2014), and Cooperative Hydrology Study (2017). The ET of irrigation water is conceptually difficult to estimate because precipitation and irrigation occur on the same area across similar time periods; therefore, the landscape ET component in table 2 combines ETp and ET of irrigation water sources.

Deep percolation past the root zone (often referred to as recharge) in the study area has been estimated at 0.2 to 2.1 in/yr below rangeland (that is, pasture), 2.7 to 6.3 in/yr below groundwater-irrigated cropland, 10 in/yr below surface-water irrigated cropland, and 0.5 to 2.5 in/yr below dry cropland (Steele and others, 2014). Additionally, recharge in the study area that occurs as leakage from the unlined irrigation canals can exceed 10 in/yr (Peterson and others, 2016). The highest recharge rates in areas without canal influence were about 4 to 6 in/yr in the flat, densely groundwater-irrigated cropland in the Platte River valley (Peterson and others, 2016).

Surface-Water Components

Surface-water inflows include streamflow that enters the study area, groundwater that discharges through the streambed as base flow, and runoff. Outflows include leakage of stream water into the underlying aquifer and outflows of streamflow where streams exit the study area. Runoff from precipitation was estimated for the study area using

Table 2. Conceptual flux estimates for pre-1940 and recent development (2011–16) periods for the landscape subsystem fluxes of evapotranspiration of precipitation and irrigation water for the Central Platte Integrated Hydrologic Model.

[nc, not calculated because there were not enough data available; negative flux values indicate outflows from the respective subsystem; positive flux values indicate inflows to the respective subsystem]

Period	Area (acres)	Irrigation wells	Evapotranspiration of precipitation and irrigation water	Evapotranspiration of precipitation and irrigation water range	Irrigation wells range	Evapotranspiration references
Landscape subsystem, in acre-feet per year						
Pre-1940	4,926,071	263,000	−8,600,000	nc	263,000–203,000	Irmak (2014), Kranz and others (2008)
2011–16	4,926,071	1,800,000	−9,500,000	−8,800,000 to −11,000,000	1,980,000–2,160,000	Irmak (2014), Kranz and others (2008)

Table 3. Conceptual flux estimates for pre-1940 and recent development (2011–16) periods for the groundwater subsystem fluxes of outflows to irrigation wells for the Central Platte Integrated Hydrologic Model.

[AET, actual evapotranspiration]

Period	Area (acres)	Outflow to irrigation wells	Irrigation wells range	Irrigation description
Groundwater subsystem, in acre-feet per year				
Pre-1940	4,926,071	−263,000	−286,000 to −203,000	Irrigated acres in 1950 multiplied by average irrigation depth of 10 inches per year based on difference between growing season precipitation and irrigated corn AET. The range was based on efficiency between 50 and 65 percent (Peterson, 2009; Irmak and others, 2011).
2011–16	4,926,071	−1,990,000	−1,990,000 to −2,190,000	Irrigated acres in 2011–16 multiplied by average irrigation depth of 10 inches per year based on difference between growing season precipitation and irrigated corn AET. The range was based on efficiency between 80 and 90 percent (Peterson, 2009; Irmak and others, 2011).

base flow separation techniques in the USGS Groundwater Toolbox (table 4; Barlow and others, 2014; 2017) from streamgage data for the Platte River, Prairie Creek, Silver Creek, and Wood River (table 4; fig. 1*A*). Streamgages were present at locations of major stream inflows and outflows in the study area for most or all of the development period, which provided adequate data to estimate the gaged flows in and out of the surface-water system. Minor streams that flowed into the study area that were ungaged along the Loup River boundary streams were estimated with flows of about 5 ft^3/s for the entire period of interest based on stream width from aerial imagery and an assumed depth of 1 ft. The largest gaged inflows are at the North Loup River near St. Paul, Nebr. (USGS streamgage 06790500; fig. 1*A*), which has an average discharge of 853 ft^3/s for the period of record 1928 to 2016 (U.S. Geological Survey, 2017). However, the Loup River system is a boundary stream; the largest gaged inflows for a nonboundary stream are at the Platte River at Brady, Nebr. (USGS and Nebraska Department of Natural Resources [NeDNR] streamgage 06766000; fig. 1*A*) with an average total inflow of about 746 ft^3/s for the period from 1939 to 2016 (table 4). The largest outflows are at the Platte River about 5 miles downstream from the Platte River near Duncan, Nebr. (USGS streamgage 06774000: fig. 1*A*), which has an average discharge of 1,742 ft^3/s for the period from 1939 to 2016 (U.S. Geological Survey, 2017). For the pregroundwater irrigation development period (pre-1940), total flow into the study area at the Platte River at Brady, Nebr. (USGS streamgage 06766000) was about 1,541 ft^3/s. The outflow at the Platte River near Duncan, Nebr. (USGS streamgage 06774000) for the pre-1940 period was about 1,620 ft^3/s; the overland flow portion of total streamflow was estimated to be an outflow of about 497 ft^3/s (about 360,000 acre-ft/yr or 1 inch) within the Platte River watershed, based on values obtained from Cooperative Hydrology Study (2017). For the recent period (2011 to 2016), total streamflow and runoff at the Platte River at Brady, Nebr. (USGS streamgage 06766000) were about 1,102 ft^3/s and 427 ft^3/s, respectively. Recent period (2011–16) total streamflow and runoff at the Platte River near Duncan, Nebr. (USGS streamgage 06774000) were about 2,495 and 884 ft^3/s, respectively (table 4). Runoff was estimated to be an outflow of about 460,000 acre-ft/yr (about 635 ft^3/s or 1.11 inches) within the Platte River watershed, which contributes to the runoff at the Platte River near Duncan, Nebr. (USGS streamgage 06774000) based on values obtained from Cooperative Hydrology Study (2017; fig. 1*A*).

Groundwater Components

Inflows to the groundwater-flow system include recharge from the landscape subsystem deep percolation component, recharge as canal leakage from the CPNRD and CNPPID canal systems, stream leakage, and cross-boundary flow into the active model area. Recharge rates are described in the “Climate and Landscape Components” section of this report. Outflows from the groundwater-flow system include cross-boundary flow out of the active model area, discharge to streams as base flow, withdrawals from irrigation wells, withdrawals from municipal wells, and ETg. Transient changes in groundwater inflows and outflows are balanced by increases or decreases of groundwater in storage. When inflows are greater than outflows, aquifer storage increases (rise in groundwater levels), and when inflows are less than outflows, aquifer storage decreases (decline in groundwater levels).

Table 4. Average base flow, runoff, and total streamflow for primary U.S. Geological Survey National Water Information System streamgages in the study area, central Nebraska.

[ID, identification; MM, month; DD, day; YYYY, year; NE, Nebraska; --, no data; NA, not available]

Site ID	Site name	Period of record (MM/DD/YYYY)	Flows, in cubic feet per second			Data source
			Average baseflow	Average runoff	Average total flow	
Period of record for each streamgage						
06766500	Platte River near Cozad, NE	10/1/1940–9/29/1991	328	347	674	U.S. Geological Survey (2017)
06770000	Platte River near Odessa, NE	10/1/1938–9/29/1991	1,002	479	1,487	U.S. Geological Survey (2017)
06770200	Platte River near Kearney, NE	1/27/1982–12/31/2016	1,080	718	1,797	U.S. Geological Survey (2017)
06770500	Platte River near Grand Island, NE	4/1/1934–12/31/2016	820	713	1,532	U.S. Geological Survey (2017)
06773050	Prairie Creek near Ovina, NE	5/30/1991–9/30/1999	6	11	18	U.S. Geological Survey (2017)
06773150	Silver Creek at Ovina, NE	5/31/1991–9/29/1995	3	7	11	U.S. Geological Survey (2017)
06773500	Prairie Creek near Silver Creek, NE	9/30/2001–1/1/2020	15	22	37	U.S. Geological Survey (2017)
06766000	Platte River at Brady, NE	3/1/1939–12/31/2016	347	394	746	Nebraska Department of Natural Resources (2019), U.S. Geological Survey (2017)
06774000	Platte River near Duncan, NE	10/25/1928–12/31/2016	923	813	1,742	Nebraska Department of Natural Resources (2019), U.S. Geological Survey (2017)
06768000	Platte River near Overton, NE	10/1/1930–12/31/2016	905	652	1,560	U.S. Geological Survey (2017)
06771000	Wood River near Grand Island, NE	3/1/2006–11/30/2011	18	19	37	U.S. Geological Survey (2017)
Pre-1940 period for each streamgage						
06766500	Platte River near Cozad, NE	--	--	--	--	NA
06770000	Platte River near Odessa, NE	10/1/1938–12/31/1939	1	145	1,108	U.S. Geological Survey (2017)
06770200	Platte River near Kearney, NE	--	--	--	--	NA
06770500	Platte River near Grand Island, NE	7/1/1934–12/31/1939	215	702	922	U.S. Geological Survey (2017)
06773050	Prairie Creek near Ovina, NE	--	--	--	--	NA
06773150	Silver Creek at Ovina, NE	--	--	--	--	NA
06773500	Prairie Creek near Silver Creek, NE	--	--	--	--	NA
06766000	Platte River at Brady, NE	3/1/1939–12/31/1939	570	474	1,541	Nebraska Department of Natural Resources (2019), U.S. Geological Survey (2017)
06774000	Platte River near Duncan, NE	11/1/1928–12/31/1939	649	962	1,620	Nebraska Department of Natural Resources (2019), U.S. Geological Survey (2017)
06768000	Platte River near Overton, NE	10/1/1930–12/31/1939	608	833	1,470	U.S. Geological Survey (2017)

Table 4. Average base flow, runoff, and total streamflow for primary U.S. Geological Survey National Water Information System streamgages in the study area, central Nebraska.—Continued

[ID, identification; MM, month; DD, day; YYYY, year; NE, Nebraska; --, no data; NA, not available]

Site ID	Site name	Period of record (MM/DD/YYYY)	Flows, in cubic feet per second			Data source
			Average baseflow	Average runoff	Average total flow	
Pre-1940 period for each streamgage—Continued						
06771000	Wood River near Grand Island, NE	--	--	--	--	NA
Average 2011–16 period for each streamgage						
06766500	Platte River near Cozad, NE	--	--	--	--	NA
06770000	Platte River near Odessa, NE	--	--	--	--	NA
06770200	Platte River near Kearney, NE	1/1/2011–12/31/2016	1,441	801	2,243	U.S. Geological Survey (2017)
06770500	Platte River near Grand Island, NE	1/1/2011–12/31/2016	1,547	744	2,291	U.S. Geological Survey (2017)
06773050	Prairie Creek near Ovina, NE	--	--	--	--	NA
06773150	Silver Creek at Ovina, NE	--	--	--	--	NA
06773500	Prairie Creek near Silver Creek, NE	1/1/2011–12/31/2016	7	11	18	U.S. Geological Survey (2017)
06766000	Platte River at Brady, NE	1/1/2011–12/31/2016	675	427	1,102	Nebraska Department of Natural Resources (2019), U.S. Geological Survey (2017)
06774000	Platte River near Duncan, NE	1/1/2011–12/31/2016	1,611	884	2,495	Nebraska Department of Natural Resources (2019), U.S. Geological Survey (2017)
06768000	Platte River near Overton, NE	1/1/2011–12/31/2016	1,449	856	2,306	U.S. Geological Survey (2017)
06771000	Wood River near Grand Island, NE	1/1/2011–11/30/2011	15	15	30	U.S. Geological Survey (2017)

Groundwater-flow subsystem components as annual inflows on the left-hand side and annual outflows on the right-hand side are presented in equation 1:

$$\textit{lake leakage} + \textit{flow from adjacent zones} + \textit{recharge} + \textit{canal leakage} + \textit{stream leakage} + \textit{releases from groundwater storage} = \textit{base flow} + \textit{groundwater evapotranspiration} + \textit{discharge to lakes} + \textit{irrigation wells} + \textit{production wells} + \textit{flow to adjacent zones} + \textit{replenishment to groundwater storage} \tag{1}$$

where

lake leakage is the water that leaks through a lakebed and becomes groundwater recharge,
flow from adjacent zones is the cross-boundary inflow of groundwater to the study area,
recharge is the deep percolation of landscape water to the groundwater-flow system,
canal leakage is the water that leaks through a canal bed and becomes groundwater recharge,
stream leakage is the water that leaks through the streambed and becomes groundwater recharge,
releases from groundwater storage is the release of groundwater from storage into the groundwater-flow system,
base flow is the discharge of groundwater to streams,
groundwater evapotranspiration is the discharge of groundwater via root uptake as transpiration or as the evaporation of groundwater,
discharge to lakes is the discharge of groundwater to lakes,
irrigation wells is the groundwater withdrawals via pumping of irrigation wells,
production wells is the groundwater withdrawals via pumping of production wells,
flow to adjacent zones is the cross-boundary outflow of groundwater from the study area, and
replenishment to groundwater storage is the replenishment of groundwater storage resulting in groundwater-level increases.

Groundwater generally flowed into the active model area at the northwestern and southwestern boundary and flowed out along portions of the southwest and eastern boundaries during pre-irrigation development period of 1895 and throughout the irrigation development period after 1895 (fig. 7*C*). Data were not available at observation wells near the study area boundaries to estimate the amount of groundwater that flowed across the study area boundaries during the pre-irrigation period. Therefore, estimates of cross-boundary flow were derived using Darcy's Law (Fetter, 2001), where hydraulic gradients were obtained from decadal groundwater levels simulated in Peterson and others (2016) and aquifer transmissivities (Kh and aquifer thickness) from Houston and others (2013) and Peterson and others (2016). Hydraulic conductivities across these boundaries were 16 to 158 ft/d, hydraulic gradients were 0.001 to 0.004, and aquifer thicknesses were about 142 to 588 ft (Houston and others 2013, Peterson and others 2016). These estimates of cross-boundary groundwater flow indicated that groundwater inflow for the pre-irrigation development period (about 1940) was about 50,000 acre-ft/yr and outflow was about 180,000 acre-ft/yr. These estimates of cross-boundary groundwater flow were assumed to be reasonable for the period prior to widespread groundwater irrigation development (about 1940) because withdrawals from the few active irrigation wells prior to 1940 were not enough to cause substantial declines in the water table at the boundaries of the study area and the decadal groundwater-level contours from Peterson and others (2016) showed little change across these boundaries for the April 30, 1940, and 1940s periods (see fig. 15 from Peterson and others, 2016). Estimates of groundwater-flow inflow to the study area for the recent period from 2011 to 2016 were about 50,000 acre-ft/yr and outflows were about 140,000 acre-ft/yr. The decrease in cross-boundary outflows is likely associated with the widespread increase in outflows to irrigation wells after 1940, which is indicated by the migration of groundwater-level contours eastward in some areas shown in the 1940s and 2000s decadal groundwater-level contours in Peterson and others (2016).

The groundwater-flow system is connected to the surface-water system through stream-aquifer interaction. Water-table contour maps indicate groundwater levels were above adjacent stream surfaces in the western portion of the active study area, which results in a net outflow from the groundwater to streams (Summerside and others, 2001; fig. 7*C*). In the eastern portion of the study area, stream surfaces are generally higher than the adjacent groundwater levels, which results in a net inflow to the groundwater from streams (Summerside and others, 2001); for example, along the Platte River approximately between Cozad and Grand Island, Nebr. (fig. 1*A*).

The Platte River, the primary stream in the study area, is connected to the groundwater-flow system for the entire length that it flows through the study area (fig. 1*A*). Along some reaches, the groundwater-flow system discharges base flow to the Platte River, and along other reaches the groundwater-flow system receives inflows from the Platte River as stream leakage (Peterson and Carney, 2002). A groundwater discharge analysis in Peterson and Carney (2002) estimated base flow at several streamgages on the Platte River during the fall low-flow season: the average groundwater discharge as base flow was from −3.0 to 4.0 ft^3/s per mile, where negative values indicate a losing reach of the stream. Estimated base flow at Platte River at Brady, Nebr., streamgage (USGS streamgage 06766000) was about 675 ft^3/s for the recent development period and 570 ft^3/s for the pre-1940 period (table 3). Estimated base flow at Platte River near Duncan, Nebr. (USGS streamgage 06774000) was estimated to be about 1,611 ft^3/s for the recent development period and 649 ft^3/s for the pre-1940 period (table 3).

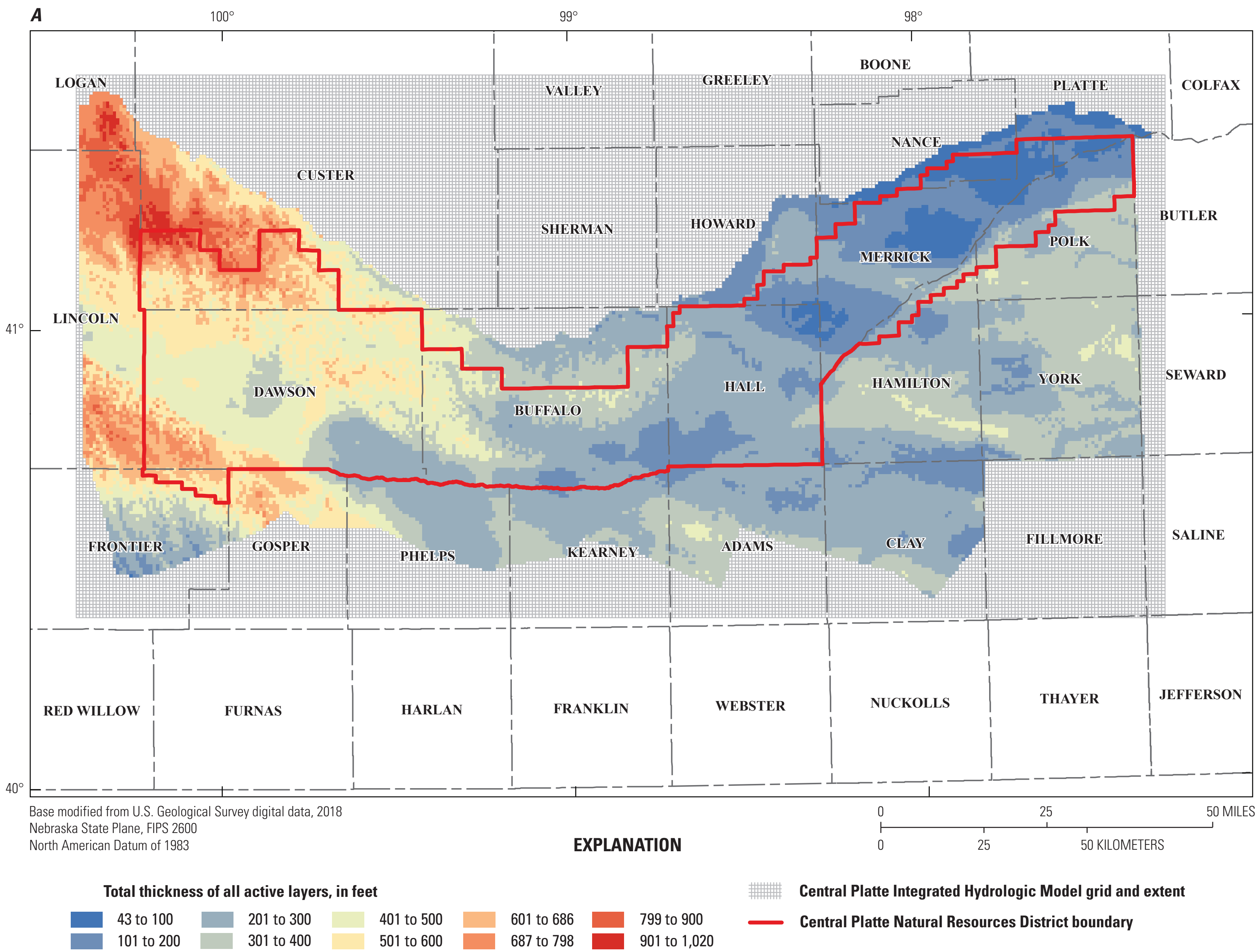

Figure 7. Map showing study area model structure, hydrologic boundaries, and conceptualized vertical layering. *A*, Orthogonal grid, active cells, and total cell thicknesses of the Central Platte Integrated Hydrologic Model. *B*, Orthogonal grid, active cells, and cell thicknesses of the Central Platte Integrated Hydrologic Model by layer (this is a layered .pdf; download at https://doi.org/10.3133/sir20235024). *C*, Simulated groundwater-level contours from 2000 to 2009 (Peterson and others, 2016) used to delineate groundwater-flow boundaries for this study and groundwater inflow, outflow, and no-flow boundaries.

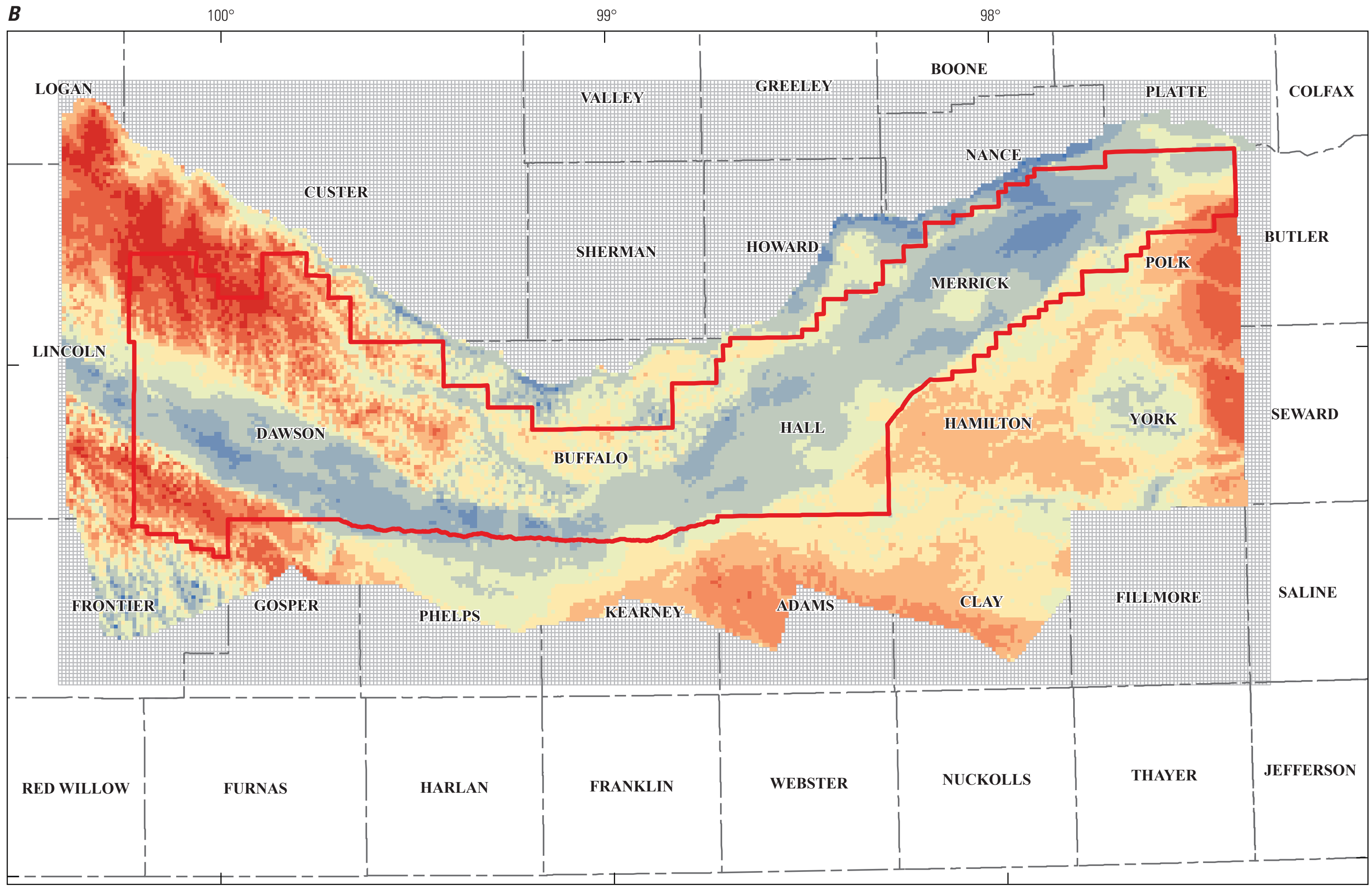

Base modified from U.S. Geological Survey digital data, 2018
Nebraska State Plane, FIPS 2600
North American Datum of 1983

EXPLANATION

Active cell thickness, in feet

10
11 to 25
26 to 50
51 to 100
101 to 150
151 to 200
201 to 250
251 to 300
301 to 400
401 to 555

Absence of layer 2 where layers 1 and 3 were present

Central Platte Integrated Hydrologic Model grid and extent

Central Platte Natural Resources District boundary

Figure 7.—Continued

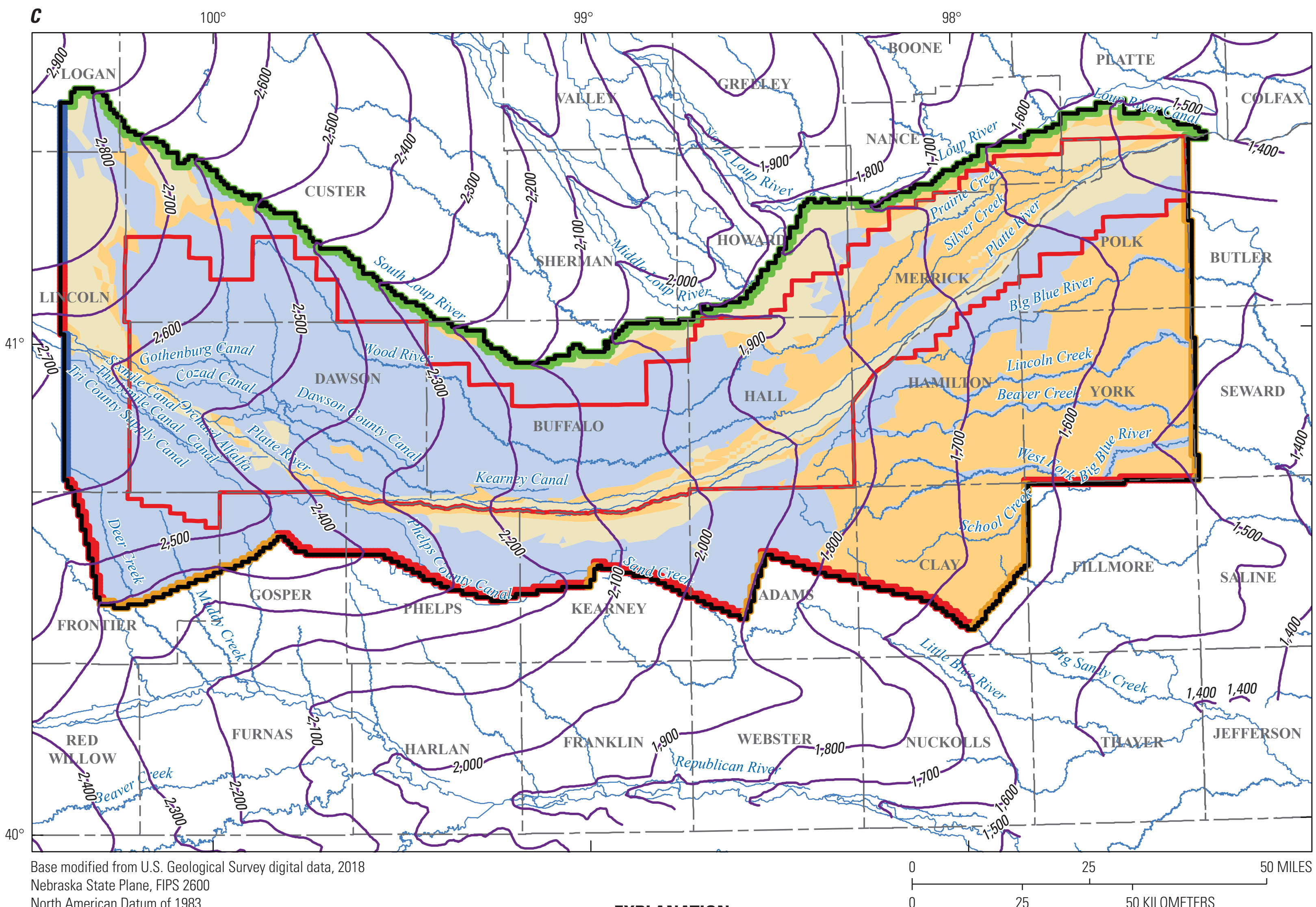

EXPLANATION

Boundary type
- Cross boundary inflow
- Cross boundary outflow
- No-flow boundary
- Stream boundary

General soil classification in the Central Platte Integrated Hydrologic Model
- Sand
- Sandy loam
- Silty clay

Simulated groundwater levels from 2000 to 2009 from Peterson and others (2016), in feet above North American Vertical Datum of 1988

Central Platte Integrated Hydrologic Model active boundary—Layer 1

Central Platte Natural Resources District boundary

Figure 7.—Continued

Recharge (analogous to deep percolation from the landscape subsystem) is the primary inflow to the groundwater-flow system for the pre-1940 and recent development periods. Recharge rates are highest on irrigated lands and lowest on rangeland (see deep percolation values described in the “Climate and Landscape Components” section of this report and based on measured values from Steele and others, 2014). Stream leakage is also estimated to be a substantial inflow to the groundwater along “losing” stream reaches of the Platte River between Overton (not shown) and Grand Island, Nebr. (fig. 1*A*). Although groundwater irrigation is the primary groundwater outflow and is typically associated with groundwater-level declines, localized increases in groundwater storage changes for the recent development period from inflows such as canal leakage and decreased outflows to groundwater ET have contributed to a small increase in storage prior to 1940 (McGuire, 2017). The increase in groundwater levels because of canal leakage has been monitored in the study area and has a local influence on the water table that does not reflect groundwater levels in other areas that do not have canal leakage inflows each year (U.S. Geological Survey, 2017).

The increase in irrigated cropland and irrigation well development has resulted in a substantial increase in outflows from groundwater irrigation wells since the 1940s (Peterson, 2009; Peterson and others, 2016). Based on a consumptive use deficit (when available precipitation is less than the amount required for a crop to fully transpire) of about 10 inches per growing season for corn, the dominant crop type, an estimated 20 inches of water was required to be pumped during an average climate year to irrigate about 158,000 acres of cropland (pre-1940 land use) for an estimated annual volume pumped of 263,000 acre-feet (table 3; Irmak and others, 2011). Estimated ranges of groundwater irrigation in table 3 are based on the range of efficiency appropriate for the time period based on values in Irmak and others (2011). Prior to the development of center pivots in the 1950s, flood or furrow irrigation was the common technique to apply groundwater pumped for irrigation, and these efficiencies had a range of 50 to 65 percent. By 2016, the number of irrigation wells was about 32,000 (fig. 3; Nebraska Department of Natural Resources, 2017) and irrigation efficiency improved with development of center-pivot technology; 80 percent of groundwater irrigation is delivered by sprinklers in Nebraska, of which most are more efficient center pivots (Irmak and others, 2011; Johnson and others, 2011). The average rate of groundwater irrigation application decreased to about 10 to 11 in/yr, but with the increase in acreage to about 2,169,000 acres of cropland, the annual estimated volume pumped increased to about 1,990,000 acre-feet (table 3). With the development of irrigation technology, such as the Low Energy Precise Application, the efficiency of groundwater pumping improved to as much as 90 percent (Irmak and others, 2011). Metered data for irrigation pumping were unavailable for more than 99 percent of irrigation wells in the CPNRD, and irrigation technology data such as traditional sprinkler or Low Energy Precise Application were also not available. Lack of these data also contributed to the uncertainty of the conceptual estimates of groundwater irrigation.

Integrated Hydrologic-Flow Model Construction

An integrated hydrologic model was constructed using the MF–OWHM software (version 2.0.1; Boyce and others, 2020). The MF–OWHM is a comprehensive version of the MODFLOW suite of groundwater-flow simulators because it is a fully integrated simulator of the landscape, surface water, and groundwater-flow system. The MF–OWHM, as described in this report, is a MODFLOW-2005 based code and therefore includes the standard MODFLOW-2005 inputs and configuration (Harbaugh, 2005) and the Newton solver (MODFLOW–NWT; Niswonger and others, 2011). The CPIHM utilized the MODFLOW–NWT (MODFLOW–NWT, ver. 2.0.0; Niswonger and others, 2011) solver because it allowed for the solution of nonlinear groundwater flow associated with the drying and rewetting of model cells in unconfined conditions without permanently deactivating those dry cells. The layers simulated in the CPIHM were thin in some areas and some cells of the model went dry under stressed conditions. The models associated with this report are available as a USGS data release (Traylor, 2023).

The CPIHM was run for three different time periods: a predevelopment period (steady state), a period representing the start and development of irrigation in the study area (the development period), and a forecast period representing possible future scenarios of pumping and changes in the groundwater (table 5). A list of processes simulated in the CPIHM and associated MF–OWHM packages and the process used to simulate those processes is provided in table 5 and 6.

Boundary Conditions

A combination of groundwater divides, surface-water features, and available input data extents were used to define the “active” domain and the boundary conditions simulated by the CPIHM around the CPNRD focus area. Simulated groundwater contours from the Northern High Plains groundwater-flow model (Peterson and others, 2016) were the principal source of information on the location of the western and southern hydrologic boundaries surrounding the CPNRD (fig. 7*B*). The western areal boundary of the study area was selected as the region extending north from central Frontier County through Brady, Nebr. (fig. 1*A*) to the South Loup River in southeastern Logan County about 10 miles upstream from South Loup River at Arnold, Nebr. (USGS streamgage 06781600, fig. 1*A*). Based on average decadal groundwater contours from Peterson and others (2016), groundwater flows into the study area across the northern and southern portions of the western boundary for this study, except for a region just north of the Platte River near Brady, Nebr., where the groundwater flows south into the Platte River, and the region in Frontier County where groundwater flows approximately southeast and creates a no-flow groundwater boundary (fig. 15 from Peterson and others, 2016; fig. 7*C*).

The South Loup River was chosen as the northern boundary of the CPIHM, west of the confluence of the Loup River (fig. 7*C*). The Loup River forms the northern boundary of the study area to its confluence with the Platte River in Platte County (fig. 7*C*). Hydrologically, the northern boundary that includes the South Loup and Loup Rivers is a mapped groundwater divide and creates a no-flow groundwater boundary (Peterson, 2009). Groundwater flows across much of the eastern boundary of the study area in Clay, York, and Polk Counties (fig. 7*C*). The northern and eastern boundaries are coincident with the boundaries from models in Peterson (2009) and Cooperative Hydrology Study (2017).

The southern boundary extended from the groundwater divide west of Deer Creek in Frontier County through central Gosper, Phelps, and Kearney Counties, then along the Big Sandy Creek in Clay County (fig. 7*C*). The southern boundary of the model approximately follows the groundwater divide created by a groundwater mound under the CNPPID canal system in central Gosper, Phelps, and Kearney Counties that is a result of persistent leakage recharge from the canals (fig. 7*C*). The southern boundary contains areas where groundwater flows east or southeast out of the study area or flows parallel to the model boundary and creates a no-flow groundwater boundary (fig. 7*C*). Vertical boundaries of the active domain of the CPIHM were the land surface as the upper boundary and top of the Pierre Shale as a no-flow lower boundary (HU 10 from Cannia and others, 2006; Peterson, 2009; Peterson and others, 2016).

Layering Scheme

The vertical discretization of the CPIHM, between the vertical boundaries (land surface and Pierre Shale), was defined by the HUs described in Cannia and others (2006) where present in the study area. The six HUs (HUs 1–6) present in the study area were combined into three hydrologically similar groups based on permeability, geologic age, and spatial relation to reduce the number of vertical layers that would need to be represented in the CPIHM (fig. 8). HUs 1 and 2 were combined into numerical model layer 1, HUs 3 and 4 were combined into numerical model layer 2, and HUs 5 and 6 were combined into numerical model layer 3 (fig. 8). Hydrologic connection remained between all three layers after grouping (figs. 6 and 8). Model layer 1 is the Quaternary alluvium and loess from HUs 1 and 2. Group 1 is present everywhere in the study area with an average thickness of 163 ft and a range from less than 10 ft in parts of the Platte River valley to greater than 500 ft in parts of Dawson and Custer counties (figs. 7*B*, 8). The alluvium and loess typically consisted of gravels, sands, and silts. Model layer 2 combined the lower Quaternary and upper Tertiary Silt identified in Cannia and others (2006) as HUs 3 and 4. There were a few areas in the central and eastern portion of the study area where these units were absent (Cannia and others, 2006). Group 2 is thicker toward the east with an average thickness of 57 ft and a range from less than 10 ft in the west and central areas to 300 ft in the eastern portion of the study area.

Model layer 3 is the Ogallala Formation identified in Cannia and others (2006) as HUs 5 and 6. Group 3 also incorporated airborne electromagnetic data from Cannia and others (2017) that were used to refine the aquifer base. The Ogallala Formation consists of sands, silts, and clays at various intervals. The Ogallala Formation is present in the western and central portions of the study area and thins eastward with an average thickness of 242 ft and ranges from less than 10 ft in the eastern portions to 500 ft in the western portions of the study area (figs. 7*B*, 8).

Spatial and Temporal Discretization

The CPIHM was spatially discretized into a grid of orthogonal blocks, called cells, horizontally and vertically. The orthogonal grid consisted of 163 rows and 327 columns with horizontal cell sides of 2,640 ft by 2,640 ft (0.5 mile by 0.5 mile or 160 acres) (table 5). The CPIHM was vertically discretized into three layers of varying spatial extents and thickness according to the hydrogeology and aquifer characteristics described in the "Study Area Description" and "Layering Scheme" sections of this report. The CPIHM includes 159,903 total cells (fig. 7*A*) where model layers 1, 2, and 3 include 30,788 active cells; 30,009 active cells; and 17,712 active cells, respectively. Based on the hydrostratigraphic data, layer 1 (Quaternary-age alluvial and loess deposits) was present, and therefore active, throughout the study area (fig. 7*A*). Layer 2 was active throughout most of the study area but was absent in some parts of the central and eastern model domain. The absence of layer 2 where layers 1 and 3 were present appeared as "holes" in the model grid and will be referred to as such throughout the report. Layer 3 was present in the west and central model domain and thinned out to the east (fig. 7*A*). MODFLOW–NWT cannot simulate discontinuous layers such as the absence of layer 2 at the "holes"; inactive cells are simulated as no-flow boundaries. Most of the layer 2 holes have layers 1 and 3 present and hydrologically connected. To simulate this hydrologic connection in the CPIHM, cells in the layer 2 holes were activated and given an artificial layer thickness of 5 ft with a hydraulic conductivity equal to the average of layers 1 and 3, and anisotropy was set to a 1:1 ratio to permit vertical flow in the artificial layer 2 (shown as "layer 2 holes" on fig. 7*B*).

The predevelopment model was run as a 500,000,000-day transient stress period to ensure that an approximate groundwater storage equilibrium was reached (table 6). The groundwater levels generated by the predevelopment model were used as the initial groundwater levels for the development model. The predevelopment model approximated average

Table 5. Central Platte Integrated Hydrologic Model spatial and physical characteristics.—Left

[FMP, Farm Process Package; GHB, General Head Boundary package; NWT, Newton Solver Package; RCH, Recharge Package; SFR, Streamflow Routing Package; UPW, Upstream weighting package; WEL, Well Package; --,not simulated because that feature was not present in the model]

Model name	Software	Cell size (feet)	Active cell count	Layers	Evapotranspiration from precipitation	Surface runoff	Groundwater recharge
Predevelopment	MODFLOW-OWHM 2.0.1	2,640	78,509	3	FMP	FMP	FMP
Development	MODFLOW-OWHM 2.0.1	2,640	78,509	3	FMP	FMP	FMP, RCH
Forecast	MODFLOW-OWHM 2.0.1	2,640	78,509	3	FMP	FMP	FMP, RCH

steady-state groundwater conditions prior to the construction of canals for surface-water irrigation and wells for groundwater irrigation.

The CPIHM development period was temporally discretized into 610 stress periods to simulate transient conditions from May 1, 1895, to December 31, 2016 (table 6). The transient simulation start date was selected as May 1, 1895, because it was coincident with the first documented surface-water diversions for irrigation in the CPIHM active domain. Also, two previous groundwater-flow models that included the CPIHM domain began transient simulations in 1895 to account for the onset of surface-water diversions for irrigation (Peterson, 2009; Peterson and others, 2016). The first 170 stress periods of the development model were discretized into periods of time that reflected the typical irrigation season from May 1 to September 30 and nonirrigation season from October 1 to April 30, with 2-week time steps and were meant to provide a reasonable starting point for the period of interest (April 1, 1982, to December 31, 2016; table 6). Stress periods 171 to 610, from May 1, 1980, to December 31, 2016, were discretized into monthly time periods to improve the temporal resolution of outputs generated for the period of interest, after April 1, 1982, again with 2-week time steps (table 6). Temporal resolution was increased after May 1980 to monthly stress periods to meet the objectives of the study and to facilitate comparison of simulated groundwater levels from different months within an irrigation season with the CPNRD's baseline groundwater levels from the spring of 1982. The CPIHM scenario period was temporally discretized into 396 stress periods to simulate transient conditions from

Table 6. Central Platte Integrated Hydrologic Model temporal characteristics.

[na, not available]

Model name	Simulation type	Stress period number	Start date	End date	Stress-period length (days)	Number of time steps	Notes
Predevelopment	Transient[1]	1	na	4/30/1895	500,000,000	1	Quasi-steady state model that simulates conditions prior to surface-water and groundwater irrigation development
Development	Transient	Even numbers from 1 to 169	5/1/1895	4/30/1980	153	11	Transient model that simulated conditions after the construction of the first irrigation development in the study area.
		Odd numbers from 2 to 170			213	15	
		171–610	5/1/1980	12/31/2016	Monthly	2	
Forecast	Transient	611–1,006	1/1/2017	12/31/2049	Monthly	2	Transient model that simulates potential future conditions

Table 5. Central Platte Integrated Hydrologic Model spatial and physical characteristics.—Right

[FMP, Farm Process Package; GHB, General Head Boundary package; NWT, Newton Solver Package; RCH, Recharge Package; SFR, Streamflow Routing Package; UPW, Upstream weighting package; WEL, Well Package; --,not simulated because that feature was not present in the model]

Surface-water routing and canal diversions	Well pumping	Groundwater Evapo-transpiration	Cross-boundary groundwater-flow	Surface-water deliveries	Groundwater-flow equation solver	Aquifer properties	Lake-groundwater interaction
SFR	none	FMP	GHB	FMP	NWT	UPW	--
SFR	FMP (irrigation), WEL (high capacity production)	FMP	GHB	FMP	NWT	UPW	GHB
SFR	FMP (irrigation), WEL (high capacity production)	FMP	GHB	FMP	NWT	UPW	GHB

January 1, 2017, to December 31, 2049 (table 6). Stress periods were discretized into monthly time periods with 2-week time steps to maintain the temporal resolution with the development period model (table 6).

Landscape Inputs and Configuration (Farm Process)

Landscape inputs are necessary for simulation of landscape processes within the MF–OWHM, as outlined in the “MODFLOW–One-Water Hydrologic Model Theory and Approach” section of this report (fig. 2). Landscape properties specified within the FMP for this study included land surface altitude, soil types, ET_{ref}, precipitation, land use and crop types, Kc, irrigation flags, root depths and pressures, fractions of transpiration (FTRs), fractions of evaporation from irrigation (FEI), fractions of inefficient losses to surface water from precipitation (FIESWP), and fractions of inefficient losses to surface water from irrigation (FIESWI). Surface-water supply sources and routing, the irrigation supply well information, and the water accounting units were specified within the FMP. The water accounting units are referred to hereafter as “water-balance subregions” (WBSs) (Hanson and others, 2014a; Boyce and others, 2020). The WBSs were delineated for the CPIHM based on subregional watersheds, surface-water irrigation zones, groundwater irrigation zones, CPNRD GWMAs, and other natural resource district boundaries. In total, there are 212 WBSs in the CPIHM (Traylor, 2023). The 212 WBSs were combined into 24 “supergroup” zones to facilitate analysis of the water budgets for areas of interest within the CPIHM (fig. 9). The 24 GWMAs within the CPNRD were used to define the supergroups (fig. 9). Hereafter, the term “GWMA” will be used to reference results pertaining to the supergroups.

The land surface altitude dataset was created using a combination of 1- and 2-meter (m) light detection and ranging (lidar) digital elevation model datasets from the Nebraska Department of Natural Resources (2018) and a 10-m digital elevation model dataset from the U.S. Geological Survey (2018) and resampled to CPIHM model cell size. The precipitation (PPT) and ET_{ref} datasets used in the CPIHM were developed for each cell and stress period, generated from interpolation of climate data at as many as 77 weather stations in the COHYST area (Cooperative Hydrology Study (2017, p. 5–9), then clipped to the study area. The PPT and ET_{ref} datasets were constructed using the same weather stations and methods described in Cooperative Hydrology Study (2017), which included data from 1950 to 2013. Outside of the 1950 to 2013 period, climate datasets were obtained from the High Plains Regional Climate Center (2018) for each weather station included in the Cooperative Hydrology Study (2017) (fig. 10*A*, *B*).

The Cooperative Hydrology Study (2017) land-use dataset specified multiple crop types per model cell in acres, and these values were converted to fractions of model cell area for use in the CPIHM (Traylor, 2023). For example, if crop type “groundwater-irrigated corn” in a specific cell was 64 acres, then the fraction used in the CPIHM cell dataset was 0.4 (for 160-acre cells). The distribution of land uses for 1982 and 2005 is shown in figure 1.1 (Dappen and others, 2007; also see figure 4-D-1 from Cooperative Hydrology Study, 2017). Soil types were grouped into sand, sandy loam, and silty clay based on classifications from a geographic information system soil dataset in University of Nebraska-Lincoln (2018) (fig. 7*B*). The land-use datasets were derived from those used in Cooperative Hydrology Study (2017) and included Cooperative Hydrology Study (2017) irrigated and dryland crop types for 1950 to 2013 partitioned into commingled irrigated, dryland uses, groundwater irrigated cropland, and surface-water irrigated cropland (table 7). The Cooperative Hydrology Study (2017) crop type “other” was then split into urban, roads, open water, and riparian forest and wetlands using the National Land Cover Database datasets to identify locations of those separate land uses (table 7) (Yang and

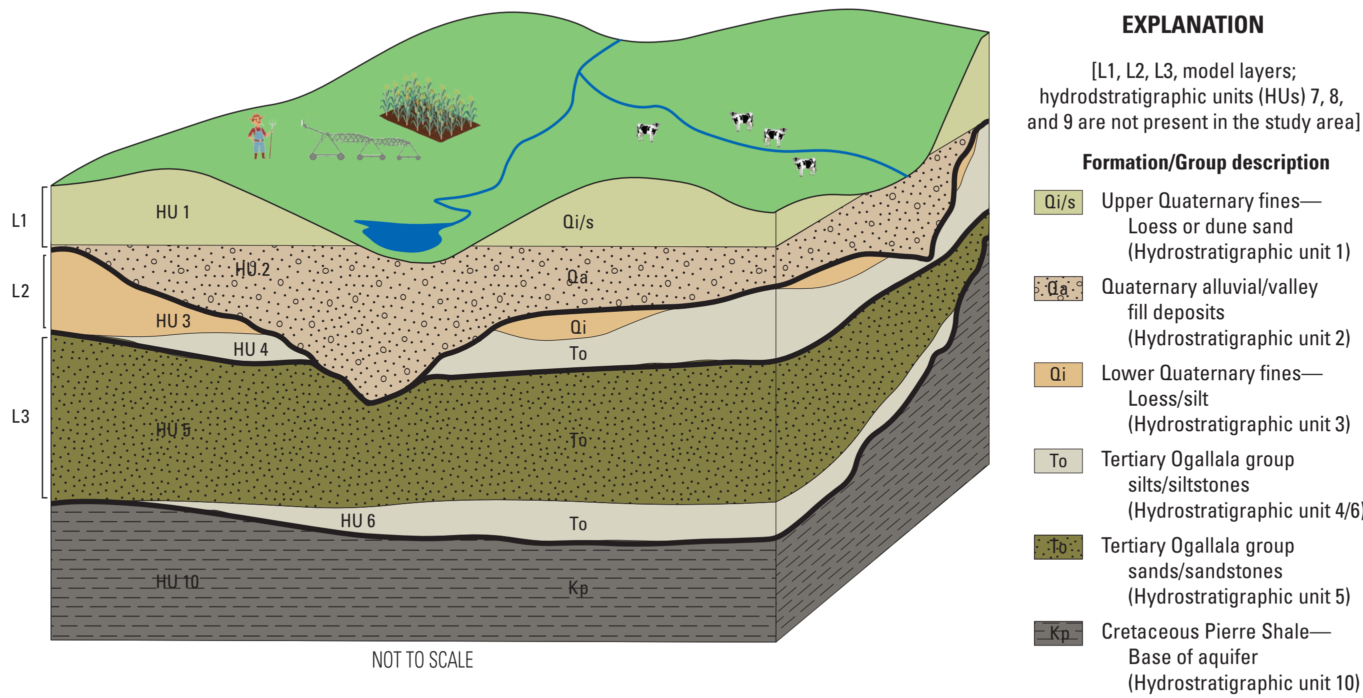

Figure 8. Conceptual diagram showing the hydrostratigraphic units from Cannia and others (2006) that were used to create the layering scheme for the Central Platte Integrated Hydrologic Model.

others, 2018). The 1950 land-use dataset was used for 1895 to 1950, which was an acceptable approximation based on Hiller and others (2009), and the 2013 dataset was repeated from 2014 to 2016.

The Kc values were specified for each crop type and stress period and interpolated and scaled to the various stress period lengths. When possible, daily Kc values were calculated following the methods used in the Cooperative Hydrology Study (2017). Additionally, the out-of-season value for cropland used in Cooperative Hydrology Study (2017) was used to represent fallow land and open water during the winter season, which was specified as November 15 to March 15. Monthly riparian forest Kc values from Hall and Rus (2013) were used for forest values. Published Kc values, planting dates, and crop growth period lengths were taken for all other land-use types from Allen and others (1998). Daily Kc values were calculated for all land uses by interpolating between the planting dates and growth stage dates. Monthly Kc values were then obtained by averaging the daily rates for the given month. Additional sources for Kc values from the Nebraska Agricultural Water Management Network (2018) were compared to the previously mentioned monthly Kc values and, where possible, were adjusted as needed to align with published values. Kc values assigned to each land use and stress period are available in the model archive associated with this report (Traylor, 2023)

Each land use was flagged for irrigation or no irrigation (dryland) for each stress period. Additionally, this "irrigation flag" included the irrigation efficiency type for the land use referenced from the separate "on-farm efficiency" (OFE) input table that specifies the irrigation efficiency as a fraction of the irrigation water pumped that is used by the crops (Boyce and others, 2020). Irrigation flags were designated for each commingled, groundwater, and surface-water crop type for potential irrigation stress periods (that is, May through September for irrigated crop types except winter wheat, which was flagged for potential irrigation from March to October). Irrigation efficiencies were specified in the development period model as 0.7, 0.55, and 0.8 for commingled, surface-water irrigated, and groundwater irrigated crops in the bi-annual irrigation stress periods from 1895 to 1980, respectively; and 0.72, 0.65, and 0.9 for commingled, surface-water irrigated, and groundwater irrigated crops in the monthly irrigation stress periods from May 1980 to December 2016, respectively, based on values from Irmak and others (2011).

Fractions of transpiration (FTRs) and FEI were assigned for each crop type. FTRs and FEI for common crop types like corn were derived from models that predicted corn transpiration and ET (Kimball and others, 2016). FTRs and FEI for winter wheat were derived from a study in China (Kang and others, 2003) and Nebraska (Irmak and others, 2016). Root depths for each land use ranged from 1 to 15 ft and were

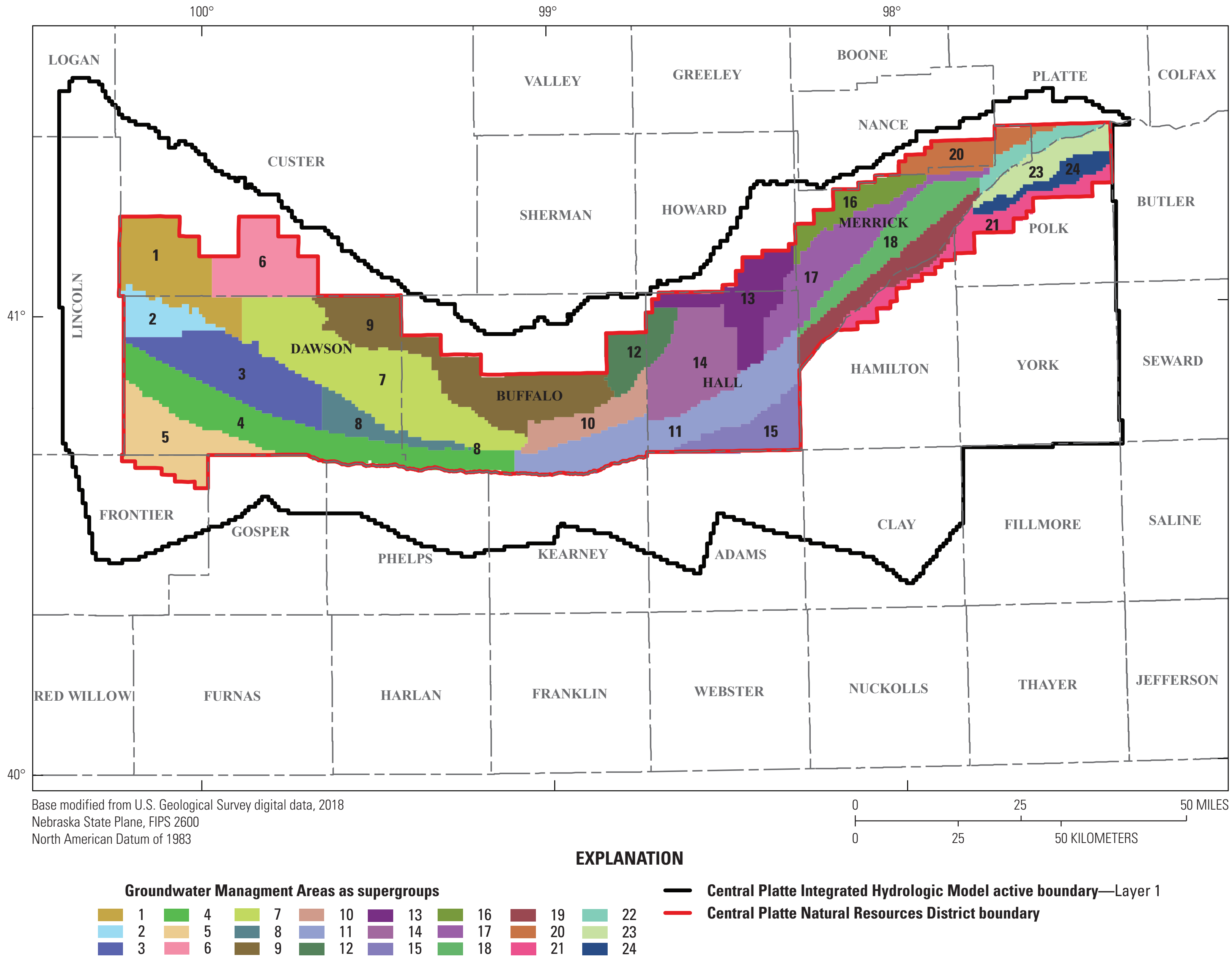

Figure 9. Supergroups (Central Platte Natural Resource District's 24 Groundwater Management Areas) defined for the Central Platte Integrated Hydrologic Model.

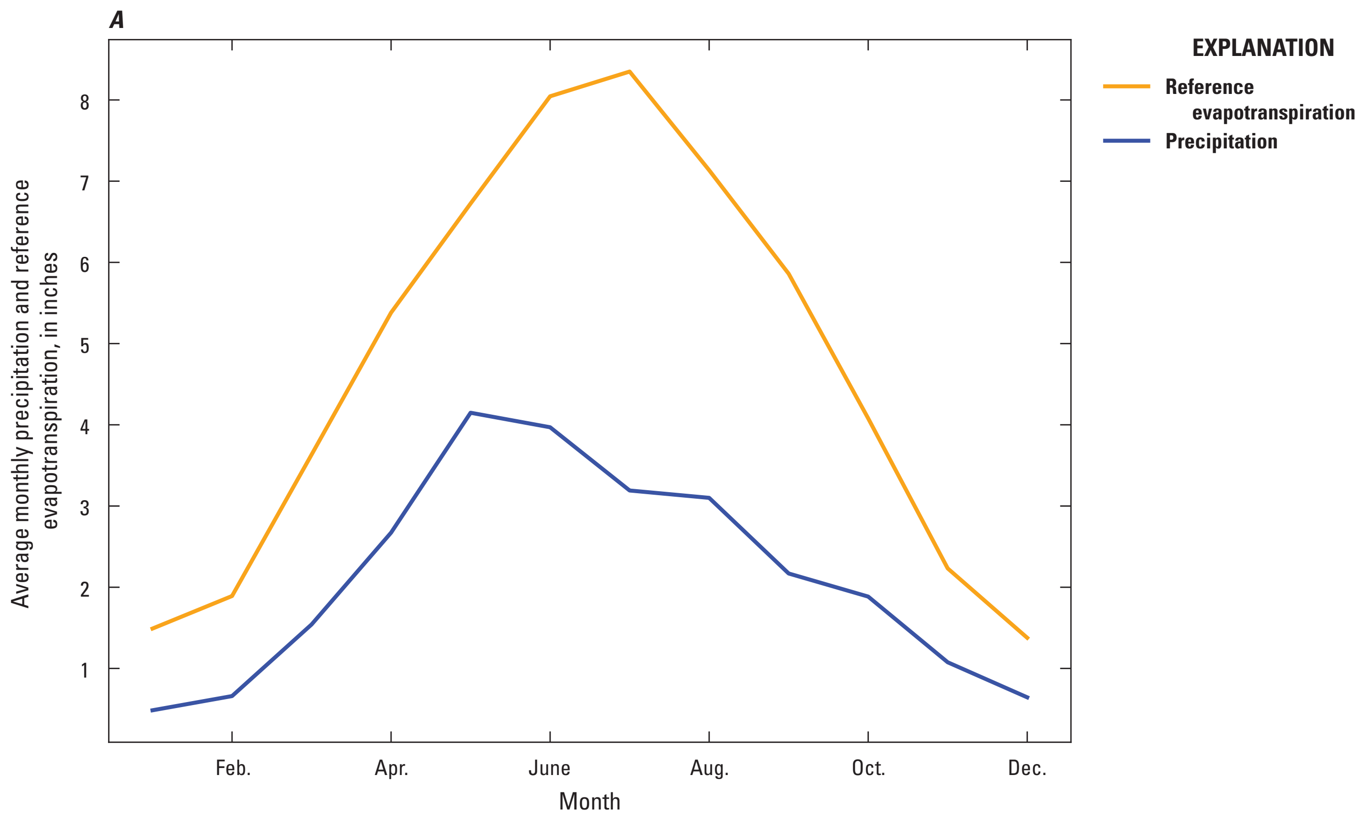

Figure 10. Plot of average precipitation and potential evapotranspiration for the Central Platte Integrated Hydrologic Model. *A*, Monthly post May 1980 model development period. *B*, Annual development period (1895 to 2016).

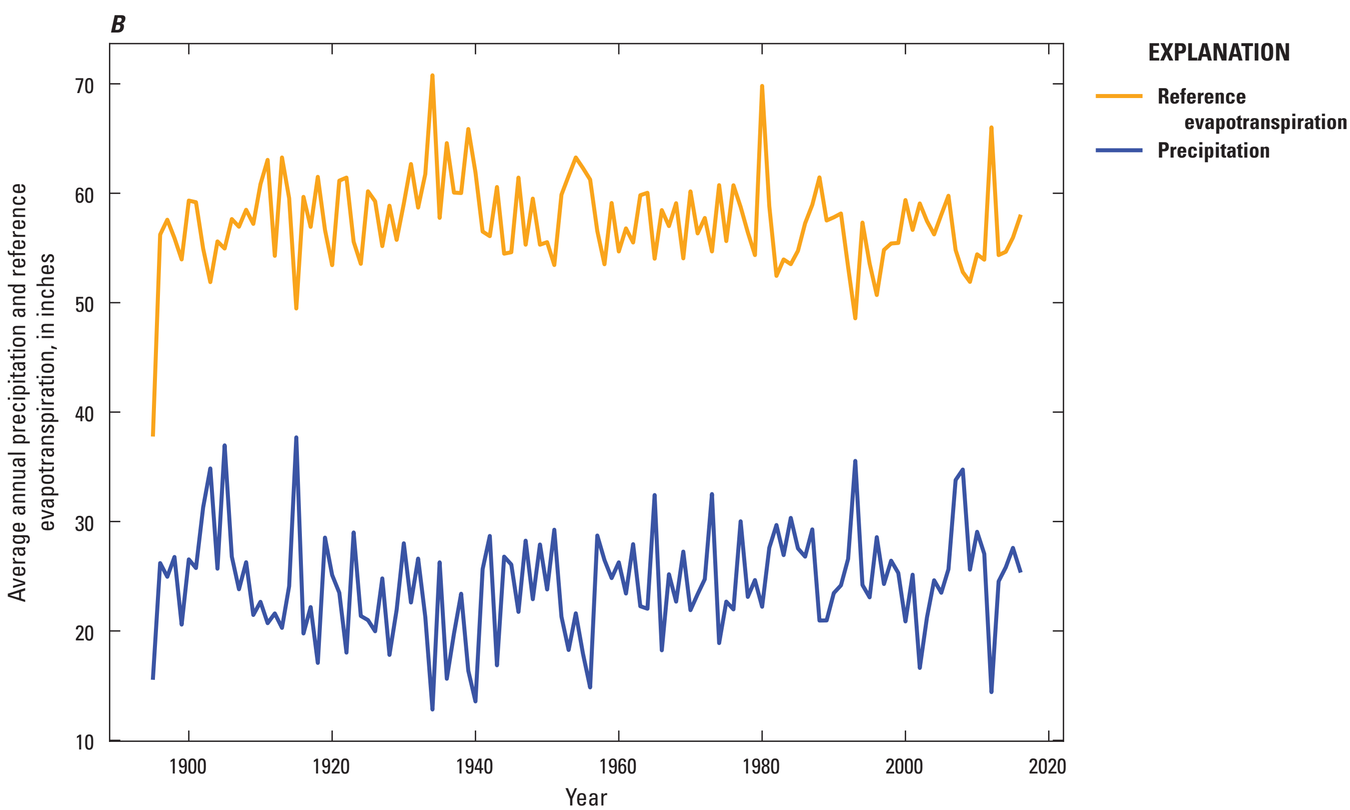

Figure 10.—Continued

Table 7. Land uses as crop types with crop numbers, crop short name, crop full name, and the source of water to meet water demand for each crop used in the Central Platte Integrated Hydrologic Model.

Crop number	Crop short name	Crop full name	Source to meet water demand
1	co_alfalfa	Commingled alfalfa	Surface water via canal deliveries and groundwater via irrigation wells
2	co_corn	Commingled corn	Surface water via canal deliveries and groundwater via irrigation wells
3	co_fallow	Commingled fallow	Surface water via canal deliveries and groundwater via irrigation wells
4	co_pasture	Commingled pasture	Surface water via canal deliveries and groundwater via irrigation wells
5	co_sorghum	Commingled sorghum	Surface water via canal deliveries and groundwater via irrigation wells
6	co_soybeans	Commingled soybeans	Surface water via canal deliveries and groundwater via irrigation wells
7	co_winterwheat	Commingled winter-wheat	Surface water via canal deliveries and groundwater via irrigation wells
8	dry_alfalfa	Dryland alfalfa	Precipitation and groundwater if roots reach the water table
9	dry_corn	Dryland corn	Precipitation and groundwater if roots reach the water table
10	dry_fallow	Dryland fallow	Precipitation and groundwater if roots reach the water table
11	dry_pasture	Dryland pasture	Precipitation and groundwater if roots reach the water table
12	dry_sorghum	Dryland sorghum	Precipitation and groundwater if roots reach the water table
13	dry_soybeans	Dryland soybeans	Precipitation and groundwater if roots reach the water table
14	dry_winterwheat	Dryland winterwheat	Precipitation and groundwater if roots reach the water table
15	dry_openwater	Dryland open water	Precipitation and groundwater if roots reach the water table
16	dry_ripforestwet	Dryland riparian forest and wetlands	Precipitation and groundwater if roots reach the water table
17	dry_urban	Dryland urban	Precipitation and groundwater if roots reach the water table
18	dry_roads	Dryland roads	Precipitation and groundwater if roots reach the water table
19	gw_alfalfa	Groundwater alfalfa	Irrigation wells
20	gw_corn	Groundwater corn	Irrigation wells
21	gw_fallow	Groundwater fallow	Irrigation wells
22	gw_pasture	Groundwater pasture	Irrigation wells
23	gw_sorghum	Groundwater sorghum	Irrigation wells
24	gw_soybeans	Groundwater soybeans	Irrigation wells
25	gw_winterwheat	Groundwater winter-wheat	Irrigation wells
26	sw_alfalfa	Surface water alfalfa	Surface water via canal deliveries
27	sw_corn	Surface water corn	Surface water via canal deliveries
28	sw_fallow	Surface water fallow	Surface water via canal deliveries
29	sw_pasture	Surface water pasture	Surface water via canal deliveries
30	sw_sorghum	Surface water sorghum	Surface water via canal deliveries
31	sw_soybeans	Surface water soybeans	Surface water via canal deliveries
32	sw_winterwheat	Surface water winter-wheat	Surface water via canal deliveries

obtained from Irmak and Rudnick (2014) and U.S. Department of Agriculture (2016). Root pressure values as depths were obtained from table 7 in Hanson and others (2014b). The FIESWP and FIESWI values were chosen based on values of similar parameters within Cooperative Hydrology Study (2017). The runoff calculated by FIESWP or FIESWI was routed to a nearby stream cell specified in the semirouted returns feature of FMP.

The development model simulated the proliferation of groundwater irrigation wells in the study area. The irrigation wells that supply the CIR for each groundwater-irrigated crop were specified in the “farm wells” block within the FMP. Each irrigation well was assigned a pumping location in the model grid (layer, row, and column designation; fig. 11) and a WBS to which the well may supply water in addition to a maximum pumping rate. Farm wells that intersected stream cells were removed to improve model stability. Irrigation well start and end dates were based on construction dates and decommission dates in the well database (Nebraska Department of Natural Resources, 2017). Surface-water deliveries from canal diversions were specified as an available source of water for 36 WBSs (156–189, 211, and 212) because they were coincident with the surface-water irrigated acres. The amount of surface deliveries available each stress period depended on the diversion amount from the streamflow routing network to the canals (Nebraska Department of Natural Resources, 2019).

MODFLOW Inputs and Configuration

MF–OWHM utilization of the Newton solver for the CPIHM required the use of the Upstream Weighting package (Niswonger and others, 2011), including hydraulic properties such as Kh, anisotropy, Sy, and specific storage (Ss) for each model layer. The precalibration initial values for the hydraulic properties are described in the “Hydrogeology and Groundwater” section. In an unconfined system, Sy is a more influential property than Ss because it quantifies 3 or 4 orders of magnitude more water. Further, assignment of a single Ss value across all active cells for each layer was a technique taken from the Northern High Plains aquifer model calibration from Peterson and others (2016). The aquifer storage (Ss and Sy), Kh, and anisotropy values were adjusted during the calibration process.

The General-Head Boundary package (GHB; Harbaugh and others, 2000) simulated inflow and outflow of groundwater across boundaries of the active model (640 cells) and the interaction of Johnson Lake and Elwood Reservoir with the groundwater-flow system (31 cells; fig. 1*A*; table 5). The GHB is a head-dependent flux boundary that requires a specified hydraulic head and conductance for each GHB designated cell. The flux between a GHB and adjacent cell is the product of the GHB cell conductance and the difference in hydraulic heads between the GHB cell and the adjacent cell. The conceptual model of groundwater flow (in the “Boundary Conditions” section of the report) indicated that there was lateral groundwater flow into the model domain along some portions of the western model boundary and lateral outflow along some southern and eastern portions of the model based on simulated groundwater-level contours from Peterson and others (2016) (fig. 7*B*). The GHB cells were assigned for these inflow and outflow edges of the model (fig. 12). The hydraulic head values were determined using a combination of rasterized decadal average groundwater levels from Peterson and others (2016) and interpolated heads from measured groundwater-level data at observation wells coincident or near boundary cells. Initial GHB heads were extracted from the rasterized grids of the decadal groundwater-level contours from Peterson and others (2016) and checked against measured groundwater levels when available (U.S. Geological Survey, 2017). For differences greater than 5 ft, GHB head values were specified by extracting values from raster grids interpolated from the measured data near boundary cells. Hydraulic conductance along the boundaries were estimated based on local aquifer properties and layer thicknesses (Peterson, 2009; Houston and others, 2013). Lake and reservoir stage data were used to specify the GHB heads for both reservoirs. Lake GHB conductance was manually adjusted such that the simulated groundwater levels below the lakes were similar to the measured groundwater levels from a nearby observation well (USGS 404046099504501) located on the southern shore of Johnson Lake (U.S. Geological Survey, 2017). Because of the proximity of Elwood Reservoir to Johnson Lake, the GHB conductance used for Elwood Reservoir was the same as that defined for Johnson Lake.

The Streamflow Routing package (SFR; Niswonger and Prudic, 2005) simulated the flow and routing of surface water in streams and canals and their interaction with the landscape and groundwater-flow system within the study area and along the northern boundary. The SFR is a head-dependent flux boundary that interacts with the groundwater-flow system of each designated SFR cell based on the relation among the stage of the stream, streambed conductance, and the hydraulic head of the aquifer. Flow of water between the SFR and the groundwater-flow system is dictated by the conductance, which is the product of the hydraulic conductivity of the streambed and the area of the stream channel, divided by the streambed thickness. The SFR network included 4,318 cells, or reaches, and 219 segments, which are a group of reaches with uniform hydraulic properties, to represent major streams such as the Platte River, South Loup River, Middle Loup River (not shown), Loup River, Wood River, Prairie Creek, Big Blue River, and the perennial reaches of their perennial tributaries (fig. 12). The upper perennial reaches of the tributaries included in the SFR network were determined based on density of streams using geographic information system techniques and assessment of satellite imagery to identify segments of streams that interact with the groundwater based on identification of a wet channel and identification of vegetation along the stream that is assumed to be supported by groundwater. Flows and stage are calculated with the SFR as the difference among inflows from upstream reaches; runoff; tributaries; groundwater discharge to the reach as base flow; and outflows

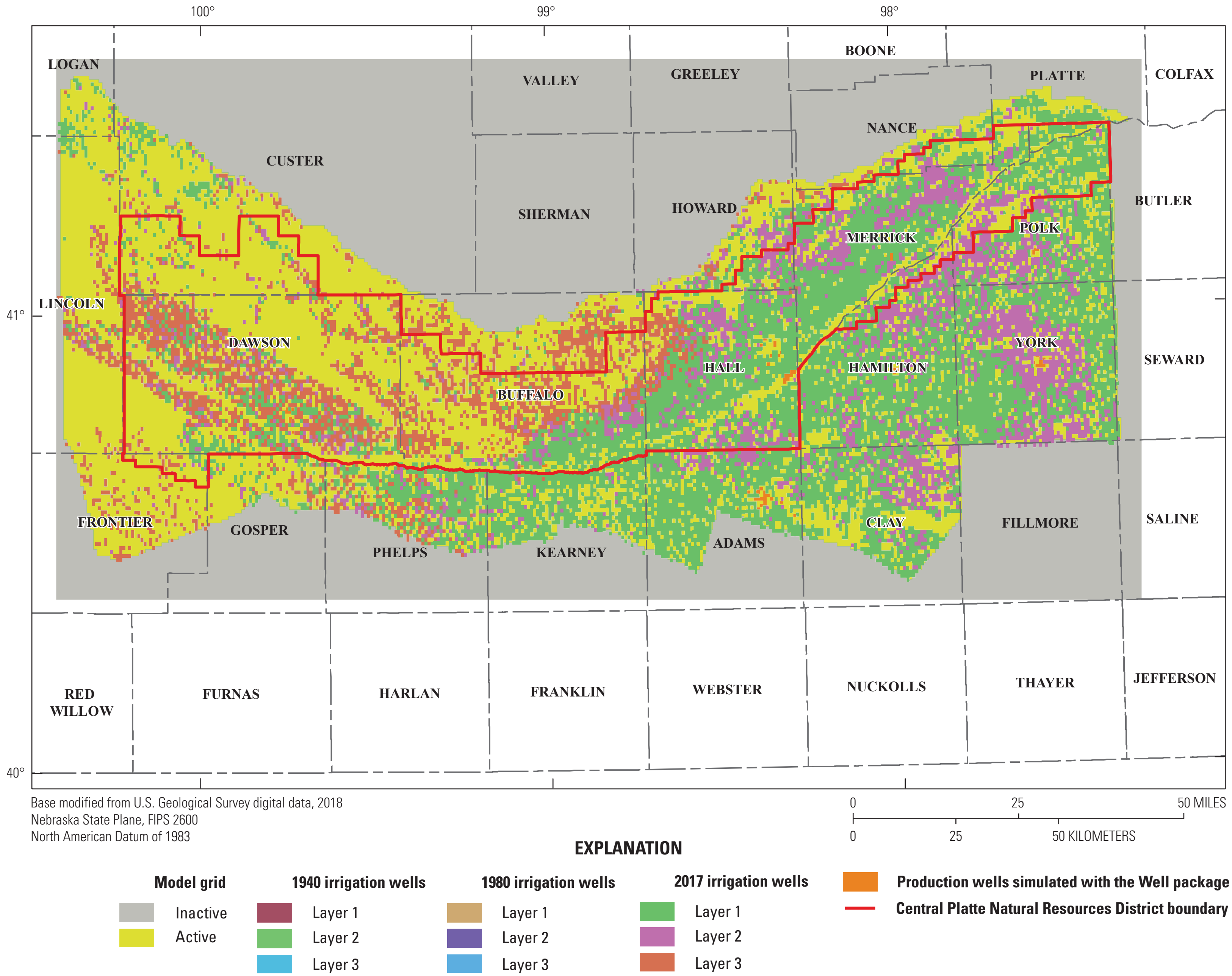

Figure 11. Irrigation well locations in the development Central Platte Integrated Hydrologic Model by layer prior to January 1, 1940; January 1, 1980; and January 1, 2017; production wells as cells simulated in the model (this is a layered .pdf; download at https://doi.org/10.3133/sir20235024).

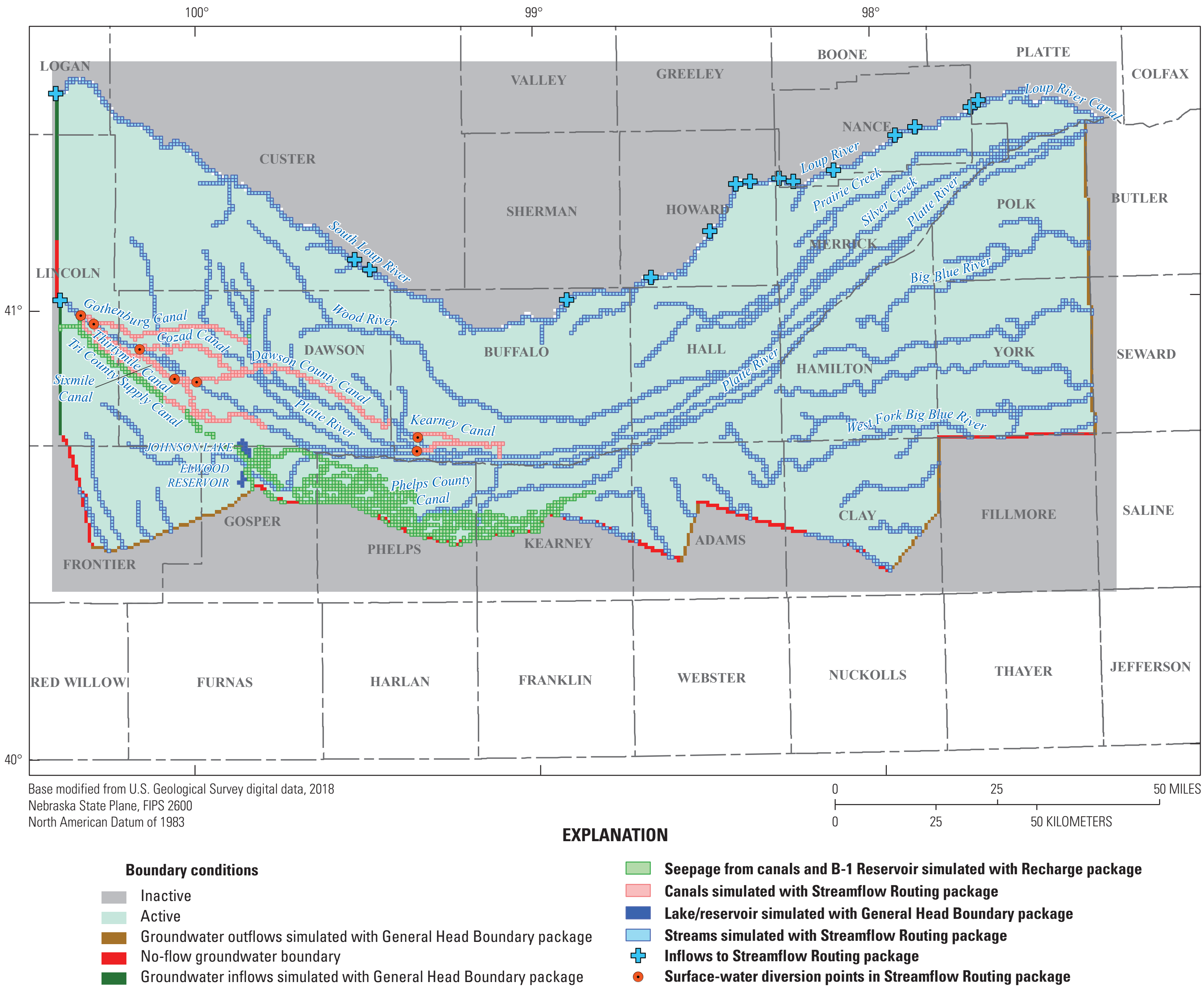

Figure 12. Boundary conditions of Central Platte Integrated Hydrologic Model.

to downstream reaches, canal diversions, and leakage into the aquifer. The SFR simulated stream depth using Manning's equation and assumed a rectangular channel (Niswonger and Prudic, 2005). Therefore, physical stream properties such as vertical hydraulic conductivity of the streambed, stream width, streambed roughness coefficient, and streambed thickness were specified for each segment. The Gage package (Merritt and Konikow, 2000) was used to extract time series of simulated streamflow for some SFR reaches for calibration to measured flow data.

Canals within the CPNRD focus area, and their associated diversions from the Platte River, were simulated with the SFR (fig. 12). The SFR simulated the routing of diverted streamflow into Cozad, Dawson, Gothenburg, Kearney, Orchard-Alfalfa, Sixmile, and Thirtymile canals (Nebraska Department of Natural Resources, 2019). Stress period averaged canal diversion values were created from daily diversions data available from the Nebraska Department of Natural Resources (2019) and were input to the SFR (table 1.1). Note that the CNPPID canal system located south of the Platte River was not simulated with the SFR. The leakage of diverted water through the canal beds of the CNPPID canals was simulated with the Recharge package (Harbaugh and others, 2000), wherein these recharge rates were estimated using change in groundwater-level values from measured groundwater-level hydrographs near the canals and mean Sy values of the aquifer. Additionally, the Recharge package was used to simulate the leakage from B-1 Reservoir in Dawson County (fig. 12); recharge rates were calculated based on the difference between reservoir inflow and evaporation data to estimate leakage through the lakebed of about 85 percent of inflows (Nebraska Department of Natural Resources, 2019).

Groundwater withdrawals for municipal supply (fig. 11) were simulated using the Well package (Harbaugh and others, 2000). The municipal well spatial and temporal information were obtained from the NeDNR Registered Well Database (Nebraska Department of Natural Resources, 2018). Well depths were used to determine the model layer from which the wells were pumped, and construction dates were used to determine the first active stress period of each well. Withdrawal rates were estimated for wells in communities or time periods without withdrawal data using withdrawal data from municipalities with similar populations. A total of 198 municipal wells were simulated (fig. 11). Municipal wells are hereafter referred to as production wells.

Calibration Approach

This section of the report describes the two-phase approach to calibration of the CPIHM. The combined predevelopment and development period transient models were used together to calibrate the CPIHM, and the calibrated inputs were then used in the forecast model. The CPIHM was linked to the Parameter Estimation (PEST) software (Doherty, 2005), which uses numerical inversion methods to adjust select model inputs, known as "calibration parameters," to improve the fit between measured data, known as "calibration targets," and their simulated equivalent outputs to constrain the range of reasonable parameter values. A two-phased calibration was used, which involved manual adjustment and fixing of some calibration parameters followed by the automated calibration, discussed in more detail in the "Two-Phase Calibration Approach" section of this report. This two-phase approach to calibration was also employed for the numerical MF–OWHM developed in Hanson and others (2018).

The CPIHM was calibrated to minimize the PEST objective function (Φ), which is the sum of squared weighted residuals between calibration targets and simulated equivalent outputs (Doherty, 2005), calculated using equation 2:

$$\Phi = \sum_{i=0}^{n} (w_i r_i)^2 \tag{2}$$

where

- n is the number of calibration targets,
- w is the weight applied to the calibration targets, and
- r is residual, as the difference between time and space equivalent calibration targets and simulated values.

In a normal PEST run, PEST requires one model run per adjustable parameter to determine the sensitivity of that parameter to the simulated model outputs equivalent to each observation. The Jacobian matrix (a matrix of parameter sensitivities to observations as derivatives) is recalculated for each iteration of the calibration process (Doherty, 2015). The CPIHM calibration was facilitated by the employment of the singular value decomposition-assist (SVDA) feature of PEST, where PEST uses the information in the first Jacobian matrix to recombine the adjustable parameters into grouped "superparameters." Fifty superparameters were established based on the most sensitive parameters in the Jacobian matrix. After the establishment of superparameters, only the most sensitive superparameters are estimated, and the less sensitive superparameters can remain fixed. In future iterations, PEST only requires one model run per adjustable superparameter to calculate a new Jacobian matrix. Therefore, SVDA facilitated the calibration process by reducing the number of parameters that PEST can adjust and thus reducing the number of model runs required for the calculation of the Jacobian matrix in subsequent PEST iterations (Doherty and Hunt, 2010). The automated PEST calibration was further facilitated by a parallel computing version of PEST called BeoPEST (Schreuder, 2009; Doherty and others, 2010a) and deployed on a cluster of machines by way of the open source, high throughput, workload management software HTCondor (Condor Team, 2012).

Calibration Parameters

A total of 740 parameters were specified for the predevelopment and development CPIHM within six parameter groups, and 435 of those parameters were adjustable during the automated calibration process (table 8). Parameterization (the specification of model inputs as calibration variables, or parameters that PEST may adjust) was based on prior data availability, local knowledge, and uncertainty in their values. In environmental modeling, there is usually a lack of available data to quantify model inputs for every model cell and stress period. The parameterization scheme (that is, the structure and number of parameters used to represent the unknown natural-system input values of a model) is an important aspect of modeling because it can have a substantial effect on the ability of a model to gain information from the calibration dataset and appropriately simulate the natural system (Fienen and others, 2010). The parameter value and its imposed lower and upper bounds represent the reasonable range of values or the precalibration (prior) uncertainty of the model input, based on prior knowledge of the system (Fienen and others, 2010). Excluding a model input from the adjustable parameter set, either as a "fixed" parameter or excluding it entirely from the PEST framework, equates to "hard coding" the model input and is similar to saying that model input is known with 100-percent certainty, which is highly unlikely in complex environmental models. However, the model may be insensitive to some model inputs, which cause far smaller effects on model outputs than other inputs. Although some parameters may be insensitive to the calibration process because they may not gain information from the calibration dataset, they can still cause changes in scenario results, which is an important consideration when specifying parameters. Additionally, some model inputs can be well constrained (less uncertainty) because they may have ample data to specify an acceptable value that produces acceptable model results, whereas others may be poorly constrained (more uncertainty) and require more freedom during calibration to find optimal values.

Calibration parameters were combined into groups defined as aquifer storage properties (aqprops), streamflow routing properties (sfrprops), farm or landscape properties (farmprops), pilot points for Kh (pilotpts), climate properties (climprops), and pilot points for aquifer anisotropy (apilotpts; table 8). As will be described in the "Two-Phase Calibration Approach" section, certain parameters were fixed to improve model stability, prevent spurious parameter values, and better simulate ET. After several calibration attempts, 305 of the 740 parameters were converted to nonadjustable or "fixed" parameters within the PEST framework so the final calibration used 435 adjustable parameters. The groups *farmprops*, *aqprops*, and *climprops* were all fixed for the final calibration, whereas the calibration treated the *sfrprops*, *pilotpts*, and *apilotpts* as adjustable.

Fixed Parameters for Final Calibration

The 305 parameters in the *farmprops*, *aqprops*, and *climprops* groups were fixed for the final calibration to combat overfitting, improve model stability, and improve the efficacy of the simulated water-budget results with the conceptual model water budget. The aquifer storage properties (*aqprops*) group of parameters included six fixed parameters for aquifer Sy and Ss values. Sy was parameterized with one multiplier for each layer and Ss values were specified as a single value for each layer. Initial Sy values were interpolated from test hole data in Houston and others (2013) (table 1) and were like values used in the COHYST model (Peterson, 2009). The three Ss parameters were fixed using literature values (Domenico and Schwartz, 1990) during the initial hand-calibration. Initial

Table 8. Description of parameters by group that includes count and whether adjustable or fixed during automated calibration.

[Ss, specific storage; Sy, specific yield; WBS, water-balance subregion; FTR, fraction of transpiration; FEI, fraction of evaporation from irrigation; OFE, on-farm efficiency; Kh, horizontal hydraulic conductivity; ET, evapotranspiration]

Parameter group	Parameter group name in model	Parameters in group	Parameter count	Adjustable or fixed during automated calibration
Aquifer storage properties	aqprops	Ss and Sy multipliers for each layer	6	Fixed
Streamflow routing properties	sfrprops	Vertical hydraulic conductivity of the streambed	11	Adjustable
Farm or landscape properties	farmprops	Irrigation pumpage scale factors for each WBS, irrigation and precipitation runoff fractions, FTR and FEI scale factors, root depths, OFEs	273	Fixed
Pilot points for Kh	pilotpts	Pilot points of horizontal hydraulic conductivity	212	Adjustable
Climate properties	climprops	Reference ET scale factors	15	Fixed
Pilot points for aquifer anisotropy	apilotpts	Pilot points and aquifer anisotropy	212	Adjustable

precalibration Ss values for model layers 1, 2, and 3 were at 2.4e-4, 9.4e-5, and 2.0e-4, respectively. The water-table layer, layer 1, used Sy to calculate storage, and layers 2 and 3, which were saturated for every stress period, used the Ss term. Lower and upper bounds for Sy multipliers were specified according to the range of values estimated from test hole data by Houston and others (2013; table 1).

The farm or landscape properties (*farmprops*) group of parameters included 273 fixed parameters for irrigation well maximum capacity scale factors, FIESWP, FIESWI, FTR, FEI, root depths, and on-farm efficiencies (table 1.2). A total of 170 parameters were defined as irrigation well maximum-capacity scale factors, which adjust the pumping capacity of the wells, for each WBS that had a designated supply from irrigation wells. The remaining 42 of the 212 WBSs were supplied irrigation by surface-water deliveries. The maximum pumping capacity was specified based on values of well yield reported in well construction logs (Nebraska Department of Natural Resources, 2018). Well yield values recorded in the logs typically represent the results of an initial well test completed immediately after construction and reported by the drillers; these values are often rounded numbers and contain some uncertainty; however, they were relatively insensitive parameters during preliminary calibration runs (table 1.3). Therefore, the well capacity scale factors were set as adjustable parameters for preliminary calibration runs but were later fixed at their initial scale factor of 1.0 for the final calibration.

The 18 FIESWI parameters, one for each irrigated crop type, were fixed for the final calibration. These parameters controlled the fraction of runoff of applied irrigation water that does not infiltrate but runs off to streams. The initial values were set between 0.001 and 0.01 because in Nebraska it is illegal to allow irrigation water pumped to run off the field (Nebraska Legislature, 2014). The 32 FIESWP parameters, one for each crop type, were fixed parameters for the final calibration. The FIESWP parameters partitioned available precipitation into runoff to streams or deep percolation past the root zone that became recharge to the water table. Initial values were set at 0.4 for most crops, like fractions of runoff in Cooperative Hydrology Study (2017), with lower and upper bounds of 0.01 and 1.0. The open water crop type land use that represents the portion of a model cell covered by open water from a stream or lake was specified an initial FIESWP value of 0.999 because precipitation that falls on this portion of the cell contributes to streamflow immediately. Similarly, the dryland urban and dryland roads crop types were specified an initial FIESWP value of 0.99 because their impervious surfaces promote runoff rather than recharge. Conversely, the dryland riparian forest and wetlands crop type was specified with an initial FIESWP value of 0.2 because the shallow water table and saturated soil of the wetlands or riparian areas promoted recharge.

A total of 14 FTR scale factors were fixed for the final calibration. FTR scale factors were parameterized by length of the stress period (irrigation season, nonirrigation season, monthly) (see table 1.2 for parameter description). The FTR scale factor parameter allowed PEST to adjust the amount of transpiration that constituted ET while maintaining the input FTR values relevant for each crop type. The FTR scale factors were specified an initial value of 1.0. Like the FTR scale factors, the FEI inputs were fixed for the final calibration. The nine FEI scale factor parameters were specified for stress periods with irrigation (irrigation season and March to September monthly stress periods). Initial values were 1.0 for each FEI scale factor. Root depth adjustable parameters were specified for 26 crop types in the model and set as fixed parameters for the final calibration. Their initial values were based on published values from Irmak and Rudnick (2014) and U.S. Department of Agriculture (2016). Four of the root depths for fallow land were not specified as parameters because fallow land does not have plants or roots; therefore, those root depths were hard coded as input values of 0 ft.

A total of six OFEs, one parameter for each of the three types of irrigation efficiencies (commingled, groundwater, and surface water), one for pre-1980 “early period” efficiencies, and one for post-1980 “recent” efficiencies, were specified to allow the model to simulate the improvement of irrigation technology and irrigation efficiency with time. However, these parameters were fixed for the final calibration at their initial values of 0.72 and 0.7 for early and recent period commingled efficiencies, respectively; 0.55 and 0.65 for early and recent period surface-water efficiencies, respectively; and 0.8 and 0.9 for early and recent period groundwater efficiencies, respectively (table 1.2).

The climate properties (*climprops*) parameters (table 1.2) included 15 ET_{ref} scale factors specified by stress period type like the FTR and FEI scale factors, except one additional ET_{ref} scale factor was parameterized for the predevelopment CPIHM. The ET_{ref} scale factors parameters were multipliers on the input ET_{ref} up or down to account for uncertainty in those datasets. All 15 of the ET_{ref} scale factors were fixed for the final calibration at values of 1.12 for the predevelopment CPIHM; 1.56 for the irrigation season stress periods and 1.0 for the nonirrigation season stress periods of the development-period CPIHM; and 1.0 for the January, February, March, April, September, October, November, and December stress periods, respectively, and 1.15, 1.20, 1.30, and 1.30 for the May, June, July, and August stress periods, respectively, for the development-period CPIHM.

Adjustable Parameters for Final Calibration

The streamflow routing properties (*sfrprops*) group of parameters included 11 adjustable parameters for vertical hydraulic conductivity of streambed (Ksb). Ksb parameters were defined for the lower and upper portion of each SFR reach and “tied” in PEST so that the Ksb remained the same for each SFR segment and did not change for reaches within a segment. Unique Ksb parameters were defined for natural streams according to soil class used in the CPIHM and for each canal simulated with the SFR (soil classification in fig. 1*B*; parameters in fig. 13). Initial values for calibration of

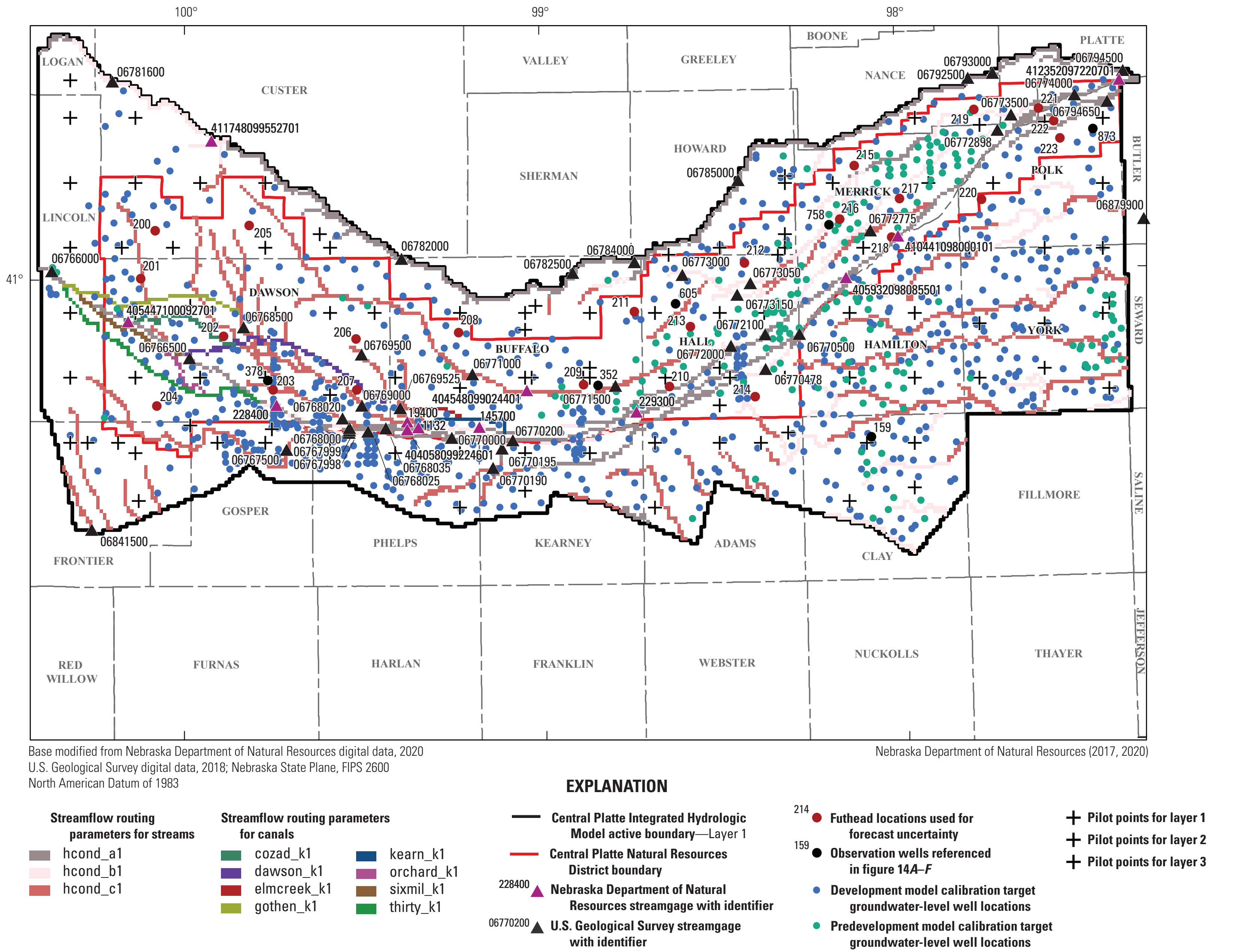

Figure 13. Locations of the observation wells, streamgages, and pilot points used during the calibration of the predevelopment (pre-May 1, 1895) and development (post May 1, 1895) Central Platte Integrated Hydrologic Model in addition to the well locations for observation wells in figure 14*A*–*F*.

Ksb for natural streams were set to less than 2 ft/d and canal Ksb values were set between 1 and 10 ft/d based on manual trial-and-error testing prior to automated calibration through which model stability was improved. The lower and upper bound were set to 0.001 and 15 ft/d, respectively, which is the acceptable range for the study area based on values from Peterson and others (2016).

Vertical hydraulic conductivity and Kh for each model cell was specified using interpolation between pilot points (see Doherty and others, 2010b). Vertical hydraulic conductivities were set using anisotropy ratios, also interpolated between pilot points. The pilot points for Kh (*pilotpts*) were specified as adjustable parameters to adequately represent the spatial heterogeneity of Kh across each model layer without needing to adjust Kh for each active model cell. A total of 124 pilot points were used: 49 for layer 1, 48 for layer 2, and 27 for layer 3 (fig. 13). In this study, pilot points were generated using the FloPy python module (Bakker and others, 2016), interpolation factors were generated using the “ppk2fac” PEST Groundwater Data Utility (Doherty 2018), and model input arrays generated from interpolation between the pilot points used the PyEmu module (White and others, 2016). The pilot point distribution was based on the presence of an active extent of each model layer. Pilot point density was chosen as one pilot point for every 25 active model cells. Pilot points within a few cells of a stream or general head boundary were manually moved away from the boundary to avoid the influence of boundary conditions. For this study, the vertical interval estimates of Kh from Houston and others (2013) were assigned to aquifer intervals that aligned with the HUs from Cannia and others (2006) and that correspond to the model layers (table 1). Initial values for individual pilot points were selected by extracting Kh values from two-dimensional arrays generated through interpolation of test hole data in Houston and others (2013) and summarized in table 1 (table 1 is a summary of the test hole data, not the interpolated grids used to extract the values).

The pilot points for aquifer anisotropy (*apilotpts*) were specified for the same locations as the Kh pilot points (fig. 13). Initial values for model layer 1 anisotropy pilot points were specified as 10:1 ratio (Kh:Kv) in accord with published values in Domenico and Schwartz (1990) for unconsolidated sands, silts, and clays of alluvial aquifers (Cannia and others, 2006). Layer 2 anisotropy at pilot points was specified as 20:1 because of the finer grained and lower Kh values of silts reported for that layer (Cannia and others, 2006). Layer 3 anisotropy at pilot points were specified as 10:1 ratio for sandstones (Domenico and Schwartz, 1990; Houston and others, 2013). Horizontal anisotropy was not simulated in the CPIHM.

Regularization of Parameters

Tikhonov regularization was employed in the CPIHM calibration process for the adjustable parameters to reduce the likeliness of overfitting during the automated calibration process (Doherty, 2015). Regularization is a mathematical preconditioning method that allows for a unique solution to an ill-posed inversion problem (many more parameters than observations) in which there is correlation between parameters (Doherty, 2015). Regularization allows for the PEST to use “prior information” or expert knowledge of the parameterized inputs as the initial preferred values unless the calibration target dataset can provide enough information to warrant deviation from those initial preferred parameter values during the calibration process (Doherty, 2015). PEST includes a weight to regularized parameters and tracks a regularized PEST objective function (Φ_r) that is added to the Φ from calibration target residuals (Doherty, 2015). Therefore, PEST imposes a penalty on the Φ if a regularized parameter deviates from its initial value. PEST will only deviate regularized parameters from their initial values if Φ_r contribution to Φ is less than the reduction in the Φ that would occur with improved fit to the calibration targets (Doherty, 2015). Regularization weights were manually adjusted from the default value of 1.0 to provide additional guidance to PEST based on the prior information.

The trial-and-error calibration demonstrated that the CPIHM adequately simulated ETp, ETg, recharge, and irrigation from wells in comparison to the conceptual flux estimates for recent years (2011–16) under the fixed climate and landscape parameter scheme (simulated values for the landscape subsystem, mentioned in this section, are presented in the “Predevelopment and Development Period Simulated Results and Water Budgets” section of this report). The comparison between the conceptual flux values (presented in tables 2 and 3 and the “Conceptual Model of the Hydrologic System” section of this report) and the manual trial-and-error calibration values verified that initial trial-and-error estimated landscape and climate parameters were acceptable values and the CPIHM accurately simulated CWD. The preliminary fit between calibration targets and their simulated equivalent values was acceptable for some stress periods and locations, whereas simulated values for other stress periods and locations exhibited some bias. This prior information gained about the CPIHM was transferred to PEST by lowering the weights of the groundwater-flow parameters to 0.5, which encouraged PEST to adjust the groundwater-flow parameters to improve the calibration.

Calibration Targets

Calibration targets are measured or estimated values assumed to represent conditions of the hydrologic system at the time of their measurement, with a degree of uncertainty that is based principally on measurement or estimation error. Calibration targets can be single measurements in time or a time series that represents the temporal behavior of the hydrologic system. PEST allows calibration targets to be clustered into groups where the contribution of each group to Φ can be assessed. The CPIHM had the following observation groups specified in PEST (table 9): development period average streamflows per stress period processed from daily

Table 9. Description of calibration targets in the Central Platte Integrated Hydrologic Model for the groundwater-level and surface-water observation groups.

[USGS, U.S. Geological Survey; NWIS, National Water Information System; CPNRD, Central Platte Natural Resources District; NeDNR, Nebraska Department of Natural Resources]

Observation group	Count	Description of observation group
Groundwater-level observation group		
realwls	10,746	Development period measured groundwater-levels from USGS NWIS (U.S. Geological Survey, 2017).
realwlst	8,916	Development period measured groundwater-levels across transects of the Platte River, collected by the CPNRD.
sswls	189	Predevelopment model average groundwater levels processed from measured pre-1950 groundwater-levels in NWIS.
realdif	9,848	Development period differences in measured groundwater levels between stress periods.
potheads[1]	12,973	Scenario period “potential” observations that can be used for dataworth analysis.
futheads[1]	24	Scenario period “future” observations used in the predictive uncertainty analysis, located at the geometric center of each Groundwater Management Area.
Surface-water observation groups		
dnrflow	2,886	Development period average streamflows per stress period processed from daily average measured streamflows from the NeDNR streamgages.
nwisflow	7,589	Development period average streamflows per stress period processed from daily average measured streamflows from the USGS NWIS streamgages.
ssflow	2	Predevelopment model average streamflows per stress period processed from daily average measured streamflows from the USGS NWIS streamgages.
sflowdiff	534	Development period model average streamflows differences per stress period processed from daily average measured stream-flows from the USGS NWIS streamgages.
ssflowdiff	1	Predevelopment model average streamflows differences per stress period processed from daily average measured streamflows from the USGS NWIS streamgages.

[1]Zero-weighted observations that did not contribute to the calibration objective function.

average measured streamflows from USGS National Water Information System (NWIS) streamgages (*nwisflow*), development period average streamflows per stress period processed from daily average measured streamflows from the NeDNR streamgages (*dnrflow*), average streamflow differences between streamgages (*sflowdiff*), predevelopment model average streamflows per stress period processed from daily average measured streamflows from the USGS NWIS streamgages (*ssflow*), Predevelopment model average streamflow differences per stress period processed from daily average measured streamflows from the USGS NWIS streamgages (*ssflowdiff*), predevelopment model average groundwater levels processed from measured pre-1950 groundwater-levels in NWIS (*sswls*), development period measured groundwater-levels from USGS NWIS (*realwls*), development period differences in measured groundwater levels between stress periods (*realdif*), and development period measured groundwater-levels across transects of the Platte River, collected by the CPNRD (*realwlst*). Two sets of observation points were included that did not involve actual measurements but were used in the analysis of the calibrated model: scenario period “potential” observations that can be used for dataworth analysis (*potheads*), and scenario period “future” observations used in the predictive uncertainty analysis, located at the geometric center of each Groundwater Management Area (*futheads*) that were incorporated for the predictive uncertainty analyses (table 9). The calibration was not affected by any observation targets in the *potheads* or *futheads* groups because they were zero weighted. The CPIHM contained 40,711 weighted calibration targets.

Groundwater Levels

The CPIHM was calibrated to groundwater levels for the predevelopment and development models. The predevelopment model was calibrated to 189 estimated groundwater levels at 189 observation wells as the average of measured groundwater levels prior to January 1, 1950, and assigned to the *sswls* observation group (table 9; fig. 13). The development model was calibrated to 19,662 measured groundwater-level observations at 963 observation wells obtained from the NWIS database (U.S. Geological Survey, 2017) and 9,848 groundwater-level differences, which were second-order observations calculated as the difference between a measured groundwater level at a single location from one stress period to the next, to ensure the model matched changes in groundwater levels in addition to the absolute groundwater level (table 9). A total of 16,840 groundwater-level observations at 725 wells completed in layer 1; 1,065 groundwater-level observations at 125 wells completed in layer 2; and 1,759 groundwater-level observations at 113 wells completed in layer 3 (table 10). Although wells were distributed across the model area, a total of 859 wells had less than 10 observations and 68 wells had 100 or more observations (fig. 13). Western regions of the active model area in Custer, Frontier, and Lincoln Counties had very few observations (fig. 13). About 95 percent of the groundwater-level observations were measured after 1980 (fig. 14); therefore, the calibration incurred a bias toward the post-1980 period. This bias was desirable because one objective of the study was to use the model results to update the CPNRD's GMP, which compared current management and MADs to 1982 groundwater levels. Consequently, the natural bias built into the model calibration (because most observations were measured after 1980) allowed PEST to focus on adjusting parameters to match observations in the post-1980 period. All groundwater-level calibration targets and locations are available in the model archive associated with this report (Traylor, 2023).

Streamflows

The CPIHM included streamflow and streamflow difference calibration targets for the predevelopment and development period models. Streamflow targets at streamgages provided the calibration with information on absolute streamflow values. Streamflow difference targets provided additional calibration information to allow the model to reasonably match streamflows between streamgages, more accurately simulate the stream-aquifer interaction, and reduce the correlation between simulated flows of upstream and downstream locations so their potential bias at one location was not passed to another location.

Two streamflow targets were used to calibrate the predevelopment CPIHM streamflows at the Platte River near Overton, Nebr., and Platte River near Duncan, Nebr., streamgages (USGS streamgages 06768000 and 06774000, respectively), and a single streamflow difference was calculated for the predevelopment model between the same streamgages on the Platte River (fig. 13). Measured streamflow data did not exist for the predevelopment period (prior to May 1, 1895); therefore, the *ssflow* observations were the average of pre-1940 streamflows for the Platte River near Overton, Nebr., and Platte River near Duncan, Nebr., streamgages (fig. 13).

The CPIHM was calibrated to 10,475 stress-period-averaged streamflows calculated from measured daily values at a combination of 53 NWIS and Nebraska Department of Natural Resources streamgages (U.S. Geological Survey, 2017; Nebraska Department of Natural Resources, 2019) for the development model (fig. 13). An additional 534 streamflow differences were calculated between the Platte River near Overton, Nebr., and Platte River near Duncan, Nebr., streamgages on the Platte River for the development model (fig. 13).

Streamflow calibration targets were spatially distributed throughout the streams of the active model area (fig. 13). The Platte River Basin had 19 streamgages and the Loup River Basin, which included the South Loup, Middle Loup, and Loup Rivers, had eight streamgages. Streamflow calibration targets at streamgages downstream from the Loup River Power Canal diversion at Genoa, Nebr. (not shown), were reduced by the diversion amount because the diversion was not simulated in the model. Further, the Johnson Power Canal (not shown) return to the Platte River return (west of Kearney, Nebr., fig. 1*A*) was not simulated; therefore, Platte River calibration targets downstream from the return point were reduced by the amount of the returns. All streamflow calibration targets and streamgage locations are available in the model archive associated with this report (Traylor, 2023).

Weighting Scheme for Calibration Targets

Weights were applied to the calibration targets to capture their uncertainty, starting with an error-based weighting scheme, then adjusting the weights to balance each

Table 10. Description of calibration targets in the Central Platte Integrated Hydrologic Model for the counts of groundwater-level calibration targets by layer.

Model layer	Count of observations	Count of observation wells
1	16,840	725
2	1,065	125
3	1,759	113

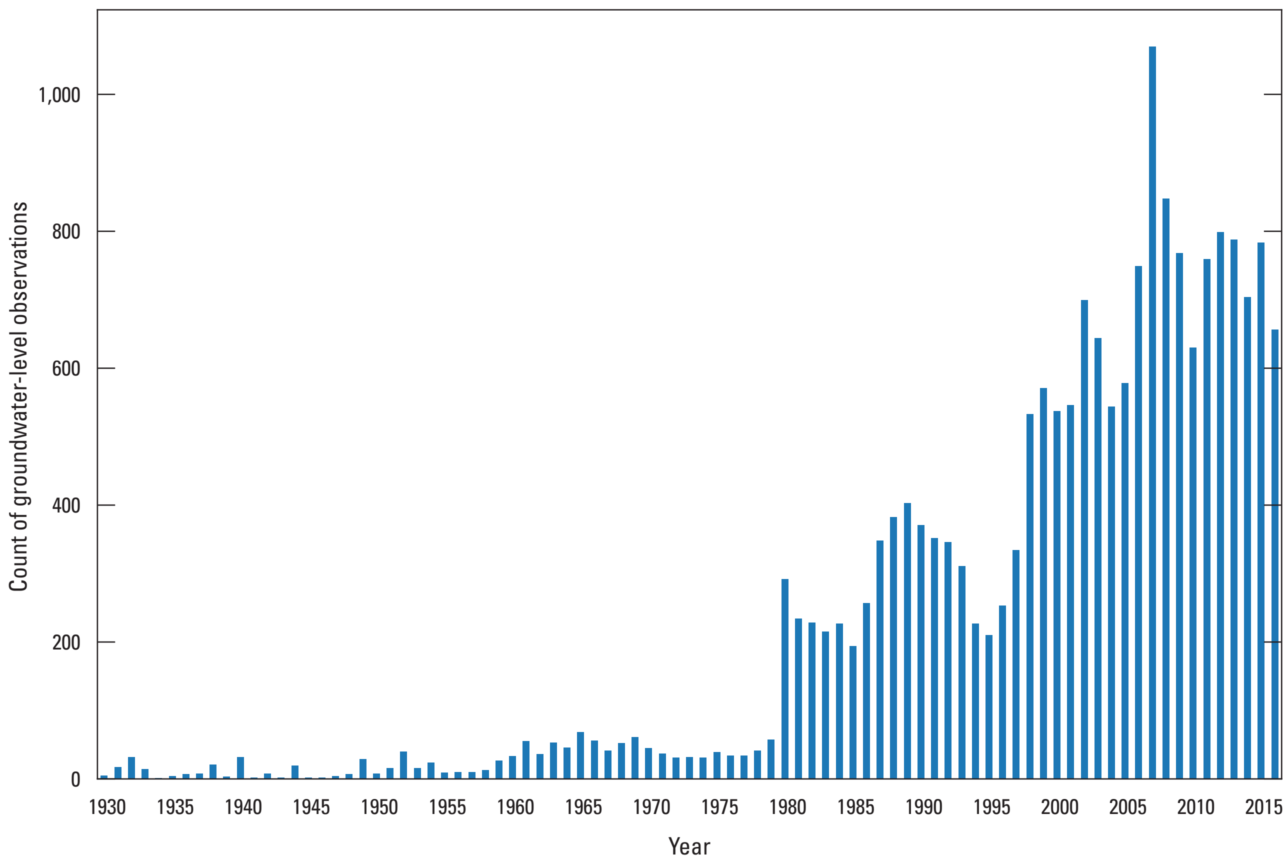

Figure 14. Count of groundwater-level observations used to calibrate the Central Platte Integrated Hydrologic Model for the development model.

observation group's contribution to Φ. Error-based weighting of the calibration targets was applied to each target based on measurement uncertainty associated with each measurement type (Hill and Tiedeman, 2007). Error-based weighting also kept PEST from being overaffected by targets with the largest magnitudes and different units. The attempts of PEST to minimize Φ are affected by the number and magnitude of the residuals in each observation group; groups with higher magnitudes or a greater number of targets have more effect on Φ than groups with smaller or fewer targets. For example, a streamflow residual of 10 ft^3/s (864,000 cubic feet per day, in model units) is three orders of magnitude larger than a groundwater-level residual of 200 ft, and when weighted equally, PEST would be more affected by the streamflow residual and become insensitive to hydrologic signal represented by the groundwater-level residual. Error-based weights for each observation were calculated using equation 3:

$$w = \frac{1}{\sigma} \tag{3}$$

where

- w is the error-based weight applied to the observation, and
- σ is the measurement uncertainty of the observation.

Measurement uncertainty varied by observation target group. The measured streamflows from USGS streamgages were assigned an uncertainty of 5 percent of their average flow for the period of record, which correlated to the 95-percent confidence interval that is typical for a "Good" rating for USGS streamgage measurements. The measured streamflows from NeDNR streamgages were assigned an uncertainty of 25 percent. Measured groundwater-level observations (*real-wls*) were assigned an uncertainty of 10 ft. This reflects the uncertainty in the grid cell altitude in which the well is located (the error in resampling a 32.8-ft digital elevation model dataset to the CPIHM cell size of 2,640 ft). Initial weights for the measured groundwater-level observation groups (*realwls*, *realdif*, *realwlst*, and *sswls*) used the error-based scheme, but were adjusted during the calibration process to increase their contribution to Φ. The final weighting scheme used during calibration reflected the CPNRD's planned use of the CPIHM to assess MADs in each GWMA, whereby smaller residuals for groundwater levels within the CPNRD were prioritized. Therefore, weights for the measured groundwater levels and groundwater-level differences were increased by about 40 percent for those measurements within the CPNRD boundary. Weights were increased for the *sswls*, *ssflowdif*, and *ssflow* to have a more balanced contribution to Φ for these observation groups.

The streamflow calibration targets were initially weighted using the error-based weighting method (Hill and Tiedeman, 2007). The calibration targets measured along the Loup River system were weighted about 75 percent lower than other targets because the Loup River system was the northern boundary of the active model area, and the hydrologic system to the north of the Loup River system that contributed base flow and runoff to those streams was not simulated in the CPIHM.

Two-Phase Calibration Approach

Calibration of the CPIHM involved two phases: a manual adjustment of parameters, followed by the automated calibration using BeoPEST. The two-phase calibration approach was adopted after several attempts to calibrate the CPIHM in a fully automated fashion because many of the adjustable parameters produced unrealistic results and resulted in significant model instability. Landscape parameters and some groundwater parameters were fixed to improve model stability during calibration, prevent spurious calibration results, and better match the conceptual estimates of landscape ET. The conceptual landscape ET estimates were based on measured data or calibrated outputs of previously developed models, which provided a blueprint for acceptable ranges of parameter values and outputs of ET and groundwater irrigation, for the CPIHM.

An assessment of parameter sensitivities to observations using a matrix of sensitivities, known as a Jacobian matrix, from a preliminary automated calibration attempt with all parameters set as adjustable, showed that the growing season ET_{ref} scale factors and Sy multipliers were some of the most sensitive (table 1.3). Preliminary automated calibration runs revealed that PEST preferred to adjust the Sy multipliers beyond acceptable ranges, even with heavy regularization weights applied, and as a result the multipliers were converted to fixed parameters before subsequent calibration. Further, the storage parameters were fixed in the calibration of layers 2–5 for the Eastern Model Unit groundwater-flow model from Peterson (2009) and the single layer Northern High Plains aquifer model from Peterson and others (2016); both models included the model domain for this study and used the same input test hole data derived from Houston and others (2013). This assessment of parameter sensitivities and methods from previous studies led to the implementation of the two-phase calibration approach that included the fixing of landscape and aquifer storage parameters to reasonable values based on available data.

In the initial manual adjustment phase, parameters were adjusted within the PEST framework to improve the fit between calibration targets and their simulated equivalent values. This phase focused on adjusting the growing season ET_{ref} scale factors to improve the CPIHM's simulation of landscape ET and irrigation pumping throughout the development period model to values that were similar to the conceptual ET values and irrigation pumping from table 2. Model outputs were postprocessed to produce annual values of those ET and irrigation fluxes, and the recent 5 years of the simulated outputs (2011–16) were compared to the conceptual values from table 3. As mentioned in the "Fixed Parameters for the Final Calibration" section of this report, the ET_{ref} scale factors required adjustment from their 1.0 values that were standard for the other scale manually adjusted factors. The unadjusted average annual inputs of ET_{ref} shown in figure 10*B* were about 57 inches, which was about 7 to 8 percent less than the measured values from Irmak and Skaggs (2011). Consequently, initial manual trial and error testing indicated that simulated total AET (which is directly controlled by the ET_{ref}, and therefore the ET_{ref} scale factors) for all crop types was too low compared to the conceptual model water-budget values. Additionally, the undersimulated AET was responsible for the undersimulation of groundwater withdrawals for irrigation compared to available data and conceptual model values described in the "Conceptual Model of the Hydrologic System" section of this report, because lower ET corresponded to lower CIR. Initial automated calibration runs, with ET_{ref} scale factor parameters set as adjustable, showed that they were highly sensitive parameters as PEST preferentially adjusted them and they hit their upper bounds when the upper limit was set to even an unrealistic 3.0 (3.0 equates to a 3 times multiplier on ET_{ref}). Trial-and-error manual adjustment was used to determine the best initial values of each ET_{ref} scale factor to combat overfitting and maintain agreement with the conceptual model landscape ET.

After manual calibration, when the simulated recent water-budget fluxes were in accord with the conceptual model values, the final set of input parameter values obtained from the manual calibration were set as the initial parameter values for the automated PEST calibration. Therefore, initial parameter values at the beginning of the automated calibration phase were derived from a combination of local knowledge of the study area, information accrued from other scientific studies of the study area or similar hydrologic settings, and information gained about the CPIHM during the manual calibration phase. To honor these initial parameter values and their information and to keep PEST from deviating too far from the initial values, Tikhonov regularization was applied during the automated calibration, also described in “Regularization of Parameters” section of this report (Doherty and Hunt, 2010; Doherty, 2015).

Calibration Results

This section of the report describes the results of the CPIHM calibration and includes an assessment of fit among the calibration targets and their simulated equivalent values, presentation of the final “best” calibrated parameter values, and parameter sensitivity and identifiability analyses. Calibration results provide an indication of a model’s ability to simulate the dynamics of the hydrologic system and reproduce outputs that are in accord with the conceptual model of the hydrologic system and measured or observed data. Additionally, the final contribution to Φ shows how the observation groups affected the automated calibration process. Additional calibration statistics and plots of measured compared to simulated values are available in appendix 2.

Comparison of Calibration Targets to Simulated Equivalent Values

The comparison of calibration targets to their simulated equivalent values is an assessment of the fit between measured or observed data such as groundwater levels and streamflows with corresponding simulated values produced by the CPIHM. During the calibration process, PEST compared the calibration targets to corresponding simulated values and calculated the difference between the observation targets and simulated equivalent values, which for the remainder of the report will be referred to as the “residual.” A positive residual indicates an underestimation of simulated values by the CPIHM and a negative residual indicates an overestimation of simulated values by the CPIHM. The Gage package extracted the simulated streamflows from SFR reaches coincident with the location of the 53 streamgages for comparison to the streamflow calibration targets. The mod2obs PEST utility was used to extract the corresponding simulated groundwater levels for comparison to the calibration target groundwater levels (Doherty, 2018).

Groundwater Levels

The calibrated predevelopment CPIHM groundwater levels displayed an adequate fit to the calibration targets for the *sswls* observation group with an average absolute residual of 8.2 ft (table 11). Therefore, the predevelopment CPIHM provided acceptable initial conditions for the transient development-period CPIHM. Spatial trends in the calibrated *sswls* included an overestimation north of the Platte River and an underestimation south and east of the Platte River and minimal bias along the Platte River and Wood River from west to east (fig. 15). The calibrated development CPIHM groundwater levels displayed an adequate fit to the calibration targets for the *realwls* and *realwlst* observation groups, with average absolute residuals of 9.6 and 2.8 ft, respectively (figs. 15, 16*A*, and 2.3; table 11). The combined *realwls* and *realwlst* average absolute groundwater-level residuals for model layers 1, 2, and 3 were 6.1, 12.4, and 7.4 ft, respectively (table 11) for the whole development-phase model, which indicated that the CPIHM adequately simulated the groundwater levels for each layer. The fit between the measured and simulated groundwater levels in the *realwls* and *realwlst* groups was somewhat

Table 11. Calibration results statistics for the groundwater-level and streamflow observation groups of the Central Platte Integrated Hydrologic Model.

[<, less than; >, greater than; --, could not calculate a value]

Observation group	Average	Standard deviation	Minimum	25 percent	50 percent	75 percent	Maximum	Average absolute residual (feet)
Calibrated groundwater-level residual statistics, in feet								
realwls	−1.4	14.2	−95.9	−5.9	0.4	5.9	137.0	9.6
realwlst	0.1	4.1	−20.6	−1.7	−0.2	2.0	21.2	2.8
sswls	2.6	11.7	−29.4	−4.1	0.7	7.2	56.8	8.2
realdif	<0.1	2.8	−80.3	−0.4	>−0.1	0.5	43.1	1.2
Calibrated streamflow statistics, in cubic feet per second								
dnrflow	15.1	1,060.7	−15,012.1	−53.7	−1.0	28.0	11,831.9	356.4
nwisflow	−191.8	833.0	−15,226.4	−191.4	−10.8	21.5	7,890.3	464.6
ssflow	2,230.0	1,518.2	1,156.4	1,693.2	2,230.0	2,766.7	3,303.5	1,073.5
sflowdiff	171.0	1,088.0	−4,230.5	−268.3	76.7	506.5	5,845.0	695.2
ssflowdif	−2,147.0	--	−2,147.0	−2,147.0	−2,147.0	−2,147.0	−2,147.0	0.0

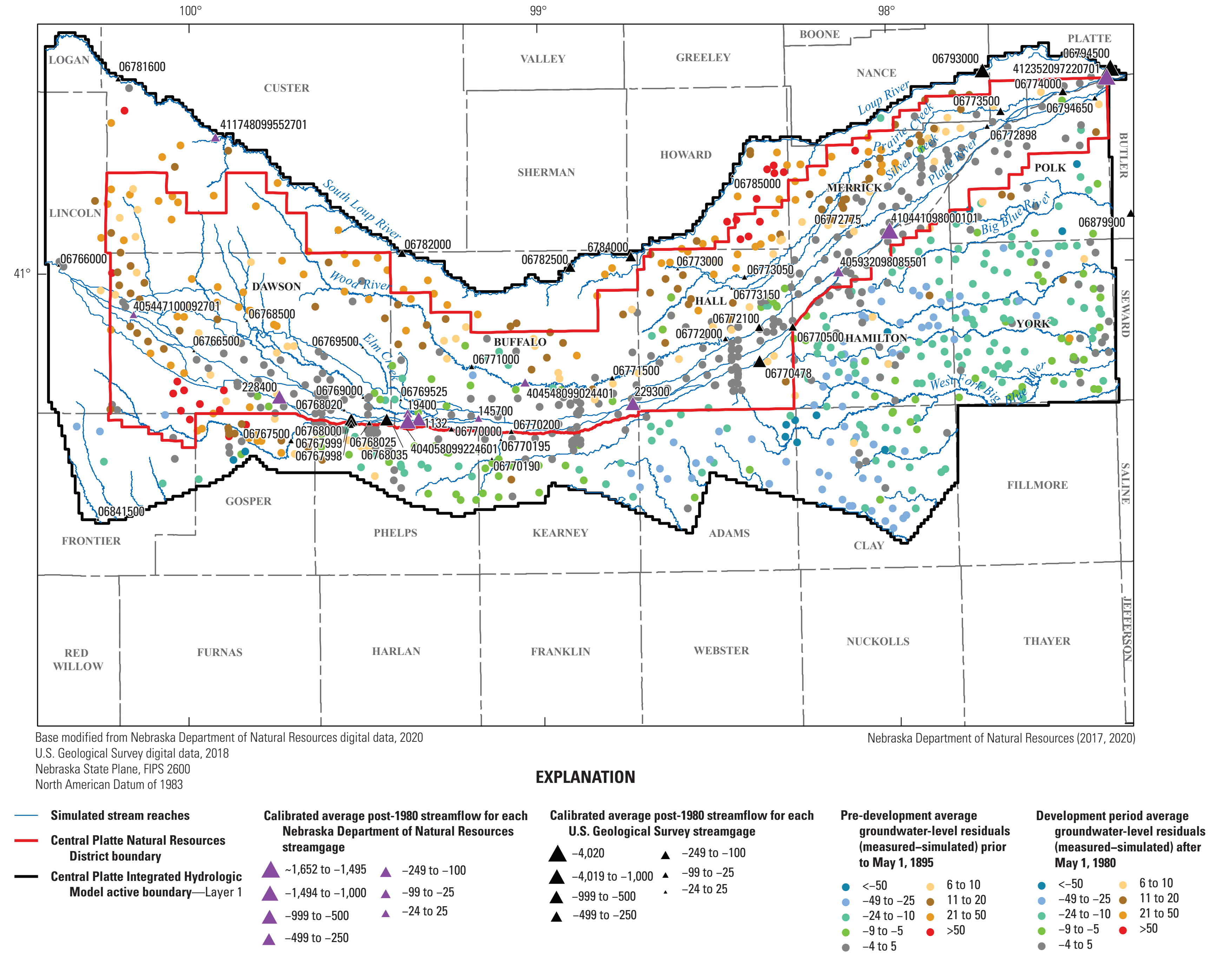

Figure 15. Spatial distribution of the average groundwater-level and streamflow residuals for the *sswls, realwls, nwisflow, and dnrflow* observation groups for the calibrated Central Platte Integrated Hydrologic Model.

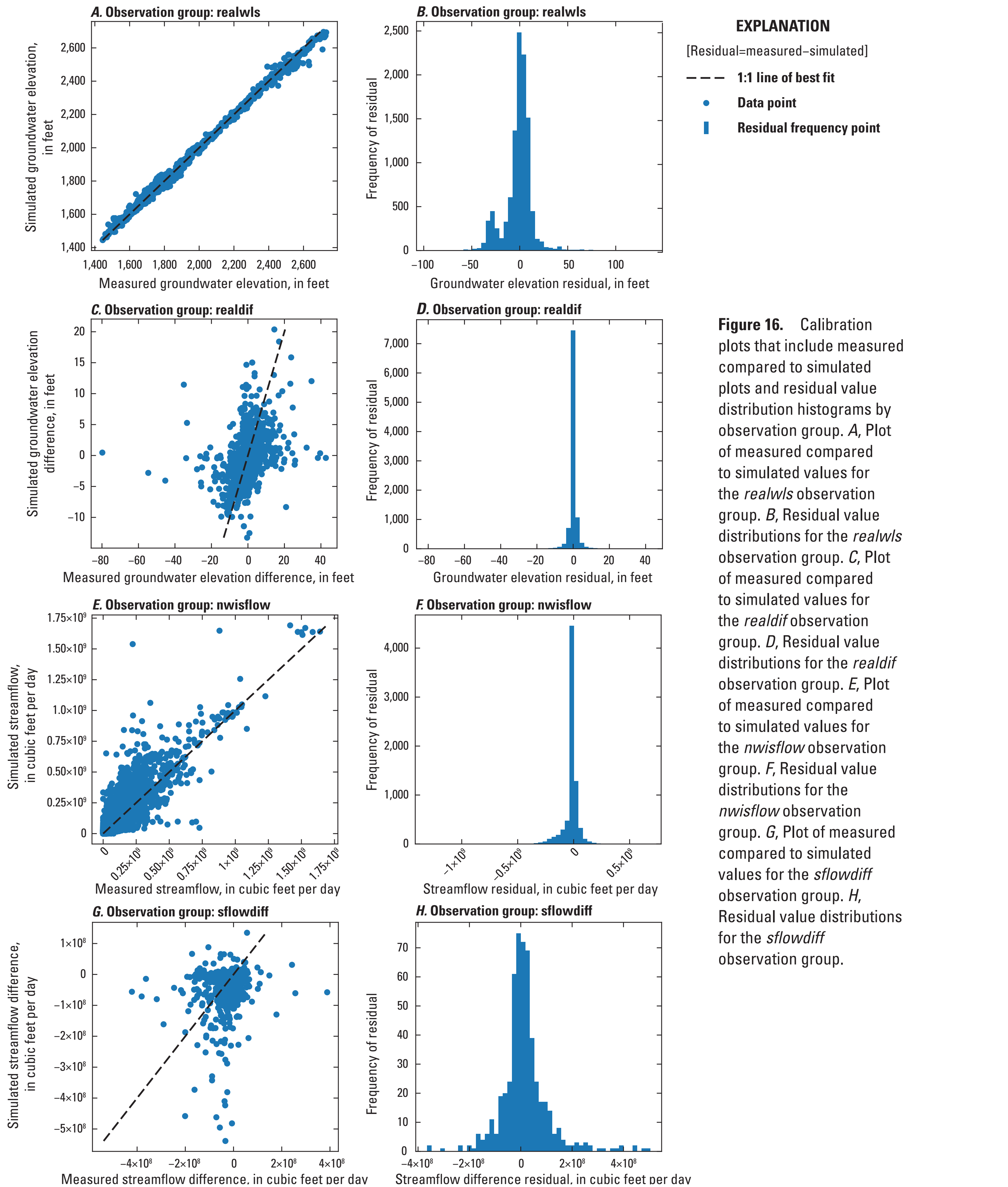

Figure 16. Calibration plots that include measured compared to simulated plots and residual value distribution histograms by observation group. *A*, Plot of measured compared to simulated values for the *realwls* observation group. *B*, Residual value distributions for the *realwls* observation group. *C*, Plot of measured compared to simulated values for the *realdif* observation group. *D*, Residual value distributions for the *realdif* observation group. *E*, Plot of measured compared to simulated values for the *nwisflow* observation group. *F*, Residual value distributions for the *nwisflow* observation group. *G*, Plot of measured compared to simulated values for the *sflowdiff* observation group. *H*, Residual value distributions for the *sflowdiff* observation group.

better within the CPNRD area after May 1, 1980, because the calibration of the CPIHM focused on the minimization of groundwater-level residuals for this area and period. This improvement in fit occurred mostly in layers 1 and 2 for the CPIHM and within the CPNRD; layer 3 exhibited an absolute residual that was larger (7.6 ft for the CPIHM and 7.5 ft for the CPNRD) after May 1, 1980, compared to the absolute residual for all time periods (7.4 ft for the CPIHM and 7.3 ft for the CPNRD); however, the difference was about 0.1 ft (table 12). The combined *realwls* and *realwlst* CPNRD average absolute groundwater-level residuals after May 1, 1980, for model layers 1, 2, and 3 were 4.0, 10.7, and 7.5 ft, respectively (table 12). Further, the calibrated development CPIHM groundwater levels displayed an adequate fit to the calibration targets for the *realdif* observation group with average absolute residuals of 1.2 ft and a standard deviation of 2.8 ft (table 11). These residuals indicated that the development-period CPIHM captured the transient nature of the groundwater-subsystem as groundwater-levels changed.

The calibrated groundwater-level residuals after May 1, 1980, exhibited spatial bias throughout the CPIHM domain. The average groundwater-level residuals at observation wells south of the Platte River were mostly negative, which indicated that the CPIHM overestimated the groundwater levels in this region; some residuals in this region exhibited a large bias of greater than 25 ft (fig. 15), including well 159 (fig. 17*A*). The average groundwater-level residuals at observation wells north of the Platte River were mostly positive, which indicated that the CPIHM underestimated the groundwater levels in this region (fig. 15), including well 352 (fig. 17*B*). Some of these wells were within the CPNRD boundary, particularly in Dawson, Buffalo, Hall, Howard, and Nance counties (fig. 15). The residuals along the Platte River were generally less than 5 ft (figs. 15 and 17*C–F*). Most of the residuals for observation wells that were overestimated by the CPIHM were located to the south and east of the Platte River outside the CPNRD boundary, particularly in Frontier, Gosper, Phelps, Kearney, Adams, Clay, Hamilton, and York Counties; because of their locations outside the CPNRD, they were weighted lower than the observations inside the CPNRD boundary, which caused them to have less effect on the Φ during the calibration. Therefore, PEST did not try to improve the fit for calibration targets outside the CPNRD boundary as much as the targets inside the CPNRD. Greater variability in groundwater levels outside of the Platte River Valley topographic region was also expected because of more dynamic terrain and depth to water in the Valley-side Slopes, Dissected Plains, and Sandhills topographic regions compared to the Valley region of the Platte River (fig. 1*B*). Additional comparisons of measured and simulated groundwater altitudes at other locations used in the model calibration process are available in the USGS data release associated with this report (Traylor, 2023).

Streamflows

The calibrated predevelopment CPIHM undersimulated streamflow by 2,230 ft^3/s for the *ssflow* observation group (table 11). However, given that (1) the *ssflow* observations were more uncertain than measured streamflows because they were estimated based on measured flows between 1930 and 1940, (2) the simulated predevelopment groundwater levels exhibited an adequate fit to the *sswls* observations, and (3) streamflow is a more dynamic observation than groundwater levels, and (4) major inflows to the Platte River are a transient input for the development CPIHM, the marginal fit to the *ssflow* observations still resulted in an adequate calibration for the development-period model. Most of the calibrated development-period CPIHM streamflows displayed a passable fit to the calibration targets (fig. 16*E–H*). Calibration targets from the *nwisflow* group exhibited a coefficient of determination of 0.776 with their simulated equivalent values. The *nwisflow* group exhibited a minor positive bias in their residuals, which indicated that the CPIHM oversimulated streamflows. The CPIHM accurately simulated the flows along the Platte River, including the outflow point of the Platte River near Duncan, Nebr. (fig. 18), streamgage (USGS streamgage 06774000; fig. 1*A*), which was important for the efficacy of the water balance during the simulation. The largest bias in flow along the Platte River occurred at splits in the complex braided network of channels such as a north and south channel at the Platte River near Overton North Channel, Nebr. (USGS streamgage 06767998) and the Platte River near Overton South Channel, Nebr. (USGS streamgage 06767999): residuals were −961 and −108 ft^3/s, respectively (fig. 15). However, the single channel Platte River near Overton, Nebr. (USGS streamgage 06768000) residual was only −31 ft^3/s (fig. 15). These residuals were expected because the model was not designed to simulate all the local complexities of a braided channel system such as Platte River; rather it was designed to simulate the primary channels of the Platte River and other streams in the study area. Further, the *dnrflow* residuals for the development-period CPIHM exhibited a large overestimation of flows on the Platte River streamgages, which was expected because these observations were weighted low in the calibration and consequently the parameters in PEST were not as sensitive to these observations compared to the *nwisflow* group. Additional comparisons of measured and simulated streamflow at 53 streamgages used in the model calibration process are available in the USGS data release associated with this report (Traylor, 2023).

The final phi distribution by observation group is presented in figure 19. The observation group with the largest contribution to Φ was from the *nwisflow* group (26.2 percent), followed by the *realdif* (24.2 percent) and *realwls* (19.9 percent) groups (fig. 19). The primary calibration focused on reducing the residuals of the *realwls, realdif,* and *nwisflow* groups more than other groups; therefore, the final Φ distribution, where the top three were *nwisflow*, *realdif*, and *realwls*, reflects the purpose of the study objectives.

Table 12. Average simulated groundwater levels and their residuals by layer in the Central Platte Integrated Hydrologic Model domain and the Central Platte Natural Resources District domain for the entire development model period (May 1, 1895, to December 31, 2016) and post-May 1, 1980.

[CPIHM, Central Platte Integrated Hydrologic Model; CPNRD, Central; Platte Natural Resources District]

Model layer	Count		CPIHM domain			CPIHM domain post-May 1, 1980		CPNRD			CPNRD domain post-May 1, 1980	
	Observ-ations	Observation wells	Average simulated groundwater-level, in feet above mean sea level	Average residual, in feet	Average absolute residual, in feet	Average residual, in feet	Average absolute residual, in feet	Average simulated groundwater-level in the CPNRD, in feet above mean sea level	Average residual, in feet	Average absolute residual, in feet	Average residual, in feet	Average absolute residual, in feet
1	16,840	725	2,052.06	−0.7	6.1	−0.4	6.0	2,010.06	2.3	4.0	2.3	4.0
2	1,065	125	2,013.42	−2.7	12.4	−3.6	11.5	1,959.01	6.9	10.3	7.4	10.7
3	1,759	113	2,211.60	1.5	7.4	1.4	7.6	2,182.39	1.1	7.3	1.1	7.5

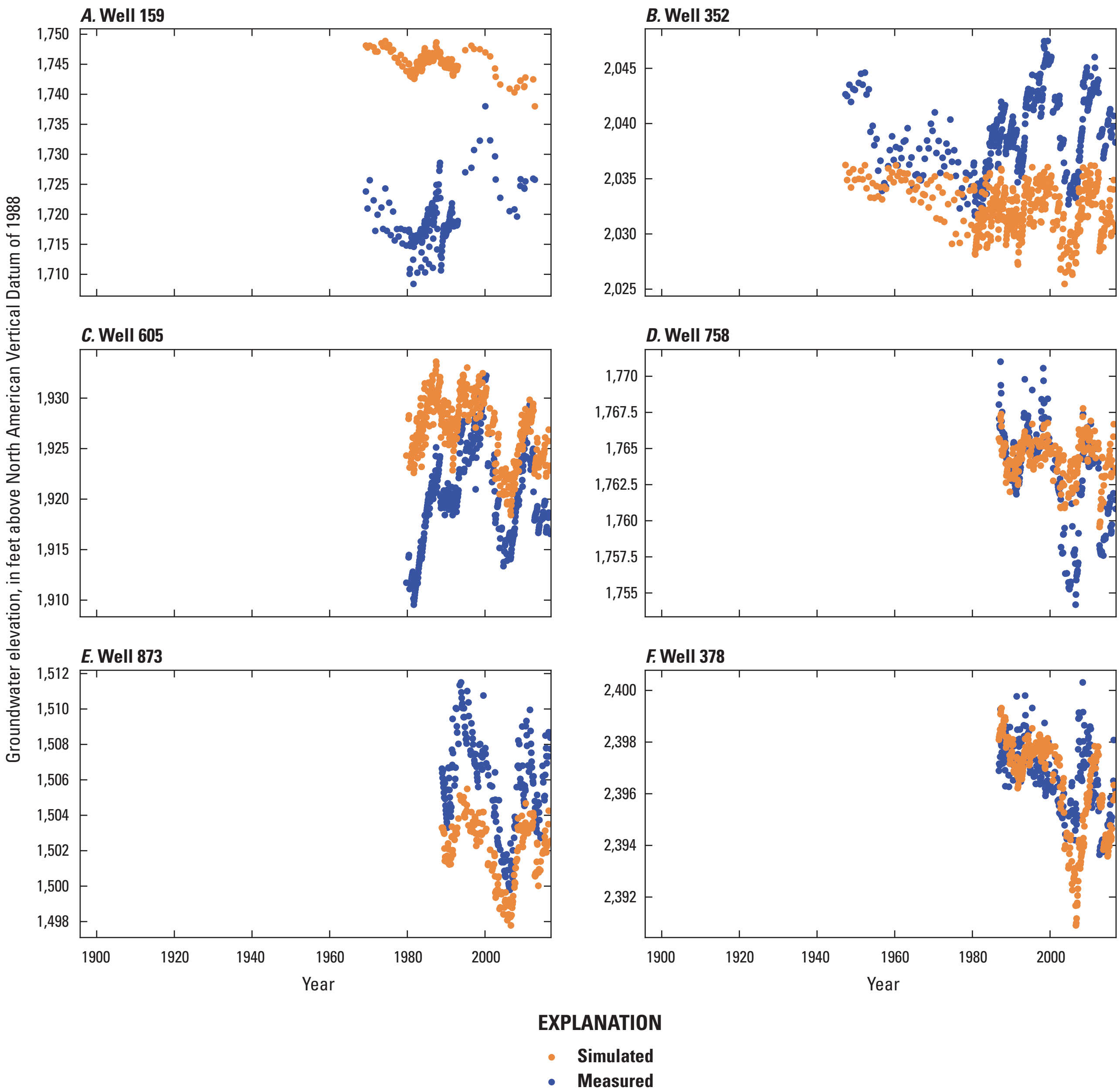

Figure 17. Measured and simulated groundwater-levels at observation wells in the Central Platte Integrated Hydrologic Model. *A*, Observation well 159. *B*, Observation well 352. *C*, Observation well 605. *D*, Observation well 758. *E*, Observation well 873. *F*, Observation well 378. Locations of observation wells shown on figure 13.

Calibrated Parameters

This section of the report describes the final calibrated values for the automated values of the 435 adjustable parameters in the six parameter groups for the CPIHM. The following sections will provide a summary of the final calibrated parameter values and a comparison to the initial parameter values to illustrate how the calibration changed the parameter values to improve the fit between the calibration targets and their simulated equivalent values. The summaries will focus on the hydraulic parameters contained in the core MODFLOW–NWT functionality of the CPIHM because the landscape and climate parameters contained in the FMP functionality of the CPIHM were fixed before the automated calibration process. A sensitivity analysis also summarizes which parameters had the largest effect on the model outputs, and parameter identifiability indicates how well the calibration target dataset informed the parameters, which is discussed in the next section of the report.

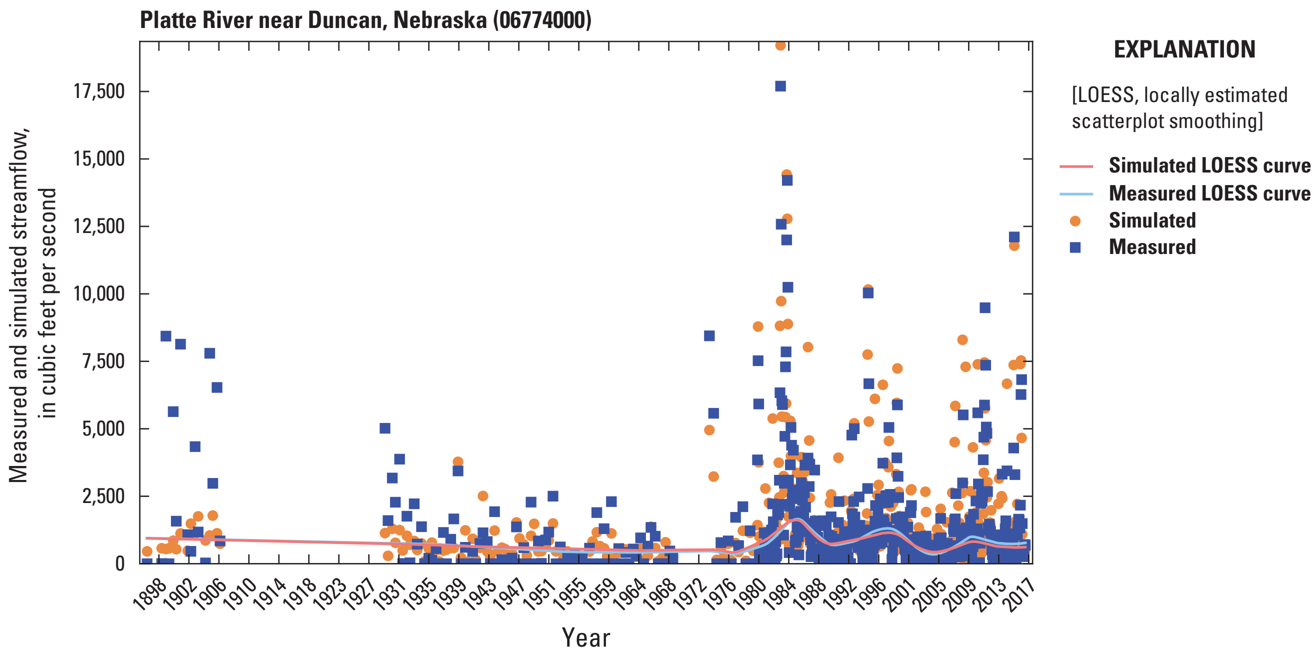

Figure 18. Measured compared to simulated streamflow and their respective locally estimated scatterplot smoothing (LOESS) line at the Platte River near Duncan, Nebraska, streamgage (U.S. Geological Survey streamgage 06774000) in the Central Platte Integrated Hydrologic Model.

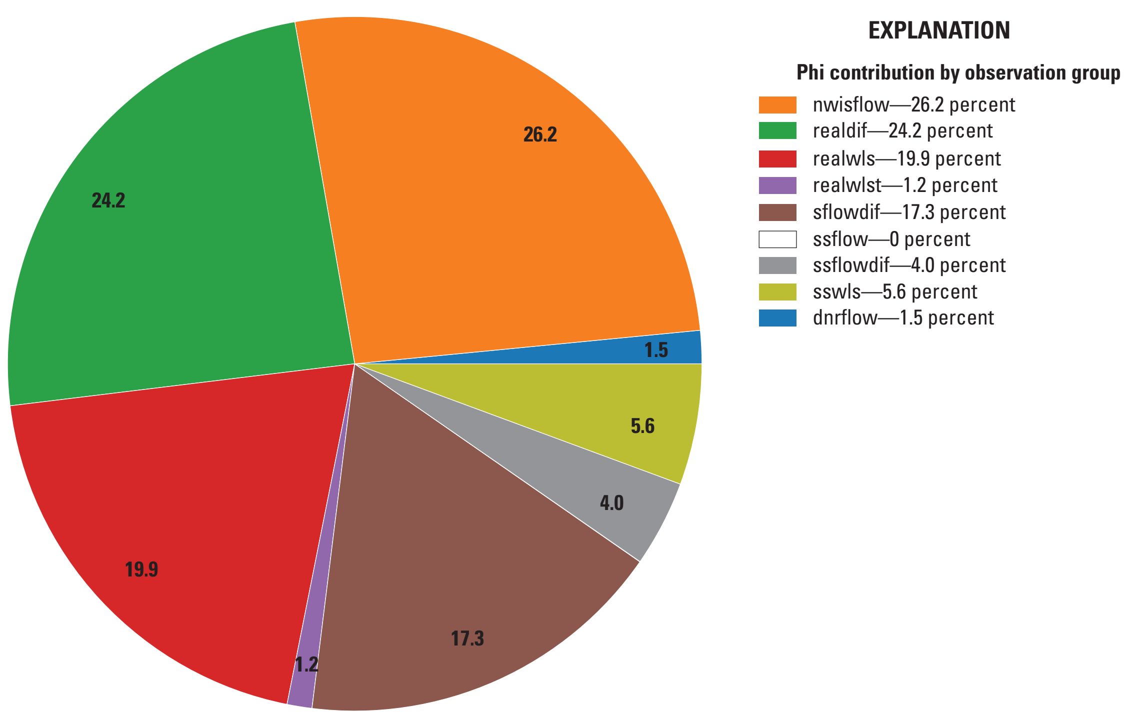

Figure 19. Distribution of phi values by observation group for the calibrated Central Platte Integrated Hydrologic Model.

Calibrated Groundwater-Flow Parameters

Calibrated Kh estimated at pilot points (fig. 13) and interpolated to the model grid kept the general trends and magnitude of the initially estimated hydraulic conductivity described in Houston and others (2013). The calibrated average Kh for layers 1, 2, and 3 were about 70, 32, and 35 ft/d, respectively (table 13). These numbers are all slightly higher (within 5 ft/d) than the initial starting values (table 1). Calibrated layer 1 Kh was generally less than 50 ft/d in the western region and more than 50 ft/d in the eastern region of the CPIHM (fig. 20*A*). Calibrated layer 2 Kh was generally less than 50 ft/d in almost all regions of the CPIHM except for the northeast corner where some Kh values were greater than 200 ft/d (fig. 20*B*); calibrated values greater than 200 ft/d were also simulated in the coincident COHYST model region in Peterson (2009). Calibrated layer 3 Kh was generally less than 40 ft/d in almost all regions of the CPIHM except for a west-central region where some Kh values were greater than 100 ft/d (fig. 20*C*). The highest Kh values for each layer were distributed around pilot points that had high initial values and were not outside the range of reasonable values for that layer; the high Kh values agreed with the test hole data from Houston and others (2013).

Calibrated anisotropy, the ratio of horizontal to vertical hydraulic conductivity (Kh:Kv) estimated at pilot points (fig. 13) and interpolated to the model grid remained in the general range of acceptable values for each layer. The average vertical anisotropy for layers 1, 2, and 3 were 9.73, 9.86, and 9.99, respectively, which were equated to vertical hydraulic conductivity values for all layers (between 0.33 and 31.70 ft/d), and the calibrated average vertical hydraulic conductivity for layers 1, 2, and 3 were 7.86, 3.41, and 3.60 ft/d, respectively (table 13). Calibrated layer 1 vertical hydraulic conductivity was between less than 7 ft/d in most of the western CPIHM domain and primarily between 7 and 20 ft/d in the southern and eastern domain (fig. 20*D*). Layer 2 vertical hydraulic conductivity was less than 10 ft/d for most of the CPIHM domain (fig. 20*E*). Calibrated layer 2 vertical hydraulic conductivity increased from the initial values in much of the central and southern CPIHM domain where it was present and generally decreased in the northern and eastern regions (fig. 20*E*). Calibrated layer 3 vertical hydraulic conductivity remained near initial values for most of the CPIHM domain except for two areas in the west where values were greater than about 10 ft/d (fig. 20*F*). The Sy, which was fixed during calibration, is shown in figure 20*G–I*.

Parameter Sensitivity and Identifiability

The automated calibration process includes the calculation of the sensitivity of simulated observations to model parameters, where sensitivity is the change in simulated observation divided by the change in a model parameter; PEST records sensitivities of simulated observations to each parameter in the Jacobian matrix (Doherty, 2005). Parameter sensitivities were extracted from the Jacobian matrix file written by PEST and composite parameter sensitivities were analyzed from the sensitivity file, also written by PEST, and are available in the model archive (Traylor, 2023). Parameter sensitivities can provide some insight into parameters that were most impactful during the calibration process. The parameter sensitivities were assessed by parameter group and the most sensitive group was the anisotropy pilot points (*apilotpts*) with an average composite sensitivity of 0.351. The Kh pilot points (*pilotpts*) group had a slightly smaller average sensitivity of 0.342. The streambed hydraulic conductivity group (*sfrprops*) was the least sensitive parameter group. The *apilopts* group and, to a slightly less extent, *pilotpts* were the most sensitive because the anisotropy parameters affected the magnitude of vertical flow in the development model. The present gradient between the layers where average simulated groundwater levels were lowest in layer 2 (table 12) coupled with the large amount of groundwater irrigation wells that pumped in the development model (more than 20,000 by 1980; fig. 3), affected the vertical flow dynamics and the groundwater levels in the transient system.

Parameter sensitivities for the final Jacobian matrix used for calibration, with fixed landscape parameters, were low compared to an assessment of parameter sensitivity with all parameters set as adjustable (fig. 21*A* and table 1.3). In the Jacobian matrix, calculated with all parameters set to adjustable, July and August development period ET_{ref} scale factor parameters were the most sensitive and, during preliminary calibration runs, exhibited large deviations from initial values that affected AET, deep percolation (recharge to the water table), and irrigation pumping (table 1.3). The Sy multiplier for layer 1 was also one of the most sensitive parameters (12 of 740) that deviated from reasonable values during preliminary calibration runs (table 1.3). The parameter sensitivities under the fixed scheme influenced the forecast uncertainties and are described in the "Forecast Uncertainty Analysis" section of this report.

Parameter sensitivities are one metric that can be useful in understanding the parameter behavior during calibration. In complex environmental models such as the CPIHM, parameters are often correlated because there are far fewer observations than parameters, which can limit the ability for PEST to fully resolve some or all parameters with a unique solution during calibration. Quantification of how PEST is able to resolve unique parameter values is known as "parameter identifiability." Parameter identifiability was assessed and provided insight into the information gained by each parameter from the calibration targets dataset during the calibration process and how well each parameter was uniquely estimated and correlated with other parameters (Doherty and Hunt, 2009; Doherty, 2015). Parameter identifiability was analyzed using pyEMU, an open-source Python module that offers a suite of tools to interrogate PEST files and analyze uncertainty (White and others, 2016). Identifiability values ranged from zero to one, where a value of one represented a parameter that could be uniquely resolved based on the information in

Table 13. Calibrated adjustable parameter summaries of the minimum, average, and maximum calibrated (posterior) values for pilot points and model grid.

[A, Soil group A; B, soil group B; C, soil group C; na, not applicable]

Parameter name	Calibrated parameter values, in feet per day					
	Pilot points			Model grid		
	Minimum	Average	Maximum	Minimum	Average	Maximum
Layer 1 horizontal hydraulic conductivity	6.90	75.41	232.96	6.90	70.38	232.96
Layer 2 horizontal hydraulic conductivity	3.48	33.19	252.00	3.48	31.63	252.00
Layer 3 horizontal hydraulic conductivity	5.04	38.19	169.23	5.04	34.50	169.23
Layer 1 vertical hydraulic conductivity	0.56	8.70	31.49	0.56 ([1]3.23)	7.86 ([1]9.73)	31.49 ([1]26.41)
Layer 2 vertical hydraulic conductivity	0.33	3.74	31.70	0.33 ([1]4.38)	3.41 ([1]9.86)	31.7 ([1]18.26)
Layer 3 vertical hydraulic conductivity	0.48	4.07	20.50	0.48 ([1]3.66)	3.6 ([1]9.99)	20.5 (23.54[1])
Streambed vertical hydraulic conductivity A	1.50	1.50	1.50	na	na	na
Streambed vertical hydraulic conductivity B	0.15	0.15	0.15	na	na	na
Streambed vertical hydraulic conductivity C	0.50	0.50	0.50	na	na	na
Streambed vertical hydraulic conductivity Cozad Canal	0.48	0.48	0.48	na	na	na
Streambed vertical hydraulic conductivity Dawson Canal	3.39	3.39	3.39	na	na	na
Streambed vertical hydraulic conductivity Elm Creek Canal	1.27	1.27	1.27	na	na	na
Streambed vertical hydraulic conductivity Gothenburg Canal	0.97	0.97	0.97	na	na	na
Streambed vertical hydraulic conductivity Kearney Canal	1.37	1.37	1.37	na	na	na
Streambed vertical hydraulic conductivity Orchard Canal	2.00	2.00	2.00	na	na	na
Streambed vertical hydraulic conductivity Six-mile Canal	5.18	5.18	5.18	na	na	na
Streambed vertical hydraulic conductivity Thirtymile Canal	10.63	10.63	10.63	na	na	na

[1]Calibrated vertical anisotropy.

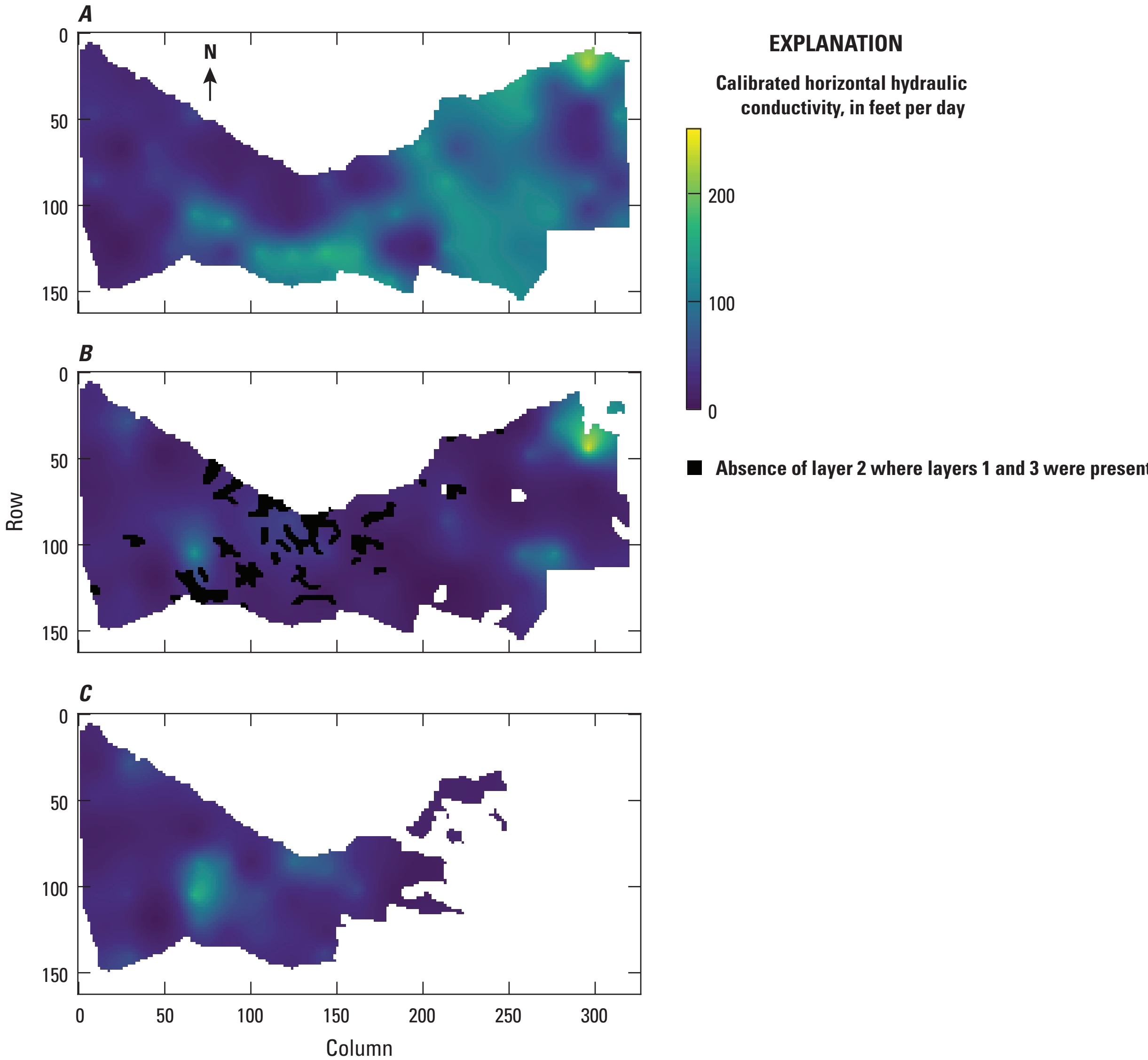

Figure 20. Central Platte Integrated Hydrologic Model calibrated aquifer properties for each layer. *A*, Horizontal hydraulic conductivity for layer 1. *B*, Horizontal hydraulic conductivity for layer 2. *C*, Horizontal hydraulic conductivity for layer 3. *D*, Anisotropy for layer 1. *E*, Anisotropy for layer 2. *F*, Anisotropy for layer 3. *G*, Input specific yield for layer 1. *H*, Input specific yield for layer 2. *I*, Input specific yield for layer 3.

the calibration target dataset; any error associated with the parameter was a result of noise or uncertainty in the calibration targets. Conversely, an identifiability of zero represented a parameter that gained no information from the calibration target dataset and did not cause a change to the residuals that were calculated at the calibration targets. Identifiability values between zero and one indicate that the parameter gained some information from the calibration targets during the calibration, but it also shares some information gained by the calibration target dataset with other parameters and cannot be uniquely solved (Doherty, 2015).

Overall, the pilot points for Kh parameters were the most identifiable as a group given the spatial distribution of the pilot points throughout the model domain and the number of observations in the calibration targets dataset. Individually, the most identifiable parameters in the CPIHM were the hcond_a2 (SFR vertical hydraulic conductivity of the streambed for soil type A), l2hkpp78 (layer 2 Kh at pilot point 78), and l3hkpp23 (layer 3 Kh at pilot point 23; fig. 21*B*), which were located downgradient of many groundwater-level observations that informed the groundwater-flow direction and reaction to stresses throughout the simulation period. Parameter hcond_a2 exhibited a low sensitivity of about 0.74 and was not in the top 50 most sensitive parameters shown in figure 21*A*. Whereas it could be the most uniquely solved in the calibration (highest identifiability, shown in figure 21*B*), the low sensitivity indicated that it did not have a substantial impact on the calibration. The high identifiability of parameter hcond_a2 is likely

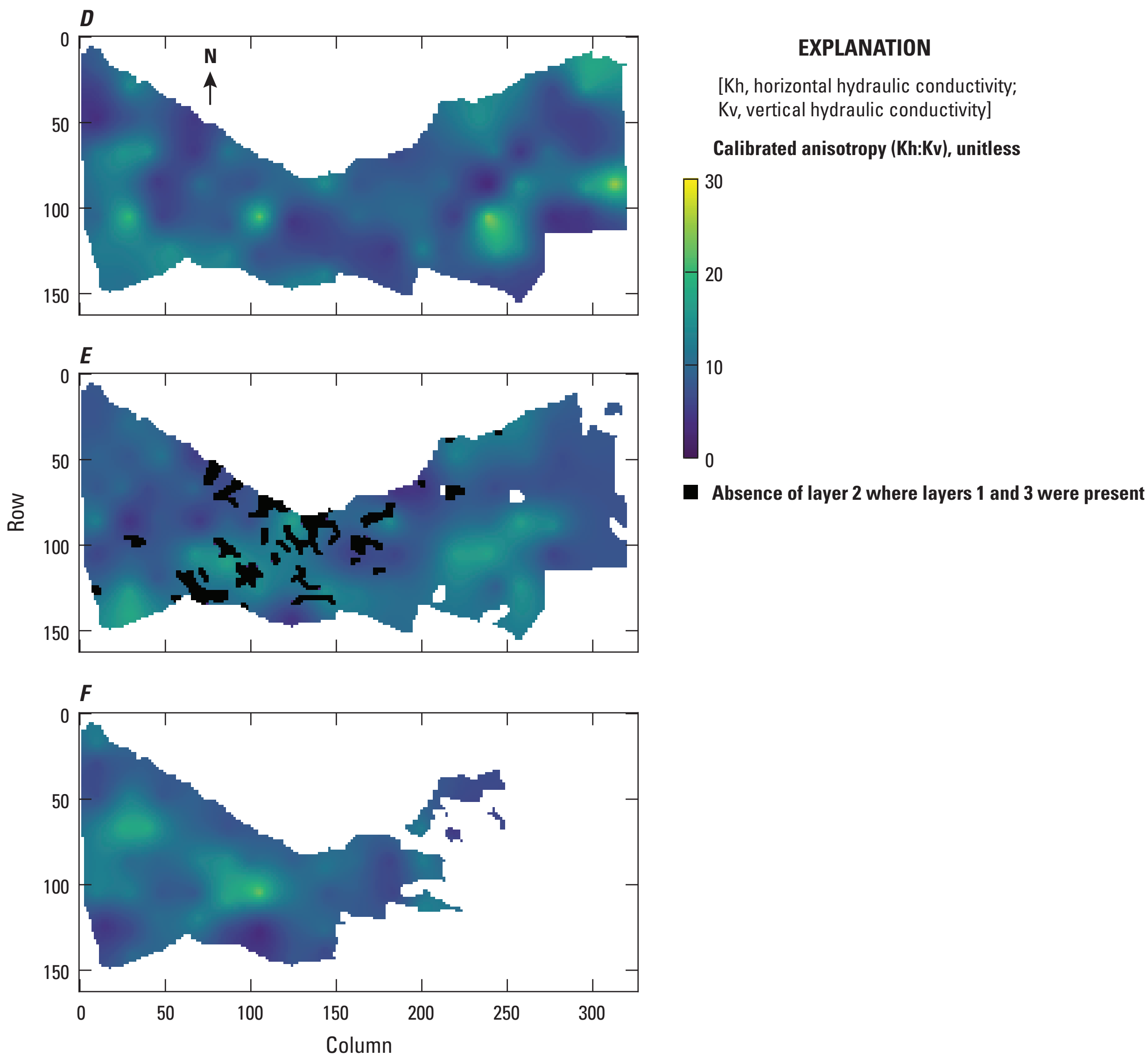

Figure 20.—Continued

because it was one of the parameters that spanned much of the model domain and could gain information from observations at many of the 53 streamgage observation locations also distributed across the model domain. Conversely, parameter l2hkpp78 exhibited a high sensitivity of about 1.54 (second most sensitive parameter), which, coupled with its high identifiability, indicated that it was more uniquely solvable and impactful to the calibration than other parameters except hcond_a2. Parameter l3hkpp23 exhibited a very low sensitivity of about 0.10 (332nd most sensitive parameters out of the 435 parameters); however, its identifiability indicated that it was more uniquely solvable than most parameters, but it was not particularly impactful to the calibration (fig. 21*A*–*B*).

Predevelopment and Development Period Simulated Results and Water Budgets

This section of the report describes the simulated landscape and groundwater-flow budgets for the CPIHM predevelopment (April 30, 1895) and development model (May 1, 1895, to December 31, 2016) and for the recent development period (January 1, 2011, to December 31, 2016). The accurate simulation of water-budget components is important to the efficacy of the model to simulate historical results and minimize or understand the bias that can transfer to the scenario results. Additionally, landscape and groundwater-flow budgets for the development model are described for the 24 GWMAs, as well as the CPNRD area, and the entire model area (called the “CPIHM domain”), which were made by grouping the 212 WBSs into larger areas of interest, in the CPIHM (fig. 9).

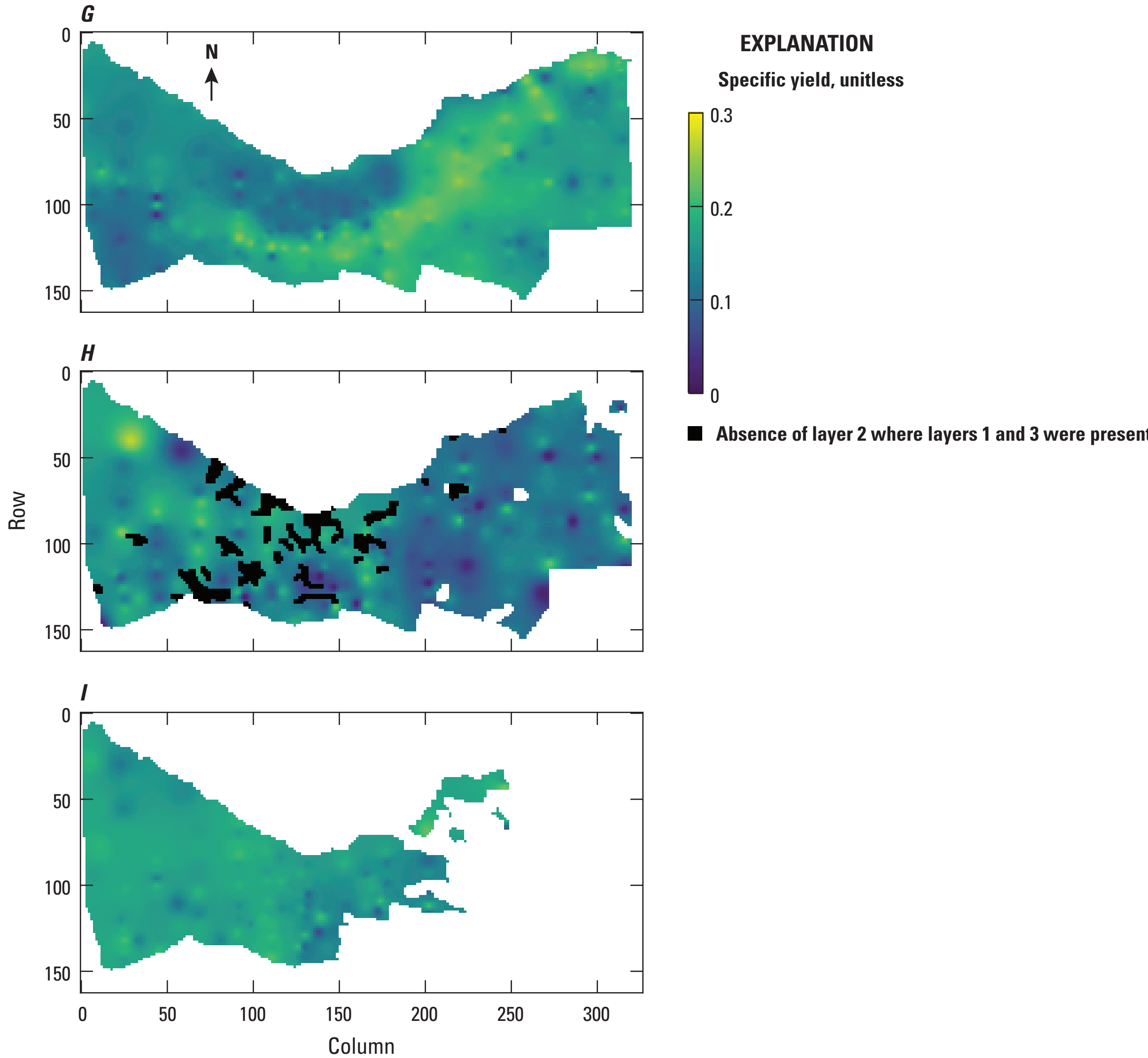

Figure 20.—Continued

Calculation of total inflows and outflows for the landscape budget does not include the hybrid Eg and Tg, as described in the "MODFLOW–One-Water Hydrologic Model Theory and Approach" section of this report. Also, where applicable, groundwater-flow budget components are expressed as net values, or the difference between inflows and outflows, for each component. Additional simulated budget details are available in appendix 3.

Landscape Water Budgets for the Central Platte Integrated Hydrological Model Domain

The calibrated predevelopment CPIHM produced landscape water-budget inflows and outflows that were meant to approximate the average conditions prior to surface-water and groundwater irrigation development and to provide reasonable initial conditions for the development CPIHM. Precipitation was the only inflow to the landscape subsystem with an average annual flux of 10,937,662 acre-ft/yr (26.6 inches). Total outflows were distributed among Ep, Tp, Ei, Ti, deep percolation, and runoff. The primary outflow was Ep with an average annual flux of about 6,362,644 acre-ft/yr (58 percent of the outflows). The sum of Ep and Tp, evapotranspiration of precipitation (ETp), accounted for 97 percent of the outflows from the landscape subsystem with an average annual flux of 10,577,561 acre-ft/yr (25.8 inches). The average annual flux for deep percolation and runoff were 91,687 acre-ft/yr (0.22 inches) and 268,414 acre-ft/yr (0.65 inches), respectively (Traylor, 2023).

The calibrated development CPIHM produced landscape water-budget inflows and outflows that maintained the general trends and magnitudes similar to the conceptual understanding of the landscape water subsystem (fig. 22; table 14). Total

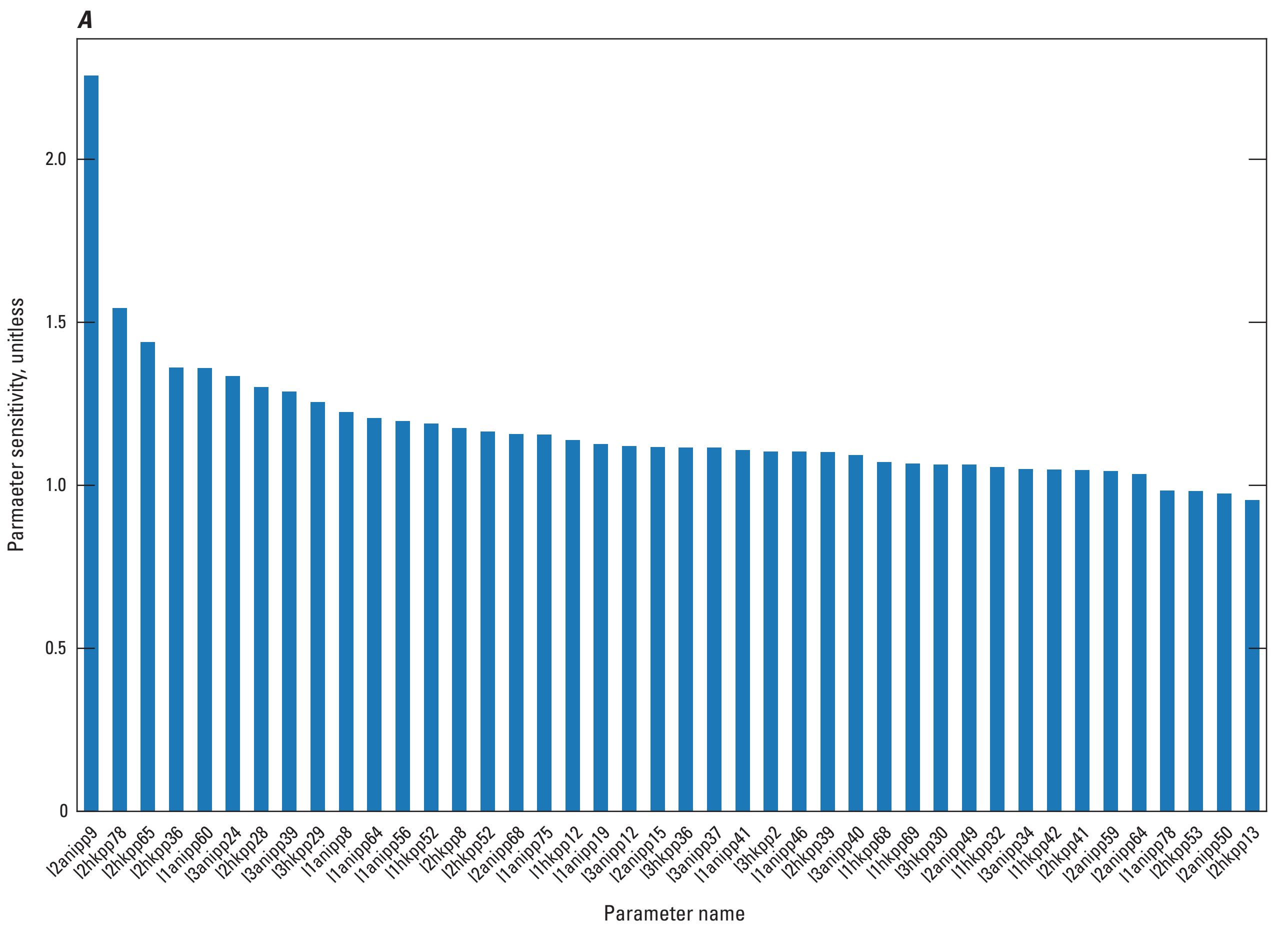

Figure 21. Sensitivity and identifiability of Central Platte Integrated Hydrologic Model Parameters. *A*, Sensitivity of the 42 most sensitive parameters. *B*, Identifiability for the 42 most identifiable parameters.

inflows to the landscape, prior to groundwater irrigation development, were largely from precipitation, with minor amounts from surface-water deliveries for irrigation. The average annual flux of precipitation was 9,978,276 acre-ft/yr (24.3 inches if spread equally across the model domain), or about 93 percent of the inflows to the landscape for the development period (May 1, 1895, to December 31, 2016) (table 14). The average annual total outflows from the landscape during the development period were 10,709,293 acre-ft/yr and the primary outflows were to Tp (4,184,162 acre-ft/yr) and Ep (3,751,102 acre-ft/yr); ETp accounted for about 80 percent of the outflows from the landscape at 7,935,263 acre-ft/yr (table 14 shows Ep and Tp). Compared to the estimates for evapotranspiration of irrigation plus precipitation for the CPIHM in table 2, which ranged from 8,600,000 to 11,000,000 acre-ft/yr, the sum of all evaporation and transpiration columns in table 14 total 8,554,930 acre-ft/yr. Deep percolation (recharge to the water table) and runoff were also substantial outflows from the landscape across the development period (1895–2016) with average annual fluxes of 1,122,257 (about 2.7 inches) and 1,032,106 (about 2.5 inches) acre-ft/yr, respectively (table 14). Further, the deep percolation values on irrigated land and dry cropland simulated by the CPIHM were in accord with recharge measurements from Steele and others (2014) and the overall average annual deep percolation of about 2.7 inches is within the ranges simulated by the models in Peterson (2009) and Peterson and others (2016) for this study area.

Temporal trends in the landscape budget were marked by the onset of widespread groundwater irrigation that was responsible for the increase in total inflows to the landscape during the development period; average annual total inflows for 1895–2016 and 2011–16 were 10,709,293 and 12,084,641 acre-ft/yr (table 14). The increase in total inflows led to an increase in total outflows primarily through an increase in deep percolation and ET of irrigation water (sum of Ei and Ti) (fig. 22). The ETp declined after about 1960; however, total landscape-derived ET, the ETp and irrigation water (sum of Ep, Ei, Tp, and Ti), exhibited less than a 2-percent increase in the recent development period (2011 to 2016) compared to the pre-1940 development period (fig. 23). The landscape water budgets for the development CPIHM were similar from 1895 to about 1960 whereby the budget was primarily affected by inflows from annual precipitation and outflows to ET of that

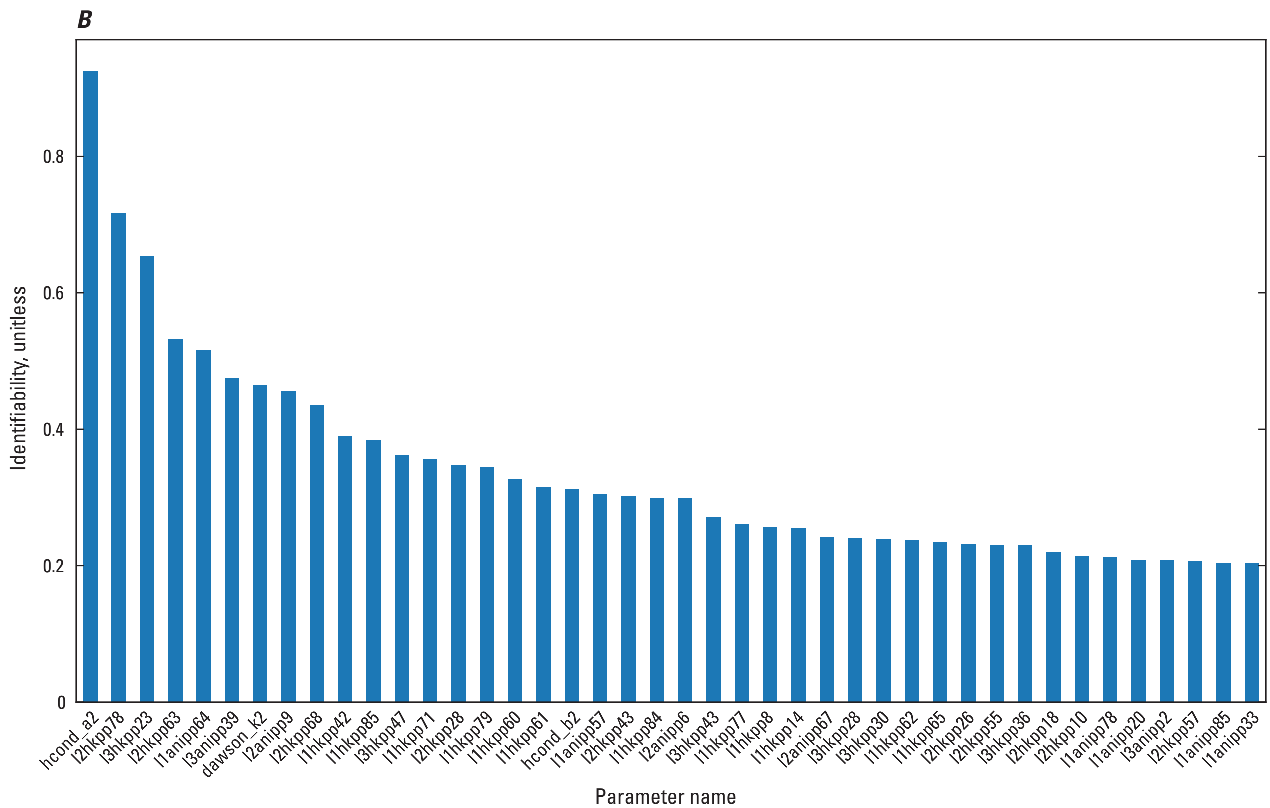

Figure 21.—Continued

precipitation. After about 1960, the increase in groundwater irrigation for crops added additional outflows as ET of the irrigation water (fig. 22, 23). The large increase in irrigation after 1960 was the primary cause of the increase in deep percolation from about 660,000 acre-ft/yr (1895–1960 average) to about 1,700,000 acre-ft/yr (1961–2016 average; fig. 22). Another factor that contributed to the substantial increase in deep percolation was a 7-percent increase in average precipitation after 1960.

In the last 5 years of the development model simulation (2011–16), the average annual volume of total landscape ET, which included ET of precipitation and irrigation water sources, was 8,420,099 acre-ft/yr, about 11 percent less than the conceptual model estimate of 9,500,000 acre-ft/yr for the same time period but only 4.5 percent less than the estimated range of uncertainty for ET from the conceptual estimates in table 2 (table 14). The average deep percolation and runoff volumes simulated for the last 5 years of the development period (2011–16) were 2,056,936 and 1,607,607 acre-ft/yr, respectively. Monthly trends from 1980–2016 indicated that the largest rates of deep percolation occurred in the spring (April and May) when precipitation was highest, and ETp was relatively low compared to peak growing season (July) ET (fig. 24).

The manually calibrated development period average annual ET_{ref} increased from 57.4 to 74.5 inches, a 30-percent increase from the precalibrated ET_{ref} (fig. 25). The reduction in ET_{ref} after 1980 is a result of different scale factors applied to the bi-annual and monthly stress periods to account for monthly dynamics in ET; however, this reduction was not present in the annual simulated total landscape ET, which increased by less than 2 percent for the development period owing to an increase in ET from irrigation water, as stated previously in the discussion of temporal trends (figs. 22, 23). The average monthly ET_{ref} increased 13-percent from the precalibrated ET_{ref}, for May through September (fig. 26, 10*B*). The increase in ET_{ref} was necessary because it led to an increase in the CWD for all crop types and increased the CIR for irrigated crops to values that were similar to conceptual estimates of total landscape ET and groundwater irrigation pumping.

Although some simulated landscape flow components such as irrigation pumping and ET were a little different than conceptual estimates, they still represented the conceptual model within expected uncertainty. The landscape budget simulated by the CPIHM can be considered a more precise representation of the landscape water budget than the conceptual flux estimates from table 2, because the conceptual estimates are uncertain, but also because the simulated budgets are calibrated and reconciled with simulated groundwater flow.

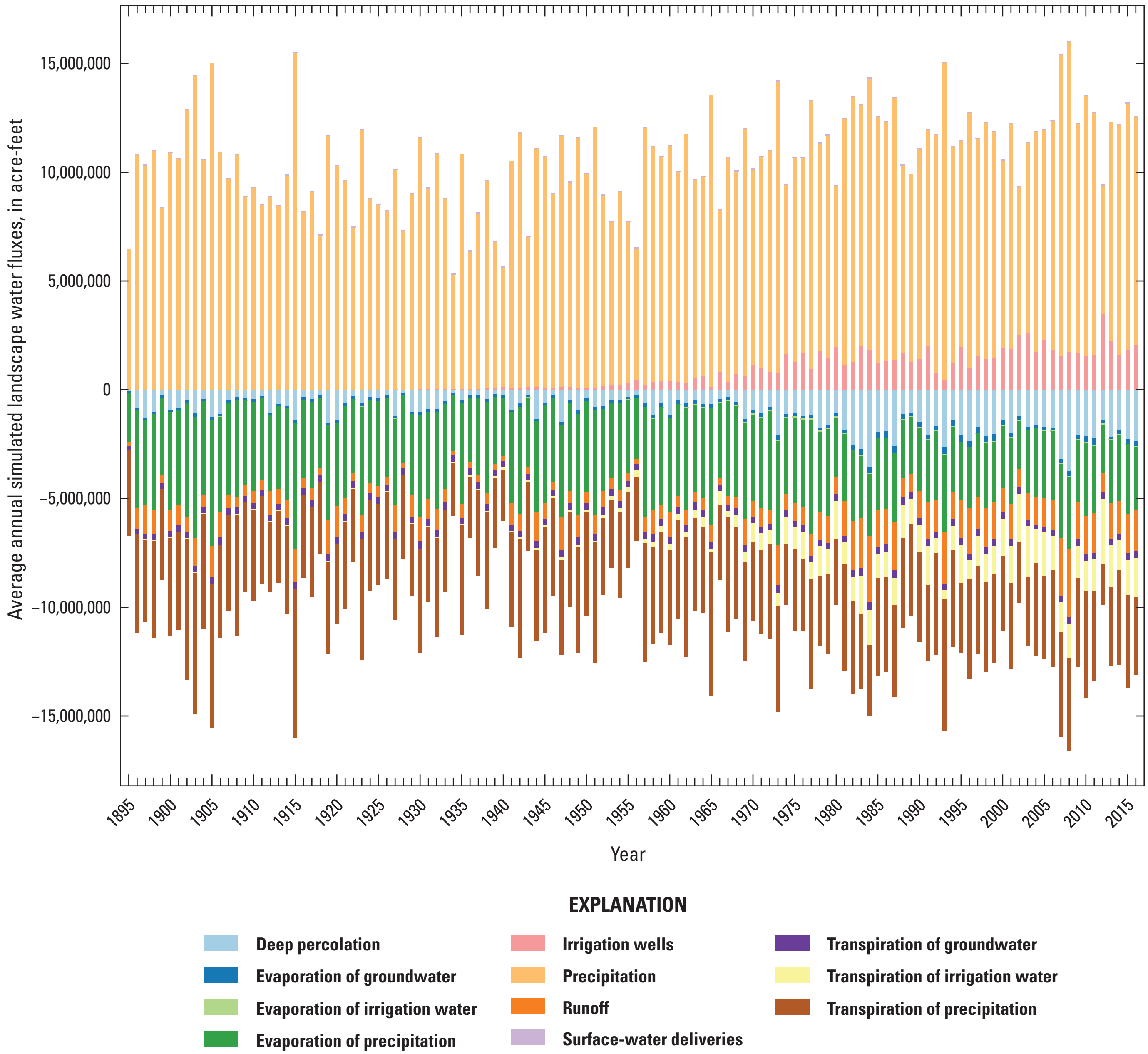

Figure 22. Simulated annual landscape water-budget volumes for the development period Central Platte Integrated Hydrologic Model (1895–2016).

Table 14. Average annual Central Platte Integrated Hydrologic Model landscape budgets for the landscape development period (1895–2016) and landscape recent development period (2011–16).

[CPIHM, Central Platte Integrated Hydrologic Model; CPNRD, Central Platte Natural Resources District; GWMA, Groundwater Management Area]

GWMA/ supergroup	Area (acres)	Inflows			Outflows							
		Precipitation	Irrigation from wells	Surface-water deliveries	Evaporation of groundwater	Transpiration of groundwater	Evaporation of irrigation water	Evaporation of precipitation	Transpiration of irrigation water	Transpiration of precipitation	Runoff	Deep percolation
Landscape water budget (1895–2016), in acre-feet per year												
1	115,520	211,042	6,642	0	0	0	−139	−80,639	−5,724	−110,884	−9,591	−10,707
2	43,360	79,564	13,052	0	0	0	−302	−31,834	−11,079	−33,475	−7,271	−8,656
3	127,040	235,973	45,399	18,200	−1,906	−6,719	−4,145	−91,826	−41,994	−93,775	−26,980	−40,853
4	180,640	343,827	21,137	16,317	−16,879	−47,146	−2,244	−129,395	−25,210	−130,223	−42,688	−51,521
5	102,720	187,826	7,506	0	0	0	−210	−76,087	−6,201	−93,233	−9,515	−10,087
6	90,240	167,749	3,814	0	0	0	−76	−61,721	−3,269	−90,478	−7,703	−8,314
7	234,880	453,336	11,584	0	−114	−156	−265	−163,501	−9,862	−246,652	−23,187	−21,454
8	40,480	79,093	9,117	1,459	−3,197	−7,286	−384	−29,205	−8,432	−28,233	−11,372	−12,041
9	179,200	353,334	23,795	0	−3	−302	−517	−129,724	−20,427	−169,350	−29,188	−27,924
10	51,360	103,333	16,882	0	−395	−225	−442	−37,252	−14,097	−40,409	−15,372	−12,643
11	154,880	320,205	19,877	0	−15,864	−53,688	−531	−115,820	−16,515	−99,928	−57,736	−49,552
12	50,240	102,419	5,383	0	0	0	−102	−37,373	−4,684	−48,452	−8,398	−8,792
13	85,280	177,461	11,970	0	0	−548	−260	−61,218	−10,265	−80,839	−20,839	−16,011
14	106,880	222,158	37,119	0	−63	−2,770	−927	−79,543	−31,144	−88,403	−28,945	−30,316
15	57,440	123,158	13,286	0	−8	−264	−299	−44,512	−11,378	−48,503	−15,788	−15,965
16	45,280	96,654	6,284	0	0	−146	−129	−33,750	−5,433	−46,162	−8,257	−9,208
17	108,640	230,811	23,034	0	−1,631	−13,799	−561	−83,513	−19,492	−83,592	−33,627	−33,059
18	73,920	158,815	6,515	0	−6,300	−20,421	−170	−57,698	−5,455	−51,939	−24,152	−25,916
19	71,200	152,210	3,189	0	−17,056	−33,286	−85	−56,417	−2,663	−41,229	−24,493	−30,512
20	51,200	112,383	4,093	0	−184	−3,530	−87	−39,800	−3,526	−50,583	−10,540	−11,939
21	67,840	149,213	7,119	0	−1,446	−3,176	−167	−53,230	−6,060	−63,664	−14,885	−18,325
22	28,000	62,221	1,941	0	−4,914	−7,925	−42	−24,168	−1,665	−19,385	−9,067	−9,836
23	45,440	101,736	994	0	−13,415	−17,486	−24	−36,634	−842	−26,954	−17,562	−20,714
24	30,560	68,758	5,371	0	−573	−1,045	−125	−24,458	−4,575	−27,475	−8,006	−9,489
CPNRD	2,142,236	4,293,620	305,102	35,976	−83,947	−219,917	−12,231	−1,579,452	−269,994	−1,813,935	−465,203	−493,883
CPIHM	4,926,071	9,978,276	693,171	37,846	−157,001	−305,327	−22,796	−3,751,102	−596,871	−4,184,162	−1,032,106	−1,122,257

Table 14. Average annual Central Platte Integrated Hydrologic Model landscape budgets for the landscape development period (1895–2016) and landscape recent development period (2011–16).—Continued

[CPIHM, Central Platte Integrated Hydrologic Model; CPNRD, Central Platte Natural Resources District; GWMA, Groundwater Management Area]

GWMA/ supergroup	Area (acres)	Inflows			Outflows							
		Precipitation	Irrigation from wells	Surface-water deliveries	Evaporation of groundwater	Transpiration of groundwater	Evaporation of irrigation water	Evaporation of precipitation	Transpiration of irrigation water	Transpiration of precipitation	Runoff	Deep percolation
Landscape water budget (2011–16), in acre-feet per year												
1	115,520	198,814	23,887	0	0	0	−473	−59,478	−20,994	−107,724	−14,770	−19,263
2	43,360	77,264	40,569	0	0	0	−796	−25,280	−35,613	−27,615	−11,064	−17,465
3	127,040	227,346	119,809	14,060	−837	−3,409	−5,957	−70,978	−100,167	−81,802	−36,643	−65,668
4	180,640	336,832	55,591	21,076	−26,778	−42,929	−3,020	−101,282	−59,627	−112,949	−57,661	−78,960
5	102,720	181,112	25,394	0	0	0	−584	−57,493	−21,866	−93,441	−14,403	−18,719
6	90,240	149,127	12,343	0	0	0	−216	−42,101	−10,893	−85,388	−10,300	−12,573
7	234,880	435,659	38,022	0	−232	−98	−757	−119,831	−33,309	−241,253	−36,987	−41,543
8	40,480	77,576	29,466	177	−575	−3,596	−723	−24,223	−25,295	−24,316	−13,851	−18,811
9	179,200	346,091	75,555	0	−3	−193	−1,471	−97,328	−66,435	−151,641	−46,428	−58,343
10	51,360	103,456	36,987	0	−189	−70	−721	−28,672	−32,518	−32,297	−22,183	−24,051
11	154,880	315,005	44,513	0	−16,829	−49,447	−795	−92,652	−39,266	−79,639	−73,674	−73,491
12	50,240	103,359	22,702	0	0	0	−415	−29,096	−20,017	−42,200	−14,860	−19,473
13	85,280	176,437	38,005	0	0	−180	−727	−47,466	−33,458	−69,439	−30,893	−32,460
14	106,880	220,260	90,130	0	−3	−640	−1,718	−64,583	−79,223	−66,668	−41,756	−56,442
15	57,440	121,699	41,155	0	−5	−164	−911	−35,532	−35,793	−36,923	−22,731	−30,963
16	45,280	99,291	21,292	0	0	−123	−416	−27,554	−18,747	−39,209	−14,908	−19,749
17	108,640	231,021	62,551	0	−1,676	−13,278	−1,214	−66,025	−55,044	−60,683	−51,405	−59,201
18	73,920	161,955	17,109	0	−9,829	−27,344	−315	−47,507	−15,083	−28,919	−40,276	−46,964
19	71,200	153,793	9,292	0	−21,642	−33,867	−169	−46,385	−8,192	−25,360	−36,796	−46,183
20	51,200	113,769	13,971	0	−306	−5,139	−308	−30,934	−12,133	−41,338	−19,208	−23,819
21	67,840	156,220	20,931	0	−1,949	−3,072	−403	−40,779	−18,434	−58,593	−25,729	−33,212
22	28,000	64,819	5,669	0	−5,480	−8,115	−108	−18,474	−4,988	−14,677	−14,553	−17,689
23	45,440	107,553	2,774	0	−22,577	−15,964	−53	−30,439	−2,443	−12,501	−28,850	−36,041
24	30,560	73,153	14,942	0	−1,248	−1,358	−289	−19,333	−13,155	−21,424	−14,748	−19,147
CPNRD	2,142,236	4,231,962	862,655	35,313	−110,158	−208,984	−22,560	−1,223,528	−762,691	−1,556,083	−694,748	−870,319
CPIHM	4,926,071	9,913,820	2,132,994	37,827	−192,152	−299,387	−53,029	−2,870,143	−1,856,977	−3,639,950	−1,607,607	−2,056,936

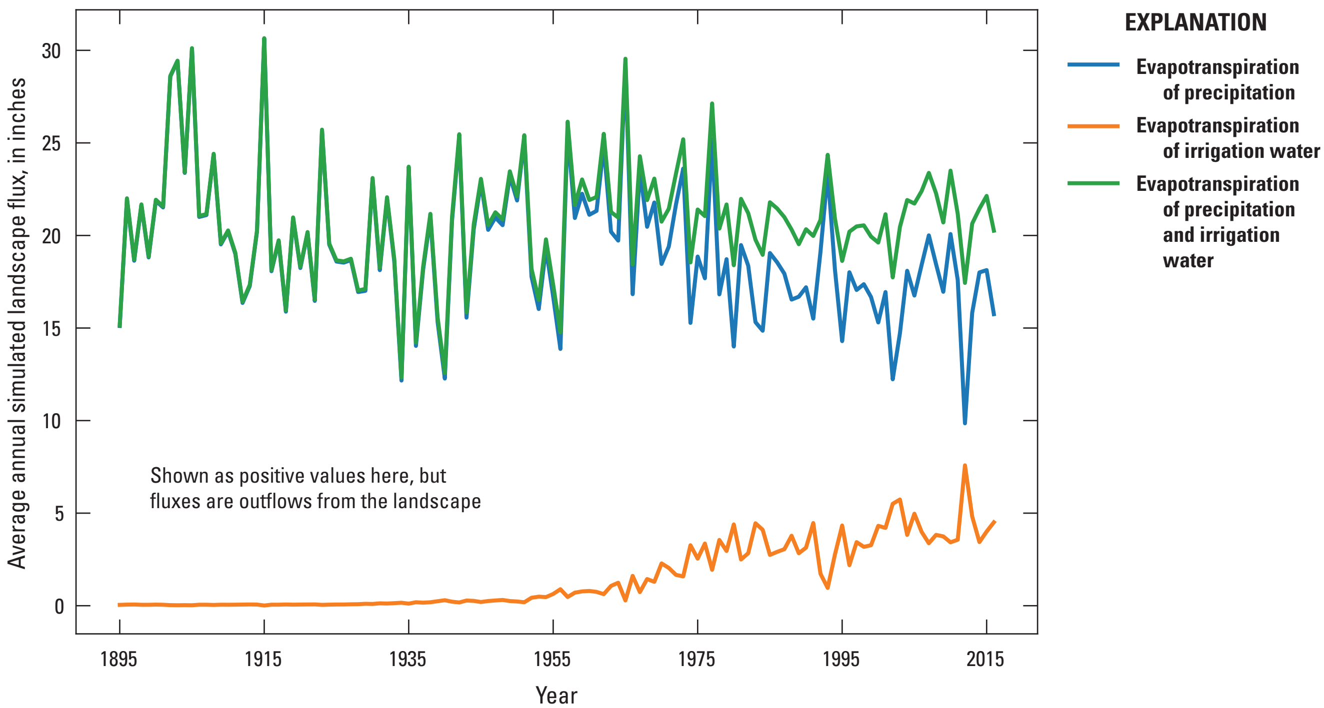

Figure 23. Simulated average annual evapotranspiration of precipitation, evapotranspiration of irrigation water, and evapotranspiration of precipitation and irrigation water for the calibrated Central Platte Integrated Hydrologic Model.

Landscape Water Budgets for Groundwater Management Areas and Other Domains

Simulated landscape water budgets were assessed for each GWMA and the CPNRD (table 14). The budgets for each GWMA and the CPNRD were similar to the CPIHM budget and were characterized by primary inflows from precipitation and large outflows to ET. Deep percolation was affected by three factors: precipitation; the amount of irrigation water from irrigation wells or surface-water deliveries; and ETg, which was linked to the depth of the water table. Like the CPIHM domain, GWMAs with large irrigation volumes per acre, such as GWMA 3 and 14 (fig. 9), also exhibited large volumes of recharge per acre (table 14, table 3.1). Similarly, GWMAs with large fluxes of precipitation (in the eastern region of the CPIHM) and shallow water tables with large fluxes of ETg, such as GWMAs 19, 22, and 23, also exhibited the large recharge volumes per acre (table 14, table 3.1). GWMAs 1, 6, and 7 exhibited the smallest deep percolation (recharge) volumes per acre because they were in the western region of the CPIHM with less precipitation and less irrigation (fig. 9; table 14, table 3.1). Larger amounts of deep percolation occurred on irrigated lands compared to dryland in the CPNRD (fig. 27). The average annual rates of deep percolation on irrigated land after 1980 (about 5.1 inches) were double the amount on nonirrigated land (about 2.4 inches), and both were within the ranges measured in Steele and others (2014). Further, the relation among precipitation, irrigation, and deep percolation was evident during years of extreme climate conditions. For example, deep percolation on irrigated and nonirrigated cropland was greater than the amount of irrigation pumpage in 1993 because it was the wettest year between 1981 and 2016 (fig. 27). As a result, the CIR was minimal and there was surplus precipitation that went to deep percolation. Conversely, 2002 and 2012 exhibited large irrigation pumpage and little recharge because these were severe drought years. CIR for the severe drought years was very high and there was minimal precipitation available for recharge (fig. 27).

Groundwater-Flow Budgets for the Central Platte Integrated Hydrologic Model Domain

The calibrated predevelopment CPIHM produced groundwater-budget inflows and outflows that were meant to approximate the average conditions prior to surface-water and groundwater irrigation development and to provide reasonable initial conditions for the development CPIHM. Total inflows and outflows were about 193,669,000 and 194,105,766 acre-ft/yr, respectively. Approximate steady-state conditions were achieved whereby the change in groundwater storage across the 500,000,000-day transient stress period was −572 acre-ft/yr. Stream leakage was the primary inflow to the groundwater subsystem, with a flux of 144,885,246 acre-ft/yr (75 percent of total inflows). Inflows to the study area across model boundaries accounted for 18 percent of total inflows and recharge from deep percolation accounted for 7 percent of total inflows. The primary outflow was to ETg, which constituted 53 percent of

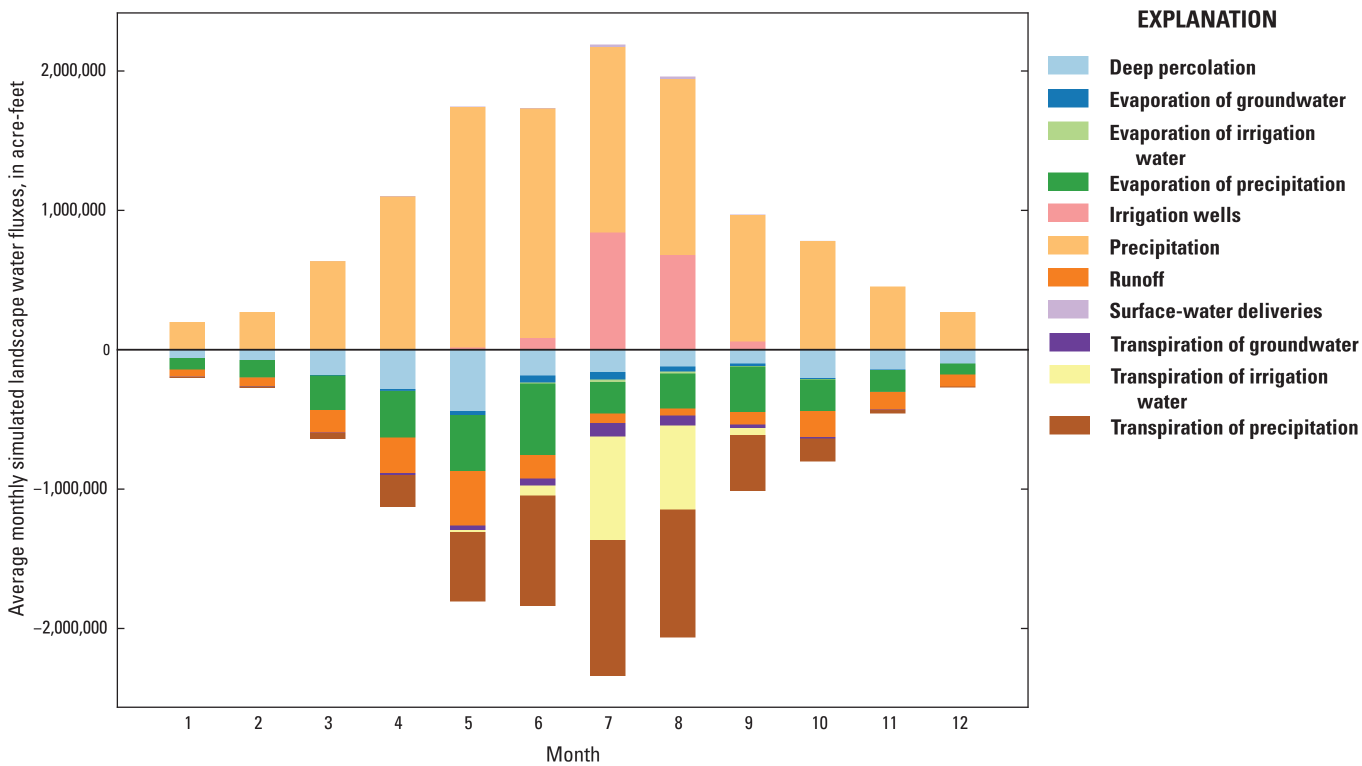

Figure 24. Simulated average monthly landscape water-budget volumes for the calibrated development period Central Platte Integrated Hydrologic Model (May 1, 1980–December 31, 2016).

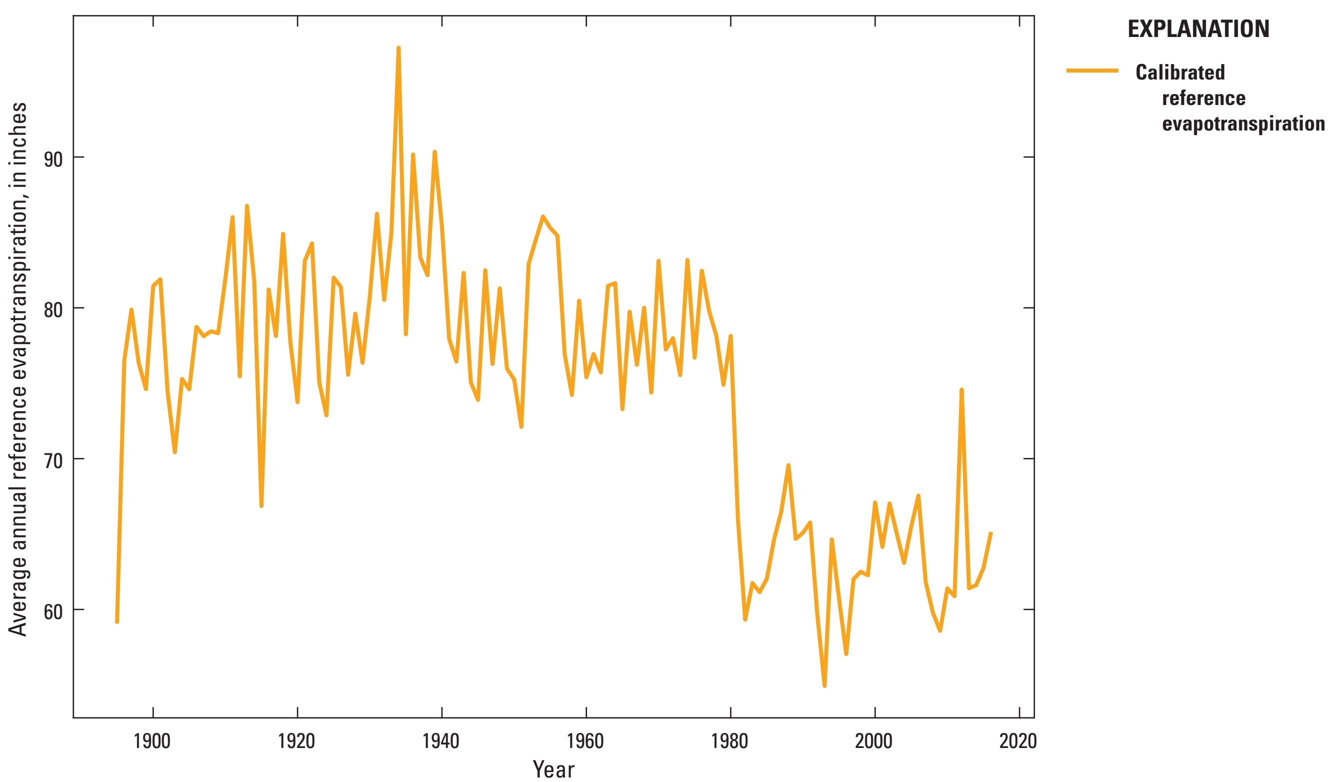

Figure 25. Simulated average annual reference evapotranspiration for the calibrated Central Platte Integrated Hydrologic Model.

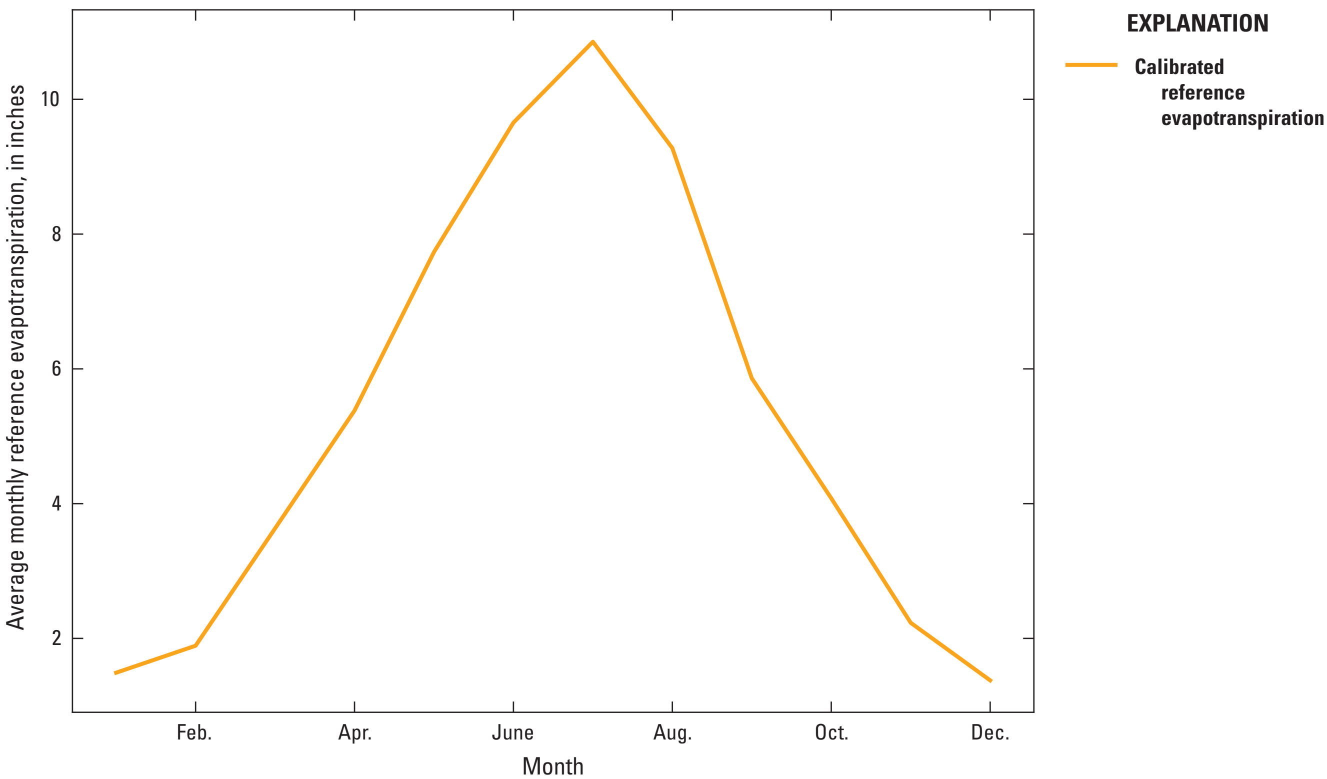

Figure 26. Simulated average monthly reference evapotranspiration for the calibrated Central Platte Integrated Hydrologic Model.

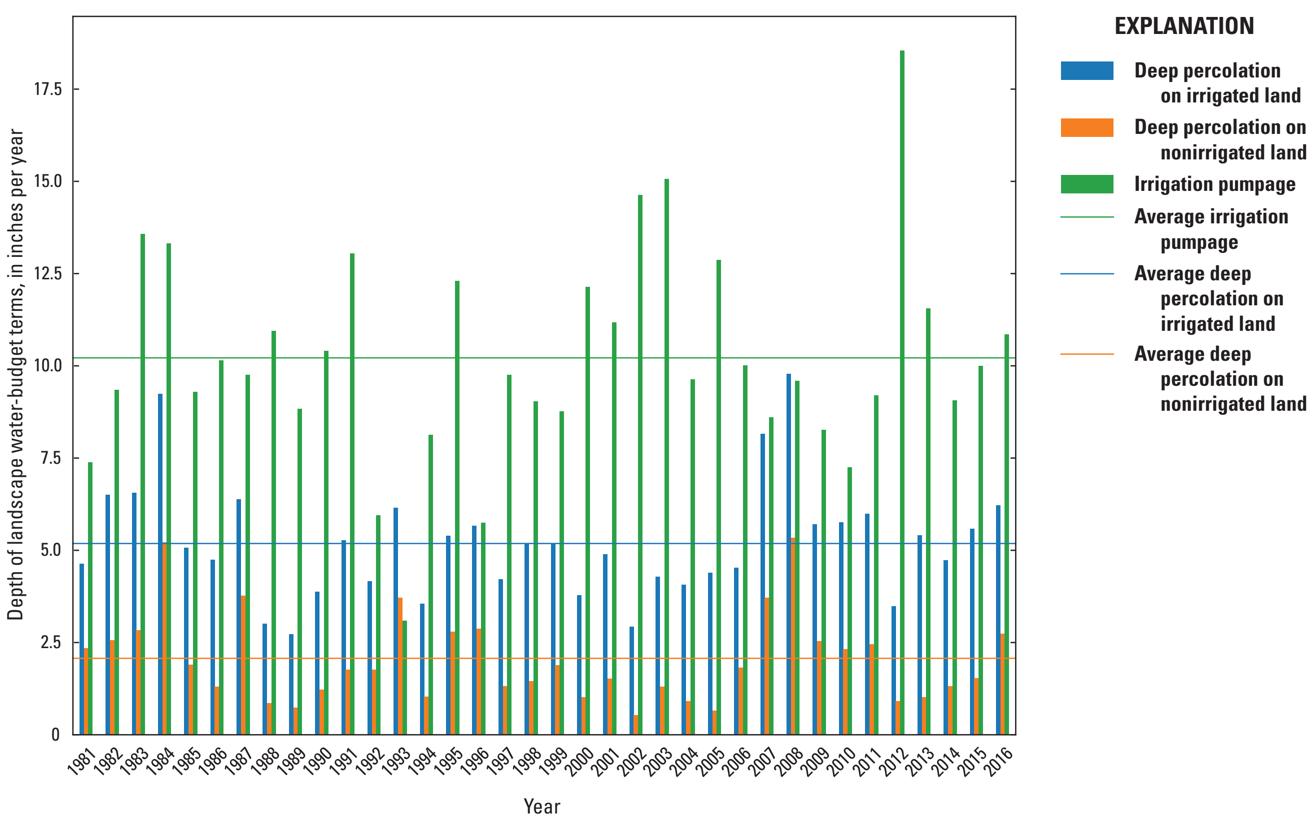

Figure 27. Average annual depths of water applied to the landscape by irrigation wells and deep percolation on irrigated land and nonirrigated land in the Central Platte Natural Resources District supergroup for the Central Platte Integrated Hydrologic Model.

Table 15. Average annual Central Platte Integrated Hydrologic Model groundwater budgets for the groundwater development period (1895–2016).—Left

[GWMA, Groundwater Management Area; CPNRD, Central Platte Natural Resources District; CPIHM, Central Platte Integrated Hydrologic Model; --, not applicable]

GWMA/supergroup	Area (acres)	Inflows					
		Inflow from general heads	Inflow from adjacent zones	Recharge (deep percolation)	Recharge from canal leakage	Release from groundwater storage	Stream leakage
Groundwater budget (1895–2016), in acre-feet per year							
1	115,520	--	15,913	10,685	--	11,052	10,483
2	43,360	--	11,417	8,619	--	12,487	5,483
3	127,040	--	27,869	37,451	1,957	36,504	46,326
4	180,640	--	87,843	30,440	3,335	29,902	83,516
5	102,720	18,381	19,327	10,066	2,342	9,811	4,325
6	90,240	--	12,619	8,299	--	5,845	5,399
7	234,880	--	35,657	21,341	--	21,548	11,874
8	40,480	--	23,022	8,280	--	11,509	22,513
9	179,200	--	32,422	27,758	--	26,724	10,200
10	51,360	--	11,307	12,473	--	14,114	4,995
11	154,880	--	19,347	26,219	--	30,646	74,597
12	50,240	--	6,669	8,780	--	7,031	556
13	85,280	--	18,410	15,855	--	14,395	2,942
14	106,880	--	9,016	29,226	--	36,107	17,627
15	57,440	--	11,985	15,792	--	13,365	1,603
16	45,280	--	5,678	9,135	--	7,843	1,310
17	108,640	--	13,182	26,894	--	28,821	17,985
18	73,920	--	17,321	15,828	--	16,052	12,136
19	71,200	--	24,077	12,628	--	13,246	23,748
20	51,200	--	4,463	10,380	--	8,252	825
21	67,840	4,299	37,007	16,714	--	10,969	1,450
22	28,000	--	10,549	5,383	--	4,549	21,337
23	45,440	924	25,879	9,154	--	7,844	9,722
24	30,560	3,217	28,011	8,807	--	6,973	0
CPNRD	2,142,236	26,820	102,659	386,219	7,634	385,597	390,951
CPIHM	4,926,071	139,233	--	1,122,257	74,005	863,519	602,318

total outflows. Discharge of groundwater to streams as base flow constituted 33 percent of total outflows, and outflows across model boundaries accounted for 14 percent of total outflows (Traylor, 2023).

The calibrated development CPIHM produced groundwater-flow budget inflows and outflows that reflected the transient conditions simulated in the development period model (table 15, 16). The largest inflow component was recharge (analogous to deep percolation from the landscape), with an average development period (May 1, 1895, to December 31, 2016) annual volume of 1,122,257 acre-ft/yr (table 15). Stream leakage (602,318 acre-ft/yr) was another major annual inflow, which indicated that the stream system in the CPIHM was an important contributor to the groundwater-flow system (table 15). The largest outflows were to irrigation wells (693,171 acre-ft/yr). Changes in groundwater storage were substantial during the development period; the replenishment of groundwater storage was −985,912 acre-ft/yr and releases from groundwater storage were 863,519 acre-ft/yr. The large releases from storage (groundwater-level declines) began to make a substantial impact on the groundwater-flow budget after about 1960 owing to the increase in groundwater pumping for irrigation (fig. 28*A*). The net storage changes were driven primarily by the relation between outflows to irrigation wells and farm net recharge each year; farm net recharge is the difference between recharge from deep percolation and ETg (fig. 28*B*). Generally, groundwater levels increased when outflows to

Table 15. Average annual Central Platte Integrated Hydrologic Model groundwater budgets for the groundwater development period (1895–2016).—Right

[GWMA, Groundwater Management Area; CPNRD, Central Platte Natural Resources District; CPIHM, Central Platte Integrated Hydrologic Model; --, not applicable]

Outflows						
Base flow	**Evapotranspiration from groundwater**	**Outflow to general heads**	**Outflow to irrigation wells**	**Outflow to production wells**	**Outflow to adjacent zones**	**Replenishment to groundwater storage**
Groundwater budget (1895–2016), in acre-feet per year						
--	--	--	−6,634	--	−24,361	−17,137
−1	--	--	−13,041	--	−12,437	−12,528
−8,575	−5,303	--	−45,330	−1,913	−50,638	−38,407
−112,468	−42,754	--	−21,117	−773	−27,019	−31,090
--	--	--	−7,497	--	−42,256	−14,501
--	--	--	−3,803	--	−17,100	−11,259
−451	−181	--	−11,561	−398	−46,296	−31,536
−12,340	−6,723	--	−9,106	--	−24,872	−12,299
−4,076	−193	--	−23,765	−254	−38,739	−30,103
−5,239	−482	--	−16,873	−225	−6,569	−13,525
−15,614	−46,109	--	−19,874	−6,728	−31,352	−31,223
--	--	--	−5,373	--	−10,154	−7,509
−3,071	−388	--	−11,959	−345	−20,795	−15,086
−3,714	−1,824	--	−37,104	−132	−14,566	−34,722
--	−185	--	−13,283	--	−15,406	−13,871
−1,283	−93	--	−6,277	--	−7,931	−8,405
−4,724	−9,315	--	−23,030	−987	−19,002	−30,039
−9,034	−16,631	--	−6,515	−194	−11,243	−18,004
−7,995	−32,344	--	−3,189	−123	−15,132	−15,044
−1,619	−2,157	--	−4,091	--	−6,997	−9,062
−816	−3,011	−6,115	−7,116	--	−40,434	−12,947
−19,498	−8,347	--	−1,941	--	−7,611	−4,433
−9,957	−19,250	−3,138	−993	--	−11,704	−8,484
−277	−934	−6,579	−5,370	--	−25,821	−8,028
−220,750	−196,223	−15,831	−304,834	−12,071	−122,123	−429,244
−492,357	−462,328	−152,343	−693,171	−16,733	--	−985,912

irrigation wells were less than farm net recharge (fig. 28*B*). The replenishment of storage came from a combination of groundwater flowing into the study area, recharge (deep percolation), and stream leakage (fig. 28*C*, shown as positive values of net streams). Prior to widespread irrigation development (about 1940), recharge was the primary source of water to replenish storage for most average and wet years. During dry periods, stream leakage became the dominant source of water to replenish storage (fig. 28*C*). After 1980, the average annual releases from groundwater storage were similar to those from recharge at about 1,957,000 acre-ft/yr and 1,941,000 acre-ft/yr, respectively. On average, the increase in outflows to irrigation wells were generally supported by increases in recharge throughout the development period except in dry years (for example, 2002, 2012) when farm net recharge was much less than outflows to irrigation wells. After 1980, even in dry years inflows from farm net recharge were generally greater than net streams (fig. 28*D*). Net replenishment to storage (negative net storage; groundwater-level rise) generally occurred during wet years or when the absolute magnitude of farm net recharge was greater than the absolute magnitude of irrigation wells (fig. 28*B*). Also, after 1980, the average annual depth (where depth represents a water-budget component expressed in terms of volume per area) of groundwater pumped by irrigation wells was 10.8 inches (1,698,000 acre-ft/yr), which was similar to the conceptual estimated depth of 10 inches (1,800,000 acre-ft/yr) from table 3 (fig. 27).

Table 16. Average annual Central Platte Integrated Hydrologic Model groundwater budgets for the groundwater recent development period (2011–16).—Left

[GWMA, Groundwater Management Area; CPNRD, Central Platte Natural Resources District; CPIHM, Central Platte Integrated Hydrologic Model; --, not applicable]

GWMA/ supergroup	Area (acres)	Inflows					
		Inflow from general heads	Inflow from adjacent zones	Recharge (deep percolation)	Recharge from canal leakage	Release from groundwater storage	Stream leakage
Groundwater budget (2011–16), in acre-feet per year							
1	115,520	--	13,877	19,263	--	34,828	10,196
2	43,360	--	17,312	17,465	--	35,336	6,973
3	127,040	--	35,546	63,435	1,990	97,729	53,465
4	180,640	--	99,933	52,653	5,711	76,728	91,236
5	102,720	28,649	23,712	18,720	4,007	30,533	5,770
6	90,240	--	12,620	12,573	--	18,836	5,433
7	234,880	--	29,056	41,431	--	59,760	10,237
8	40,480	--	25,639	16,742	--	25,921	8,485
9	179,200	--	34,869	58,241	--	79,794	16,430
10	51,360	--	11,485	23,974	--	35,532	9,529
11	154,880	--	16,230	47,633	--	73,638	89,961
12	50,240	--	6,517	19,474	--	24,429	452
13	85,280	--	16,798	32,400	--	39,480	4,701
14	106,880	--	9,569	56,071	--	88,657	27,849
15	57,440	--	16,360	30,875	--	37,356	1,508
16	45,280	--	5,643	19,673	--	22,836	2,781
17	108,640	--	13,854	52,158	--	70,391	20,825
18	73,920	--	15,441	30,754	--	35,765	12,535
19	71,200	--	22,958	23,081	--	29,644	18,299
20	51,200	--	4,046	21,034	--	20,813	1,530
21	67,840	4,405	35,149	31,169	--	27,299	1,612
22	28,000	--	11,461	10,967	--	11,597	17,884
23	45,440	807	27,908	17,125	--	16,294	6,999
24	30,560	3,204	30,730	17,851	--	16,189	0
CPNRD	2,142,236	37,064	111,827	734,785	11,709	1,009,413	424,690
CPIHM	4,926,071	184,003	--	2,056,936	124,583	2,326,871	673,118

The monthly trend in the simulated groundwater-flow budgets was typical of systems with large amounts of groundwater-irrigated cropland and characterized by large irrigation demands during the growing season. Monthly trends were assessed for the 1981 to 2016 period when the development model stress periods lengths changed to monthly (table 6). Recharge was the largest average monthly inflow from October to June (fig. 29). The largest volumes of recharge occurred in April, May, and October when groundwater pumping to irrigation wells was minimal or absent and precipitation was relatively high (fig. 29). The highest average monthly precipitation in the CPIHM was in June, but there was less recharge compared to April and May because the high landscape ET (1,306,656 acre-ft/yr) removed much of the precipitation that would have otherwise become recharge to the water table. The lowest volumes of recharge occurred in driest months of December, January, and February (fig. 29). The largest inflows to the groundwater-flow system during the 2 months with the highest irrigation (July and August) were caused by the release of groundwater from storage that supported the groundwater pumping during that time; the replenishment to storage occurred primarily during April, May, and October when recharge was highest (fig. 29). The average volume of water pumped for irrigation during July (814,815 acre-ft/yr) was more than twice as large as any other outflows for any month (replenishment to groundwater storage in May: −428,771 acre-ft/yr) (fig. 29).

Table 16. Average annual Central Platte Integrated Hydrologic Model groundwater budgets for the groundwater recent development period (2011–16).—Right

[GWMA, Groundwater Management Area; CPNRD, Central Platte Natural Resources District; CPIHM, Central Platte Integrated Hydrologic Model; --, not applicable]

Outflows						
Base flow	Evapotranspiration from groundwater	Outflow to general heads	Outflow to irrigation wells	Outflow to production wells	Outflow to adjacent zones	Replenishment to groundwater storage
Groundwater budget (2011–16), in acre-feet per year						
--	--	--	−23,887	--	−28,453	−25,824
0	--	--	−40,569	--	−9,903	−26,615
−3,259	−2,012	--	−119,810	−4,572	−39,640	−82,889
−126,514	−43,400	--	−55,591	−2,446	−28,103	−70,392
--	--	--	−25,394	--	−59,133	−26,864
--	--	--	−12,343	--	−21,112	−16,008
−479	−217	--	−38,022	−1,213	−53,624	−46,930
−3,289	−2,101	--	−29,466	--	−18,754	−23,205
−3,057	−92	--	−75,556	−809	−40,969	−68,884
−2,898	−182	--	−36,987	−536	−7,930	−32,080
−14,531	−40,418	--	−44,513	−22,330	−38,932	−67,127
--	--	--	−22,702	--	−9,102	−19,067
−1,282	−57	--	−38,005	−376	−19,243	−34,467
−1,208	−272	--	−90,130	−312	−12,306	−78,042
--	−81	--	−41,155	--	−13,138	−31,725
−1,833	−46	--	−21,292	--	−7,187	−20,586
−4,263	−7,911	--	−62,551	−1,881	−17,374	−63,358
−10,145	−20,962	--	−17,109	−351	−13,236	−32,905
−9,379	−32,407	--	−9,292	−394	−15,439	−27,282
−3,033	−2,659	--	−13,971	--	−7,673	−20,090
−458	−2,978	−6,342	−20,931	--	−44,472	−24,480
−21,111	−6,873	--	−5,669	--	−7,078	−11,222
−14,057	−19,625	−3,653	−2,774	--	−12,004	−17,025
−380	−1,310	−6,602	−14,942	--	−28,236	−16,503
−221,179	−183,604	−16,598	−862,661	−35,220	−128,184	−883,590
−500,972	−491,539	−153,012	−2,132,994	−43,314	--	−2,045,430

Groundwater-Flow Budgets for the Groundwater Management Areas and Other Domains

Individual simulated groundwater-flow budgets were assessed for each GWMA and the CPNRD for the development CPIHM. The budgets for each area were similar to the CPIHM budget, which is characterized by the largest inflows of recharge, largest outflows to irrigation wells, and large fluxes to and from groundwater storage (table 15). Other major inflows to many GWMAs and the CPNRD were the groundwater flows from adjacent zones upgradient and stream leakage (table 15). The spatial orientation of the CPNRD and the 24 GWMAs within the CPNRD along the Platte River corridor, perpendicular to the regional west to east direction of groundwater flow, caused most of the GWMAs to exhibit substantial inflows of groundwater from adjacent zones upgradient and outflows to adjacent downgradient zones (table 15). In the CPNRD, prior to 1960, the primary inflow was from streams and after 1960 the primary inflow was farm net recharge (recharge from deep percolation minus ETg) (fig. 28*D*). Like the CPIHM, the relation between outflows to irrigation wells and farm net recharge was the primary driver of net changes to storage within the CPNRD later in the development period; net replenishment to storage (groundwater-level rise) generally occurred when the difference between the absolute value of irrigation wells and farm net recharge was small (less than 270,000 acre-ft/yr). These results indicated that the groundwater was under more stress when irrigation

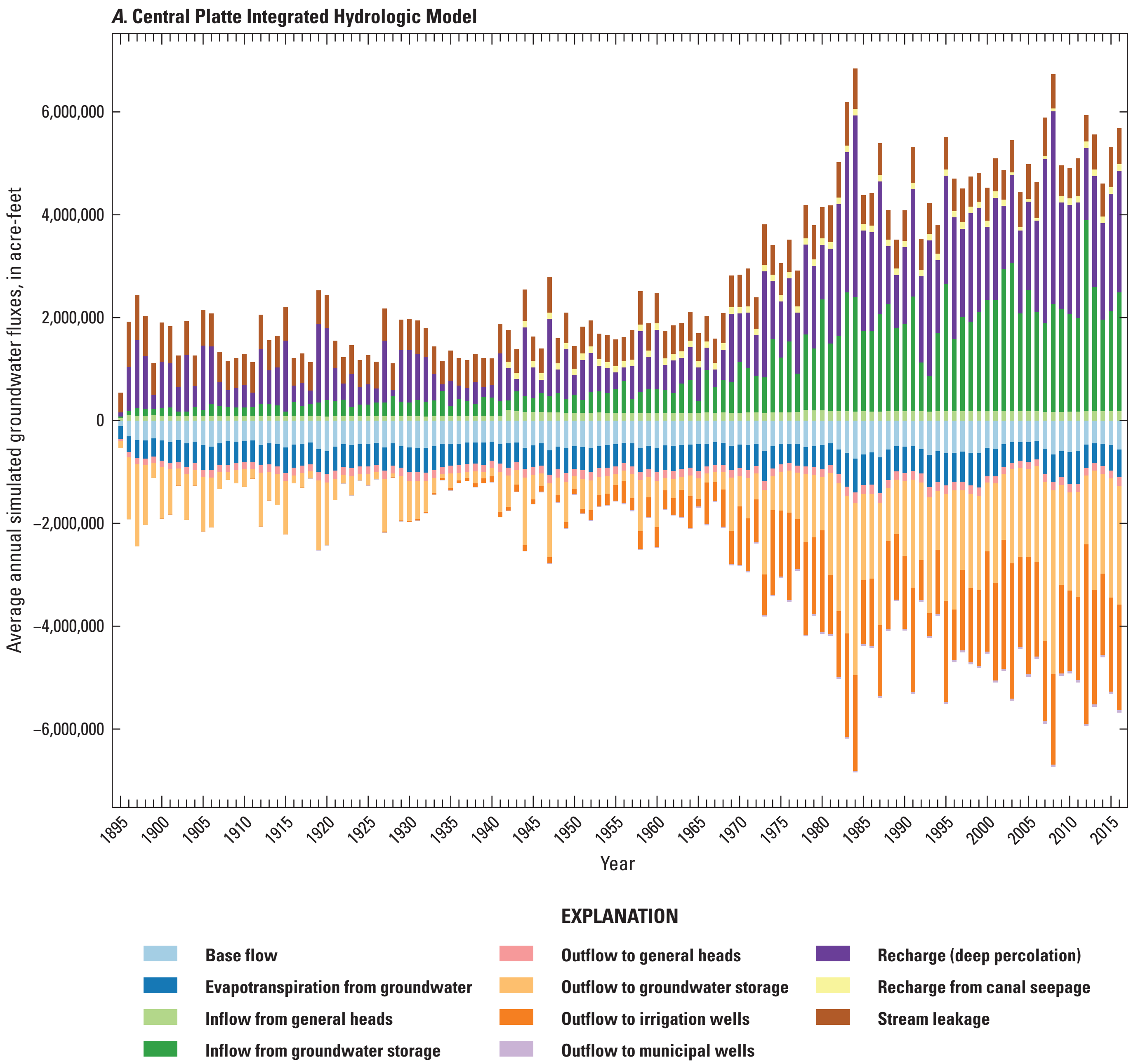

Figure 28. Simulated development period annual groundwater-flow budget components. *A*, Inflows and outflows by volume. *B*, Difference between the absolute value of outflows to irrigation wells and farm net recharge. *C*, Net components by volume for the Central Platte Integrated Hydrologic Model domain. *D*, Net components, for the Central Platte Natural Resource District. *E*, Difference between the absolute value of outflows to irrigation wells and farm net recharge for the Central Platte Natural Resource District. *F*, Net components by volumetric rate for the recent development period (2011–16) by Groundwater Management Area. *G*, Net volumetric rates for the difference between the absolute value of outflows to irrigation wells and farm net recharge, net storage, and net zone flow for the recent development period (2011–16) by Groundwater Management Area in the Central Platte Integrated Hydrologic Model.

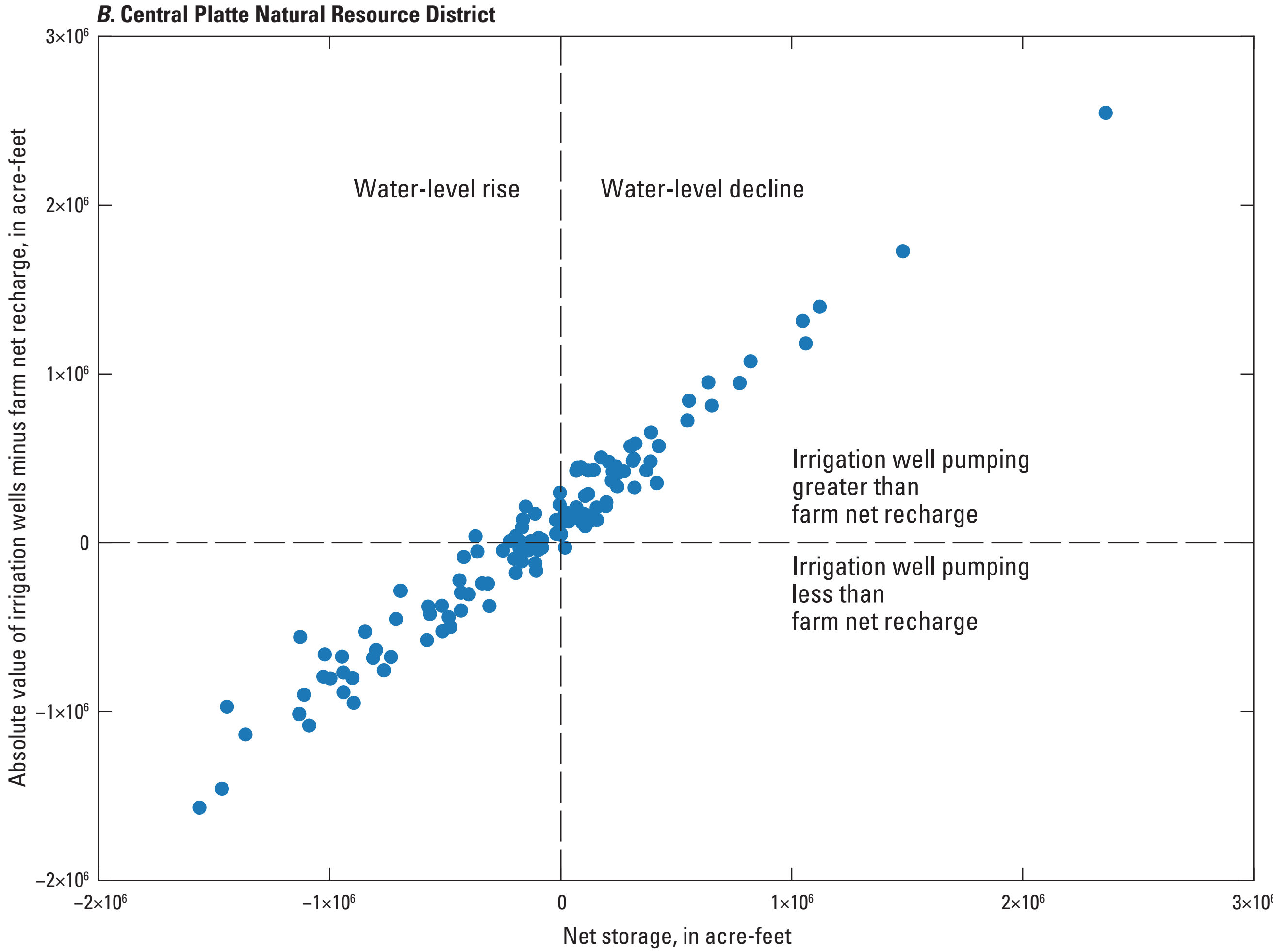

Figure 28.—Continued

pumping was high or recharge was low (fig. 28*E*). Net flow to and from the CPNRD (net zone flow) was a net outflow for 106 of the 122 years simulated in the development period and indicated that the loss of groundwater within the CPNRD may be attributed to a combination ETg, base flow, and outflow to irrigation wells (fig. 28*D*).

For the recent development period (2011–16), groundwater wells were the largest outflow for 21 of the 24 GWMAs, indicating that irrigation pumping is the dominant stress on most regions of the CPNRD. GWMAs 5, 19, and 23 were dominated by outflows of net zone flow, farm net recharge, and net streams, respectively, rather than irrigation pumping (fig. 28*F*, table 3.6). On average, changes in storage were driven by outflows to irrigation wells and farm net recharge for most GWMAs (fig. 28*F*, outflows are negative net values). Generally, GWMAs that exhibited net release to storage (groundwater-level decline) from 2011 to 2016 had larger imbalances between the magnitude of irrigation and farm net recharge, which indicated that recharge increases owing to pumping in these areas were less substantial and not enough to support those levels of pumping during that time period (fig. 28*F*, *G*). Further, the GWMAs that had smaller outflows to irrigation wells, coupled with low amounts of recharge, but exhibited net releases from storage (groundwater-level declines) generally had larger net outflows to adjacent zones, which indicated that net zone flow was an important contributor to the stability of the groundwater-flow system for these GWMAs (for example, GWMAs 1, 5, 6, 7; fig. 28*G*). Inflows from adjacent zones were larger than recharge (deep percolation) in 15 of the 24 GWMAs; however, net zone flow was less than zero (a net outflow) for 14 of 24 GWMAs, which indicated that more groundwater leaves a zone than enters (fig. 28*F*, table 15). For example, GWMAs 20 and 21 exhibited net releases from storage (positive net storage) despite having more net inflows from farm net recharge than irrigation pumping because they had substantial net outflows to adjacent zones (as negative net zones) (fig. 28*F*). The source of inflows to a GWMA was important in understanding the stability of the groundwater-flow system. The stability of the groundwater-flow system for each GWMA is influenced by activities and stresses within that area, such as pumping and recharge, but also the activities in GWMAs upgradient.

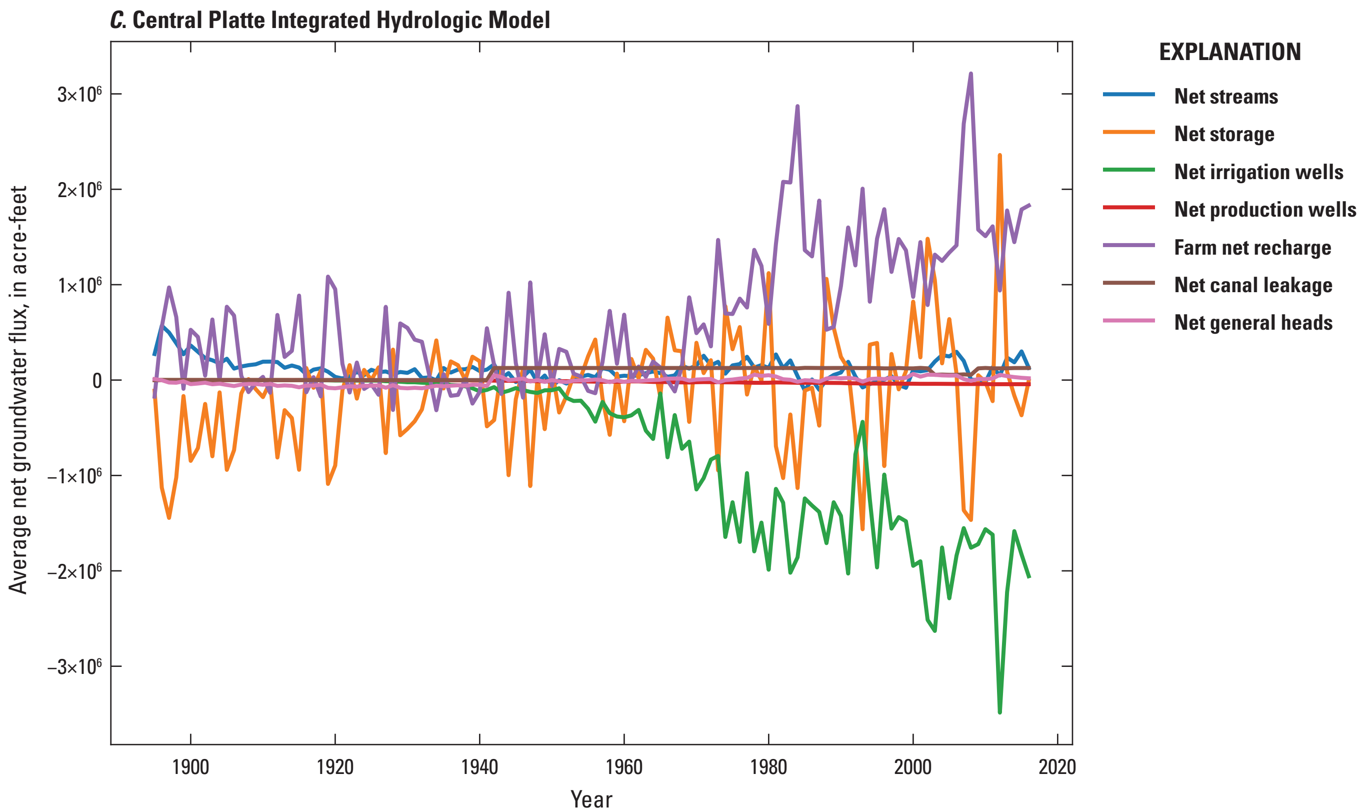

Figure 28.—Continued

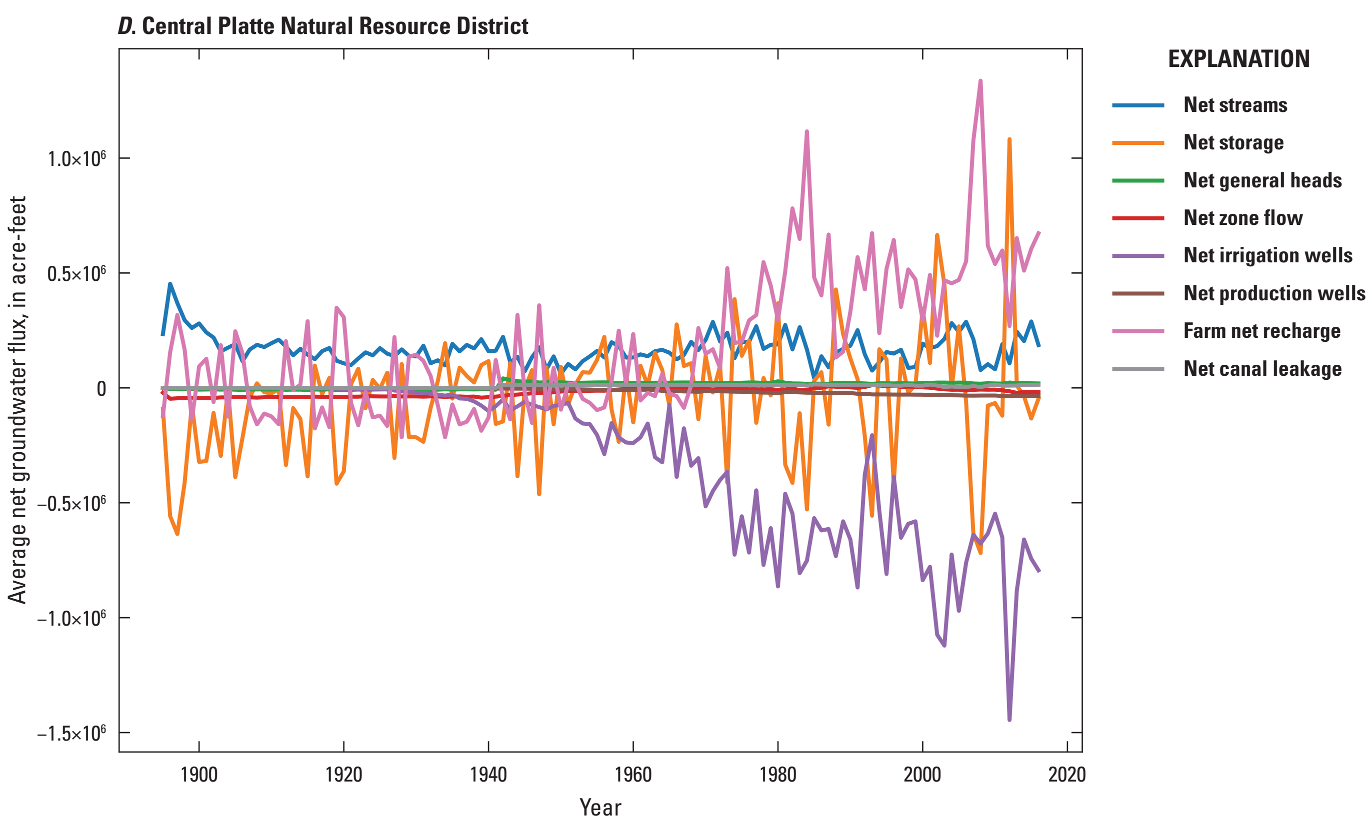

Figure 28.—Continued

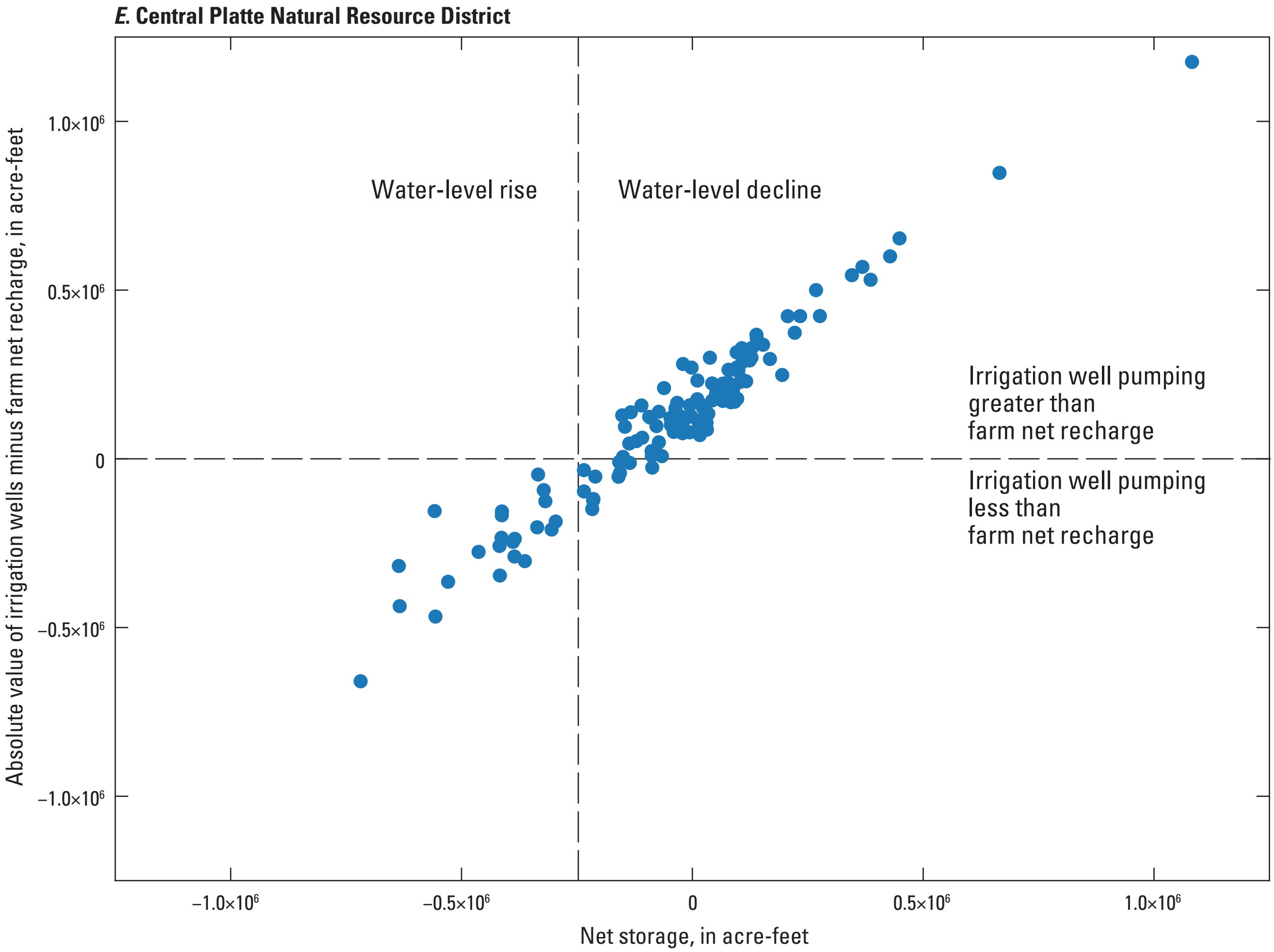

Figure 28.—Continued

Declines in an upgradient GWMA can cause less inflow of groundwater to the adjacent downgradient GWMAs even if the activities and stresses in the downgradient GWMA remain constant. If a GWMA receives more inflows from adjacent zones than other inflows, the groundwater-flow system of the GWMA is more influenced on activities upgradient. GWMAs 4, 8, 21, 23, and 24 each have greater than double the volume of inflows from adjacent zones compared to recharge (deep percolation) and are examples of areas that are more influenced by activities upgradient (table 15).

Scenario Simulated Groundwater Levels and Water Budgets Results

The CPIHM simulated the effects of eight different potential future climate and irrigation pumping scenarios on the landscape and groundwater-flow systems for 396 monthly stress periods from January 1, 2017, to December 31, 2049 (table 5 and 6). Initial conditions for each of the eight scenarios were specified using the simulated groundwater levels from the final stress period of the development-period CPIHM (stress period 610, with end date of December 31, 2016). The primary input datasets for each scenario were selected from the post-1980 development-period CPIHM to use realistic climate inputs of precipitation and ET_{ref}, land-use input, and stream inflows to the SFR network (table 17). The climate and streamflow inputs were selected as the year with climate and streamflow that most closely matched the monthly average for a moderately dry, very dry, or average condition. The averages were calculated from post-1980 monthly time series of precipitation and stream inflows used in the development-period CPIHM for a given condition. The monthly average for each condition was then compared to the post-1980 monthly time series of precipitation and stream inflows used in the development-period CPIHM where the year of data with the lowest coefficient of determination (R^2) to the monthly average determined the best match to the calculated average monthly average for a given condition. For example, to select an "average" year of precipitation data that was most representative of the typical month for a year of "average" precipitation, all "average" years of precipitation (40th to 60th percentile) post-1980 were averaged together to create an "average year month" dataset for comparison. The precipitation dataset

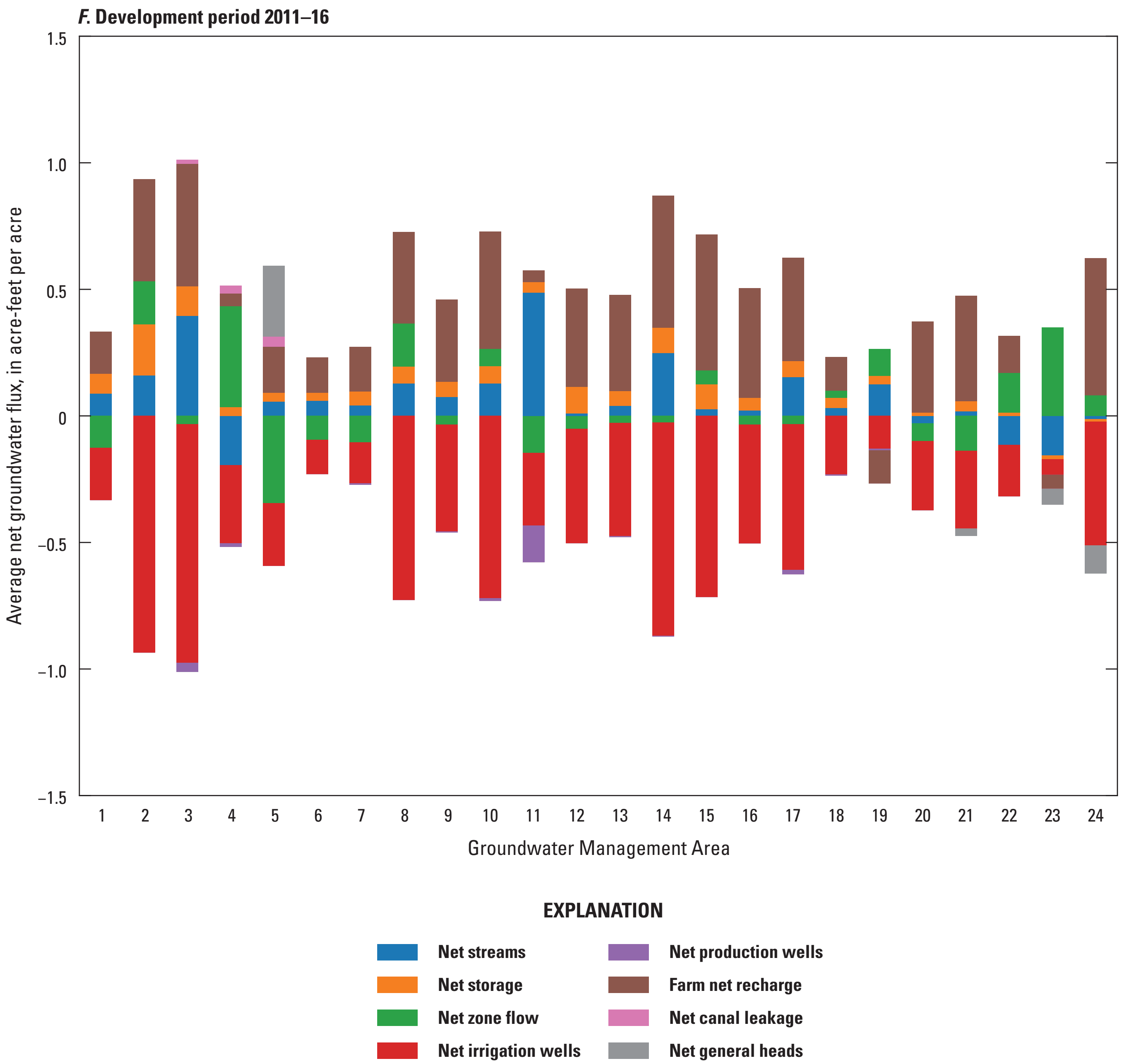

Figure 28.—Continued

from 1999 had the lowest R^2, indicating the January to December 1999 precipitation was most representative of the average monthly trend of an "average" year of precipitation. Drought years were also selected based on the intensity of the drought. The 3-year drought was an intense drought with total annual precipitation less than the 25th percentile post-1980, and the 10-year drought was a moderate drought with total annual precipitation between the 25th and 40th percentile post-1980. As with the "average" year selection, the moderate drought year was selected based on the month R^2 comparison to the "moderate drought year monthly trend." The intense 3-year drought was chosen based on recent familiarity with the 2012 drought. The climate input selected was from 1999 for average conditions, from 2012 for a 3-year drought, from 2013 for a 10-year drought, from 2013 for a mid-growing season drought, and from 1997 for an early growing season drought (table 17). Stream inflows specified were primarily the average year of 1991 inflows, considered average with respect to stream inflows, or the 2002 and 2003 inflows, considered dry years with respect to inflows, although 2003 inflows were less than 2002 owing to decreased releases in 2003 from Lake McConaughy (not shown), located about 70 miles upstream from the study area (table 17). Other model inputs such as GHB flow or crop parameters were held constant at their end of development period values for the entire scenario period. The 2016 land-use dataset was repeated each year for all

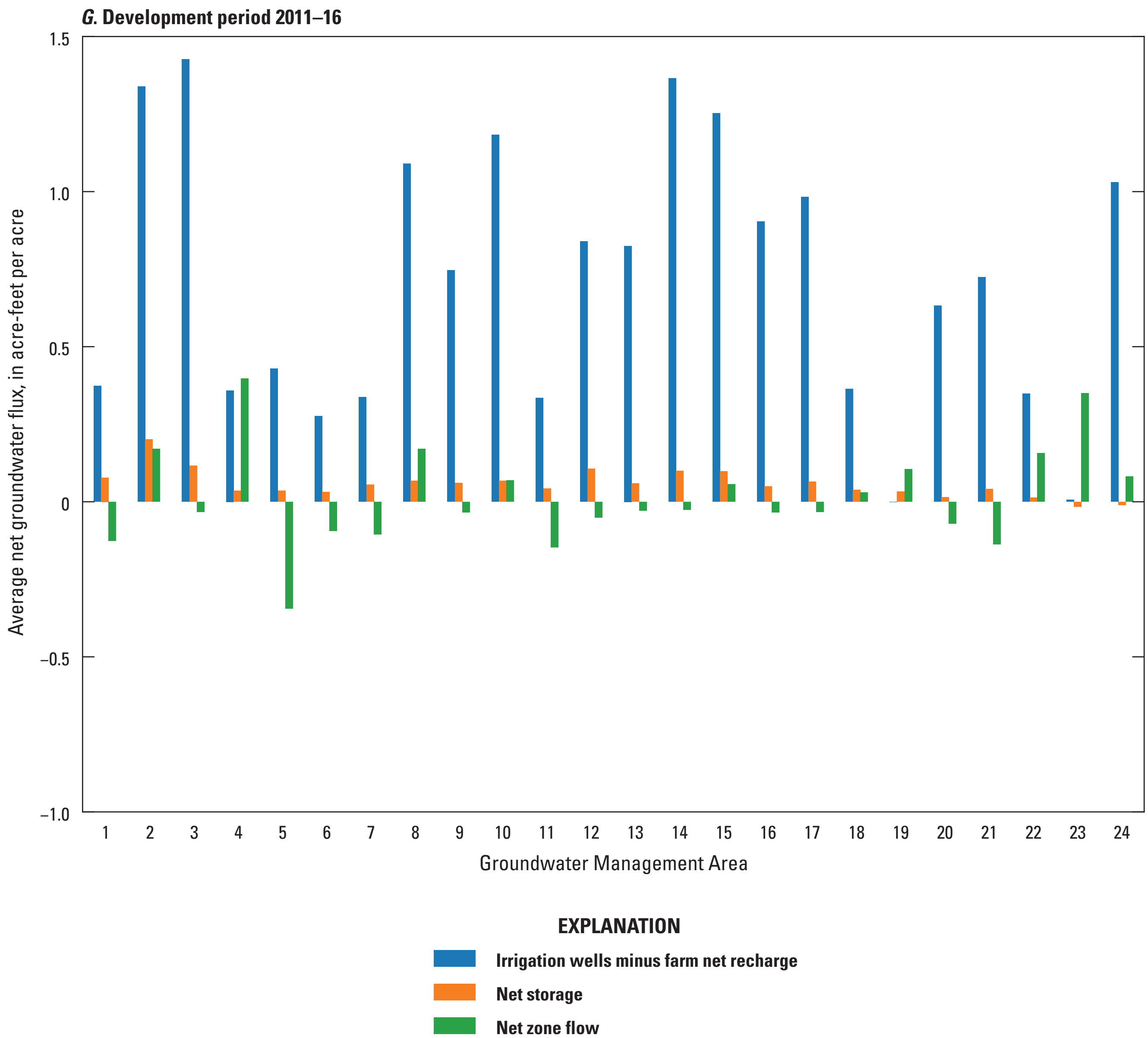

Figure 28.—Continued

scenario models. The differences in climate, land use, and stream inflows for each scenario are summarized in table 17. Input datasets varied by time period within each scenario and are denoted by "Input I," "Input II," and "Input III" in table 17. Additional plots of simulated groundwater levels for each scenario by GWMA are available in appendix 5.

The CPIHM that simulated average conditions was called the "FutBase" model; the monthly precipitation and ET_{ref} datasets for 1999 were repeated for each year of the FutBase model, as were the 1991 SFR inflows (table 17). The four drought scenarios simulated were (1) a short and intense 3-year drought ("Futdrought3yr"); (2) a long, moderate 10-year drought ("Futdrought10yr"); (3) a mid-growing-season drought from June to September each year of the scenario ("Futdroughtjun2sep"); and (4) an early growing-season drought from March to May each year of the scenario ("Futdroughtmar2may") (table 11). The three irrigation scenarios that simulated limits on groundwater irrigation were (1) an annual 7-inch depth limit ("Futirr7in"), (2) an annual 9-inch depth limit ("Futirr9in"), and (3) an annual 10-inch depth limit ("Futirr10in"). The depth limits on irrigation pumping were specified as monthly depths in the FMP's ALLOTMENT block using the GROUNDWATER feature (Boyce and others, 2020).

The simulated groundwater levels for each CPIHM scenario were compared to the baseline 1982 (April 30, 1982) average groundwater levels simulated by the development model (referred to hereafter as the "baseline 1982 gwlevels").

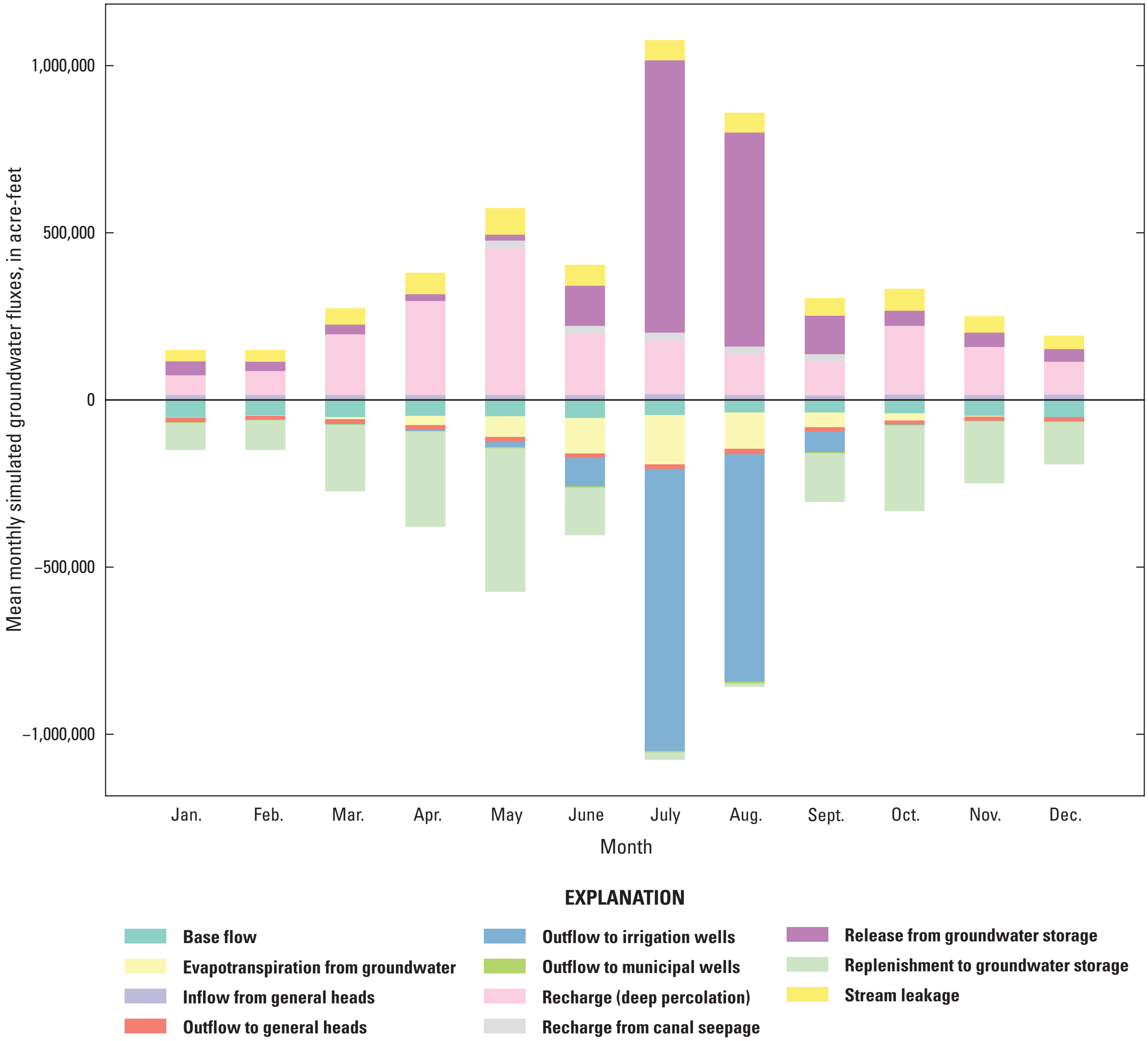

Figure 29. Simulated average monthly groundwater-flow budget from 1981 to 2016 of the development period Central Platte Integrated Hydrologic Model.

The comparison was calculated as the difference between the simulated average groundwater levels at the end of each scenario (December 31, 2049) and the baseline 1982 gwlevels by supergroup (table 12). Negative values indicated that the simulated average groundwater levels at the end of the scenario period (December 31, 2049) were below the baseline 1982 gwlevels and positive values indicated that the simulated average groundwater levels at the end of the scenario period were above the baseline 1982 gwlevels (table 18). The average groundwater levels simulated by the CPIHM for each scenario were also compared to the predrought (December 31, 2016) groundwater levels and the baseline 1982 gwlevels at three time periods (December 31, 2019; December 31, 2026; and December 31, 2049) for each GWMA, the CPNRD, and the CPIHM (table 19).

Base Scenario Simulated Results

The FutBase scenario results provided a reference point for the effects of average climate conditions on the landscape and groundwater-flow systems that may be compared to results from other scenarios simulated by the CPIHM. By the end of the scenario, the groundwater levels for 12 GWMAs were 0.2 to 10.0 ft below their levels at the beginning of the

Table 17. Summary of the main input datasets that include a scenario name, description of each scenario, climate inputs, land-use inputs, and stream inflow inputs for each scenario simulated with the Central Platte Integrated Hydrologic Model.

[AVG, average; --, not applicable]

Names and descriptions		Climate input (Type, year, simulation period)			Land-use input (Type, year, simulation period)	Stream-inflow input (Type, year, simulation period)		
Forecast name	**Description**	**Input I**	**Input II**	**Input III**	**Input I**	**Input I**	**Input II**	**Input III**
FutBase	Base forecast with constant precipitation and potential evapotranspiration and average stream inflows.	AVG, 1999, January 2017–December 2049	--	--	Land-use, 2016, January 2017–December 2049	AVG, 1991, January 2017–December 2049	--	--
Futdrought3yr	Drought forecast with three years consecutive of a severe drought and very low stream inflows followed by average climate conditions and stream inflows.	DRY, 2012, January 2017–December 2019	AVG, 1999, January 2020–December 2049	--	Land-use, 2016, January 2017–December 2049	DRY, 2003, January 2017–December 2019	AVG, 1991, January 2020–December 2049	--
Futdrought10yr	Drought forecast with 10 consecutive years of a moderate drought and average stream inflows followed by average climate conditions and stream inflows.	DRY, 2013, January 2017–December 2026	AVG, 1999, January 2027–December 2049	--	Land-use, 2016, January 2017–December 2049	AVG, 1991, January 2017–December 2049	--	--
Futdroughtjun-2sep	Mid-growing season drought forecast with a moderate drought from June to September and moderately low stream inflows preceded and followed by average climate conditions and stream inflows.	AVG, 1999, January–May	DRY, 2013, June–September, reduced by 11 percent	AVG, 1999, October–December	Land-use, 2016, January 2017–December 2049	AVG, 1991, January–May	DRY, 2002, June–September	AVG, 1991, October–December 2049
Futdroughtmar-2may	Early growing season drought forecast with a moderate drought from March to May and moderately low stream inflows preceded and followed by average climate conditions and stream inflows.	AVG, 1999, January–February	DRY, 1997, March–May	AVG, 1999, June–December	Land-use, 2016, January 2017–December 2049	AVG, 1991, January–February	DRY, 2002, March–May	AVG, 1991, June–December
Futirr7in	Irrigation forecast with an annual limit on groundwater irrigation withdrawals of 7 inches with constant average climate and stream inflows.	AVG, 1999, January 2017–December 2049	--	--	Land-use, 2016, January 2017–December 2049	AVG, 1991, January 2017–December 2049	--	--
Futirr9in	Irrigation forecast with an annual limit on groundwater irrigation withdrawals of 9 inches with constant average climate and stream inflows.	AVG, 1999, January 2017–December 2049	--	--	Land-use, 2016, January 2017–December 2049	AVG, 1991, January 2017–December 2049	--	--
Futirr10in	Irrigation forecast with an annual limit on groundwater irrigation withdrawals of 10 inches with constant average climate and stream inflows.	AVG, 1999, January 2017–December 2049	--	--	Land-use, 2016, January 2017–December 2049	AVG, 1991, January 2017–December 2049	--	--

Table 18. Change in simulated groundwater-level between baseline 1982 (April 30, 1982) average groundwater levels and the final stress period (December 31, 2049) for each scenario by supergroup in the Central Platte Integrated Hydrologic Model.

[GWMA, Groundwater Management Area; NAVD 88, North American Vertical Datum of 1988; CPNRD, Central Platte Natural Resources District; CPIHM, Central Platte Integrated Hydrologic Model]

GWMA/ supergroup	Simulated December 2016 groundwater level (feet above NAVD 88)	Baseline 1982 groundwater level (feet above NAVD 88)	Forecast name and change in groundwater level, in feet[1]							
			FutBase	Futdrought3yr	Futdrought10yr	Futdroughtjun2sep	Futdroughtmar2may	irr7in	Futirr9in	Futirr10in
1	2,600.4	2,599.3	−8.9	−12.3	−12.8	−22	−20.6	6.5	4	2.8
2	2,557.6	2,565.8	−13.7	−18.4	−18.5	−38.8	−33.7	16.6	12.7	10.8
3	2,455.5	2,457.3	−4.5	−6.5	−6.7	−30.1	−15.3	10.6	10	9.8
4	2,387.5	2,387.8	−0.5	−0.6	−0.6	−3	−1.7	0.7	0.6	0.5
5	2,515.2	2,509.1	6.3	4.7	3.7	−3.2	−4.3	13.8	12.4	11.8
6	2,468	2,459.7	0.6	−1.1	−2.4	−8.7	−5.4	8.8	7.2	6.5
7	2,329.7	2,329.2	−0.6	−2.8	−4.3	−22.4	−12.9	10	8.3	7.6
8	2,312.6	2,315.9	−2.3	−2.8	−3.2	−19.6	−9.1	3.5	2.8	2.6
9	2,187	2,186.1	7.3	5	3.5	−15.5	−8.4	16.8	14.1	12.9
10	2,047.7	2,048.9	5.5	4.2	3.9	−12.5	−4.9	10.9	9.5	8.8
11	1,970.9	1,971.4	0.7	0.6	0.6	−4	−2.1	1.4	1.3	1.2
12	1,974.1	1,980.1	0.1	−5.6	−5.6	−23.9	−33	18.1	13.1	10.9
13	1,847.7	1,848.8	−3.7	−6	−3.8	−16.2	−22.6	5.9	3.1	1.9
14	1,918.4	1,921.4	−0.2	−2.6	−1.8	−23.1	−23.1	10.4	8.2	7
15	1,882.9	1,889.1	−5	−7.6	−7.8	−26.5	−24	9.9	5.9	4
16	1,703.8	1,704.2	−1.5	−2.8	−1.3	−9.3	−16.4	6.1	3.5	2.3
17	1,749	1,749.1	0.6	0.1	0.5	−9	−10	3.1	2.3	2
18	1,680.5	1,679.9	1.4	1.4	1.4	−3.8	−3.9	1.7	1.6	1.5
19	1,709.6	1,709.7	0.1	−0.1	0	−3.1	−3.2	0.9	0.6	0.5
20	1,576.2	1,575.5	1.3	1.2	1.3	−4.4	−3.2	2.8	2.1	1.9
21	1,626.9	1,624.5	1.6	−0.1	0.5	−12.5	−12.9	9.7	6.7	5.4
22	1,518.3	1,518.4	−0.4	−0.5	−0.4	−2.1	−1.5	-0.1	-0.2	-0.3
23	1,513	1,512.5	−0.4	−0.5	−0.4	−2.4	−2.1	0.2	-0.1	-0.2
24	1,528.3	1,525.1	2.2	1.8	2	−5.8	−5.4	5.5	4.2	3.6
CPNRD	2,105.7	2,105.6	−0.2	−1.7	−2	−13.8	−11	7.6	6.1	5.4
CPIHM	2,059.0	2,059.3	−1.4	−3.2	−3.3	−16.1	−13.6	7.2	4.9	3.8

[1]Forecast names defined in table 17.

Table 19. Average simulated groundwater-level changes from baseline 1982 groundwater levels (April 30, 1982) and prescenario groundwater levels (December 31, 2016) to December 31, 2019; December 31, 2026; and December 31, 2049, by Groundwater Management Area, Central Platte Natural Resource District domain, and the Central Platte Integrated Hydrologic Model.

[GWMA, Groundwater Management Area; NAVD 88, North American Vertical Datum of 1988; WL, water level; CPNRD, Central Platte Natural Resources District; CPIHM, Central Platte Integrated Hydrologic Model]

GWMA/ supergroup	December 2016 groundwater level, in feet above NAVD 88	Baseline 1982 groundwater level, in feet above NAVD 88	WL change from baseline 1982–December 2019	WL change from baseline 1982–December 2026	WL change from baseline 1982–December 2049	WL change December 2016 to baseline 1982 ground-water level	WL change December 2016 to December 2019	WL change December 2016 to December 2026	WL change December 2019 to December 2026	WL change December 2016 to December 2049	WL change December 2019 to December 2049	WL change December 2026 to December 2049
FutBase scenario groundwater-level change, in feet[1]												
1	2,600.4	2,599.3	0	−2.4	−8.9	1.1	−1.1	−3.5	−2.4	−10.0	−8.9	−6.7
2	2,557.6	2,565.8	−8.5	−9.6	−13.7	−8.2	−0.3	−1.4	−1.1	−5.5	−5.2	−4.8
3	2,455.5	2,457.3	−2.4	−3.1	−4.5	−1.8	−0.6	−1.3	−0.7	−2.7	−2.1	−1.7
4	2,387.5	2,387.8	−0.5	−0.5	−0.5	−0.3	−0.2	−0.2	0	−0.2	0.0	0
5	2,515.2	2,509.1	6	6	6.3	6.1	−0.1	−0.1	0	0.2	0.3	0.3
6	2,468.0	2,459.7	7.4	5.5	0.6	8.3	−0.9	−2.8	−1.9	−7.7	−6.8	−4.7
7	2,329.7	2,329.2	0.5	0.3	-0.6	0.5	0.0	−0.2	−0.2	−1.1	−1.1	−1
8	2,312.6	2,315.9	−2.6	−2.4	−2.3	−3.3	0.7	0.9	0.2	1.0	0.3	0.1
9	2,187.0	2,186.1	2.3	4.5	7.3	0.9	1.4	3.6	2.2	6.4	5.0	2.6
10	2,047.7	2,048.9	1	3.3	5.5	−1.2	2.2	4.5	2.3	6.7	4.5	2.2
11	1,970.9	1,971.4	−0.1	0.5	0.7	−0.5	0.4	1.0	0.6	1.2	0.8	0.2
12	1,974.1	1,980.1	−5.3	−3.8	0.1	−6.0	0.7	2.2	1.5	6.1	5.4	3.9
13	1,847.7	1,848.8	−1.4	−2.2	−3.7	−1.1	−0.3	−1.1	−0.8	−2.6	−2.3	−1.6
14	1,918.4	1,921.4	−2.5	−1.6	−0.2	−3.0	0.5	1.4	0.9	2.8	2.3	1.4
15	1,882.9	1,889.1	−5.7	−5.2	−5	−6.2	0.5	1.0	0.5	1.2	0.7	0.4
16	1,703.8	1,704.2	−0.3	−0.4	−1.5	−0.4	0.1	0.0	−0.1	−1.1	−1.2	−0.9
17	1,749.0	1,749.1	0.2	0.6	0.6	−0.1	0.3	0.7	0.4	0.7	0.4	0.1
18	1,680.5	1,679.9	1	1.4	1.4	0.6	0.4	0.8	0.4	0.8	0.4	0.2
19	1,709.6	1,709.7	0	0.1	0.1	−0.1	0.1	0.2	0.1	0.2	0.1	0.1
20	1,576.2	1,575.5	0.9	1.2	1.3	0.7	0.2	0.5	0.3	0.6	0.4	0.2
21	1,626.9	1,624.5	2.3	2.1	1.6	2.4	−0.1	−0.3	−0.2	−0.8	−0.7	−0.1
22	1,518.3	1,518.4	−0.5	−0.4	−0.4	−0.1	−0.4	−0.3	0.1	−0.3	0.1	0
23	1,513.0	1,512.5	−0.3	−0.4	−0.4	0.5	−0.8	−0.9	−0.1	−0.9	−0.1	0
24	1,528.3	1,525.1	2.6	2.4	2.2	3.2	−0.6	−0.8	−0.2	−1.0	−0.4	−0.2
CPNRD	2,105.7	2,105.6	0.2	0.3	−0.2	0.1	0.1	0.2	0.1	−0.3	−0.4	−0.5
CPIHM	2,059.0	2,059.3	−0.4	−0.6	−1.4	−0.3	−0.1	−0.3	−0.2	−1.1	−1.0	−0.7

Table 19. Average simulated groundwater-level changes from baseline 1982 groundwater levels (April 30, 1982) and prescenario groundwater levels (December 31, 2016) to December 31, 2019; December 31, 2026; and December 31, 2049, by Groundwater Management Area, Central Platte Natural Resource District domain, and the Central Platte Integrated Hydrologic Model.—Continued

[GWMA, Groundwater Management Area; NAVD 88, North American Vertical Datum of 1988; WL, water level; CPNRD, Central Platte Natural Resources District; CPIHM, Central Platte Integrated Hydrologic Model]

GWMA/ supergroup	December 2016 groundwater level, in feet above NAVD 88	Baseline 1982 groundwater level, in feet above NAVD 88	WL change from baseline 1982–December 2019	WL change from baseline 1982–December 2026	WL change from baseline 1982–December 2049	WL change December 2016 to baseline 1982 ground-water level	WL change December 2016 to December 2019	WL change December 2016 to December 2026	WL change December 2019 to December 2026	WL change December 2016 to December 2049	WL change December 2019 to December 2049	WL change December 2026 to December 2049
Futdrought3yr scenario groundwater-level change, in feet[1]												
1	2,600.4	2,599.3	−3.2	−6	−12.3	1.1	−4.3	−7.1	−2.8	−13.4	−9.1	−6.3
2	2,557.6	2,565.8	−20.1	−18.5	−18.4	−8.2	−11.9	−10.3	1.6	−10.2	1.7	−0.6
3	2,455.5	2,457.3	−15.5	−9.6	−6.5	−1.8	−13.7	−7.8	5.9	−4.7	9.0	2.9
4	2,387.5	2,387.8	−3.7	−0.9	−0.6	−0.3	−3.4	−0.6	2.8	−0.3	3.1	0.4
5	2,515.2	2,509.1	2	3	4.7	6.1	−4.1	−3.1	1	−1.4	2.7	1.6
6	2,468.0	2,459.7	5.9	4.2	−1.1	8.3	−2.4	−4.1	−1.7	−9.4	−7.0	−5.1
7	2,329.7	2,329.2	−4.1	−4.3	−2.8	0.5	−4.6	−4.8	−0.2	−3.3	1.3	1.3
8	2,312.6	2,315.9	−11.4	−5	−2.8	−3.3	−8.1	−1.7	6.4	0.5	8.6	2.1
9	2,187.0	2,186.1	−6	−1	5	0.9	−6.9	−1.9	5	4.1	11.0	5.7
10	2,047.7	2,048.9	−10.7	−1.2	4.2	−1.2	−9.5	0.0	9.5	5.4	14.9	5.3
11	1,970.9	1,971.4	−5.3	−0.7	0.6	−0.5	−4.8	−0.2	4.6	1.1	5.9	1.5
12	1,974.1	1,980.1	−16	−14	−5.6	−6.0	−10.0	−8.0	2	0.4	10.4	8.2
13	1,847.7	1,848.8	−7.9	−7.1	−6	−1.1	−6.8	−6.0	0.8	−4.9	1.9	1.2
14	1,918.4	1,921.4	−14.6	−9.4	−2.6	−3.0	−11.6	−6.4	5.2	0.4	12.0	7.3
15	1,882.9	1,889.1	−14.4	−11	−7.6	−6.2	−8.2	−4.8	3.4	−1.4	6.8	3.7
16	1,703.8	1,704.2	−7.6	−4.6	−2.8	−0.4	−7.2	−4.2	3	−2.4	4.8	2.1
17	1,749.0	1,749.1	−8.7	−2.7	0.1	−0.1	−8.6	−2.6	6	0.2	8.8	4.2
18	1,680.5	1,679.9	−6.9	−0.2	1.4	0.6	−7.5	−0.8	6.7	0.8	8.3	3.3
19	1,709.6	1,709.7	−4.8	−0.8	−0.1	−0.1	−4.7	−0.7	4	0.0	4.7	1.4
20	1,576.2	1,575.5	−4.5	−0.5	1.2	0.7	−5.2	−1.2	4	0.5	5.7	2.1
21	1,626.9	1,624.5	−4.2	−2.1	−0.1	2.4	−6.6	−4.5	2.1	−2.5	4.1	2.4
22	1,518.3	1,518.4	−3.1	−0.7	−0.5	−0.1	−3.0	−0.6	2.4	−0.4	2.6	0.5
23	1,513.0	1,512.5	−2.5	−0.7	−0.5	0.5	−3.0	−1.2	1.8	−1.0	2.0	0.3
24	1,528.3	1,525.1	−3.1	0.4	1.8	3.2	−6.3	−2.8	3.5	−1.4	4.9	1.4
CPNRD	2,105.7	2,105.6	−6.4	−3.5	−1.7	0.1	−6.5	−3.6	2.9	−1.8	4.7	1.9
CPIHM	2,059.0	2,059.3	−6.5	−4.5	−3.2	−0.3	−6.2	−4.2	2	−2.9	3.3	1.5

Table 19. Average simulated groundwater-level changes from baseline 1982 groundwater levels (April 30, 1982) and prescenario groundwater levels (December 31, 2016) to December 31, 2019; December 31, 2026; and December 31, 2049, by Groundwater Management Area, Central Platte Natural Resource District domain, and the Central Platte Integrated Hydrologic Model.—Continued

[GWMA, Groundwater Management Area; NAVD 88, North American Vertical Datum of 1988; WL, water level; CPNRD, Central Platte Natural Resources District; CPIHM, Central Platte Integrated Hydrologic Model]

GWMA/ supergroup	December 2016 groundwater level, in feet above NAVD 88	Baseline 1982 groundwater level, in feet above NAVD 88	WL change from baseline 1982–December 2019	WL change from baseline 1982–December 2026	WL change from baseline 1982–December 2049	WL change December 2016 to baseline 1982 ground-water level	WL change December 2016 to December 2019	WL change December 2016 to December 2026	WL change December 2019 to December 2026	WL change December 2016 to December 2049	WL change December 2019 to December 2049	WL change December 2026 to December 2049
Futdrought10yr scenario groundwater-level change, in feet[1]												
1	2,600.4	2,599.3	−1.1	−6.2	−12.8	1.1	−2.2	−7.3	−5.1	−13.9	−11.7	−6.6
2	2,557.6	2,565.8	−11.7	−18.9	−18.5	−8.2	−3.5	−10.7	−7.2	−10.3	−6.8	0.4
3	2,455.5	2,457.3	−5	−10	−6.7	−1.8	−3.2	−8.2	−5	−4.9	−1.7	3.3
4	2,387.5	2,387.8	−1.1	−1.7	−0.6	−0.3	−0.8	−1.4	−0.6	−0.3	0.5	1.1
5	2,515.2	2,509.1	4.4	1.3	3.7	6.1	−1.7	−4.8	−3.1	−2.4	−0.7	2.4
6	2,468.0	2,459.7	6.3	2.1	−2.4	8.3	−2.0	−6.2	−4.2	−10.7	−8.7	−4.5
7	2,329.7	2,329.2	−1.8	−7	−4.3	0.5	−2.3	−7.5	−5.2	−4.8	−2.5	2.7
8	2,312.6	2,315.9	−5.3	−8.4	−3.2	−3.3	−2.0	−5.1	−3.1	0.1	2.1	5.2
9	2,187.0	2,186.1	−1.5	−6	3.5	0.9	−2.4	−6.9	−4.5	2.6	5.0	9.5
10	2,047.7	2,048.9	−2.3	−4.2	3.9	−1.2	−1.1	−3.0	−1.9	5.1	6.2	8.1
11	1,970.9	1,971.4	−1	−1.5	0.6	−0.5	−0.5	−1.0	−0.5	1.1	1.6	2.1
12	1,974.1	1,980.1	−8.5	−13.8	−5.6	−6.0	−2.5	−7.8	−5.3	0.4	2.9	8.2
13	1,847.7	1,848.8	−1.7	−2.7	−3.8	−1.1	−0.6	−1.6	−1	−2.7	−2.1	−1.1
14	1,918.4	1,921.4	−4.2	−6.5	−1.8	−3.0	−1.2	−3.5	−2.3	1.2	2.4	4.7
15	1,882.9	1,889.1	−8.3	−12.1	−7.8	−6.2	−2.1	−5.9	−3.8	−1.6	0.5	4.3
16	1,703.8	1,704.2	−0.7	−1.2	−1.3	−0.4	−0.3	−0.8	−0.5	−0.9	−0.6	−0.1
17	1,749.0	1,749.1	−0.7	−1.3	0.5	−0.1	−0.6	−1.2	−0.6	0.6	1.2	1.8
18	1,680.5	1,679.9	0.3	0	1.4	0.6	−0.3	−0.6	−0.3	0.8	1.1	1.4
19	1,709.6	1,709.7	−0.5	−0.7	0	−0.1	−0.4	−0.6	−0.2	0.1	0.5	0.7
20	1,576.2	1,575.5	1.3	1.7	1.3	0.7	0.6	1.0	0.4	0.6	0.0	−0.4
21	1,626.9	1,624.5	1.4	−0.6	0.5	2.4	−1.0	−3.0	−2	−1.9	−0.9	1.1
22	1,518.3	1,518.4	−0.3	−0.3	−0.4	−0.1	−0.2	−0.2	0	−0.3	−0.1	−0.1
23	1,513.0	1,512.5	0	−0.2	−0.4	0.5	−0.5	−0.7	−0.2	−0.9	−0.4	−0.2
24	1,528.3	1,525.1	2.3	1.4	2	3.2	−0.9	−1.8	−0.9	−1.2	−0.3	0.6
CPNRD	2,105.7	2,105.6	−1.4	−4.1	−2	0.1	−1.5	−4.2	−2.7	−2.1	−0.6	2.1
CPIHM	2,059.0	2,059.3	−1.9	−4.9	−3.3	−0.3	−1.6	−4.6	−3	−3.0	−1.4	1.6

Table 19. Average simulated groundwater-level changes from baseline 1982 groundwater levels (April 30, 1982) and prescenario groundwater levels (December 31, 2016) to December 31, 2019; December 31, 2026; and December 31, 2049, by Groundwater Management Area, Central Platte Natural Resource District domain, and the Central Platte Integrated Hydrologic Model.—Continued

[GWMA, Groundwater Management Area; NAVD 88, North American Vertical Datum of 1988; WL, water level; CPNRD, Central Platte Natural Resources District; CPIHM, Central Platte Integrated Hydrologic Model]

GWMA/ supergroup	December 2016 groundwater level, in feet above NAVD 88	Baseline 1982 groundwater level, in feet above NAVD 88	WL change from baseline 1982–December 2019	WL change from baseline 1982–December 2026	WL change from baseline 1982–December 2049	WL change December 2016 to baseline 1982 ground-water level	WL change December 2016 to December 2019	WL change December 2016 to December 2026	WL change December 2019 to December 2026	WL change December 2016 to December 2049	WL change December 2019 to December 2049	WL change December 2026 to December 2049
Futdroughtjun2sep scenario groundwater-level change, in feet[1]												
1	2,600.4	2,599.3	−1	−6.1	−22	1.1	−2.1	−7.2	−5.1	−23.1	−21.0	−15.9
2	2,557.6	2,565.8	−12	−19.8	−38.8	−8.2	−3.8	−11.6	−7.8	−30.6	−26.8	−19
3	2,455.5	2,457.3	−6.7	−14.7	−30.1	−1.8	−4.9	−12.9	−8	−28.3	−23.4	−15.4
4	2,387.5	2,387.8	−1.2	−1.9	−3	−0.3	−0.9	−1.6	−0.7	−2.7	−1.8	−1.1
5	2,515.2	2,509.1	4.7	2.2	−3.2	6.1	−1.4	−3.9	−2.5	−9.3	−7.9	−5.4
6	2,468.0	2,459.7	6.5	2.7	−8.7	8.3	−1.8	−5.6	−3.8	−17.0	−15.2	−11.4
7	2,329.7	2,329.2	−1.8	−7.4	−22.4	0.5	−2.3	−7.9	−5.6	−22.9	−20.6	−15
8	2,312.6	2,315.9	−6.1	−10.4	−19.6	−3.3	−2.8	−7.1	−4.3	−16.3	−13.5	−9.2
9	2,187.0	2,186.1	−1.5	−5.7	−15.5	0.9	−2.4	−6.6	−4.2	−16.4	−14.0	−9.8
10	2,047.7	2,048.9	−3.4	−6.5	−12.5	−1.2	−2.2	−5.3	−3.1	−11.3	−9.1	−6
11	1,970.9	1,971.4	−1.6	−2.5	−4	−0.5	−1.1	−2.0	−0.9	−3.5	−2.4	−1.5
12	1,974.1	1,980.1	−7.7	−12	−23.9	−6.0	−1.7	−6.0	−4.3	−17.9	−16.2	−11.9
13	1,847.7	1,848.8	−3	−6.8	−16.2	−1.1	−1.9	−5.7	−3.8	−15.1	−13.2	−9.4
14	1,918.4	1,921.4	−5.9	−11	−23.1	−3.0	−2.9	−8.0	−5.1	−20.1	−17.2	−12.1
15	1,882.9	1,889.1	−9.1	−14.7	−26.5	−6.2	−2.9	−8.5	−5.6	−20.3	−17.4	−11.8
16	1,703.8	1,704.2	−2	−4.7	−9.3	−0.4	−1.6	−4.3	−2.7	−8.9	−7.3	−4.6
17	1,749.0	1,749.1	−2.4	−5.2	−9	−0.1	−2.3	−5.1	−2.8	−8.9	−6.6	−3.8
18	1,680.5	1,679.9	−0.7	−2.1	−3.8	0.6	−1.3	−2.7	−1.4	−4.4	−3.1	−1.7
19	1,709.6	1,709.7	−1.2	−1.9	−3.1	−0.1	−1.1	−1.8	−0.7	−3.0	−1.9	−1.2
20	1,576.2	1,575.5	−1.2	−3.2	−4.4	0.7	−1.9	−3.9	−2	−5.1	−3.2	−1.2
21	1,626.9	1,624.5	−0.1	−4.4	−12.5	2.4	−2.5	−6.8	−4.3	−14.9	−12.4	−8.1
22	1,518.3	1,518.4	−1.2	−1.7	−2.1	−0.1	−1.1	−1.6	−0.5	−2.0	−0.9	−0.4
23	1,513.0	1,512.5	−1	−1.5	−2.4	0.5	−1.5	−2.0	−0.5	−2.9	−1.4	−0.9
24	1,528.3	1,525.1	0.4	−2.4	−5.8	3.2	−2.8	−5.6	−2.8	−9.0	−6.2	−3.4
CPNRD	2,105.7	2,105.6	−2	−5.7	−13.8	0.1	−2.1	−5.8	−3.7	−13.9	−11.8	−8.1
CPIHM	2,059.0	2,059.3	−2.6	−6.6	−16.1	−0.3	−2.3	−6.3	−4	−15.8	−13.5	−9.5

Table 19. Average simulated groundwater-level changes from baseline 1982 groundwater levels (April 30, 1982) and prescenario groundwater levels (December 31, 2016) to December 31, 2019; December 31, 2026; and December 31, 2049, by Groundwater Management Area, Central Platte Natural Resource District domain, and the Central Platte Integrated Hydrologic Model.—Continued

[GWMA, Groundwater Management Area; NAVD 88, North American Vertical Datum of 1988; WL, water level; CPNRD, Central Platte Natural Resources District; CPIHM, Central Platte Integrated Hydrologic Model]

GWMA/ supergroup	December 2016 groundwater level, in feet above NAVD 88	Baseline 1982 groundwater level, in feet above NAVD 88	WL change from baseline 1982–December 2019	WL change from baseline 1982–December 2026	WL change from baseline 1982–December 2049	WL change December 2016 to baseline 1982 groundwater level	WL change December 2016 to December 2019	WL change December 2016 to December 2026	WL change December 2019 to December 2026	WL change December 2016 to December 2049	WL change December 2019 to December 2049	WL change December 2026 to December 2049
Futdroughtmar2may scenario groundwater-level change, in feet[1]												
1	2,600.4	2,599.3	−1	−6	−20.6	1.1	−2.1	−7.1	−5	−21.7	−19.6	−14.6
2	2,557.6	2,565.8	−11.2	−17.6	−33.7	−8.2	−3.0	−9.4	−6.4	−25.5	−22.5	−16.1
3	2,455.5	2,457.3	−4.3	−8	−15.3	−1.8	−2.5	−6.2	−3.7	−13.5	−11.0	−7.3
4	2,387.5	2,387.8	−0.9	−1.3	−1.7	−0.3	−0.6	−1.0	−0.4	−1.4	−0.8	−0.4
5	2,515.2	2,509.1	4.6	1.8	−4.3	6.1	−1.5	−4.3	−2.8	−10.4	−8.9	−6.1
6	2,468.0	2,459.7	6.9	3.8	−5.4	8.3	−1.4	−4.5	−3.1	−13.7	−12.3	−9.2
7	2,329.7	2,329.2	−1	−4.5	−12.9	0.5	−1.5	−5.0	−3.5	−13.4	−11.9	−8.4
8	2,312.6	2,315.9	−4.1	−5.6	−9.1	−3.3	−0.8	−2.3	−1.5	−5.8	−5.0	−3.5
9	2,187.0	2,186.1	−0.2	−2.5	−8.4	0.9	−1.1	−3.4	−2.3	−9.3	−8.2	−5.9
10	2,047.7	2,048.9	−1.3	−2.1	−4.9	−1.2	−0.1	−0.9	−0.8	−3.7	−3.6	−2.8
11	1,970.9	1,971.4	−1.1	−1.5	−2.1	−0.5	−0.6	−1.0	−0.4	−1.6	−1.0	−0.6
12	1,974.1	1,980.1	−9.1	−15.9	−33	−6.0	−3.1	−9.9	−6.8	−27.0	−23.9	−17.1
13	1,847.7	1,848.8	−3.7	−8.9	−22.6	−1.1	−2.6	−7.8	−5.2	−21.5	−18.9	−13.7
14	1,918.4	1,921.4	−5.8	−11	−23.1	−3.0	−2.8	−8.0	−5.2	−20.1	−17.3	−12.1
15	1,882.9	1,889.1	−8.7	−13.5	−24	−6.2	−2.5	−7.3	−4.8	−17.8	−15.3	−10.5
16	1,703.8	1,704.2	−3	−7.5	−16.4	−0.4	−2.6	−7.1	−4.5	−16.0	−13.4	−8.9
17	1,749.0	1,749.1	−2.3	−5.2	−10	−0.1	−2.2	−5.1	−2.9	−9.9	−7.7	−4.8
18	1,680.5	1,679.9	−0.8	−2.3	−3.9	0.6	−1.4	−2.9	−1.5	−4.5	−3.1	−1.6
19	1,709.6	1,709.7	−1.2	−2.1	−3.2	−0.1	−1.1	−2.0	−0.9	−3.1	−2.0	−1.1
20	1,576.2	1,575.5	−0.7	−2.2	−3.2	0.7	−1.4	−2.9	−1.5	−3.9	−2.5	−1
21	1,626.9	1,624.5	−0.3	−4.8	−12.9	2.4	−2.7	−7.2	−4.5	−15.3	−12.6	−8.1
22	1,518.3	1,518.4	−1	−1.4	−1.5	−0.1	−0.9	−1.3	−0.4	−1.4	−0.5	−0.1
23	1,513.0	1,512.5	−0.8	−1.3	−2.1	0.5	−1.3	−1.8	−0.5	−2.6	−1.3	−0.8
24	1,528.3	1,525.1	0.5	−2.2	−5.4	3.2	−2.7	−5.4	−2.7	−8.6	−5.9	−3.2
CPNRD	2,105.7	2,105.6	−1.6	−4.5	−11	0.1	−1.7	−4.6	−2.9	−11.1	−9.4	−6.5
CPIHM	2,059.0	2,059.3	−2.2	−5.6	−13.6	−0.3	−1.9	−5.3	−3.4	−13.3	−11.4	−8

Table 19. Average simulated groundwater-level changes from baseline 1982 groundwater levels (April 30, 1982) and prescenario groundwater levels (December 31, 2016) to December 31, 2019; December 31, 2026; and December 31, 2049, by Groundwater Management Area, Central Platte Natural Resource District domain, and the Central Platte Integrated Hydrologic Model.—Continued

[GWMA, Groundwater Management Area; NAVD 88, North American Vertical Datum of 1988; WL, water level; CPNRD, Central Platte Natural Resources District; CPIHM, Central Platte Integrated Hydrologic Model]

GWMA/ supergroup	December 2016 groundwater level, in feet above NAVD 88	Baseline 1982 groundwater level, in feet above NAVD 88	WL change from baseline 1982–December 2019	WL change from baseline 1982–December 2026	WL change from baseline 1982–December 2049	WL change December 2016 to baseline 1982 groundwater level	WL change December 2016 to December 2019	WL change December 2016 to December 2026	WL change December 2019 to December 2026	WL change December 2016 to December 2049	WL change December 2019 to December 2049	WL change December 2026 to December 2049
irr7in scenario groundwater-level change, in feet[1]												
1	2,600.4	2,599.3	1.2	2.1	6.5	1.1	0.1	1.0	0.9	5.4	5.3	4.4
2	2,557.6	2,565.8	−4	3.8	16.6	−8.2	4.2	12.0	7.8	24.8	20.6	12.8
3	2,455.5	2,457.3	2.2	7.2	10.6	−1.8	4.0	9.0	5	12.4	8.4	3.4
4	2,387.5	2,387.8	0.2	0.5	0.7	−0.3	0.5	0.8	0.3	1.0	0.5	0.2
5	2,515.2	2,509.1	7.1	9.1	13.8	6.1	1.0	3.0	2	7.7	6.7	4.7
6	2,468.0	2,459.7	8.2	8.1	8.8	8.3	−0.1	−0.2	−0.1	0.5	0.6	0.7
7	2,329.7	2,329.2	1.8	4.6	10	0.5	1.3	4.1	2.8	9.5	8.2	5.4
8	2,312.6	2,315.9	−0.7	1.4	3.5	−3.3	2.6	4.7	2.1	6.8	4.2	2.1
9	2,187.0	2,186.1	3.9	8.9	16.8	0.9	3.0	8.0	5	15.9	12.9	7.9
10	2,047.7	2,048.9	2.7	6.9	10.9	−1.2	3.9	8.1	4.2	12.1	8.2	4
11	1,970.9	1,971.4	0.3	1	1.4	−0.5	0.8	1.5	0.7	1.9	1.1	0.4
12	1,974.1	1,980.1	−2.7	4.5	18.1	−6.0	3.3	10.5	7.2	24.1	20.8	13.6
13	1,847.7	1,848.8	0.2	2.4	5.9	−1.1	1.3	3.5	2.2	7.0	5.7	3.5
14	1,918.4	1,921.4	0.5	5.5	10.4	−3.0	3.5	8.5	5	13.4	9.9	4.9
15	1,882.9	1,889.1	−3	2	9.9	−6.2	3.2	8.2	5	16.1	12.9	7.9
16	1,703.8	1,704.2	1.4	3.9	6.1	−0.4	1.8	4.3	2.5	6.5	4.7	2.2
17	1,749.0	1,749.1	1.2	2.4	3.1	−0.1	1.3	2.5	1.2	3.2	1.9	0.7
18	1,680.5	1,679.9	1.2	1.6	1.7	0.6	0.6	1.0	0.4	1.1	0.5	0.1
19	1,709.6	1,709.7	0.1	0.5	0.9	−0.1	0.2	0.6	0.4	1.0	0.8	0.4
20	1,576.2	1,575.5	1.6	2.5	2.8	0.7	0.9	1.8	0.9	2.1	1.2	0.3
21	1,626.9	1,624.5	3.7	6	9.7	2.4	1.3	3.6	2.3	7.3	6.0	3.7
22	1,518.3	1,518.4	−0.3	−0.2	−0.1	−0.1	−0.2	−0.1	0.1	0.0	0.2	0.1
23	1,513.0	1,512.5	−0.2	0	0.2	0.5	−0.7	−0.5	0.2	−0.3	0.4	0.2
24	1,528.3	1,525.1	3.6	4.5	5.5	3.2	0.4	1.3	0.9	2.3	1.9	1
CPNRD	2,105.7	2,105.6	1.7	4.1	7.6	0.1	1.6	4.0	2.4	7.5	5.9	3.5
CPIHM	2,059.0	2,059.3	1.1	3.5	7.2	−0.3	1.4	3.8	2.4	7.5	6.1	3.7

Table 19. Average simulated groundwater-level changes from baseline 1982 groundwater levels (April 30, 1982) and prescenario groundwater levels (December 31, 2016) to December 31, 2019; December 31, 2026; and December 31, 2049, by Groundwater Management Area, Central Platte Natural Resource District domain, and the Central Platte Integrated Hydrologic Model.—Continued

[GWMA, Groundwater Management Area; NAVD 88, North American Vertical Datum of 1988; WL, water level; CPNRD, Central Platte Natural Resources District; CPIHM, Central Platte Integrated Hydrologic Model]

GWMA/ supergroup	December 2016 groundwater level, in feet above NAVD 88	Baseline 1982 groundwater level, in feet above NAVD 88	WL change from baseline 1982–December 2019	WL change from baseline 1982–December 2026	WL change from baseline 1982–December 2049	WL change December 2016 to baseline 1982 ground-water level	WL change December 2016 to December 2019	WL change December 2016 to December 2026	WL change December 2019 to December 2026	WL change December 2016 to December 2049	WL change December 2019 to December 2049	WL change December 2026 to December 2049
Futirr9in scenario groundwater-level change, in feet[1]												
1	2,600.4	2,599.3	1	1.3	4	1.1	−0.1	0.2	0.3	2.9	3.0	2.7
2	2,557.6	2,565.8	−4.6	1.9	12.7	−8.2	3.6	10.1	6.5	20.9	17.3	10.8
3	2,455.5	2,457.3	2	6.8	10	−1.8	3.8	8.6	4.8	11.8	8.0	3.2
4	2,387.5	2,387.8	0.2	0.5	0.6	−0.3	0.5	0.8	0.3	0.9	0.4	0.1
5	2,515.2	2,509.1	6.9	8.5	12.4	6.1	0.8	2.4	1.6	6.3	5.5	3.9
6	2,468.0	2,459.7	8.1	7.5	7.2	8.3	−0.2	−0.8	-0.6	−1.1	-0.9	-0.3
7	2,329.7	2,329.2	1.5	3.8	8.3	0.5	1.0	3.3	2.3	7.8	6.8	4.5
8	2,312.6	2,315.9	−1	0.9	2.8	−3.3	2.3	4.2	1.9	6.1	3.8	1.9
9	2,187.0	2,186.1	3.4	7.6	14.1	0.9	2.5	6.7	4.2	13.2	10.7	6.5
10	2,047.7	2,048.9	2.2	5.8	9.5	−1.2	3.4	7.0	3.6	10.7	7.3	3.7
11	1,970.9	1,971.4	0.2	0.9	1.3	−0.5	0.7	1.4	0.7	1.8	1.1	0.4
12	1,974.1	1,980.1	−3.5	2	13.1	−6.0	2.5	8.0	5.5	19.1	16.6	11.1
13	1,847.7	1,848.8	−0.3	1.1	3.1	−1.1	0.8	2.2	1.4	4.2	3.4	2
14	1,918.4	1,921.4	−0.3	3.8	8.2	−3.0	2.7	6.8	4.1	11.2	8.5	4.4
15	1,882.9	1,889.1	−3.7	0.1	5.9	−6.2	2.5	6.3	3.8	12.1	9.6	5.8
16	1,703.8	1,704.2	0.7	2.2	3.5	−0.4	1.1	2.6	1.5	3.9	2.8	1.3
17	1,749.0	1,749.1	0.8	1.8	2.3	−0.1	0.9	1.9	1	2.4	1.5	0.5
18	1,680.5	1,679.9	1.1	1.5	1.6	0.6	0.5	0.9	0.4	1.0	0.5	0.1
19	1,709.6	1,709.7	0	0.4	0.6	−0.1	0.1	0.5	0.4	0.7	0.6	0.2
20	1,576.2	1,575.5	1.2	1.8	2.1	0.7	0.5	1.1	0.6	1.4	0.9	0.3
21	1,626.9	1,624.5	3.2	4.5	6.7	2.4	0.8	2.1	1.3	4.3	3.5	2.2
22	1,518.3	1,518.4	−0.4	−0.3	−0.2	−0.1	−0.3	−0.2	0.1	−0.1	0.2	0.1
23	1,513.0	1,512.5	−0.2	−0.2	−0.1	0.5	−0.7	−0.7	0	−0.6	0.1	0.1
24	1,528.3	1,525.1	3.2	3.7	4.2	3.2	0.0	0.5	0.5	1.0	1.0	0.5
CPNRD	2,105.7	2,105.6	1.3	3.3	6.1	0.1	1.2	3.2	2	6.0	4.8	2.8
CPIHM	2,059.0	2,059.3	0.7	2.3	4.9	−0.3	1.0	2.6	1.6	5.2	4.2	2.6

Table 19. Average simulated groundwater-level changes from baseline 1982 groundwater levels (April 30, 1982) and prescenario groundwater levels (December 31, 2016) to December 31, 2019; December 31, 2026; and December 31, 2049, by Groundwater Management Area, Central Platte Natural Resource District domain, and the Central Platte Integrated Hydrologic Model.—Continued

[GWMA, Groundwater Management Area; NAVD 88, North American Vertical Datum of 1988; WL, water level; CPNRD, Central Platte Natural Resources District; CPIHM, Central Platte Integrated Hydrologic Model]

GWMA/ supergroup	December 2016 groundwater level, in feet above NAVD 88	Baseline 1982 groundwater level, in feet above NAVD 88	WL change from baseline 1982–December 2019	WL change from baseline 1982–December 2026	WL change from baseline 1982–December 2049	WL change December 2016 to baseline 1982 groundwater level	WL change December 2016 to December 2019	WL change December 2016 to December 2026	WL change December 2019 to December 2026	WL change December 2016 to December 2049	WL change December 2019 to December 2049	WL change December 2026 to December 2049
Futirr10in scenario groundwater-level change, in feet[1]												
1	2,600.4	2,599.3	0.9	0.9	2.8	1.1	−0.2	−0.2	0	1.7	1.9	1.9
2	2,557.6	2,565.8	−5	1	10.8	−8.2	3.2	9.2	6	19.0	15.8	9.8
3	2,455.5	2,457.3	1.9	6.6	9.8	−1.8	3.7	8.4	4.7	11.6	7.9	3.2
4	2,387.5	2,387.8	0.1	0.4	0.5	−0.3	0.4	0.7	0.3	0.8	0.4	0.1
5	2,515.2	2,509.1	6.8	8.3	11.8	6.1	0.7	2.2	1.5	5.7	5.0	3.5
6	2,468.0	2,459.7	8	7.3	6.5	8.3	−0.3	−1.0	−0.7	−1.8	−1.5	−0.8
7	2,329.7	2,329.2	1.4	3.4	7.6	0.5	0.9	2.9	2	7.1	6.2	4.2
8	2,312.6	2,315.9	−1.1	0.6	2.6	−3.3	2.2	3.9	1.7	5.9	3.7	2
9	2,187.0	2,186.1	3.2	7	12.9	0.9	2.3	6.1	3.8	12.0	9.7	5.9
10	2,047.7	2,048.9	2	5.3	8.8	−1.2	3.2	6.5	3.3	10.0	6.8	3.5
11	1,970.9	1,971.4	0.1	0.8	1.2	−0.5	0.6	1.3	0.7	1.7	1.1	0.4
12	1,974.1	1,980.1	−3.8	1	10.9	−6.0	2.2	7.0	4.8	16.9	14.7	9.9
13	1,847.7	1,848.8	−0.5	0.5	1.9	−1.1	0.6	1.6	1	3.0	2.4	1.4
14	1,918.4	1,921.4	−0.6	2.9	7	−3.0	2.4	5.9	3.5	10.0	7.6	4.1
15	1,882.9	1,889.1	−4	−0.8	4	−6.2	2.2	5.4	3.2	10.2	8.0	4.8
16	1,703.8	1,704.2	0.5	1.6	2.3	−0.4	0.9	2.0	1.1	2.7	1.8	0.7
17	1,749.0	1,749.1	0.7	1.5	2	−0.1	0.8	1.6	0.8	2.1	1.3	0.5
18	1,680.5	1,679.9	1.1	1.5	1.5	0.6	0.5	0.9	0.4	0.9	0.4	0
19	1,709.6	1,709.7	0	0.3	0.5	−0.1	0.1	0.4	0.3	0.6	0.5	0.2
20	1,576.2	1,575.5	1.1	1.6	1.9	0.7	0.4	0.9	0.5	1.2	0.8	0.3
21	1,626.9	1,624.5	3	3.9	5.4	2.4	0.6	1.5	0.9	3.0	2.4	1.5
22	1,518.3	1,518.4	−0.4	−0.3	−0.3	−0.1	−0.3	−0.2	0.1	−0.2	0.1	0
23	1,513.0	1,512.5	−0.3	−0.2	−0.2	0.5	−0.8	−0.7	0.1	−0.7	0.1	0
24	1,528.3	1,525.1	3	3.3	3.6	3.2	−0.2	0.1	0.3	0.4	0.6	0.3
CPNRD	2,105.7	2,105.6	1.2	2.9	5.4	0.1	1.1	2.8	1.7	5.3	4.2	2.5
CPIHM	2,059.0	2,059.3	0.5	1.8	3.8	−0.3	0.8	2.1	1.3	4.1	3.3	2

[1]Forecast names defined in table 17.

scenario and 12 GWMAs exhibited groundwater levels that were 0.2 to 6.7 ft above their levels at the beginning of the scenario (table 19). Many of the GWMAs in the western portion of the CPNRD exhibited groundwater levels that were below the beginning of the scenario levels, which indicated that the groundwater-flow system was still stressed enough by the balance between irrigation pumping and farm net recharge under average climate conditions to cause a net release from storage (table 19).

The landscape water budget for the FutBase model was like the average conditions from the development model, characterized by large inflows from precipitation and large outflows of ET of precipitation, which was expected because of the recycling of the "average" condition datasets from the development model. Lower total ET values generally occurred in the more densely irrigated and wetter supergroups, where wetter areas in the eastern portion of the model had lower ET_{ref} values (except GWMAs 2 and 3), which resulted in greater values of deep percolation for 22 of the 25 supergroups and the CPIHM domain; GWMAs 2 and 3 contain canals that increased ET and deep percolation in the drier conditions of the western region (table 20). GWMAs 1, 5, 6, and 7 did not follow this pattern because they were in the drier western region of the CPIHM and had less irrigated land where ET_{ref} rates were higher and removed a higher percentage of precipitation from the landscape (table 20).

The groundwater-flow budget for the FutBase model exhibited similar trends to the average conditions from the development model marked by large inflows from recharge (deep percolation) and large outflows to irrigation wells (table 21). The positive net change in groundwater storage for the CPIHM indicated that on average there was a net release from storage (corresponding to groundwater-level declines). Of the GWMAs, 10 exhibited negative average annual net changes in storage (rise in groundwater level) and were generally located in the central and eastern region of the CPIHM domain. Average annual groundwater irrigation pumping depth was 9.3 inches for the CPNRD (table 22). GWMA 6 had the largest average annual irrigation depth of 15.1 inches and GWMA 23 had the lowest depth of 0.7 inch. These irrigation pumping depths were about 1 inch lower than the average development period irrigation pumping depths, which indicated that overall, the pumping stress for the FutBase scenario across the CPIHM was slightly less than the average from the development period.

Alternate Irrigation Pumping Scenario Simulated Results

Three alternative irrigation pumping scenarios (called the Futirr7in, Futirr9in, and Futirr10in scenarios) limited annual groundwater withdrawals to depths of 7, 9, and 10 inches, respectively, under average climate and stream inflow conditions (table 17). The limits on irrigation were imposed as a depth for each month of the irrigation season (May to September) by scaling the average monthly trend simulated by the development model from 1981 to 2016 to the desired annual scenario limit. For each alternative groundwater pumping scenario, an irrigation well could pump less than the monthly limit, but not more, if that met the CIR. Results from these scenario simulations highlighted GWMAs with the most limited groundwater supply in the CPIHM.

The average outflows to irrigation wells, as depth, for each alternate pumping scenario were compared to the average outflows to irrigation wells for the FutBase scenario CPIHM for each GWMA to understand which areas had limited groundwater supply under the same average climate and stream inflow conditions (table 22). A positive value represented a higher FutBase scenario average than the scenario pumping cap limit and indicated a supply limited groundwater area in which a limit on irrigation pumping caused an irrigation deficit where the CWD was not met from irrigation (referred to hereafter as a "deficit irrigation state"; table 22); conversely a negative value represented a lower FutBase scenario average than the scenario pumping cap limit and indicated a supply surplus groundwater area in which a limit on irrigation pumping did not restrict the ET of the crop (referred to hereafter as a "surplus irrigation state").

The groundwater levels for each alternate irrigation pumping limit scenario approached a new dynamic equilibrium compared to those of the development period and the FutBase scenario (table 19). By the end of the forecast period, the groundwater levels increased 0.0 to 24.8 ft from their prescenario levels for most GWMAs; only GWMAs 6, 22, and 23 exhibited groundwater levels that were lower than their initial scenario levels and baseline 1982 gwlevels, but these GWMAs also exhibited groundwater-level declines for the FutBase scenario. GWMAs 2 and 9 had the largest rise in groundwater levels, which indicated that the aquifer in this area was more responsive to the limits on irrigation pumping than other GWMAs and that the development period irrigation had a more substantial impact on the aquifer than for other GWMAs (table 18). Conversely, GWMAs 19 and 23 were the least responsive to limits on irrigation pumping because their difference in pumping from the irrigation limits was largest, indicating they required less pumping in average conditions to meet their CIR; the balance between their average irrigation rate and other stresses such as recharge throughout the development period was much less than the limits imposed by the cap on irrigation (table 18, 22). Generally, groundwater levels for GWMAs that did not exhibit a substantial change owing to limits on irrigation correlate to areas with less irrigation and net inflows from adjacent zones (table 20).

Across all three of these forecasts, the drier western region GWMAs (GWMAs 1, 2, 5, and 6) were also the regions that were most groundwater supply limited. The number of GWMAs that were in a deficit irrigation state also decreased as the irrigation cap increased (table 22). For all three alternate pumping forecasts, GMWAs 19 and 23 exhibited the highest surplus irrigation state where the average irrigation difference for the FutBase scenario was 6.3, 8.3, and 9.3 inches, which is less than the Futirr7in, Futirr9in, and Futirr10in scenario pumping limits because their irrigation requirements were small when compared to other GWMAs and they exhibited substantial net inflow from adjacent zones (table 22). Conversely, for all three alternate pumping scenarios, GMWA 6 exhibited the highest deficit irrigation state where the average irrigation for the FutBase scenario was 8.1, 6.1, and 5.1 inches, which is greater than the Futirr7in, Futirr9in, and Futirr10in scenario pumping limits because it had one of the lowest rates of farm net recharge and lacked other inflows such as net inflows from adjacent zones and limited net inflow from streams (table 22).

Alternate Climate Scenario Simulated Results

Four alternate climate scenarios simulated various lengths of drier than average climate and stream inflow conditions. A 3-year intense drought, called “Futdrought3yr,” was simulated from the beginning of the scenario model period (January 1, 2017) to December 31, 2019 (Input I in table 17), and was followed by average climate and stream inflow conditions simulated from January 1, 2020, to the end of the scenario model period (December 31, 2049) (Input II in table 17). A 10-year moderate drought, called “Futdrought10yr,” was simulated from the beginning of the scenario model period to December 31, 2026 (Input I in table 17), and was followed by average climate and stream inflow conditions simulated from January 1, 2027, to the end of the scenario model period (December 31, 2049) (Input II in table 17). In addition, the 10-year drought precipitation was reduced by 11 percent using a multiplier of 0.89 applied to the precipitation input file because locally the precipitation for several GWMAs was greater in the drought year compared to the average year even though precipitation was less than average across the CPIHM. A mid-growing season drought, called “Futdroughtjun2sep,” was simulated for each year of the scenario model period (2017 to 2049). Within each year, average monthly climate and stream inflow conditions were simulated from January to May (Input I, table 17) and October to December (Input III, table 17) and a moderate drought was simulated from June to September (Input II, table 17). An early growing season drought, called “Futdroughtmar2may,” simulated each year of the scenario model period (2017 to 2049). Within each year, average monthly climate and stream inflow conditions were simulated from January to February (Input I, table 17) and June to December (Input III, table 17), and a moderate drought was simulated from March to May (Input II, table 17).

3-Year Drought Scenario Results

The Futdrought3yr scenario average groundwater levels decreased during the drought and ended below their predrought levels for all GWMAs and the CPNRD (table 19). GWMA 6 exhibited the least amount of drawdown during the 3-year drought period (2.4 ft) and GWMA 3 exhibited the most amount of drawdown during the 3-year drought period (13.7 ft) (table 19). GWMAs 3, 14, and 17 had the largest declines during the drought (January 1, 2017, to December 31, 2019) because they had larger outflows to irrigation wells than other areas. GWMA 2 also exhibited large declines during the drought (11.9 ft) owing to having the third highest rate of outflows to irrigation wells and the lowest amount of recharge to the water table by area of any GWMA (table 21). By the end of the forecast, the groundwater levels fully recovered (equal to or above their predrought levels) for 10 GWMAs, whereas the groundwater levels for the other 14 GWMAs, CPNRD, and CPIHM did not recover to their predrought levels. Groundwater levels in GWMA 1 exhibited the largest drawdown from their predrought (January 1, 2017) levels at 13.4 ft, and GWMA 10 exhibited groundwater levels that recovered most compared to their predrought levels at 5.4 ft. Groundwater levels did not recover for GWMAs 1 and 6 after the end of the drought; instead, they continued to decline by 9.1 and 7.0 ft, respectively, until the end of the scenario period owing to a combination of net outflows to adjacent zones, low farm net recharge rates, and large CIR during drought and average conditions compared to other GWMAs (table 19). These continued declines postdrought indicated that areas with large CIR and low rates of recharge (large difference in irrigation and recharge) that are similar to average conditions are more vulnerable to severe droughts (fig. 30*A*). GWMAs 10, 14, 17, and 18 recovered the most after the end of the drought because they had more sources of water to replenish storage, such as larger farm net recharge, net inflows from adjacent zones, or net inflows from streams (figs. 30*B*, 5.10). Five GWMAs (11, 18, 19, 22, and 23) exhibited average annual recharge rates on irrigated land that were greater than the rates of groundwater irrigation; GWMA 23 exhibited the largest difference of 8 inches more recharge than irrigation and had other sources of water to draw from, which included large net inflows from adjacent zones and connection to streams (fig. 30*C*). GWMA 23 also exhibited fewer declines in groundwater levels at the end of the drought (3.0 ft), which indicated that these areas are more resilient to severe droughts and do not have the lasting effects like some of the heavily irrigated areas in the drier western region (table 19).

10-Year Drought Scenario Results

The average groundwater levels simulated in the Futdrought10yr scenario were below levels for the FutBase scenario for most GWMAs (table 19). After 3 years of the moderate drought (December 31, 2019), average groundwater levels were below their predrought levels for 23 GWMAs and the CPNRD and CPIHM supergroups (table 19). Only GWMA 20 exhibited groundwater levels above predrought levels (0.6 ft) after 3 years of moderate drought. These results indicated that, in general, the moderate drought was more stressful on the groundwater-flow system across the study area compared to conditions at the beginning of the forecast. Compared to the 3-year intense drought, the average groundwater levels were 5.0 ft higher for the CPNRD and all 24 GWMAs exhibited higher groundwater levels in the same period (table 19).

At the end of the 10-year drought (December 31, 2026), average groundwater levels were below their predrought levels for 23 GWMAs and the CPNRD and CPIHM (table 19). Only GWMA 20 exhibited groundwater levels above their predrought levels (1.0 ft); this GWMA exhibited a decrease in outflows to irrigation wells for the 10-year moderate drought compared to the recent development period owing to an increase in precipitation compared to the recent development period (2011–16), which reduced the primary outflow from groundwater, indicating that this GWMA's groundwater was more stressed in the development period compared to other GWMAs (table 22). By the end of the scenario (December 31, 2049), with average climate and stream inflow conditions simulated from January 1, 2027, to December 31, 2049, the groundwater levels fully recovered (equal to or above their predrought levels) for 10 GWMAs, whereas groundwater levels for the other 15 GWMAs, CPNRD, and CPIHM were below their predrought levels. Groundwater levels in GWMA 1 exhibited the largest drawdown from their predrought (December 3, 2016) levels at 13.9 ft, and GWMA 10 exhibited groundwater levels that recovered most compared to their predrought levels at 5.1 ft. Groundwater levels did not recover for seven GWMAs (1, 6, 13, 16, 20, 22, and 23) after the end of the drought; instead, they continued to decline by 0.1 to 6.6 ft, respectively, until the end of 2049 (table 19).

Outflows to irrigation wells, inflows to recharge, and the difference between irrigation and recharge on irrigated land affected the recovery of groundwater levels by the end of the forecast. GWMAs that exhibited the largest differences between irrigation depths and recharge depths on irrigated land (GWMAs 1, 6, and 13) did not recover at the end of the 10-year drought; instead, they continued to decline between 1.1 and 6.6 ft (table 19). GWMAs 1 and 6 were in the drier western region of the CPIHM where recharge was lowest compared to other regions and did not vary much from drought to average conditions, and GWMA 13 also exhibited a minimal difference in recharge during drought and average conditions (table 21). These GWMAs exhibited declines throughout the FutBase forecast, and their net outflows to irrigation wells were similar for the 10-year moderate drought and FutBase forecasts, which indicated that the groundwater-flow system in these areas was stressed enough under average conditions to illicit net releases from storage (table 22, fig. 5.11).

GWMAs that exhibited the most recharge (14, 15, and 24) also exhibited moderate differences between irrigation and recharge on irrigated land, which resulted in moderate recoveries (tables 19 and 21). GWMAs that recovered the most after the end of the 10-year moderate drought exhibited the smallest difference between irrigation and recharge on irrigated land (GWMAs 9 and 12). These GWMAs also exhibited farm net recharge rates that were similar to net outflows to irrigation wells and low net flow to or from adjacent zones, which indicated that recharge supported irrigation pumping, and there were minimal other outflows. These GWMAs were located in the central region of the CPIHM where irrigation pumping increased enough during the drought to cause declines, and after the drought ended, pumping was reduced enough and recharge was high enough to allow the system to recover, which indicated the groundwater-flow system was more responsive to changes in climate than other regions (table 19). Further, the five GWMAs (11, 18, 19, 22, and 23) that exhibited more recharge on irrigated land than outflows to irrigation wells and exhibited small differences between net irrigation wells and farm net recharge were generally in the wetter eastern region of the CPIHM; recharge and irrigation amounts were also similar between the drought and average conditions, which indicated that those GWMAs were less stressed than other GWMAs for the conditions simulated by the Futdrought10yr forecast and that storage was replenished primarily through net inflows from recharge.

Mid-Growing Season Drought Scenario Results

The average groundwater levels simulated by the CPIHM for the Futdroughtjun2sep (mid-growing season drought) scenario were below levels for the FutBase scenario for all GWMAs and the CPNRD and CPIHM (table 19). After 3 years of a mid-growing season drought (January 1, 2017, to December 31, 2019, with each June through September simulated as drought conditions), average groundwater levels were 0.9 to 4.9 ft below their predrought levels for all 24 GWMAs. GWMA 2 exhibited second largest declines (3.8 ft) after 3 years. By December 31, 2026, with mid-growing season drought conditions simulated from January 1, 2017, to December 31, 2026, all 24 GWMAs exhibited groundwater levels 1.6 to 12.9 ft below the predrought groundwater levels (December 31, 2016). These results indicated that a mid-growing season drought bookended by average climate and stream inflow conditions for January through May and October through December caused groundwater-level declines across all regions of the CPIHM (table 19). GWMAs 2, 3, and 15 exhibited the largest declines (11.6, 12.9, and 8.5 ft, respectively) during the 10-year period (January 1, 2017, to December 31, 2026) and GWMAs 4 and 22 exhibited the lowest declines (1.6 and 1.6 ft, respectively) (table 19).

By the end of the scenario (December 31, 2049), with mid-growing season drought conditions simulated from January 1, 2017, to December 31, 2049, all 24 GWMAs exhibited groundwater levels that were 2.0 to 30.6 ft below their initial predrought scenario levels. These results indicated that groundwater levels in all regions of the CPIHM continued to decline below their predrought levels each year of the scenario. The drier western GWMAs 1, 2, and 3 exhibited the largest declines (23.1, 30.6, and 28.3 ft, respectively) and GWMAs 4 and 22 exhibited the lowest declines (2.7 and 2.0 ft, respectively) (table 19). By the end of the scenario, 13 GWMAs exhibited declines of greater than 10 ft and six GWMAs exhibited declines of greater than 20 ft. The GWMAs that exhibited the largest declines in groundwater

Table 20. Average landscape water-budget component results for each scenario (January 1, 2017, to December 31, 2049) by Groundwater Management Area, Central Platte Natural Resource District domain, and the Central Platte Integrated Hydrologic Model.

[GWMA, Groundwater Management Area; CPNRD, Central Platte Natural Resources District; CPIHM, Central Platte Integrated Hydrologic Model]

GWMA/ super-group	Area (acres)	Inflows			Outflows							
		Precipitation	Irrigation wells	Surface-water deliveries	Evaporation of groundwater	Transpiration of groundwater	Evaporation of irrigation water	Evaporation of precipitation	Transpiration of irrigation water	Transpiration of precipitation	Runoff	Deep percolation
FutBase, in acre-feet per year[1]												
1	115,520	205,966	20,119	0	0	0	−378	−58,773	−17,702	−122,233	−11,616	−15,382
2	43,360	83,156	30,399	0	0	0	−604	−26,087	−26,679	−34,749	−10,128	−15,307
3	127,040	239,528	99,615	8,332	−902	−3,125	−4,797	−71,630	−80,829	−96,179	−35,568	−58,472
4	180,640	365,103	39,001	17,661	−24,072	−41,091	−2,251	−103,314	−44,070	−133,530	−60,731	−77,868
5	102,720	194,990	19,938	0	0	0	−441	−58,174	−17,179	−109,871	−12,869	−16,394
6	90,240	141,996	12,236	0	0	0	−211	−37,831	−10,802	−87,622	−7,861	−9,906
7	234,880	465,020	31,668	0	−345	−94	−619	−113,573	−27,756	−274,979	−38,281	−41,480
8	40,480	83,700	21,817	846	−661	−4,147	−566	−23,998	−19,285	−26,923	−15,624	−19,965
9	179,200	393,700	55,974	0	−26	−317	−1,093	−95,660	−49,222	−182,137	−55,454	−66,107
10	51,360	122,196	24,770	0	−298	−68	−485	−28,697	−21,775	−43,274	−26,386	−26,349
11	154,880	352,344	23,147	0	−19,860	−56,959	−431	−93,618	−20,401	−80,234	−91,322	−89,485
12	50,240	113,485	19,053	0	0	0	−339	−27,571	−16,809	−47,481	−17,826	−22,513
13	85,280	180,581	32,351	0	0	−172	−598	−43,961	−28,502	−79,502	−30,016	−30,353
14	106,880	234,805	75,972	0	−2	−753	−1,384	−61,766	−66,845	−76,126	−45,453	−59,204
15	57,440	131,075	36,719	0	−43	−232	−790	−33,296	−31,957	−39,576	−26,849	−35,326
16	45,280	104,965	19,753	0	0	−114	−370	−27,128	−17,407	−42,070	−16,411	−21,331
17	108,640	248,468	50,453	0	−1,925	−15,715	−981	−65,585	−44,392	−65,701	−57,590	−64,672
18	73,920	177,263	5,399	0	−19,370	−26,833	−110	−51,223	−4,748	−16,355	−51,468	−58,757
19	71,200	168,267	3,106	0	−28,783	−32,086	−61	−49,704	−2,735	−18,751	−44,856	−55,268
20	51,200	119,193	13,427	0	−803	−6,912	−306	−30,148	−11,659	−38,260	−23,529	−28,718
21	67,840	161,501	20,169	0	−1,805	−2,999	−369	−40,081	−17,783	−59,916	−27,926	−35,596
22	28,000	65,776	4,881	0	−5,983	−8,838	−98	−18,152	−4,290	−12,786	−16,024	−19,307
23	45,440	107,351	1,198	0	−24,383	−15,890	−25	−30,138	−1,052	−9,904	−30,084	−37,345
24	30,560	72,421	15,618	0	−1,216	−1,549	−292	−18,445	−13,760	−19,432	−15,738	−20,372
CPNRD	2,142,236	4,533,231	676,782	26,838	−130,478	−217,892	−17,600	−1,208,657	−597,640	−1,717,689	−769,689	−925,578
CPIHM	4,926,071	10,407,613	1,790,361	28,721	−242,387	−308,235	−42,946	−2,806,218	−1,560,437	−3,969,984	−1,716,545	−2,130,566

Table 20. Average landscape water-budget component results for each scenario (January 1, 2017, to December 31, 2049) by Groundwater Management Area, Central Platte Natural Resource District domain, and the Central Platte Integrated Hydrologic Model.—Continued

[GWMA, Groundwater Management Area; CPNRD, Central Platte Natural Resources District; CPIHM, Central Platte Integrated Hydrologic Model]

GWMA/ super-group	Area (acres)	Inflows			Outflows							
		Precipitation	Irrigation wells	Surface-water deliveries	Evaporation of groundwater	Transpiration of groundwater	Evaporation of irrigation water	Evaporation of precipitation	Transpiration of irrigation water	Transpiration of precipitation	Runoff	Deep percolation
Futdrought3yr, in acre-feet per year[1]												
1	115,520	196,750	21,663	0	0	0	−419	−57,117	−19,049	−115,593	−11,191	−15,044
2	43,360	79,141	33,394	0	0	0	−676	−25,283	−29,295	−32,805	−9,553	−14,923
3	127,040	228,619	112,486	6,402	−508	−2,136	−5,345	−69,531	−89,015	−92,032	−33,331	−58,252
4	180,640	349,048	46,506	18,809	−21,428	−38,747	−2,602	−100,368	−50,919	−129,874	−56,367	−74,232
5	102,720	186,218	21,591	0	0	0	−491	−56,578	−18,590	−104,226	−12,138	−15,786
6	90,240	135,842	12,898	0	0	0	−226	−36,753	−11,382	−82,851	−7,719	−9,810
7	234,880	444,721	34,145	0	−287	−90	−681	−111,025	−29,913	−260,601	−36,585	−40,060
8	40,480	80,206	25,920	777	−311	−3,194	−664	−23,281	−22,763	−26,915	−14,334	−18,944
9	179,200	375,668	61,668	0	−15	−259	−1,221	−93,549	−54,210	−172,290	−52,557	−63,508
10	51,360	116,526	27,766	0	−255	−47	−551	−28,152	−24,401	−40,831	−24,991	−25,366
11	154,880	337,196	32,707	0	−15,124	−50,785	−612	−90,785	−28,824	−84,603	−83,233	−81,845
12	50,240	108,155	20,756	0	0	0	−376	−26,936	−18,304	−44,780	−16,900	−21,615
13	85,280	172,286	35,192	0	0	−81	−663	−43,125	−30,992	−74,953	−28,489	−29,256
14	106,880	224,584	82,542	0	0	−338	−1,536	−60,713	−72,593	−72,261	−42,984	−57,038
15	57,440	126,538	39,029	0	−7	−153	−847	−33,192	−33,960	−38,260	−25,414	−33,894
16	45,280	100,453	21,334	0	0	−87	−409	−26,511	−18,792	−39,823	−15,654	−20,599
17	108,640	237,185	60,396	0	−1,095	−11,035	−1,190	−63,571	−53,129	−66,345	−52,845	−60,502
18	73,920	169,509	15,136	0	−13,574	−23,866	−300	−48,741	−13,323	−23,615	−45,677	−52,990
19	71,200	160,718	8,293	0	−22,036	−29,952	−162	−47,444	−7,300	−24,295	−40,099	−49,712
20	51,200	114,742	15,263	0	−476	−5,639	−349	−29,382	−13,247	−37,844	−22,012	−27,171
21	67,840	155,666	21,681	0	−1,283	−3,140	−405	−39,319	−19,108	−57,338	−26,786	−34,390
22	28,000	63,466	6,034	0	−5,304	−8,421	−121	−17,670	−5,303	−12,811	−15,186	−18,408
23	45,440	103,783	2,335	0	−20,893	−16,524	−48	−29,291	−2,054	−10,964	−28,388	−35,373
24	30,560	70,161	17,366	0	−831	−1,152	−330	−17,998	−15,296	−19,213	−15,008	−19,683
CPNRD	2,142,236	4,337,543	776,100	25,988	−103,427	−195,647	−20,223	−1,176,417	−681,763	−1,665,212	−717,520	−878,496
CPIHM	4,926,071	9,998,842	1,997,494	28,057	−183,050	−277,130	−48,736	−2,742,479	−1,736,195	−3,839,477	−1,616,552	−2,040,955

Table 20. Average landscape water-budget component results for each scenario (January 1, 2017, to December 31, 2049) by Groundwater Management Area, Central Platte Natural Resource District domain, and the Central Platte Integrated Hydrologic Model.—Continued

[GWMA, Groundwater Management Area; CPNRD, Central Platte Natural Resources District; CPIHM, Central Platte Integrated Hydrologic Model]

GWMA/ super-group	Area (acres)	Inflows			Outflows							
		Precipitation	Irrigation wells	Surface-water deliveries	Evaporation of groundwater	Transpiration of groundwater	Evaporation of irrigation water	Evaporation of precipitation	Transpiration of irrigation water	Transpiration of precipitation	Runoff	Deep percolation
Futdrought10yr, in acre-feet per year[1]												
1	115,520	197,608	21,133	0	0	0	−397	−58,279	−18,595	−117,039	−10,354	−14,077
2	43,360	80,095	33,319	0	0	0	−645	−26,052	−29,259	−32,499	−9,772	−15,188
3	127,040	228,077	108,730	8,653	−505	−2,323	−5,105	−71,167	−88,055	−91,119	−32,763	−57,250
4	180,640	344,088	45,374	19,694	−20,665	−39,423	−2,502	−101,812	−50,825	−129,242	−53,662	−71,114
5	102,720	184,096	21,746	0	0	0	−488	−57,156	−18,732	−103,037	−11,410	−15,020
6	90,240	133,856	12,417	0	0	0	−209	−37,269	−10,966	−83,347	−6,294	−8,189
7	234,880	437,340	33,877	0	−242	−88	−659	−114,380	−29,694	−259,073	−32,166	−35,245
8	40,480	78,231	26,006	1,079	−230	−3,021	−651	−23,793	−23,125	−26,518	−13,360	−17,870
9	179,200	370,945	62,532	0	−10	−234	−1,212	−96,575	−54,995	−170,453	−49,727	−60,515
10	51,360	115,197	28,875	0	−236	−54	−567	−28,657	−25,382	−39,116	−24,878	−25,472
11	154,880	335,468	32,860	0	−14,793	−51,084	−601	−92,707	−28,973	−84,408	−81,678	−79,962
12	50,240	109,218	19,668	0	0	0	−355	−28,416	−17,346	−46,291	−15,994	−20,485
13	85,280	178,879	33,907	0	0	−130	−638	−45,243	−29,862	−75,636	−30,339	−31,068
14	106,880	227,505	80,505	0	0	−515	−1,510	−61,703	−70,788	−71,766	−44,096	−58,146
15	57,440	124,572	39,521	0	−2	−134	−890	−32,571	−34,354	−36,403	−25,629	−34,245
16	45,280	102,572	20,571	0	0	−105	−393	−27,032	−18,122	−39,761	−16,416	−21,421
17	108,640	241,974	56,561	0	−1,496	−13,918	−1,104	−64,392	−49,765	−62,894	−56,355	−64,027
18	73,920	171,227	9,997	0	−14,710	−27,263	−191	−48,811	−8,806	−20,630	−47,788	−54,998
19	71,200	162,496	5,446	0	−22,851	−32,306	−102	−48,056	−4,799	−22,451	−41,419	−51,115
20	51,200	119,262	13,583	0	−729	−6,708	−306	−30,359	−11,796	−37,660	−23,743	−28,980
21	67,840	156,749	21,396	0	−1,408	−3,155	−394	−39,636	−18,863	−56,280	−27,628	−35,346
22	28,000	65,263	5,253	0	−5,413	−8,615	−103	−17,910	−4,619	−12,974	v15,853	−19,056
23	45,440	105,698	1,640	0	−21,489	−16,414	−32	−29,700	−1,444	−10,961	−29,053	−36,148
24	30,560	70,942	16,576	0	−1,000	−1,318	−306	−18,070	−14,608	−18,752	−15,545	−20,238
CPNRD	2,142,236	4,341,726	751,494	29,426	−105,781	−206,806	−19,359	−1,199,844	−663,774	−1,648,397	−716,001	−875,272
CPIHM	4,926,071	9,976,889	1,978,282	31,495	−173,841	−285,729	−48,025	−2,772,823	−1,721,997	−3,795,896	−1,611,424	−2,036,502

Table 20. Average landscape water-budget component results for each scenario (January 1, 2017, to December 31, 2049) by Groundwater Management Area, Central Platte Natural Resource District domain, and the Central Platte Integrated Hydrologic Model.—Continued

[GWMA, Groundwater Management Area; CPNRD, Central Platte Natural Resources District; CPIHM, Central Platte Integrated Hydrologic Model]

GWMA/ super-group	Area (acres)	Inflows			Outflows							
		Precipitation	Irrigation wells	Surface-water deliveries	Evaporation of groundwater	Transpiration of groundwater	Evaporation of irrigation water	Evaporation of precipitation	Transpiration of irrigation water	Transpiration of precipitation	Runoff	Deep percolation
Futdroughjun2sep, in acre-feet per year[1]												
1	115,520	180,809	22,371	0	0	0	−404	−58,568	−19,700	−104,324	−8,348	−11,835
2	43,360	70,951	38,459	0	0	0	−701	−27,134	−33,814	−27,856	−7,241	−12,663
3	127,040	203,904	129,501	3,857	−50	−708	−5,417	−73,571	−100,515	−81,199	−25,005	−51,555
4	180,640	296,695	57,755	22,801	−16,117	−34,810	−2,888	−97,568	−63,356	−118,615	−38,648	−56,176
5	102,720	161,974	24,707	0	0	0	−554	−55,505	−21,287	−86,826	−9,418	−13,090
6	90,240	126,766	12,333	0	0	0	−190	−39,172	−10,909	−80,062	−3,596	−5,169
7	234,880	382,273	37,216	0	−74	−111	−698	−110,448	−32,646	−226,788	−22,721	−26,188
8	40,480	67,580	34,591	0	−13	−875	−768	−23,439	−29,663	−24,813	−9,347	−14,143
9	179,200	309,022	74,080	0	0	−73	−1,387	−93,065	−65,193	−144,860	−34,157	−44,440
10	51,360	89,685	36,706	0	−35	−72	−716	−26,204	−32,264	−29,787	−17,762	−19,657
11	154,880	265,084	55,152	0	−7,468	−34,766	−994	−78,950	−48,643	−85,523	−53,258	−52,869
12	50,240	100,903	19,696	0	0	0	−362	−28,749	−17,364	−44,516	−12,808	−16,798
13	85,280	150,479	35,564	0	0	−37	−675	−42,643	−31,313	−65,692	−22,280	−23,441
14	106,880	193,333	85,988	0	0	−93	−1,665	−60,020	−75,555	−63,835	−32,728	−45,518
15	57,440	98,786	43,837	0	0	−38	−1,054	−29,740	−38,038	−29,559	−18,234	−25,997
16	45,280	88,431	21,161	0	0	−54	−403	−26,412	−18,642	−34,704	−12,535	−16,897
17	108,640	201,245	71,897	0	−236	−4,580	−1,384	−60,712	−63,285	−60,104	−39,823	−47,834
18	73,920	144,352	30,867	0	−2,867	−16,888	−547	−43,201	−27,233	−36,184	−30,760	−37,294
19	71,200	135,968	15,647	0	−11,012	−27,310	−276	−41,911	−13,804	−32,301	−28,007	−35,316
20	51,200	95,575	14,996	0	−30	−2,237	−328	−29,802	−13,020	−39,214	−12,275	−15,933
21	67,840	131,205	22,989	0	−829	−2,893	−411	−38,816	−20,279	−48,056	−20,114	−26,519
22	28,000	53,095	6,500	0	−3,760	−7,455	−119	−17,038	−5,722	−14,047	−10,138	−12,529
23	45,440	87,107	3,729	0	−11,044	−17,263	−66	−27,196	−3,291	−17,536	−18,830	−23,918
24	30,560	58,771	17,994	0	−256	−479	−316	−18,149	−15,873	−17,889	−10,345	−14,192
CPNRD	2,142,236	3,694,302	913,733	26,658	−53,789	−150,742	−22,322	−1,148,112	−801,411	−1,514,362	−498,439	−650,048
CPIHM	4,926,071	8,484,816	2,293,265	29,049	−90,692	−209,025	−54,845	−2,667,532	−1,988,888	−3,406,041	−1,145,406	−1,544,417

Table 20. Average landscape water-budget component results for each scenario (January 1, 2017, to December 31, 2049) by Groundwater Management Area, Central Platte Natural Resource District domain, and the Central Platte Integrated Hydrologic Model.—Continued

[GWMA, Groundwater Management Area; CPNRD, Central Platte Natural Resources District; CPIHM, Central Platte Integrated Hydrologic Model]

GWMA/ super-group	Area (acres)	Inflows			Outflows							
		Precipitation	Irrigation wells	Surface-water deliveries	Evaporation of groundwater	Transpiration of groundwater	Evaporation of irrigation water	Evaporation of precipitation	Transpiration of irrigation water	Transpiration of precipitation	Runoff	Deep percolation
Futdroughtmar2may, in acre-feet per year[1]												
1	115,520	173,429	20,238	0	0	0	−380	−49,063	−17,808	−111,676	−5,870	−8,870
2	43,360	67,305	31,293	0	0	0	−617	−23,407	−27,469	−32,182	−5,324	−9,598
3	127,040	195,376	103,767	7,530	−332	−1,928	−4,891	−63,772	−83,483	−90,727	−21,260	−42,540
4	180,640	298,238	44,495	17,695	−18,792	−36,560	−2,396	−87,727	−48,659	−130,186	−38,572	−52,887
5	102,720	157,873	20,042	0	0	0	−442	−47,264	−17,272	−98,524	−5,854	−8,561
6	90,240	117,788	12,328	0	0	0	−212	−29,299	−10,884	−76,581	−5,677	−7,463
7	234,880	381,381	31,853	0	−152	−94	−621	−92,822	−27,919	−245,241	−22,285	−24,346
8	40,480	68,622	25,881	861	−19	−2,195	−640	−21,531	−22,855	−28,240	−9,176	−12,922
9	179,200	320,696	56,638	0	0	−160	−1,102	−84,290	−49,809	−166,376	−33,910	−41,847
10	51,360	99,743	25,029	0	−232	−42	−489	−26,930	−22,004	−41,241	−17,275	−16,832
11	154,880	282,237	36,034	0	−9,120	−40,867	−659	−81,408	−31,772	−101,033	−53,046	−50,353
12	50,240	86,989	19,256	0	0	0	−341	−24,250	−16,989	−43,475	−8,930	−12,260
13	85,280	139,949	32,892	0	0	−29	−605	−38,595	−28,981	−72,550	−16,090	−16,019
14	106,880	183,517	76,885	0	0	−98	−1,396	−58,160	−67,654	−73,362	−24,767	−35,062
15	57,440	102,844	36,934	0	0	−48	−793	−32,679	−32,147	−38,248	−14,795	−21,116
16	45,280	81,952	19,857	0	0	−26	−373	−24,145	−17,498	−39,316	−8,454	−12,023
17	108,640	192,761	61,771	0	−215	−3,666	−1,187	−58,137	−54,371	−73,819	−30,930	−36,088
18	73,920	137,837	27,939	0	−3,017	−14,276	−530	−42,117	−24,614	−44,976	−24,234	−29,304
19	71,200	130,203	13,919	0	−12,817	−24,223	−267	−40,436	−12,260	−39,977	−22,290	−28,893
20	51,200	98,675	15,557	0	−29	−2,892	−351	−25,837	−13,489	−39,651	−15,380	−19,523
21	67,840	126,868	20,302	0	−844	−2,856	−371	−35,030	−17,901	−55,983	−16,206	−21,679
22	28,000	54,051	6,369	0	−4,446	−7,640	−124	−15,557	−5,600	−13,844	−11,352	−13,943
23	45,440	87,047	2,798	0	−12,725	−17,387	−57	−24,885	−2,461	−17,162	−20,023	−25,257
24	30,560	57,991	17,070	0	−256	−466	−317	−16,235	−15,042	−19,952	−9,929	−13,586
CPNRD	2,142,236	3,643,669	759,147	26,086	−62,994	−155,454	−19,164	−1,043,674	−668,941	−1,694,419	−441,675	−561,028
CPIHM	4,926,071	8,493,446	1,914,760	27,979	−118,830	−228,981	−45,698	−2,511,695	−1,666,925	−3,868,004	−1,010,274	−1,333,589

Table 20. Average landscape water-budget component results for each scenario (January 1, 2017, to December 31, 2049) by Groundwater Management Area, Central Platte Natural Resource District domain, and the Central Platte Integrated Hydrologic Model.—Continued

[GWMA, Groundwater Management Area; CPNRD, Central Platte Natural Resources District; CPIHM, Central Platte Integrated Hydrologic Model]

GWMA/ super-group	Area (acres)	Inflows			Outflows							
		Precipitation	Irrigation wells	Surface-water deliveries	Evaporation of groundwater	Transpiration of groundwater	Evaporation of irrigation water	Evaporation of precipitation	Transpiration of irrigation water	Transpiration of precipitation	Runoff	Deep percolation
Futirr7in, in acre-feet per year[1]												
1	115,520	205,966	10,603	0	0	0	−175	−58,773	−9,354	−122,233	−11,615	−14,419
2	43,360	83,156	13,193	18	0	0	−223	−26,087	−11,648	−34,749	−10,126	−13,534
3	127,040	239,528	18,117	17,289	−2,664	−8,017	−1,411	−72,035	−27,314	−90,915	−37,628	−45,632
4	180,640	365,103	18,134	17,392	−29,346	−45,155	−1,377	−103,841	−27,565	−127,436	−63,176	−77,234
5	102,720	194,990	10,144	0	0	0	−199	−58,174	−8,764	−109,871	−12,866	−15,260
6	90,240	141,996	5,160	0	0	0	−77	−37,831	−4,566	−87,622	−7,861	−9,199
7	234,880	465,020	17,456	0	−405	−126	−298	−113,576	−15,345	−274,945	−38,293	−40,019
8	40,480	83,700	8,620	813	−4,201	−6,032	−208	−24,469	−8,044	−23,116	−17,132	−20,163
9	179,200	393,700	32,445	0	−92	−441	−549	−95,676	−28,617	−181,956	−55,523	−63,823
10	51,360	122,196	14,606	0	−583	−870	−253	−28,864	−12,872	−42,425	−26,693	−25,696
11	154,880	352,344	19,603	0	−25,312	−57,956	−353	−94,415	−17,289	−73,153	−94,169	−92,567
12	50,240	113,485	11,322	0	0	−8	−175	−27,572	−10,015	−47,476	−17,827	−21,743
13	85,280	180,581	18,700	0	0	−632	−301	−43,989	−16,519	−79,155	−30,159	−29,156
14	106,880	234,805	44,603	0	−297	−3,078	−722	−62,128	−39,340	−74,261	−46,114	−56,842
15	57,440	131,075	20,536	0	−231	−424	−392	−33,351	−17,924	−39,285	−26,956	−33,704
16	45,280	104,965	12,022	0	0	−295	−201	−27,138	−10,619	−42,018	−16,430	−20,581
17	108,640	248,468	34,976	0	−3,664	−20,480	−618	−66,359	−30,831	−59,111	−60,250	−66,275
18	73,920	177,263	4,951	0	−21,014	−26,582	−101	−51,401	−4,354	−14,916	−52,049	−59,393
19	71,200	168,267	2,620	0	−34,593	−31,640	−51	−50,042	−2,307	−15,376	−46,129	−56,981
20	51,200	119,193	9,000	0	−1,411	−8,312	−179	−30,419	−7,839	−36,563	−24,182	−29,010
21	67,840	161,501	13,091	0	−2,665	−2,609	−217	−40,091	−11,565	−59,764	−27,989	−34,966
22	28,000	65,776	4,312	0	−6,257	−9,172	−79	−18,210	−3,800	−12,406	−16,160	−19,434
23	45,440	107,351	1,076	0	−27,610	−15,214	−23	−30,225	−946	−9,160	−30,378	−37,696
24	30,560	72,421	10,938	0	−2,331	−2,191	−188	−18,683	−9,654	−18,408	−16,093	−20,333
CPNRD	2,142,236	4,533,231	356,227	35,512	−162,676	−239,235	−8,371	−1,213,453	−337,090	−1,676,419	−785,877	−903,761
CPIHM	4,926,071	10,407,613	1,041,458	37,392	−315,970	−337,015	−22,215	−2,814,468	−932,520	−3,898,276	−1,744,558	−2,074,425

Table 20. Average landscape water-budget component results for each scenario (January 1, 2017, to December 31, 2049) by Groundwater Management Area, Central Platte Natural Resource District domain, and the Central Platte Integrated Hydrologic Model.—Continued

[GWMA, Groundwater Management Area; CPNRD, Central Platte Natural Resources District; CPIHM, Central Platte Integrated Hydrologic Model]

GWMA/ super-group	Area (acres)	Inflows			Outflows							
		Precipitation	Irrigation wells	Surface-water deliveries	Evaporation of groundwater	Transpiration of groundwater	Evaporation of irrigation water	Evaporation of precipitation	Transpiration of irrigation water	Transpiration of precipitation	Runoff	Deep percolation
Futirr9in, in acre-feet per year[1]												
1	115,520	205,966	12,642	0	0	0	−211	−58,773	−11,151	−122,233	−11,615	−14,625
2	43,360	83,156	16,065	0	0	0	−274	−26,087	−14,163	−34,749	−10,126	−13,822
3	127,040	239,528	22,049	16,806	−2,417	−7,583	−1,506	−71,992	−30,124	−91,389	−37,436	−45,937
4	180,640	365,103	21,113	17,434	−28,761	−44,715	−1,471	−103,791	−30,030	−128,030	−62,932	−77,395
5	102,720	194,990	11,920	0	0	0	−237	−58,174	−10,296	−109,871	−12,867	−15,466
6	90,240	141,996	6,627	0	0	0	−99	−37,831	−5,865	−87,622	−7,861	−9,345
7	234,880	465,020	21,227	0	−393	−118	−365	−113,575	−18,656	−274,956	−38,289	−40,406
8	40,480	83,700	10,161	804	−3,190	−5,908	−243	−24,403	−9,357	−23,678	−16,907	−20,076
9	179,200	393,700	39,551	0	−52	−408	−675	−95,672	−34,877	−182,017	−55,500	−64,509
10	51,360	122,196	17,834	0	−378	−541	−312	−28,785	−15,715	−42,841	−26,540	−25,839
11	154,880	352,344	20,775	0	−23,788	−57,769	−383	−94,215	−18,315	−74,908	−93,459	−91,839
12	50,240	113,485	13,718	0	0	−1	−214	−27,571	−12,132	−47,480	−17,826	−21,980
13	85,280	180,581	22,520	0	0	−436	−367	−43,978	−19,891	−79,308	−30,095	−29,462
14	106,880	234,805	52,445	0	−164	−2,079	−862	−61,962	−46,240	−75,067	−45,828	−57,290
15	57,440	131,075	24,311	0	−168	−340	−470	−33,334	−21,213	−39,376	−26,923	−34,071
16	45,280	104,965	15,066	0	0	−199	−253	−27,133	−13,307	−42,040	−16,422	−20,876
17	108,640	248,468	40,802	0	−2,978	−18,765	−729	−66,074	−35,960	−61,614	−59,234	−65,659
18	73,920	177,263	5,117	0	−20,348	−26,720	−105	−51,328	−4,500	−15,592	−51,769	−59,086
19	71,200	168,267	2,732	0	−32,649	−32,077	−53	−49,947	−2,406	−16,290	−45,782	−56,522
20	51,200	119,193	11,434	0	−1,067	−7,457	−225	−30,269	−9,963	−37,555	−23,797	−28,816
21	67,840	161,501	15,532	0	−2,341	−2,744	−261	−40,086	−13,717	−59,822	−27,968	−35,179
22	28,000	65,776	4,543	0	−6,178	−9,035	−85	−18,185	−4,000	−12,560	−16,104	−19,385
23	45,440	107,351	1,117	0	−26,415	−15,457	−24	−30,200	−982	−9,385	−30,288	−37,591
24	30,560	72,421	12,981	0	−1,776	−1,920	−225	−18,586	−11,454	−18,812	−15,954	−20,370
CPNRD	2,142,236	4,533,231	422,282	35,045	−153,064	−234,272	−9,650	−1,212,055	−394,316	−1,687,291	−781,601	−905,646
CPIHM	4,926,071	10,407,613	1,255,678	36,925	−291,681	−329,340	−26,553	−2,811,861	−1,118,272	−3,919,891	−1,736,131	−2,087,508

Table 20. Average landscape water-budget component results for each scenario (January 1, 2017, to December 31, 2049) by Groundwater Management Area, Central Platte Natural Resource District domain, and the Central Platte Integrated Hydrologic Model.—Continued

[GWMA, Groundwater Management Area; CPNRD, Central Platte Natural Resources District; CPIHM, Central Platte Integrated Hydrologic Model]

GWMA/ super-group	Area (acres)	Inflows			Outflows							
		Precipitation	Irrigation wells	Surface-water deliveries	Evaporation of groundwater	Transpiration of groundwater	Evaporation of irrigation water	Evaporation of precipitation	Transpiration of irrigation water	Transpiration of precipitation	Runoff	Deep percolation
Futirr10in, in acre-feet per year[1]												
1	115,520	205,966	13,519	0	0	0	−227	−58,773	−11,922	−122,233	−11,615	−14,714
2	43,360	83,156	17,485	0	0	0	−299	−26,087	−15,415	−34,749	−10,126	−13,966
3	127,040	239,528	23,678	16,569	−2,323	−7,403	−1,545	−71,974	−31,259	−91,583	−37,357	−46,057
4	180,640	365,103	22,216	17,447	−28,539	−44,561	−1,511	−103,773	−30,927	−128,244	−62,845	−77,467
5	102,720	194,990	12,818	0	0	0	−256	−58,174	−11,070	−109,871	−12,867	−15,570
6	90,240	141,996	7,366	0	0	0	−110	−37,831	−6,519	−87,622	−7,861	−9,419
7	234,880	465,020	22,746	0	−387	−113	−394	−113,575	−19,988	−274,960	−38,287	−40,561
8	40,480	83,700	10,921	802	−2,814	−5,837	−261	−24,376	−10,005	−23,928	−16,806	−20,047
9	179,200	393,700	42,789	0	−42	−391	−734	−95,670	−37,730	−182,041	−55,491	−64,824
10	51,360	122,196	19,443	0	−332	−405	−341	−28,756	−17,132	−42,982	−26,489	−25,940
11	154,880	352,344	21,221	0	−23,092	−57,670	−394	−94,116	−18,705	−75,767	−93,113	−91,469
12	50,240	113,485	14,641	0	0	0	−230	−27,571	−12,947	−47,481	−17,825	−22,072
13	85,280	180,581	24,126	0	0	−389	−395	−43,974	−21,307	−79,350	−30,078	−29,603
14	106,880	234,805	56,358	0	−110	−1,703	−932	−61,906	−49,685	−75,348	−45,728	−57,565
15	57,440	131,075	26,219	0	−139	−310	v510	−33,326	−22,875	−39,412	−26,910	−34,262
16	45,280	104,965	16,159	0	0	−176	−273	−27,132	−14,271	−42,046	−16,420	−20,983
17	108,640	248,468	43,097	0	−2,738	-18,153	−776	−65,971	−37,978	−62,500	−58,876	−65,463
18	73,920	177,263	5,185	0	−20,109	−26,725	−106	−51,303	−4,561	−15,799	−51,685	−58,994
19	71,200	168,267	2,801	0	−31,838	−32,159	−55	−49,902	−2,466	−16,743	−45,603	−56,300
20	51,200	119,193	11,939	0	−1,009	−7,320	−236	−30,243	−10,405	−37,721	−23,733	−28,794
21	67,840	161,501	16,614	0	−2,209	−2,818	−281	−40,085	−14,671	−59,844	−27,958	−35,275
22	28,000	65,776	4,605	0	−6,150	−8,993	−87	−18,178	−4,054	−12,603	−16,089	−19,371
23	45,440	107,351	1,137	0	−25,828	−15,589	−24	−30,187	−999	−9,493	−30,244	−37,541
24	30,560	72,421	13,969	0	−1,560	−1,806	−243	−18,541	−12,325	−19,007	−15,887	−20,387
CPNRD	2,142,236	4,533,231	451,054	34,818	−149,220	−232,523	−10,220	−1,211,529	−419,216	−1,691,422	−779,976	−906,741
CPIHM	4,926,071	10,407,613	1,345,271	36,699	−281,730	−326,730	−28,452	−2,810,846	−1,195,783	−3,928,489	−1,732,761	−2,093,251

[1]Forecast names defined in table 17.

Table 21. Average groundwater-flow budget component results for each scenario (January 1, 2017 to December 31, 2049) of the Central Platte Integrated Hydrologic Model by supergroup.

[GWMA, Groundwater Management Area; --, not applicable; CPNRD, Central Platte Natural Resources District; CPIHM, Central Platte Integrated Hydrologic Model]]

		Inflows						Outflows						
GWMA/ supergroup	Area (acres)	Inflow from general heads	Inflow from adjacent zones	Recharge (deep percolation)	Recharge from canal leakage	Release from groundwater storage	Stream leakage	Base flow	Evapotranspiration from groundwater	Outflow to general heads	Outflow to irrigation wells	Outflow to production wells	Outflow to adjacent zones	Replenishment to groundwater storage
							FutBase, in acre-feet per year[1]							
1	115,520	--	14,096	15,334	--	29,453	9,386	--	--	--	−20,116	--	−26,602	−21,552
2	43,360	--	15,865	15,228	--	26,292	7,289	--	--	--	−30,379	--	−9,612	−24,684
3	127,040	--	32,569	55,795	3,922	85,259	53,062	-2,529	-1,517	--	−99,612	−4,571	−41,236	−81,164
4	180,640	--	104,338	46,301	5,711	58,530	71,585	-128,622	-33,680	--	−38,996	−2,446	−25,861	−56,933
5	102,720	28,296	23,513	16,331	4,007	23,822	5,666	--	--	--	−19,935	--	−57,675	−24,024
6	90,240	--	12,666	9,895	--	18,166	4,710	--	--	--	−12,236	--	−19,730	−13,471
7	234,880	--	30,206	41,259	--	50,355	10,184	−520	−257	--	−31,668	−1,213	−49,668	−48,679
8	40,480	--	23,588	17,103	--	21,700	8,226	−4,333	−1,973	--	−21,816	--	−20,603	−21,894
9	179,200	--	31,979	65,836	--	65,527	13,761	−5,467	−128	--	−55,970	−808	−43,814	−70,918
10	51,360	--	12,149	26,189	--	25,515	3,045	−7,862	−217	--	−24,765	−521	−6,210	−27,324
11	154,880	--	19,213	52,157	--	53,935	71,874	−19,792	−39,443	--	−23,142	−22,306	−37,706	−54,847
12	50,240	--	6,990	22,473	--	21,186	394	--	--	--	−19,053	--	−9,249	−22,742
13	85,280	--	16,590	30,237	--	34,454	3,664	−1,065	−47	--	−32,341	−376	−18,388	−32,787
14	106,880	--	9,542	58,607	--	75,098	22,937	−1,211	−249	--	−75,963	−312	−12,138	−76,354
15	57,440	--	15,714	35,156	--	34,231	1,272	--	−112	--	−36,717	--	−14,833	−34,711
16	45,280	--	5,656	21,187	--	21,642	1,452	−2,114	−14	--	−19,752	--	−6,878	−21,192
17	108,640	--	12,737	55,500	--	60,402	16,072	−4,698	−8,591	--	−50,452	−1,878	−19,070	−60,169
18	73,920	--	16,837	34,676	--	26,450	8,673	−17,006	−22,200	--	−5,398	−345	−12,969	−28,848
19	71,200	--	23,031	25,161	--	22,360	15,561	−11,853	−30,788	--	−3,106	−394	−16,124	−23,892
20	51,200	--	3,611	24,545	--	22,832	1,040	−3,578	−3,589	--	−13,424	--	−8,342	−23,095
21	67,840	4,447	34,342	33,234	--	27,564	1,379	−339	−2,533	−6,496	−20,168	--	−44,108	−27,322
22	28,000	--	12,206	12,307	--	10,255	18,571	−24,078	−7,854	--	−4,881	--	−6,343	−10,183
23	45,440	1,001	28,128	17,846	--	14,662	6,396	−14,658	−20,814	−3,341	−1,198	--	−12,288	−15,734
24	30,560	3,150	30,462	18,966	--	17,533	--	−396	−1,420	−6,684	−15,618	--	−28,401	−17,593
CPNRD	2,142,236	36,893	115,928	751,364	13,640	847,256	356,196	−250,119	−175,425	−16,521	−676,704	−35,169	−127,783	−840,150
CPIHM	4,926,071	190,595	--	2,133,797	126,515	2,042,779	583,174	−538,073	−550,306	−146,353	−1,790,361	−43,632	--	−2,008,865

Table 21. Average groundwater-flow budget component results for each scenario (January 1, 2017 to December 31, 2049) of the Central Platte Integrated Hydrologic Model by supergroup.—Continued

[GWMA, Groundwater Management Area; --, not applicable; CPNRD, Central Platte Natural Resources District; CPIHM, Central Platte Integrated Hydrologic Model]]

		Inflows						Outflows						
GWMA/ supergroup	Area (acres)	Inflow from general heads	Inflow from adjacent zones	Recharge (deep percolation)	Recharge from canal leakage	Release from groundwater storage	Stream leakage	Base flow	Evapotranspiration from groundwater	Outflow to general heads	Outflow to irrigation wells	Outflow to production wells	Outflow to adjacent zones	Replenishment to groundwater storage
Futdrought3yr, in acre-feet per year[1]														
1	115,520	--	14,317	14,996	--	31,958	8,979	--	--	--	−21,660	--	−27,140	−21,451
2	43,360	--	17,509	14,843	--	28,296	6,932	--	--	--	−33,374	--	−8,904	−25,302
3	127,040	--	35,963	56,475	3,565	93,672	53,964	-1,360	-1,035	--	−112,483	−4,571	−35,788	−88,412
4	180,640	--	93,481	45,928	5,386	63,737	80,464	−116,058	−31,958	--	−46,500	−2,446	−30,747	−61,480
5	102,720	28,450	23,781	15,723	3,783	25,014	5,374	--	--	--	−21,588	--	−56,307	−24,230
6	90,240	--	12,446	9,799	--	19,240	4,490	--	--	--	−12,898	--	−19,576	−13,501
7	234,880	--	29,761	39,860	--	53,149	9,655	−481	−216	--	−34,145	−1,213	−48,054	−48,315
8	40,480	--	22,735	16,797	--	23,491	8,753	−2,361	−1,386	--	−25,919	--	−18,644	−23,490
9	179,200	--	32,653	63,287	--	68,888	15,294	−3,872	−109	--	−61,663	−808	−41,590	−72,095
10	51,360	--	11,068	25,244	--	28,008	5,869	−5,104	−191	--	−27,762	−521	−7,385	−29,252
11	154,880	--	15,109	50,339	--	60,712	82,196	−15,590	−34,374	--	−32,703	−22,306	−42,527	−61,174
12	50,240	--	7,020	21,575	--	22,576	382	--	--	--	−20,755	--	−8,087	−22,712
13	85,280	--	15,426	29,194	--	36,790	4,992	−545	−13	--	−35,181	−376	−16,521	−33,811
14	106,880	--	9,648	56,735	--	81,265	27,757	−638	−125	--	−82,533	−312	−10,736	−81,102
15	57,440	--	18,276	33,789	--	35,403	1,275	--	−63	--	−39,027	--	−14,768	−34,885
16	45,280	--	5,299	20,471	--	22,651	2,341	−1,455	−4	--	−21,333	--	−6,215	−21,787
17	108,640	--	13,411	54,134	--	66,138	19,502	−2,760	−5,891	--	−60,394	−1,878	−17,231	−65,260
18	73,920	--	15,194	34,176	--	32,294	11,111	−11,813	−18,709	--	−15,136	−345	−13,532	−33,443
19	71,200	--	20,433	24,752	--	25,038	17,505	−8,975	−27,059	--	−8,293	−394	−17,396	−25,808
20	51,200	--	3,948	23,939	--	23,156	1,338	−2,927	−2,931	--	−15,260	--	−7,895	−23,373
21	67,840	4,670	32,029	32,220	--	28,046	2,074	−152	−2,344	−6,248	−21,680	--	−41,533	−27,095
22	28,000	--	11,624	11,999	--	10,992	18,258	−21,769	−7,349	--	−6,033	--	−6,918	−10,830
23	45,440	1,104	25,990	17,468	--	15,706	6,697	−12,992	−19,556	−3,178	−2,335	--	−12,479	−16,434
24	30,560	3,274	29,438	18,647	--	17,621	--	−333	−1,010	−6,549	−17,367	--	−26,137	−17,583
CPNRD	2,142,236	37,497	107,675	732,432	12,734	913,872	395,201	−209,185	−154,321	−15,975	−776,021	−35,169	−127,265	−882,865
CPIHM	4,926,071	196,598	--	2,039,490	120,028	2,171,586	641,745	−466,883	−460,240	−135,699	−1,997,494	−43,632	--	−2,067,083

Table 21. Average groundwater-flow budget component results for each scenario (January 1, 2017 to December 31, 2049) of the Central Platte Integrated Hydrologic Model by supergroup.—Continued

[GWMA, Groundwater Management Area; --, not applicable; CPNRD, Central Platte Natural Resources District; CPIHM, Central Platte Integrated Hydrologic Model]]

GWMA/ supergroup	Area (acres)	Inflows						Outflows						
		Inflow from general heads	Inflow from adjacent zones	Recharge (deep percolation)	Recharge from canal leakage	Release from groundwater storage	Stream leakage	Base flow	Evapotranspiration from groundwater	Outflow to general heads	Outflow to irrigation wells	Outflow to production wells	Outflow to adjacent zones	Replenishment to groundwater storage
Futdrought10yr, in acre-feet per year[1]														
1	115,520	--	14,267	14,029	--	31,329	8,998	--	--	--	−21,130	--	−27,057	−20,436
2	43,360	--	17,243	15,109	--	28,393	6,845	--	--	--	−33,299	--	−8,935	−25,356
3	127,040	--	34,128	55,407	3,922	90,704	54,504	−1,407	−1,152	--	−108,727	−4,571	−37,777	−85,040
4	180,640	--	92,502	44,122	5,711	62,004	83,037	−115,671	−33,186	--	−45,369	−2,446	−30,806	−60,031
5	102,720	28,469	23,761	14,956	4,007	25,007	5,246	--	--	--	−21,743	--	−56,098	−23,605
6	90,240	--	12,465	8,178	--	18,437	4,398	--	--	--	−12,417	--	−19,129	−11,933
7	234,880	--	31,089	35,060	--	50,912	9,356	−459	−183	--	−33,877	−1,213	−46,669	−44,016
8	40,480	--	22,320	15,907	--	23,312	9,398	−2,049	−1,316	--	−26,004	--	−18,363	−23,229
9	179,200	--	33,251	60,318	--	67,421	14,355	−3,235	−103	--	−62,528	−808	−39,566	−69,116
10	51,360	--	11,007	25,356	--	28,666	6,294	−4,541	−187	--	−28,870	−521	−7,486	−29,753
11	154,880	--	14,285	49,993	--	58,574	84,710	−14,881	−35,881	--	−32,856	−22,306	−42,725	−59,049
12	50,240	--	6,928	20,445	--	21,103	413	--	--	--	−19,668	--	−7,990	−21,231
13	85,280	--	16,114	30,982	--	35,530	4,056	−991	−35	--	−33,897	−376	−17,671	−33,774
14	106,880	--	9,164	57,733	--	79,492	26,717	−814	−192	--	−80,497	−312	−11,661	−79,704
15	57,440	--	17,822	34,156	--	35,504	1,325	--	−56	--	−39,518	--	−14,322	−34,911
16	45,280	--	5,572	21,288	--	22,229	2,020	−1,945	−17	--	−20,570	--	−6,787	−21,803
17	108,640	--	13,193	56,362	--	64,826	17,910	−4,096	−7,875	--	−56,560	−1,878	−17,757	−64,267
18	73,920	--	15,796	34,965	--	30,736	9,945	−13,922	−22,021	--	−9,997	−345	−13,277	−32,020
19	71,200	--	21,598	25,311	--	24,418	16,116	−10,309	−29,383	--	−5,446	−394	−16,616	−25,374
20	51,200	--	3,502	25,093	--	23,152	1,034	−3,806	−3,598	--	−13,579	--	−8,402	−23,396
21	67,840	4,546	32,913	33,138	--	28,161	1,797	−234	−2,446	−6,382	−21,395	--	−42,621	−27,476
22	28,000	--	12,187	12,586	--	10,906	18,337	−24,096	−7,591	--	−5,252	--	−6,324	−10,755
23	45,440	1,034	27,037	18,424	--	15,606	6,398	−14,483	−20,223	−3,275	−1,640	--	−12,482	−16,395
24	30,560	3,197	29,824	19,092	--	17,858	--	−371	−1,233	−6,624	−16,576	--	−27,303	−17,861
CPNRD	2,142,236	37,245	106,832	728,053	13,640	894,314	393,208	−217,308	−166,678	−16,281	−751,415	−35,169	−126,730	−860,569
CPIHM	4,926,071	195,864	--	2,035,733	126,515	2,142,206	633,971	−480,213	−459,474	−137,264	−1,978,282	−43,632	--	−2,036,445

Table 21. Average groundwater-flow budget component results for each scenario (January 1, 2017 to December 31, 2049) of the Central Platte Integrated Hydrologic Model by supergroup.—Continued

[GWMA, Groundwater Management Area; --, not applicable; CPNRD, Central Platte Natural Resources District; CPIHM, Central Platte Integrated Hydrologic Model]]

GWMA/ supergroup	Area (acres)	Inflows						Outflows						
		Inflow from general heads	Inflow from adjacent zones	Recharge (deep perco- lation)	Recharge from canal leakage	Release from ground- water storage	Stream leakage	Base flow	Evapotranspiration from groundwater	Outflow to general heads	Outflow to irrigation wells	Outflow to produc- tion wells	Outflow to adjacent zones	Replenishment to groundwater storage
Futdroughtjun2sep, in acre-feet per year[1]														
1	115,520	--	14,533	11,787	--	35,835	7,163	--	--	--	−22,368	--	−29,142	−17,809
2	43,360	--	20,126	12,584	--	31,881	5,360	--	--	--	−38,438	--	−8,631	−22,881
3	127,040	--	49,847	50,958	1,476	98,890	32,989	−253	−329	--	−129,498	−4,571	−25,831	−73,691
4	180,640	--	75,683	38,634	5,711	74,789	106,450	−93,243	−33,483	--	−57,748	−2,446	−47,222	−67,465
5	102,720	28,646	24,241	13,027	4,007	28,497	3,914	--	--	--	−24,703	--	−54,829	−22,800
6	90,240	--	12,428	5,158	--	19,125	3,322	--	--	--	−12,333	--	−18,864	−8,837
7	234,880	--	26,630	26,070	--	64,215	6,098	−361	−107	--	−37,217	−1,213	−51,716	−32,400
8	40,480	--	23,913	13,563	--	27,650	5,448	−245	−339	--	−34,589	--	−12,293	−23,123
9	179,200	--	35,370	44,347	--	76,918	14,232	−776	−37	--	−74,075	−808	−34,389	−60,812
10	51,360	--	10,137	19,601	--	36,615	12,865	−322	−63	--	−36,701	−521	−9,197	−32,527
11	154,880	--	11,548	39,481	--	70,392	113,588	−7,732	−28,842	--	−55,148	−22,306	−55,946	−65,476
12	50,240	--	6,215	16,759	--	22,556	366	--	--	--	−19,696	--	−8,305	−17,895
13	85,280	--	13,143	23,408	--	38,390	5,907	−163	−12	--	−35,553	−376	−15,068	−29,697
14	106,880	--	10,943	45,382	--	85,974	24,667	−73	−48	--	−85,979	−312	−8,084	−72,522
15	57,440	--	23,840	25,970	--	38,303	1,184	--	−20	--	−43,835	--	−14,875	−30,568
16	45,280	--	5,102	16,810	--	22,700	3,258	−757	−12	--	−21,160	--	−6,120	−19,894
17	108,640	--	15,279	45,589	--	73,421	22,052	−855	−2,701	--	−71,894	−1,878	−13,561	−65,670
18	73,920	--	12,648	30,100	--	42,311	14,231	−2,813	−12,659	--	−30,866	−345	−14,517	−38,504
19	71,200	--	17,772	21,694	--	28,807	23,841	−5,061	−24,751	--	−15,647	−394	−19,121	−27,380
20	51,200	--	5,065	14,804	--	18,709	2,474	−1,161	−1,187	--	−14,992	--	−6,647	−17,123
21	67,840	5,277	29,474	25,015	--	28,631	3,361	−76	−2,310	−5,539	−22,988	--	−38,036	−22,818
22	28,000	--	9,809	8,003	--	10,168	19,701	−16,077	−6,725	--	−6,499	--	−8,688	−9,717
23	45,440	1,285	21,532	12,765	--	15,351	8,674	−8,461	−17,209	−2,609	−3,729	--	−12,689	−14,968
24	30,560	3,586	27,206	13,799	--	15,955	--	−178	−404	−6,182	−17,994	--	−21,300	−14,489
CPNRD	2,142,236	38,793	99,356	575,345	11,195	1,006,115	441,147	−138,604	−131,235	−14,330	−913,649	−35,169	−131,971	−809,106
CPIHM	4,926,071	210,402	--	1,547,662	124,069	2,349,747	706,026	−353,411	−299641.1	−109,795	−2,293,265	−43,632	--	−1,840,506

Table 21. Average groundwater-flow budget component results for each scenario (January 1, 2017 to December 31, 2049) of the Central Platte Integrated Hydrologic Model by supergroup.—Continued

[GWMA, Groundwater Management Area; --, not applicable; CPNRD, Central Platte Natural Resources District; CPIHM, Central Platte Integrated Hydrologic Model]]

GWMA/ supergroup	Area (acres)	Inflows						Outflows						
		Inflow from general heads	Inflow from adjacent zones	Recharge (deep percolation)	Recharge from canal leakage	Release from groundwater storage	Stream leakage	Base flow	Evapotranspiration from groundwater	Outflow to general heads	Outflow to irrigation wells	Outflow to production wells	Outflow to adjacent zones	Replenishment to groundwater storage
Futdroughtmar2may, in acre-feet per year[1]														
1	115,520	--	14,518	8,869	--	31,353	7,318	--	--	--	−20,233	--	−27,463	−14,362
2	43,360	--	18,327	9,594	--	24,972	4,333	--	--	--	−31,256	--	−8,503	−17,468
3	127,040	--	37,177	41,153	2,971	84,980	49,929	−739	−871	--	−103,761	−4,571	−34,324	−71,953
4	180,640	--	86,905	29,188	5,711	57,764	88,347	−102,331	−31,551	--	−44,486	−2,446	−33,944	−53,404
5	102,720	28,627	23,951	8,560	4,007	22,241	2,837	--	--	--	−20,036	--	−54,227	−15,960
6	90,240	--	12,333	7,464	--	19,087	3,423	--	--	--	−12,328	--	−19,240	−10,738
7	234,880	--	30,577	24,221	--	50,471	6,735	−401	−120	--	−31,854	−1,213	−46,601	−31,816
8	40,480	--	21,901	11,544	--	21,801	9,260	−958	−832	--	−25,877	--	−16,826	−20,071
9	179,200	--	34,451	41,758	--	59,433	12,571	−1,528	−71	--	−56,632	−808	−39,128	−50,083
10	51,360	--	9,368	16,731	--	23,850	7,926	−1,333	−173	--	−25,022	−521	−8,499	−22,453
11	154,880	--	12,139	28,778	--	51,087	100,122	−9,370	−28,353	--	−36,028	−22,306	−47,941	−48,429
12	50,240	--	6,733	12,260	--	20,912	300	--	--	--	−19,255	--	−7,165	−13,784
13	85,280	--	12,622	16,015	--	34,242	6,384	−52	−4	--	−32,875	−376	−13,575	−22,407
14	106,880	--	10,165	35,003	--	75,551	26,607	−61	−41	--	−76,872	−312	−8,031	−62,101
15	57,440	--	22,966	21,087	--	31,583	1,142	--	−19	--	−36,931	--	−15,033	−24,794
16	45,280	--	5,085	11,999	--	20,371	3,736	−315	−2	--	−19,855	--	−5,249	−15,830
17	108,640	--	14,611	33,936	--	62,262	23,263	−406	−1,727	--	−61,765	−1,878	−14,213	−54,321
18	73,920	--	12,796	21,191	--	33,968	15,048	−1,364	−9,167	--	−27,936	−345	−14,092	−30,508
19	71,200	--	17,459	13,385	--	21,274	26,707	−3,988	−21,471	--	−13,919	−394	−19,409	−19,788
20	51,200	--	4,434	18,116	--	20,119	1,412	−1,276	−1,513	--	−15,550	--	−6,877	−18,898
21	67,840	5,146	30,047	20,129	--	23,972	3,580	−34	−2,142	−5,616	−20,300	--	−36,818	−17,963
22	28,000	--	10,134	8,773	--	9,347	20,161	−18,232	−6,891	--	−6,369	--	−7,911	−9,069
23	45,440	1,203	21,436	12,417	--	13,755	8,671	−8,413	−17,209	−2,720	−2,798	--	−12,817	−13,525
24	30,560	3,513	27,020	13,229	--	14,683	--	−183	−363	−6,258	−17,070	--	−21,258	−13,314
CPNRD	2,142,236	38,488	100,829	465,435	12,690	829,091	429,811	−150,984	−122,521	−14,594	−759,008	−35,169	−122,826	−673,078
CPIHM	4,926,071	208,030	--	1,336,832	125,564	1,972,428	684,473	−366,121	-347,674	−110,500	−1,914,760	−43,632	--	−1,546,763

Table 21. Average groundwater-flow budget component results for each scenario (January 1, 2017 to December 31, 2049) of the Central Platte Integrated Hydrologic Model by supergroup.—Continued

[GWMA, Groundwater Management Area; --, not applicable; CPNRD, Central Platte Natural Resources District; CPIHM, Central Platte Integrated Hydrologic Model]]

		Inflows						Outflows						
GWMA/ supergroup	Area (acres)	Inflow from general heads	Inflow from adjacent zones	Recharge (deep perco-lation)	Recharge from canal leakage	Release from ground-water storage	Stream leakage	Base flow	Evapotranspiration from groundwater	Outflow to general heads	Outflow to irrigation wells	Outflow to produc-tion wells	Outflow to adjacent zones	Replenishment to groundwater storage
Futirr7in, in acre-feet per year[1]														
1	115,520	--	14,634	14,371	--	17,207	9,544	--	--	--	−10,603	--	−23,567	−21,587
2	43,360	--	11,016	13,456	--	13,294	7,470	−81	--	--	−13,193	--	−11,069	−20,895
3	127,040	--	28,595	40,031	3,922	42,001	42,925	−21,134	−5,242	--	−18,117	−4,571	−55,976	−52,469
4	180,640	--	127,142	42,727	5,711	48,672	59,387	−152,592	−40,065	--	−18,134	−2,446	−20,931	−49,521
5	102,720	28,007	23,057	15,197	4,007	15,881	5,664	--	--	--	−10,144	--	−60,782	−20,887
6	90,240	--	12,636	9,188	--	11,147	4,759	--	--	--	−5,160	--	−21,120	−11,450
7	234,880	--	32,770	39,785	--	33,867	11,382	−602	−335	--	−17,456	−1,213	−51,238	−46,965
8	40,480	--	24,173	15,184	--	17,466	15,887	−14,187	−5,278	--	−8,620	--	−25,343	−19,295
9	179,200	--	31,440	63,460	--	49,989	11,363	−10,659	−225	--	−32,446	−808	−48,021	−64,119
10	51,360	--	13,665	25,001	--	20,962	1,464	−14,831	−770	--	−14,606	−521	−5,947	−24,418
11	154,880	--	26,661	51,804	--	50,589	62,188	−24,958	−42,452	--	−19,603	−22,306	−29,260	−52,685
12	50,240	--	6,738	21,698	--	14,596	395	--	−2	--	−11,322	--	−11,452	−20,649
13	85,280	--	17,949	28,781	--	24,474	2,665	−3,983	−246	--	−18,700	−376	−22,105	−28,467
14	106,880	--	9,151	55,029	--	52,398	12,415	−7,004	−1,650	--	−44,604	−312	−14,197	−61,276
15	57,440	--	10,787	33,355	--	23,763	1,278	--	−314	--	−20,536	--	−18,224	−30,109
16	45,280	--	5,989	20,405	--	16,836	1,084	−4,143	−163	--	−12,022	--	−9,401	−18,586
17	108,640	--	13,392	53,658	--	51,322	13,836	−8,876	−11,648	--	−34,976	−1,878	−21,262	−53,619
18	73,920	--	19,369	34,495	--	25,545	8,312	−20,086	−22,772	--	−4,951	−345	−11,375	−28,309
19	71,200	--	27,187	24,870	--	21,942	15,104	−13,652	−34,136	--	−2,620	−394	−14,424	−23,895
20	51,200	--	3,568	23,882	--	20,578	885	−4,251	−4,639	--	−9,001	--	−9,364	−21,659
21	67,840	3,987	39,363	32,480	--	23,016	623	−1,235	−2,878	−6,979	−13,091	--	−49,151	−26,135
22	28,000	--	12,998	12,236	--	10,012	18,311	−25,122	−8,263	--	−4,312	--	−5,869	−9,991
23	45,440	955	31,676	17,537	--	14,335	6,273	−16,278	−22,699	−3,416	−1,076	--	−11,598	−15,708
24	30,560	2,991	32,523	18,400	--	15,987	--	−484	−2,649	−6,897	−10,938	--	−31,986	−16,946
CPNRD	2,142,236	35,938	127,029	707,074	13,640	635,908	313,213	−344,158	−206,426	−17,292	−356,230	−35,169	−134,249	−739,672
CPIHM	4,926,071	175,242	--	2,077,650	126,515	1,535,874	499,169	−716,845	−652,566	−175,554	−1,041,458	−43,632	--	−1,784,933

Table 21. Average groundwater-flow budget component results for each scenario (January 1, 2017 to December 31, 2049) of the Central Platte Integrated Hydrologic Model by supergroup.—Continued

[GWMA, Groundwater Management Area; --, not applicable; CPNRD, Central Platte Natural Resources District; CPIHM, Central Platte Integrated Hydrologic Model]]

GWMA/ supergroup	Area (acres)	Inflows						Outflows						
		Inflow from general heads	Inflow from adjacent zones	Recharge (deep percolation)	Recharge from canal leakage	Release from groundwater storage	Stream leakage	Base flow	Evapotranspiration from groundwater	Outflow to general heads	Outflow to irrigation wells	Outflow to production wells	Outflow to adjacent zones	Replenishment to groundwater storage
Futirr9in, in acre-feet per year[1]														
1	115,520	--	14,555	14,577	--	19,424	9,529	--	--	--	−12,642	--	−23,653	−21,791
2	43,360	--	11,404	13,744	--	15,470	7,404	−7	--	--	−16,065	--	−10,068	−21,883
3	127,040	--	27,539	40,577	3,922	43,669	43,834	−19,299	−4,801	--	−22,049	−4,571	−55,268	−53,589
4	180,640	--	124,902	43,101	5,711	49,940	60,343	−149,637	−39,254	--	−21,113	−2,446	−21,173	−50,417
5	102,720	28,060	23,132	15,403	4,007	17,292	5,664	--	--	--	−11,920	--	−60,208	−21,430
6	90,240	--	12,632	9,335	--	12,574	4,754	--	--	--	−6,627	--	−20,744	−11,923
7	234,880	--	33,006	40,176	--	37,294	11,309	−568	−319	--	−21,227	−1,213	−50,467	−47,995
8	40,480	--	23,570	15,465	--	18,412	14,924	−12,640	−4,510	--	−10,161	--	−25,124	−19,951
9	179,200	--	31,723	64,184	--	54,413	11,905	−8,924	−191	--	−39,551	−808	−46,662	−66,105
10	51,360	--	13,000	25,386	--	22,181	1,827	−12,463	−478	--	−17,835	−521	−5,904	−25,194
11	154,880	--	24,363	51,938	--	51,554	64,933	−23,488	−41,605	--	−20,776	−22,306	−31,388	−53,247
12	50,240	--	6,810	21,939	--	16,652	394	--	0	--	−13,718	--	−10,632	−21,446
13	85,280	--	17,635	29,191	--	27,292	2,757	−3,062	−155	--	−22,520	−376	−21,109	−29,665
14	106,880	--	9,074	55,960	--	57,555	14,249	−4,698	−1,001	--	−52,445	−312	−13,719	−64,735
15	57,440	--	11,945	33,773	--	26,206	1,275	--	−219	--	−24,312	--	−17,695	−30,974
16	45,280	--	5,899	20,709	--	18,733	1,216	−3,301	−77	--	−15,067	--	−8,378	−19,742
17	108,640	--	13,193	54,353	--	54,469	14,898	−7,472	−10,559	--	−40,803	−1,878	−20,475	−55,791
18	73,920	--	18,506	34,558	--	25,908	8,470	−18,997	−22,616	--	−5,117	−345	−11,960	−28,525
19	71,200	--	25,537	24,971	--	22,046	15,460	−12,817	−33,192	--	−2,733	−394	−15,065	−23,832
20	51,200	--	3,558	24,218	--	21,940	1,000	−3,833	−3,972	--	−11,434	--	−8,955	−22,522
21	67,840	4,165	37,274	32,736	--	24,583	805	−775	−2,732	−6,785	−15,532	--	−47,293	−26,447
22	28,000	--	12,581	12,271	--	10,158	18,494	−24,597	−8,132	--	−4,543	--	−6,138	−10,093
23	45,440	971	30,277	17,653	--	14,409	6,348	−15,584	−21,971	−3,391	−1,117	--	−11,873	−15,723
24	30,560	3,060	31,817	18,626	--	16,570	--	−447	−2,013	−6,805	−12,981	--	−30,544	−17,282
CPNRD	2,142,236	36,256	123,068	714,890	13,640	678,774	321,793	−322,607	−197,797	−16,981	−422,285	−35,169	−133,676	−760,337
CPIHM	4,926,071	179,604	--	2,090,735	126,515	1,680,150	522,548	−661,257	−620,631	−165,919	−1,255,678	−43,632	--	−1,853,033

Table 21. Average groundwater-flow budget component results for each scenario (January 1, 2017 to December 31, 2049) of the Central Platte Integrated Hydrologic Model by supergroup.—Continued

[GWMA, Groundwater Management Area; --, not applicable; CPNRD, Central Platte Natural Resources District; CPIHM, Central Platte Integrated Hydrologic Model]]

GWMA/ supergroup	Area (acres)	Inflows						Outflows						
		Inflow from general heads	Inflow from adjacent zones	Recharge (deep perco-lation)	Recharge from canal leakage	Release from ground-water storage	Stream leakage	Base flow	Evapotranspiration from groundwater	Outflow to general heads	Outflow to irrigation wells	Outflow to produc-tion wells	Outflow to adjacent zones	Replenishment to groundwater storage
Futirr10in, in acre-feet per year[1]														
1	115,520	--	14,494	14,666	--	20,439	9,522	--	--	--	−13,519	--	−23,728	−21,874
2	43,360	--	11,615	13,888	--	16,596	7,391	0	--	--	−17,486	--	−9,576	−22,428
3	127,040	--	27,056	40,792	3,922	44,480	44,203	−18,534	−4,622	--	−23,679	−4,571	−54,942	−54,139
4	180,640	--	123,763	43,264	5,711	50,498	60,789	−148,379	−38,971	--	−22,217	−2,446	−21,300	−50,745
5	102,720	28,086	23,164	15,507	4,007	18,027	5,664	--	--	--	−12,818	--	−59,912	−21,727
6	90,240	--	12,639	9,409	--	13,313	4,752	--	--	--	−7,366	--	−20,546	−12,201
7	234,880	--	33,093	40,333	--	38,747	11,248	−559	−311	--	−22,746	−1,213	−50,159	−48,439
8	40,480	--	23,352	15,599	--	18,859	14,551	−11,953	−4,227	--	−10,921	--	−24,992	−20,282
9	179,200	--	31,870	64,512	--	56,536	12,193	−8,218	−178	--	−42,790	−808	−46,029	−67,113
10	51,360	--	12,761	25,573	--	22,865	2,060	−11,348	−381	--	−19,444	−521	−5,917	−25,650
11	154,880	--	23,256	51,996	--	51,997	66,202	−22,750	−41,238	--	−21,222	−22,306	−32,458	−53,509
12	50,240	--	6,813	22,032	--	17,491	394	--	--	--	−14,641	--	−10,356	−21,733
13	85,280	--	17,452	29,360	--	28,481	2,869	−2,659	−136	--	−24,126	−376	−20,708	−30,174
14	106,880	--	9,112	56,431	--	60,395	15,319	−3,804	−769	--	−56,358	−312	−13,465	−66,634
15	57,440	--	12,520	33,985	--	27,441	1,274	--	−181	--	−26,219	--	−17,337	−31,484
16	45,280	--	5,817	20,819	--	19,456	1,271	−3,018	−57	--	−16,160	--	−8,003	−20,137
17	108,640	--	13,152	54,637	--	55,805	15,295	−6,908	−10,187	--	−43,097	−1,878	−20,080	−56,810
18	73,920	--	18,092	34,588	--	26,037	8,534	−18,509	−22,504	--	−5,185	−345	−12,215	−28,607
19	71,200	--	24,836	25,001	--	22,076	15,631	−12,517	−32,716	--	−2,801	−394	−15,349	−23,786
20	51,200	--	3,551	24,289	--	22,231	1,015	−3,778	−3,872	--	−11,939	--	−8,773	−22,724
21	67,840	4,243	36,429	32,854	--	25,324	927	−615	−2,695	−6,700	−16,614	--	−46,518	−26,635
22	28,000	--	12,458	12,279	--	10,191	18,541	−24,451	−8,084	--	−4,605	--	−6,205	−10,123
23	45,440	979	29,608	17,706	--	14,460	6,385	−15,267	−21,620	−3,379	−1,137	--	−12,011	−15,724
24	30,560	3,093	31,558	18,752	--	16,890	--	−430	−1,792	−6,761	−13,969	--	−29,855	−17,486
CPNRD	2,142,236	36,402	121,154	718,314	13,640	698,666	326,029	−313,697	−194,539	−16,840	−451,056	−35,169	−133,167	−770,198
CPIHM	4,926,071	181,673	--	2,096,479	126,515	1,743,165	533,104	−640,183	−608,085	−161,925	−1,345,271	−43,632	--	−1,882,454

[1]Forecast names defined in table 17.

Table 22. Average annual depths of irrigation withdrawals for each scenario, the difference from the irrigation limit for the Futirr7in, Futirr9in, and Futirr10in scenarios, and the difference between the FutBase scenario irrigation withdrawal and the scenario limit, by supergroup/Groundwater Management Area.—Left

[GWMA, Groundwater Management Area]

GWMA/ super-group	Average annual groundwater irrigation pumping by scenario, in inches[1]								
	Development model, 1981–2016	FutBase	Futdrought-3yr	Futdrought-10yr	Futdrought-jun2sep	Futdrought-mar2may	Futirr7in	Futirr9in	Futirr10in
1	13.6	12.3	13.2	12.9	13.8	12.3	6.4	7.5	8.1
2	13.6	11.4	12.5	12.5	14.4	11.6	5.3	6.4	6.9
3	12.1	11.4	13.2	12.7	15.9	12.3	4.9	5.9	6.3
4	8	7.1	7.1	7.3	9.1	6.7	4.4	5.2	5.5
5	14.1	12	13	13	14.8	12	6.1	7.1	7.7
6	13.9	15.1	15.9	15.3	15.2	15.2	6.6	8.4	9.4
7	12.8	11.3	12.2	12.2	13.8	11.5	6	7.3	7.9
8	10.1	8.6	10	10	13.8	9.7	4.4	5.2	5.6
9	12.5	10.8	11.8	11.7	13.1	10.9	6	7.3	7.9
10	12.1	8.5	9.6	10	12.9	8.6	5	6.1	6.7
11	6.9	4.6	5.7	5.8	8	4.9	3.4	3.8	3.9
12	12	11.1	12.1	11.5	11.4	11.3	6.6	8	8.6
13	11.5	11.1	12.1	11.5	11.5	11.4	6.3	7.7	8.3
14	11.7	10.7	11.7	11.5	12.5	10.9	6.2	7.3	7.9
15	11.3	10.5	11.2	11.3	12.6	10.6	5.9	7	7.5
16	11	10.9	11.7	11.3	11.5	10.9	6.5	8.2	8.9
17	9.4	8.7	10.1	9.6	11.7	10	5.6	6.7	7.2
18	2.4	1	3	1.7	5.9	5.5	0.9	0.9	0.9
19	1.8	0.7	2.3	1.4	4.5	3.9	0.6	0.6	0.6
20	8	7.6	8.9	7.7	9.4	9.5	5.1	6.2	6.6
21	10.5	10.1	10.9	10.8	11.7	10.1	6.5	7.7	8.2
22	4.5	3.9	4.9	4.2	5.4	5.1	3.4	3.6	3.7
23	1.5	0.7	1.3	0.9	2.1	1.6	0.6	0.6	0.7
24	9.7	9.6	10.5	10.1	10.8	10.2	6.4	7.8	8.4
CPNRD	10.2	9.3	10.2	10	11.7	9.7	5.2	6.2	6.7

levels across the entire scenario period were generally in the western region (GWMAs 1, 2, and 3) and received less recharge compared to the GWMAs in the wetter eastern region, or they were in the most heavily irrigated regions (GWMAs 14 and 15) with high outflow rates to irrigation wells (table 21).

Early Growing Season Drought Scenario Results

The average groundwater levels simulated by the CPIHM for the Futdroughtmar2may (early growing season drought) scenario were below FutBase scenario levels for all GWMAs and the CPNRD and the CPIHM (table 19). After 3 years of an early growing season drought (January 1, 2017, to December 31, 2019, with each March through May simulated as drought conditions), average groundwater levels for all 24 GWMAs were below their predrought levels. By December 31, 2026, all 24 GWMAs exhibited continued declines in groundwater levels 0.9 to 9.9 ft below the predrought groundwater levels (December 31, 2016), which indicated that an early growing season drought bookended by average climate and stream inflow conditions for January through February and June through December caused groundwater-level declines across all regions of the CPIHM (table 19). By the end of the scenario (December 31, 2049), all 24 GWMAs exhibited further groundwater-level declines

Table 22. Average annual depths of irrigation withdrawals for each scenario, the difference from the irrigation limit for the Futirr7in, Futirr9in, and Futirr10in scenarios, and the difference between the FutBase scenario irrigation withdrawal and the scenario limit, by supergroup/Groundwater Management Area.—Right

[GWMA, Groundwater Management Area]

Difference from limit, in inches			Difference from FutBase, in inches		
7 inch limit–average Futirr7in scenario withdrawal	9 inch limit–average Futirr9in scenario withdrawal	10 inch limit–average Futirr10in scenario withdrawal	Difference (Fut-Base–7 inch limit)	Difference (Fut-Base–9 inch limit)	Difference (Fut-Base–10 inch limit)
0.6	1.5	1.9	5.3	3.3	2.3
1.7	2.6	3.1	4.4	2.4	1.4
2.1	3.1	3.7	4.4	2.4	1.4
2.6	3.8	4.5	0.1	−1.9	−2.9
0.9	1.9	2.3	5	3	2
0.4	0.6	0.6	8.1	6.1	5.1
1	1.7	2.1	4.3	2.3	1.3
2.6	3.8	4.4	1.6	−0.4	−1.4
1	1.7	2.1	3.8	1.8	0.8
2	2.9	3.3	1.5	−0.5	−1.5
3.6	5.2	6.1	−2.4	−4.4	−5.4
0.4	1	1.4	4.1	2.1	1.1
0.7	1.3	1.7	4.1	2.1	1.1
0.8	1.7	2.1	3.7	1.7	0.7
1.1	2	2.5	3.5	1.5	0.5
0.5	0.8	1.1	3.9	1.9	0.9
1.4	2.3	2.8	1.7	−0.3	−1.3
6.1	8.1	9.1	−6	−8	−9
6.4	8.4	9.4	−6.3	−8.3	−9.3
1.9	2.8	3.4	0.6	−1.4	−2.4
0.5	1.3	1.8	3.1	1.1	0.1
3.6	5.4	6.3	−3.1	−5.1	−6.1
6.4	8.4	9.3	−6.3	−8.3	−9.3
0.6	1.2	1.6	2.6	0.6	−0.4
1.8	2.8	3.3	2.3	0.3	−0.7

[1]Forecast names defined in table 17.

of 1.4 to 27.0 ft below their initial predrought scenario levels. GWMAs 2 and 12 exhibited the largest total declines (25.5 and 27.0 ft, respectively) for the entire forecast and GWMAs 4 and 22 exhibited the lowest declines (1.4 and 1.4 ft, respectively) (table 19). The GWMAs that exhibited the largest declines in groundwater levels across the entire forecast period were generally in the western region (GWMA 1 and 2) and received less recharge compared to the GWMAs in the wetter eastern region, or they were in the most heavily irrigated regions (GWMAs 12, 13, and 14) with the high rates of outflows to irrigation wells (table 21, fig. 5.12).

Comparison Between Early Growing Season and Mid-Growing Season Drought Scenarios

Comparison between the average change in groundwater levels across the scenario period for the early growing season and mid-growing season drought scenario indicated two general trends for the GWMAs in the CPNRD: 16 GWMAs exhibited 0.3 to 14.8 ft greater declines in groundwater levels by the end of the scenario period for the mid-growing season drought scenario, and 8 GWMAs exhibited 0.1 to 9.1 ft greater declines for the early growing season drought; GWMA 14

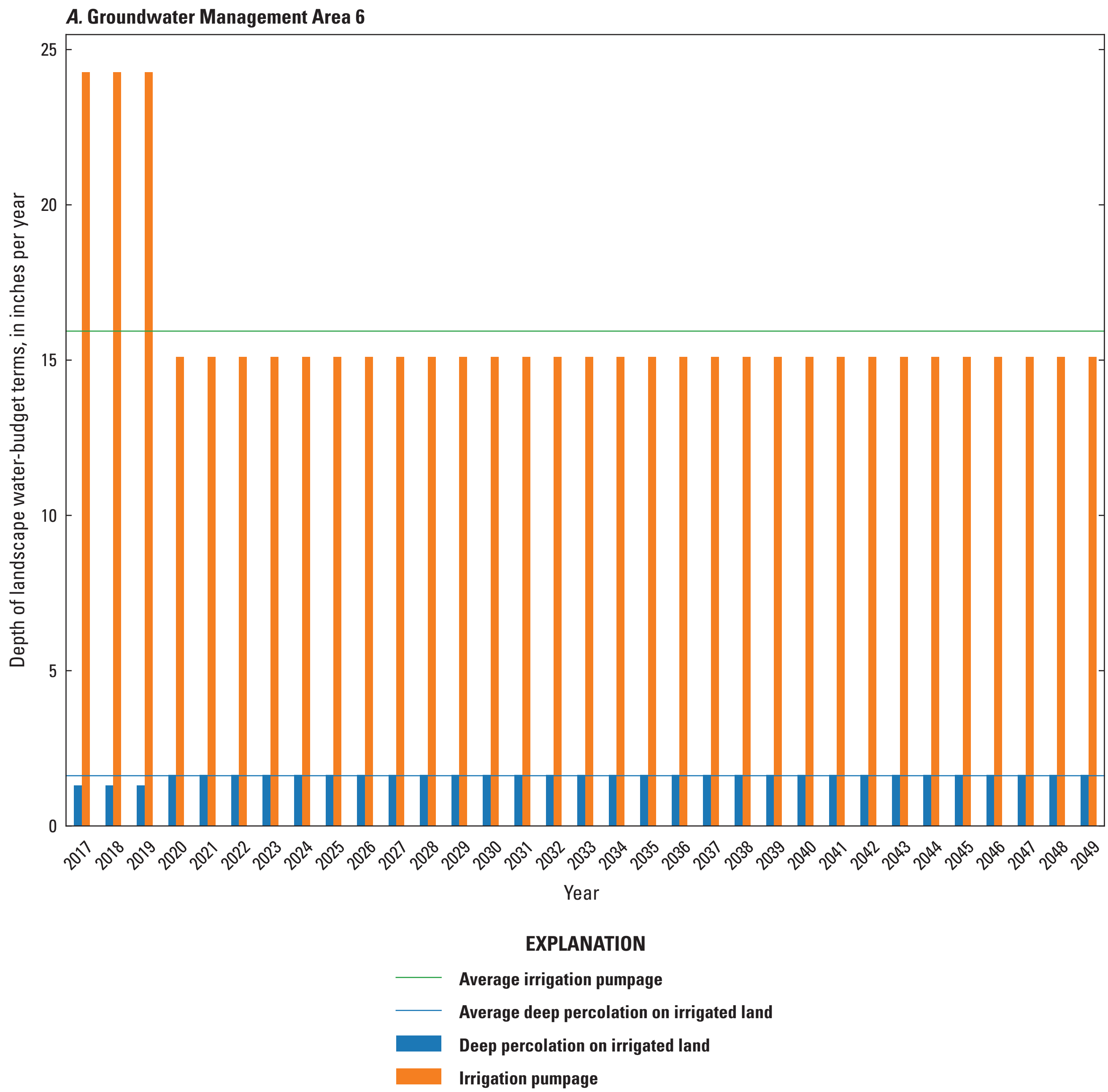

Figure 30. Drought3yr scenario simulated average annual groundwater irrigation pumping and recharge on irrigated land depths for the Central Platte Integrated Hydrologic Model. *A*, Groundwater Management Area (GWMA) 6. *B*, GWMA 10. *C*, GWMA 23.

exhibited the same change in groundwater levels (−20.1) for both scenarios, which indicated that an early and mid-growing season drought had the same effect on the system (table 19). The GWMAs that exhibited larger declines for the early growing season drought (GWMAs 5, 12, 13, 16, 17, 18, 19, and 21) also had smaller net outflows to irrigation wells compared to the mid-growing season drought, but the groundwater levels declined because there was also less farm net recharge. These results indicated that for these GWMAs, less precipitation and recharge during spring (March to May) had a larger effect on net storage than irrigation wells. Conversely, the GWMAs that exhibited larger declines in groundwater levels for the mid-growing season drought had larger net outflows to irrigation wells but were also accompanied by larger farm net recharge. Despite the larger values of farm net recharge compared to other GWMAs, the increased outflows to irrigation wells in response to less precipitation and recharge in the summer months was the major stress that caused the larger declines in groundwater levels for the mid-growing season drought (table 19, figs. 5.12 and 5.13).

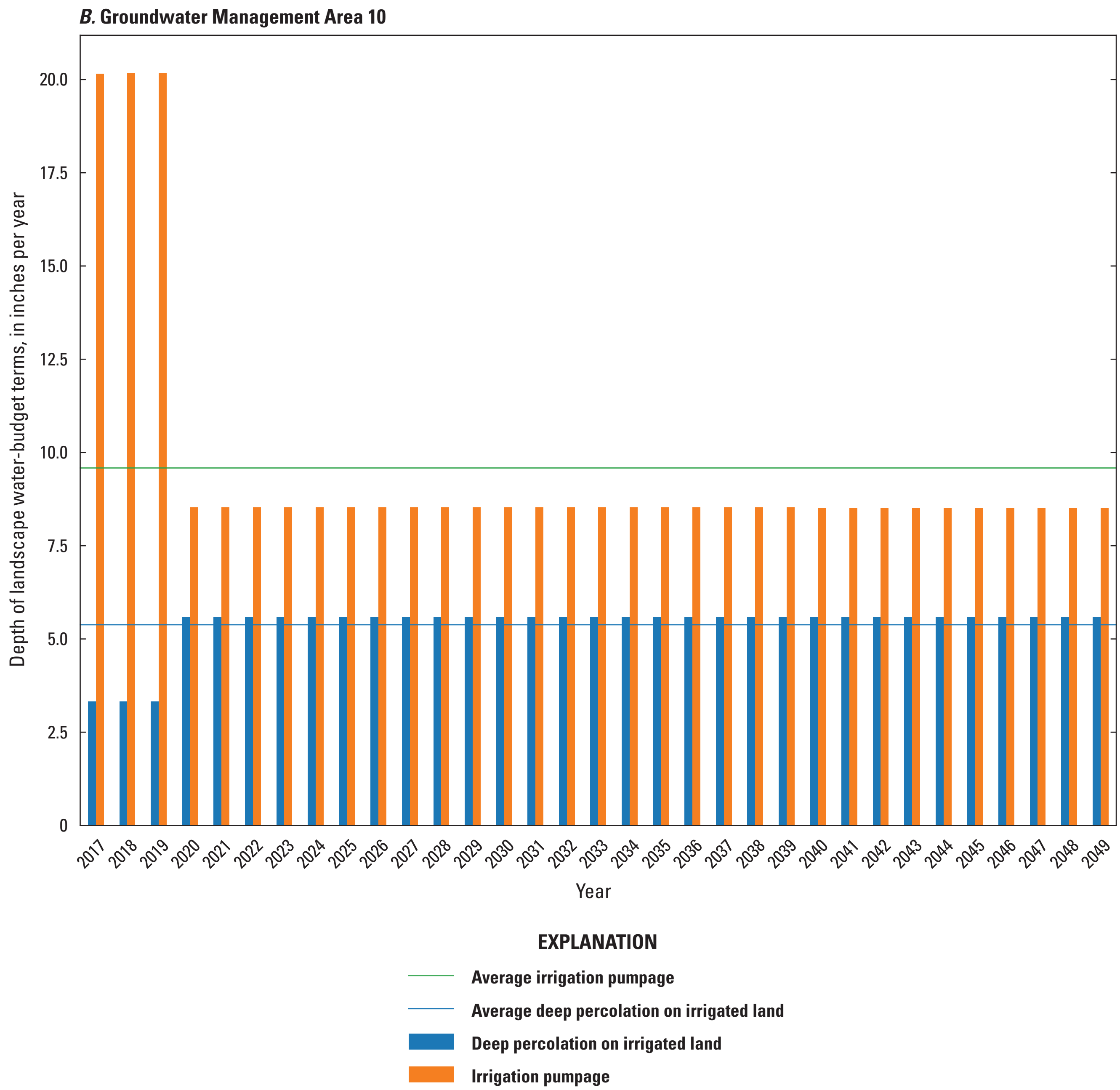

Figure 30.—Continued

Scenario Differences Between Irrigation and Recharge from Deep Percolation

In all scenarios, outflows to irrigation wells, recharge from deep percolation, and farm net recharge were key components of the groundwater-flow system that influenced changes in storage and groundwater levels. Annual relations between inflows to recharge from deep percolation and outflows to irrigation wells exhibited two general trends among GWMAs related to location and climate. Outflows to irrigation wells in the drier central and western region GWMAs (GWMAs 1–16) exhibited approximately constant outflows to irrigation wells for each scenario, except the 3- and 10-year droughts, which were marked by substantial increases in pumping for most GWMAs during the drought periods and shown for GWMA 2 in figure 31*A*. Additionally, outflows to irrigation wells for these western and central region GWMAs were higher for the mid-growing season drought (futdroughtjun2sep) because there was less precipitation to support ETp, which resulted in a larger CIR that was met through increased pumping during the peak irrigation season (fig. 31*A*). Conversely, outflows to irrigation for the early season drought were similar to the FutBase scenario, because the drought occurred from March to May, which were not peak irrigation

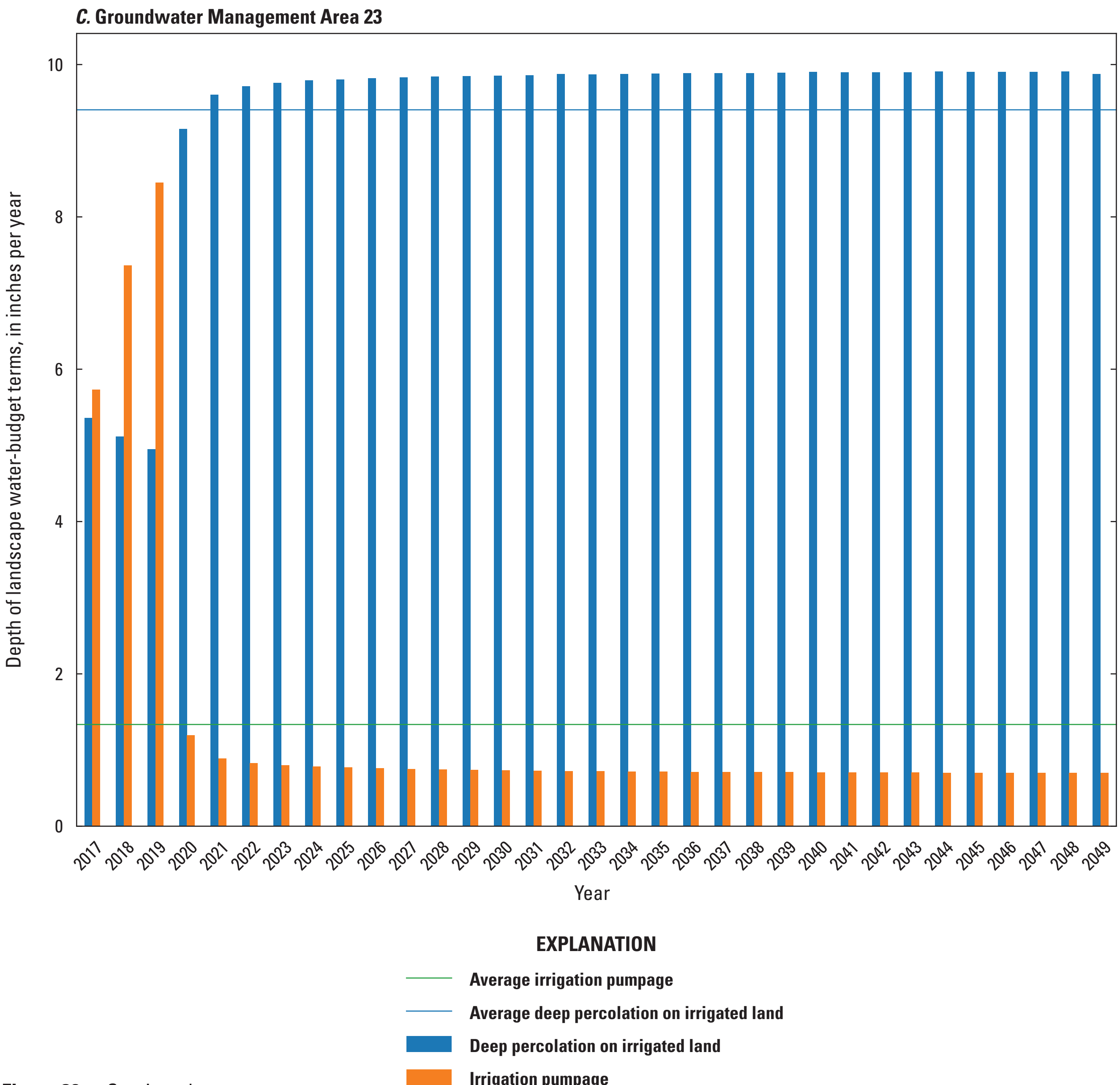

Figure 30.—Continued

months (fig. 31*A*). During the peak irrigation season (June to September), the FutBase and early season drought scenarios had similar CIR, resulting in similar outflows to irrigation for each season (fig. 31*A*).

The wetter eastern region (GWMAs 17–24), with shallower water tables and larger outflows to ETg, generally exhibited a gradual increase in outflows to irrigation wells and annual inflows from recharge that indicated the seasonal climatic stresses had a lasting effect on the irrigation pumping as groundwater levels and ETg declined as crop roots were less able to reach the water table and shown for GWMA 18 in figure 31*B*. Outflows to irrigation wells increased for the duration of each drought period compared to the FutBase scenario owing to a decrease in precipitation and recharge and an increase in CWD and CIR (fig. 31*B*). Like the western and central region GWMAs, the outflows to irrigation wells were larger for the mid-growing season drought (fut-droughtjun2sep) as there was less precipitation to support ETp during the peak irrigation season resulting in a larger CIR met by pumping from irrigation wells (fig. 31*B*). Further, annual recharge was larger in the mid-growing season drought scenario because recharge occurred more during the spring months when CWD and CIR were lower. The increase in recharge throughout the

A. Groundwater Management Area 2

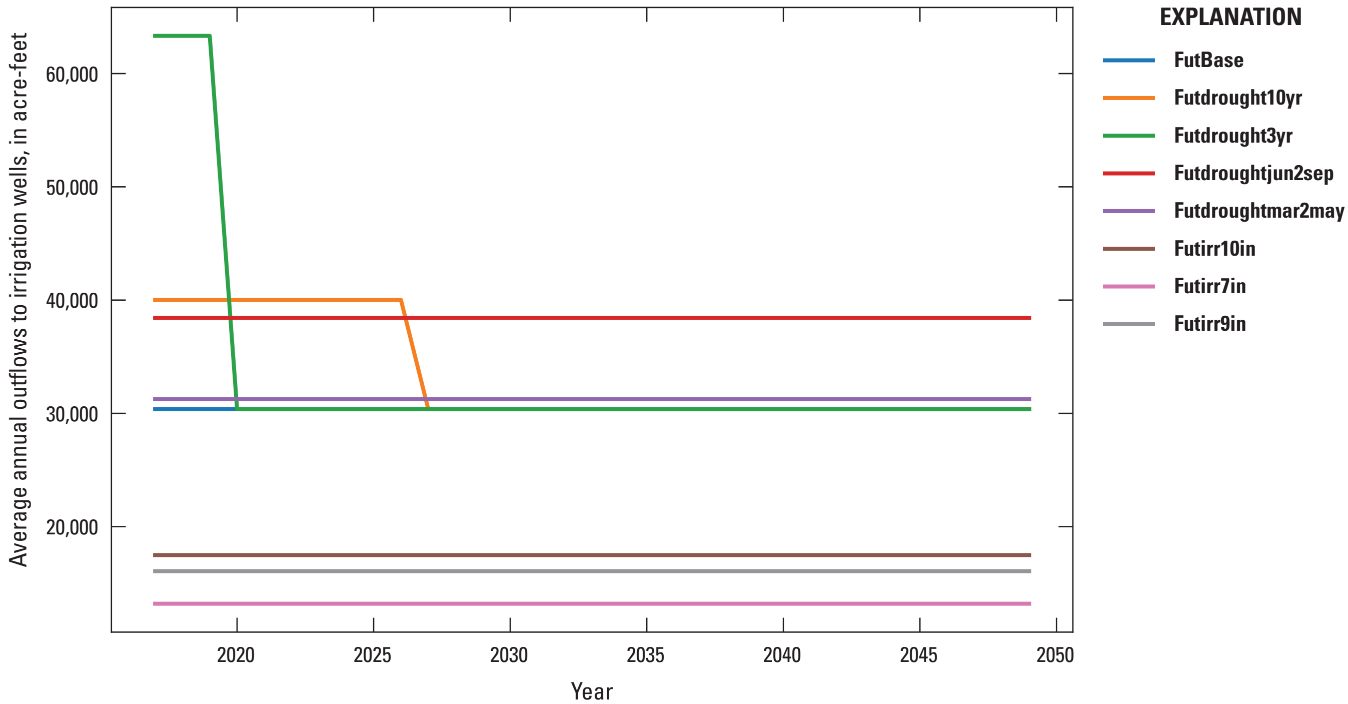

Figure 31. Plot of average annual outflows to irrigation wells for each scenario. *A*, Groundwater Management Area 2. *B*, Groundwater Management Area 18.

B. Groundwater Management Area 18

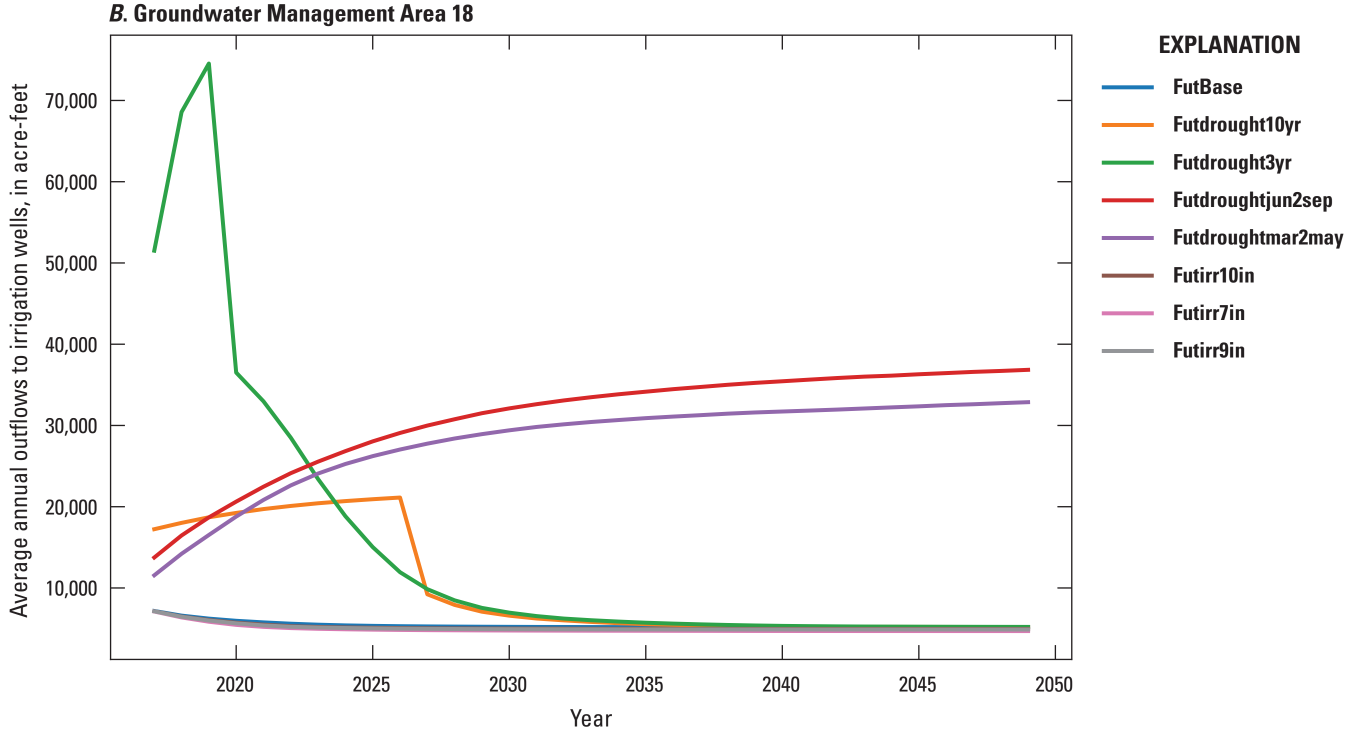

Figure 31.—Continued

scenario period resulted from the increase in irrigation, which led to an increase in inefficient irrigation water that became recharge. Conversely, for the western and central region GWMAs, the early growing season drought (futdroughtmar2may) exhibited outflows to irrigation that were larger than the FutBase scenario because the reduced recharge from March to May also caused a reduction in the mid-growing season ETg (crops roots had less access to the water table that did not receive typical spring recharge) (fig. 31*B*). For readers interested in additional detail, irrigation pumping for each scenario by GWMA is provided in the model archive (Traylor, 2023).

Inflows to recharge from deep percolation in the drier western and central GWMAs (1–16) generally exhibited constant annual recharge throughout the simulation period for each scenario (fig. 32*A*). GWMA 2 exhibits a typical trend where a large reduction in recharge occurs in the 3-year drought scenario and a moderate reduction in recharge for the 10-year drought scenario, each followed by an increase to match the FutBase postdrought recharge (fig. 32*A*). Further, the increase in irrigation also increased recharge from deep percolation as seen in the comparison between the alternate irrigation scenarios where the 10-inch alternate pumping scenario (Futirr10in) exhibited the highest annual recharge, and the 7-inch alternate pumping scenario (Futirr7in) exhibited the lowest annual recharge (fig. 32*A*). Also, the FutBase scenario, with identical climate to the alternate irrigation scenarios, exhibited larger irrigation and recharge than the 10-inch alternate pumping scenario. Irrigation efficiency was constant for different irrigation amounts and therefore the increases in recharge for the highest irrigation limits were because of more inefficient losses of irrigation water applied to crops compared to the lower irrigation limit scenarios.

Inflows to recharge from deep percolation in the wetter eastern GWMAs (17–24) exhibited a general increase because of an increase in irrigation pumping for the drought scenarios and a decrease because of a decrease in pumping for the alternate pumping scenarios that resulted from a change in inefficient losses of irrigation water (fig. 32*B*). The drought scenarios required a higher CIR each year that necessitated more irrigation pumping during the drought months and years; for the 3-year and 10-year drought scenarios, the postdrought average conditions caused a reduction of CIR and outflows to irrigation wells, which led to a reduction in recharge from deep percolation back to average amounts exhibited by the FutBase scenario (fig. 32*B*). The seasonal droughts indicated that the amount of precipitation that occurred in the spring months was a major contributor to total annual recharge; annual recharge was larger for the mid-growing season drought compared to the early growing season drought (fig. 32*B*). The recharge figures for each scenario for the other GWMAs are available in the model archive associated with this report (Traylor, 2023).

Comparison of Simulated Groundwater Levels to Maximum Acceptable Declines

The current CPNRD GMP specifies MADs for each GWMA (described in the “Introduction” section of this report). In this section of the report, simulated groundwater levels for each scenario were compared to the baseline 1982 gwlevels and MADs for each GWMA to assess the effect of the scenario stresses on current management thresholds set by the CPNRD (appendix 5). In general, by the end of the scenario period (December 31, 2049) for the FutBase, Futirr7in, Futirr9in, and Futirr10in scenarios, most GWMAs exhibited an increase in groundwater levels above their baseline 1982 gwlevels with seasonal irrigation related drawdowns that never approached the MAD during any period of the scenario (appendix 5). Only GWMA 6 exhibited groundwater-level declines for the FutBase and alternate irrigation scenarios owing to small inflow rates of farm net recharge and stream leakage and relatively large zone outflow. The declines for those scenarios indicated that the groundwater in GWMA 6 was not in a dynamic equilibrium with average climate and irrigation pumping conditions prior to the scenario period (fig. 5.5). Groundwater levels declined for all GWMAs during drought periods; groundwater levels continued to decline for some GWMAs postdrought, whereas other GWMAs recovered from droughts. GWMAs 2, 3, 8, and 12–17 exhibited groundwater levels that declined below their MADs for at least one scenario (fig. 33*A*, *B*; appendix 5).

For the FutBase scenario, most (21 of 25) GWMAs exhibited groundwater levels at the beginning of the forecast that were less than 5 ft from the baseline 1982 gwlevels (table 19). Deviations occurred because of dynamic climate and water use between April 1982 and December 2016. Twelve GWMAs exhibited groundwater levels from 0.2 to 13.7 ft below the baseline 1982 gwlevels at the end of the FutBase scenario (table 19). None of the GWMA exhibited declines in groundwater levels for the FutBase scenario that were below the MADs (appendix 5). GWMA 9 exhibited simulated groundwater levels 7.3 ft above the baseline 1982 gwlevels, which was attributed to the drier conditions from 1971 to 1982 and lower average deep percolation during that period (about 39,400 acre-ft/yr) in the development model compared to the FutBase model deep percolation of (66,107 acre-ft/yr). Additionally, recent development period net outflow to irrigation wells for GWMA 9 was greater than for the FutBase forecast, which contributed to less stress on the groundwater-flow system during the FutBase forecast (tables 14 and 20). The largest difference from the baseline 1982 gwlevels was in GWMA 2 (13.7 ft below baseline 1982 gwlevels), which was attributed to less irrigation pumping

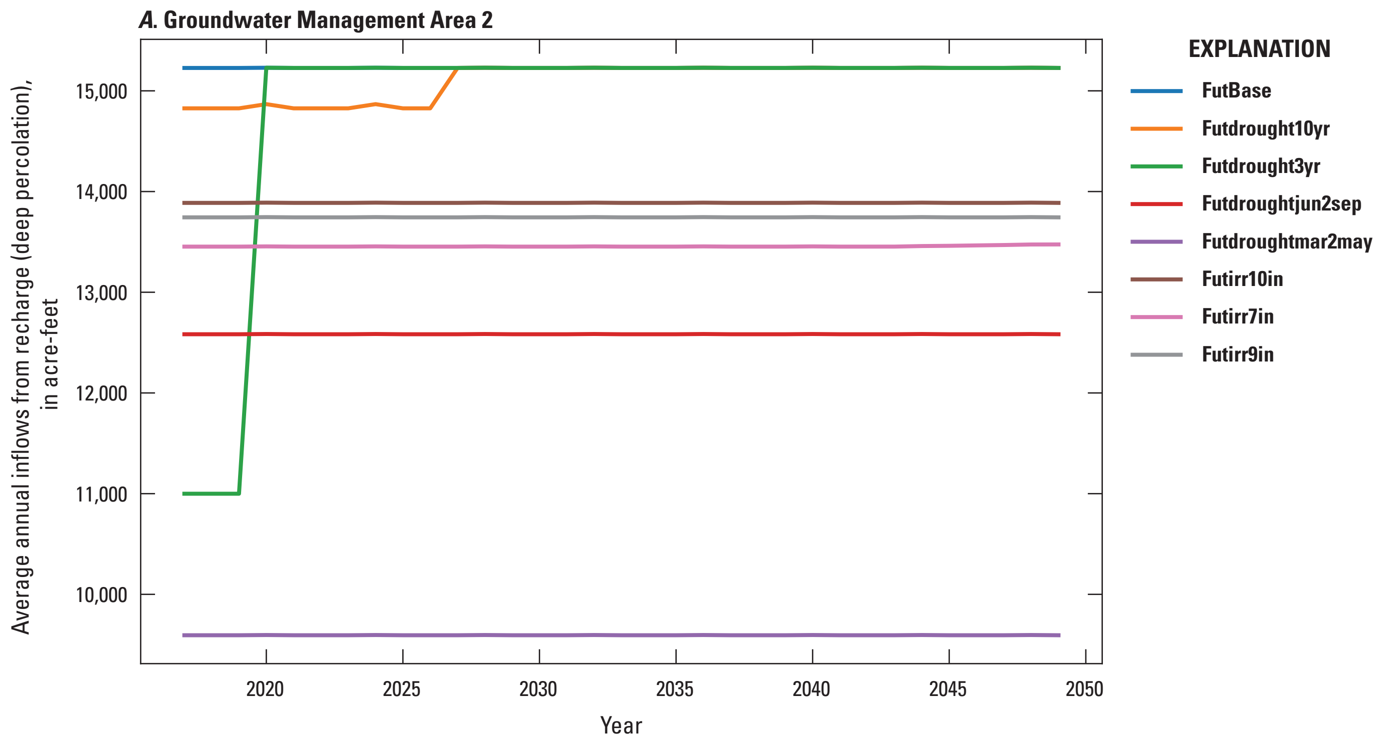

Figure 32. Plots of average annual recharge from deep percolation for each scenario. *A*, Groundwater Management Area 2. *B*, Groundwater Management Area 18.

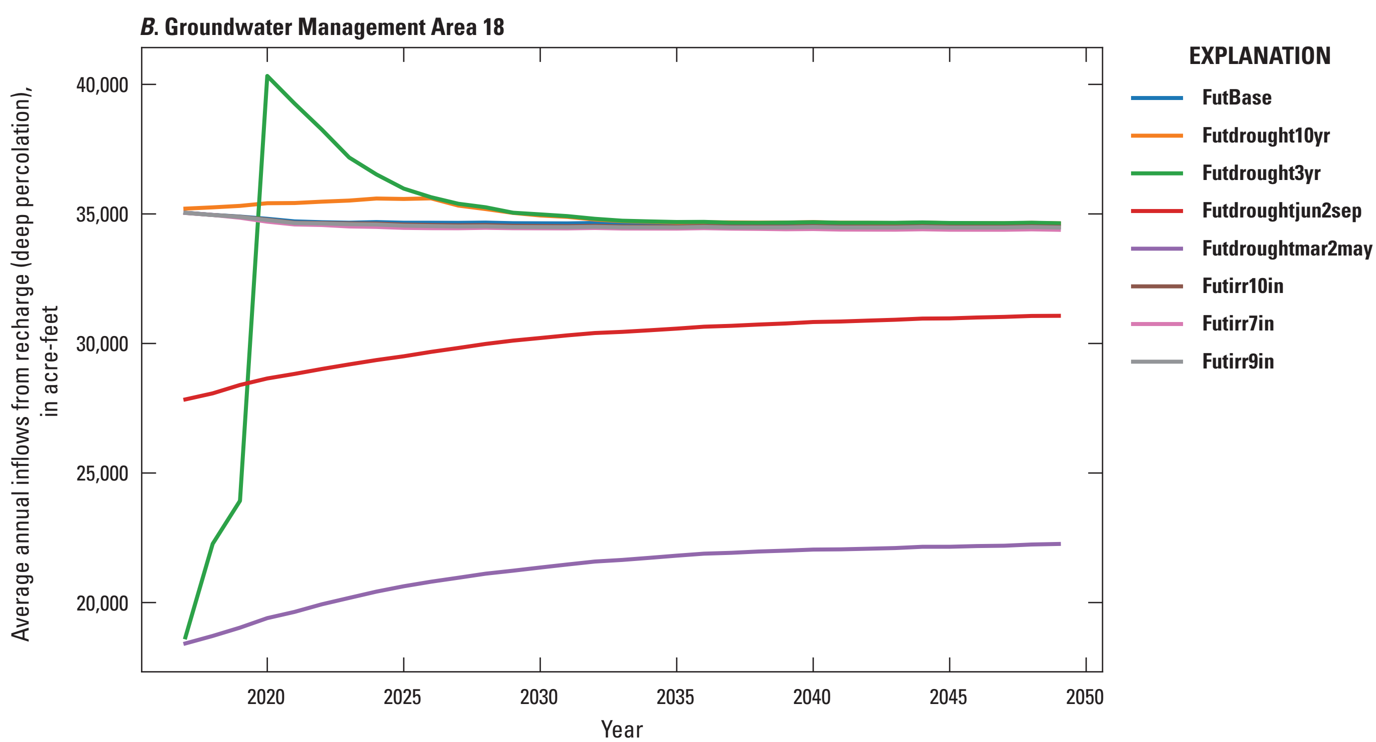

Figure 32.—Continued

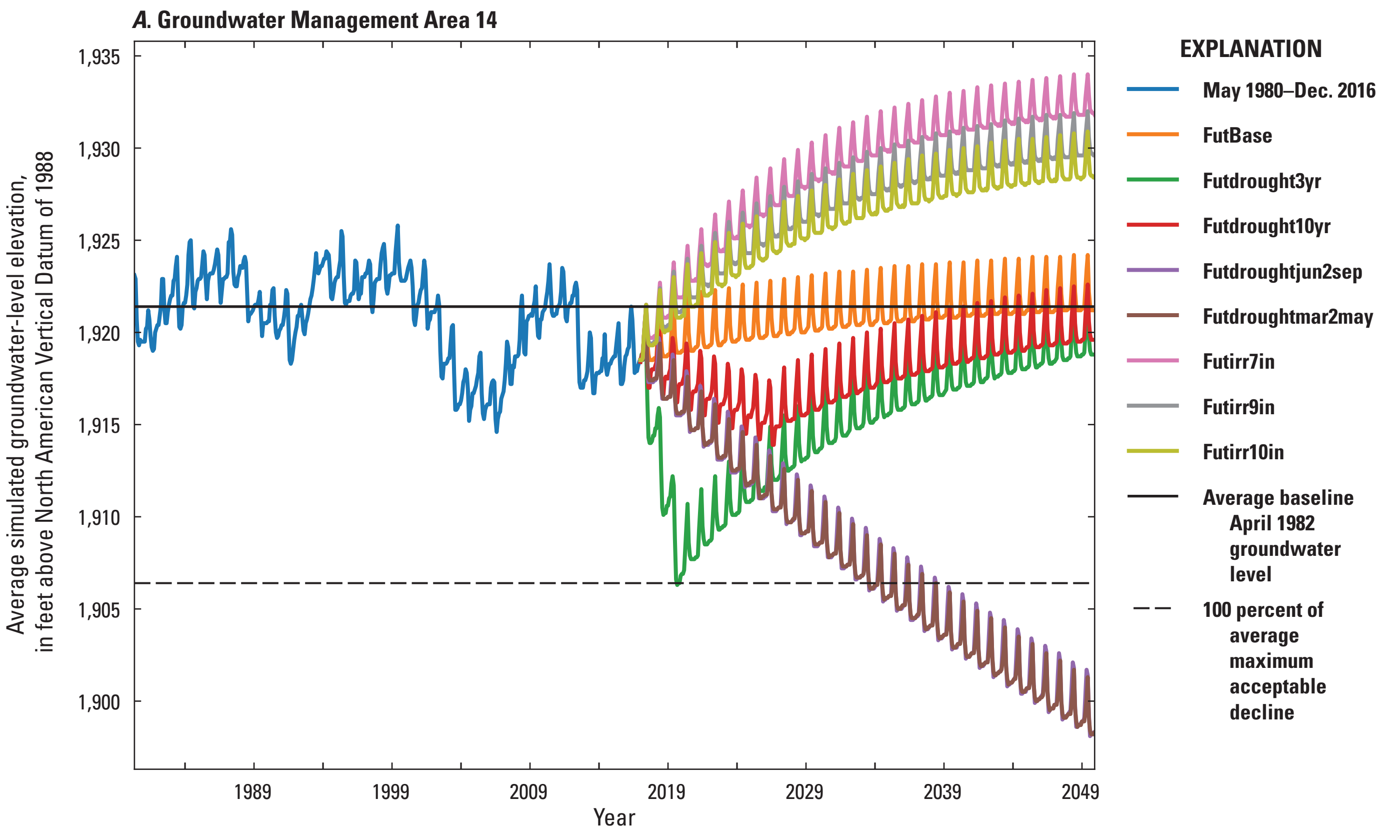

Figure 33. Simulated groundwater levels from May 1980 to December 2016 development period and January 2017 to December 2049 scenario period for the Central Platte Integrated Hydrologic Model. *A*, Groundwater Management Area 14. *B*, Groundwater Management Area 2.

and more recharge owing to wetter conditions in 1981 and 1982 compared to those simulated in the FutBase model; the CPNRD supergroup average groundwater levels were 0.2 ft below the baseline 1982 gwlevels, which indicated that overall, the groundwater-flow system in the CPNRD was similar to levels in 1982 (table 19).

For the Futdrought3yr scenario, groundwater levels at the end of the scenario were 0.1 to 18.4 ft below the baseline 1982 gwlevels for 16 GWMAs (table 19). Groundwater levels exceeded the MAD by 0.3 and 0.1 ft, respectively, for GWMAs 2 and 14 by the end of the 3-year drought (September 2019); GWMA 15 was 0.1 ft above the MAD by that time (fig. 5.13). These areas were characterized by a high demand for groundwater to irrigate crops that was met by large rates of irrigation pumping and small rates of stream leakage that could not recharge the aquifer during extended drought conditions and led to the simulated larger declines in groundwater levels during the 3-year severe drought (table 4.18).

For the Futdrought10yr scenario, groundwater levels at the end of the scenario were 0.4 to 18.5 ft below the baseline 1982 gwlevels for 14 GWMAs (table 19). Groundwater levels did not exceed the MAD for any GWMA throughout the scenario (appendix 5). After 3 years of the moderate drought (December 31, 2019), average groundwater levels for 17 GWMAs and the CPNRD and CPIHM were below the baseline 1982 gwlevels. At the end of the 10-year drought (December 31, 2026), average groundwater levels for 19 GWMAs and the CPNRD and CPIHM were below the baseline 1982 gwlevels. GWMA 2 exhibited an average groundwater level more than 10 ft below the baseline 1982 gwlevels because of high outflows from irrigation wells and less recharge compared to many other GWMAs (10.7 ft; table 19).

For the mid-growing season drought scenario (Futdroughtjun2sep), all 24 GWMAs exhibited groundwater levels that ranged from 2.1 to 38.8 ft below the baseline 1982 gwlevels (table 19) by the end of the scenario (December 31, 2049), with mid-growing season drought conditions simulated from January 1, 2017, to December 31, 2049. After 3 years of a mid-growing season drought (January 1, 2017, to December 31, 2019, with each June through September simulated as drought conditions), average groundwater levels for 21 GWMAs were 0.1 to 12 ft below the baseline 1982 gwlevels (table 19). GWMA 2 exhibited the largest average groundwater-level difference from the baseline 1982 gwlevels at −12 ft. Five GWMAs (GWMAs 2, 3, 8, 13, 14, and 15) exhibited groundwater levels below their MADs by the end of the scenario (see appendix 5 figures for each GWMA). Each

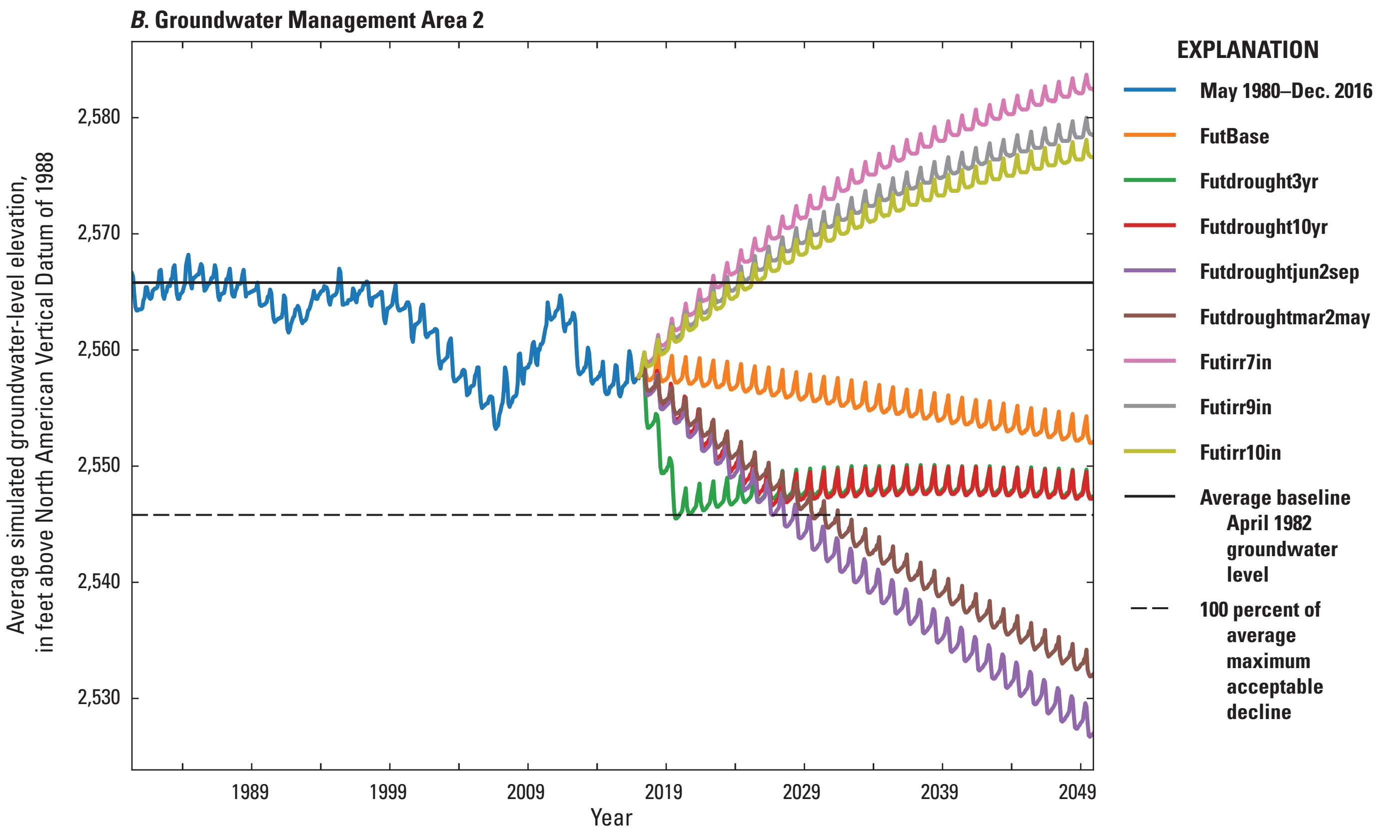

Figure 33.—Continued

of these GWMAs were characterized by large irrigation pumping rates and small rates of stream leakage compared to other GWMAs, which had less irrigation pumping or more stream leakage that recharged the aquifer (table 4.20).

For the early growing season drought scenario (Futdroughtmar2may), all 24 GWMAs exhibited groundwater levels that ranged from 1.5 to 33.7 ft below the baseline 1982 gwlevels (table 19) by the end of the scenario (December 31, 2049), with early growing season drought conditions simulated from January 1, 2017, to December 31, 2049. After 3 years of a mid-growing season drought (January 1, 2017, to December 31, 2019, with each June through September simulated as drought conditions), average groundwater levels for 21 GWMAs were 0.1 to 12 ft below the baseline 1982 gwlevels (table 19). GWMA 2 exhibited the largest average groundwater-level difference from the baseline 1982 gwlevels at −11.2 ft. Five GWMAs (GWMAs 2, 12, 13, 14, 15, 16, and 17) exhibited groundwater levels below their MADs by the end of the scenario (see appendix 5 figures for each GWMA). Like the GWMAs for the other drought scenarios, each GWMA that exhibited groundwater-level declines below their MADs were characterized by large irrigation pumping rates and small rates of stream leakage, which was an indication that stream leakage supplies recharge to the aquifer during dry periods and reduces the impact of irrigation pumping on the aquifer (table 4.21).

Forecast Uncertainty Analysis

In a complex hydrologic model, the calibrated parameter set can be varied by large amounts and still generate similar model results with a similar objective function value (Anderson and others, 2015). Thus, the final calibrated parameter set calculated in the "Calibration Results" section can be viewed as a single set of parameters from an entire range. This parameter nonuniqueness can generate a range of reasonable outputs or results of a scenario, which can be thought of as the forecast uncertainty. Quantification of the forecast uncertainty can improve the understanding of the usefulness of the model. A large forecast uncertainty can correspond to a wider range of simulated model results, such as groundwater levels at the end of a scenario period, whereas a small forecast uncertainty can correspond to less variation in the same simulated groundwater level at the end of a scenario.

Forecast uncertainty was assessed for this study using the linear "first order second moment" uncertainty analysis techniques within the PEST++GLM code to generate an ensemble of 500 combinations of parameters (realizations) for a Monte Carlo analysis. A comprehensive description of this process, including its theoretical and mathematical underpinnings, can be found in the PEST++GLM documentation (White and others, 2019). The analysis was executed on the Denali supercomputer (U.S. Geological Survey, 2020).

Forecast uncertainty was evaluated for 24 theoretical future groundwater altitudes (futheads200 to futheads223) in the FutBase scenario, corresponding to end of scenario (December 31, 2049) groundwater altitudes at the center of GWMAs 1 to 24 (table 23). Uncertainty in the forecasted groundwater altitude at each location (fig. 13) was reduced from an average of 15.47 ft prior to the model calibration to 0.14 ft after the model calibration (posterior; table 23). Therefore, prior to model calibration, using acceptable ranges of input parameter values, the average standard deviation of a simulated groundwater altitude for the FutBase scenario of the CPIHM was 15.47 ft and post calibration standard deviation was 0.14 ft. Groundwater levels in GWMAs 2, 14, and 15 exhibited the highest reduction in uncertainty as indicated by the percentage change in standard deviation. These GWMAs contained more groundwater-level calibration targets than were in GWMAs 6, 17, and 20, which exhibited the lowest reduction in forecast uncertainty, because more observations in a region provide more information to parameters during the calibration process (fig. 13; Doherty, 2015). The large reduction in forecast uncertainty for all regions in the CPIHM was mainly a product of the fixed landscape parameters, particularly the ET_{ref} scale factors, which exhibited a large uncertainty and sensitivity during preliminary calibrations, and the relatively small sensitivities of the remaining adjustable parameters during the final calibration process (Kh, aquifer anisotropy, and streamed vertical hydraulic conductivity), discussed in the “Parameter Sensitivity and Identifiability” section of this report.

Assumptions and Limitations

The CPIHM was constructed to simulate the important hydrologic processes for the CPNRD. The calibration results indicated agreement between calibration targets and simulated equivalents, the results were deemed adequate, and the spatial and temporal resolutions of the CPIHM were appropriate to simulate and characterize landscape water and groundwater flow in the CPNRD and semiregional scale processes. Nonetheless, limitations exist with respect to applying the CPIHM for purposes beyond those for which it was designed. For example, local hydrologic processes may not have been represented or were combined with more regional processes; ephemeral channels were not simulated in this model and runoff that flows to these channels during precipitation events was instead routed directly to the closest perennial stream. The seasonal temporal discretization of the development CPIHM for stress periods 1 to 170 and monthly from 171 to 610 only allows the model to simulate the prevailing average conditions each month. Consequently, this model should not be used to study any hydrologic processes with less than a 1-month duration, such as the peak flows of streams during daily precipitation events (for example, thunderstorms) that produce heavy rainfall in a few minutes or hours. Model cell size limits the characterization of hydrologic properties and features to greater than or equal to a single model cell (160 acres) and includes land use, which was specified using fractions of a cell, but the total effect on the hydrologic system was the combination of each land-use fraction within a cell. Any properties of features less than 160 acres were effectively combined with other features. The CPIHM simulated landscape and groundwater hydrologic processes and did not simulate the soil moisture changes or processes in the unsaturated zone. Therefore, the CPIHM should not be used to assess the effects of hydrologic stresses on soil moisture or the unsaturated zone. Additionally, the CPIHM does not include porosity of aquifer layers and should not be used to conduct a particle travel time analysis without the implementation of porosity values.

The CPIHM should not be used to assess the impacts of stresses on total streamflow and base flow for the South Loup River, Middle Loup River, and Loup River. These streams interact with the groundwater-flow system and surface-water system to the north, but the region north of these streams was not simulated in the CPIHM because that was not within the scope of the study; the Loup River system was simulated as a boundary condition for the CPIHM. Therefore, the simulated flows for these streams did not include groundwater (base flow) and surface-water (run off) contributions from the north side because that was not included in the CPIHM. The CPIHM should not be used to assess the impacts of stresses on total streamflow and base flow for other boundary streams that include Sand Creek in Adams County, Big Sandy Creek in Clay County, and School Creek in Clay and York Counties.

The CPIHM should not be used to assess groundwater levels, streamflow, or impacts to either of those features from irrigation, climate change, or other stresses outside of the boundary of the CPNRD. The objective of the study and focus area of the model development and the calibration was the CPNRD. Physical properties, such as Kh and anisotropy, were adjusted during calibration to preferentially improve the fit between measured data and simulated equivalent values inside the CPNRD, and weighting of the groundwater-level calibration targets was larger for targets inside the CPNRD. Aquifer storage properties (Sy and Ss) of each model layer were not adjusted during calibration, but simulated groundwater-level hydrographs compared to high resolution temporal data from figure 17 showed that the amplitudes of measured and simulated groundwater levels were very similar, which indicated that the input storage values were accurate; however, local refinement of the storage properties and a different calibration parameter scheme may further improve the fit between the measured and simulated groundwater levels. Spatial bias in the groundwater-level residuals, as documented in this report, did not affect the ability of the CPIHM to meet the objectives of the study, particularly with respect to assessment of the scenario stresses on MADs because they were relative to simulated values for the baseline 1982 gwlevels and simulated end of development period (December 31, 2016) groundwater levels. The bias in the groundwater levels does affect the

Table 23. Summary of FutBase scenario uncertainty for each potential observation in each Groundwater Management Area.

[GWMA, Groundwater Management Area; --, not applicable]

Forecast name	GWMA/ supergroup	Average forecast groundwater altitude, in feet above sea level	Prior standard deviation, in feet	Posterior standard deviation, in feet	Change in standard deviation, in feet	Change in standard deviation, in percent
FUTHEADS200	1	2,595.37	33.98	0.31	33.67	99.08
FUTHEADS201	2	2,560.97	52.62	0.24	52.39	99.55
FUTHEADS202	3	2,457.15	14.82	0.09	14.74	99.40
FUTHEADS203	4	2,387.07	3.34	0.02	3.32	99.31
FUTHEADS204	5	2,509.06	10.92	0.07	10.85	99.34
FUTHEADS205	6	2,467.40	21.10	0.30	20.80	98.60
FUTHEADS206	7	2,340.15	16.28	0.16	16.12	99.01
FUTHEADS207	8	2,312.41	6.03	0.05	5.98	99.24
FUTHEADS208	9	2,174.51	14.46	0.14	14.32	99.02
FUTHEADS209	10	2,056.01	3.10	0.04	3.07	98.78
FUTHEADS210	11	1,971.04	62.58	0.80	61.79	98.72
FUTHEADS211	12	1,984.84	12.98	0.09	12.89	99.31
FUTHEADS212	13	1,847.50	8.21	0.06	8.14	99.22
FUTHEADS213	14	1,891.47	23.72	0.11	23.61	99.52
FUTHEADS214	15	1,882.74	9.82	0.04	9.78	99.61
FUTHEADS215	16	1,706.36	15.53	0.12	15.41	99.24
FUTHEADS216	17	1,747.41	28.49	0.39	28.11	98.64
FUTHEADS217	18	1,677.01	5.52	0.08	5.44	98.61
FUTHEADS218	19	1,706.41	5.06	0.04	5.02	99.29
FUTHEADS219	20	1,576.70	2.43	0.03	2.39	98.62
FUTHEADS220	21	1,635.29	10.97	0.15	10.82	98.62
FUTHEADS221	22	1,515.29	0.46	0.01	0.46	98.84
FUTHEADS222	23	1,511.23	1.03	0.01	1.02	99.02
FUTHEADS223	24	1,528.52	7.74	0.07	7.67	99.05
Average	--	--	15.47	0.14	15.32	99.07

ability of the CPIHM to simulate absolute groundwater-level altitudes in the northern and southern regions of the model domain at the edges of the CPNRD boundary.

The conveyance and routing of surface water for the CNPPID canals was not simulated by the CPIHM; only leakage losses from the CNPPID canals were simulated. In addition to the CNPPID canals residing outside the CPNRD focus area, the CPIHM should not be used to assess the impact of Phelps County Supply Canal on the hydrologic system. The scenarios simulated by the CPIHM were theoretical and provided information on general hydrologic trends in each GWMA under different potential future conditions in a transient system. The scenarios analyzed with CPIHM were not intended to predict future climate.

The landscape parameters were not well constrained during preliminary calibration attempts because there were no calibration target datasets with adequate spatial or temporal coverage available to constrain inputs such as ET_{ref}, FTR, irrigation efficiencies, runoff, or recharge. Therefore, as discussed in the “Parameter Sensitivity and Identifiability” and “Forecast Uncertainty Analysis” sections of this report, the fixing of landscape parameters introduced a low bias in the uncertainty of model results. Although the simulated model results were in agreement with the conceptual understanding of the hydrologic system and the results presented in this report are acceptable with respect to the calibration targets and the conceptual understanding of the study area processes, the fixing of the landscape parameters limited the flexibility of the model during the calibration process. A calibration with all landscape parameters set as “adjustable” and accompanied by additional calibration targets to provide information and constrain the adjustable landscape parameters may have resulted in PEST finding a different combination of acceptable parameter values. A predictive uncertainty was performed and demonstrated that simulated groundwater levels in the CPNRD area have a very small predictive uncertainty related to the fixing of some of the most sensitive parameters such as the ET_{ref} scale factors, but the uncertainty in other model outputs or in groundwater levels outside of the CPNRD was not evaluated.

Potential Topics for Additional Study

Data collection and monitoring are essential for informing construction and calibration of hydrologic models, as well as assessment of results. A data-worth analysis may quantify the worth of new data collected and how the data would improve the calibration, such as new observations at existing sites, new observations at new sites, and new types of observations. A data-worth analysis may also quantify the impact of removal of observations on the calibration. Such information could be used to select new locations for data collection or removal of data collection sites if necessary. The unsaturated zone was not simulated in the CPIHM because it was not critical to the study objectives or model calibration and results within the CPNRD. A study to simulate the unsaturated zone in the CPIHM using the Unsaturated Zone Flow (UZF) package could be used to assess rejected infiltration and attenuation of deep percolation recharge past the root zone to the water table (Niswonger and others, 2006). Recent feature updates to the MF–OWHM code allow the FMP and the UZF package to be linked so that FMP-calculated deep percolation is passed as an inflow to UZF, as an infiltration rate, and is used as unsaturated flow (Boyce and others, 2020).

The scenarios simulated by the CPIHM provide information on the response of the hydrologic system to selected potential future climate and irrigation pumping conditions. Additional studies of the effects of other future climate conditions on recharge, runoff, ET, groundwater storage, stream leakage, and saturated thickness and availability would likely improve the understanding of the response of the system to those potential scenarios. For example, simulation of potential scenarios that include continuous warmer and drier conditions and continuous colder and wetter conditions on the hydrologic system in the CPIHM could improve the understanding of the response of the hydrologic system to a wider variety of potential future climate change conditions. This approach was used in a groundwater-flow model of the Northern High Plains aquifer to evaluate hydrologic responses induced by potential future conditions from downscaled global climate models (Peterson and others, 2020).

The MF–OWHM contains functionality to simulate more complex surface-water features. The simulations of the irrigation canals in the CPIHM used constant surface-water diversions from a year that matched climate trends. A study to simulate alternative surface-water diversions to canals could likely improve the understanding of those potential changes on the hydrologic-flow system. Additional scenarios to assess managed aquifer recharge using canals or new reservoirs may also quantify the impact of such practices on the hydrologic-flow system.

The CPIHM simulated subregional stresses, but localized stresses and their impact on the hydrologic system could be simulated and studied with an inset hydrologic-flow model within the CPNRD using a finer spatial resolution within the regional CPIHM domain that would produce higher resolution outputs. Additionally, the CPIHM could be linked to an economic model to create a full decision support system that may inform management decisions on economic factors or vice versa. Water-quality and particle tracking could be the focus of an additional study if permeability inputs were specified, which might allow for accurate simulation of particle paths and travel times. Water-quality data, such as age dating, might be useful to corroborate transit and residence times within the aquifer and possibly improve the understanding of water sources to streams and irrigation wells.

The complexity of a fully integrated model like the CPIHM would benefit from an increase in parameterization to better capture the unknowns and uncertainty in model inputs and allow for more flexibility for these model inputs during the calibration process. An increase in the number of adjustable parameters would improve the CPIHM's ability to simulate the natural system and provide a more robust characterization of scenario uncertainty. The latest advancements in the PEST++ suite of calibration software includes the iterative ensemble smoother (PESTPP–IES) code, which was not available at the time of model development and calibration. PESTPP–IES can accommodate millions of parameters without the prohibitive increase in computational burden that is required for calculation of the derivatives of parameters to observations (Jacobian sensitivity matrix) when using traditional PEST and BeoPEST codes. Further, the addition of observations such as AET, recharge, and metered pumping as calibration targets to constrain landscape parameters also might improve the calibration of the CPIHM with respect to the landscape processes that influence recharge to the groundwater system. Additional AET observations from Reitz and others (2017) may improve the ability of PEST to constrain the ET_{ref} scale factors in an automated calibration rather than manual adjustments.

Summary

The Central Platte Natural Resources District (CPNRD) is responsible for regulating groundwater use of the district. The groundwater and surface-water supply of the CPNRD is one of its most valuable natural resources and supports an agricultural economy that generates more than $2 billion per year. The CPNRD's main groundwater quantity management goal is the utilization of its water resources through proper management and conservation to ensure an adequate supply for feasible and beneficial uses. State law requires the CPNRD to develop a Groundwater Management Plan. The CPNRD's initial Groundwater Management Plan was adopted in 1987. The CPNRD Groundwater Management Plan specifies maximum acceptable declines of 10 to 30 feet for 24 Groundwater Management Areas (GWMAs) across the CPNRD, with the declines based on spring 1982 (approximately April 30, 1982) groundwater levels. The CPNRD management strategy has employed advanced numerical flow models since the creation of their first Groundwater Management Plan, initially adopted in 1987. The purpose of this report is to document and describe the construction, calibration, and results of a numerical fully integrated hydrologic model using the U.S. Geological Survey MODFLOW-based software called MODFLOW–One-Water Hydrologic Model code that simulated the CPNRD hydrologic system under past development conditions from 1895 to 2016 and eight future scenarios simulated from 2017 to 2049. Results of the potential future scenarios are described in this report along with information about potential future water availability and changes in groundwater levels for each scenario with respect to the baseline 1982 groundwater levels, and maximum acceptable declines, that can be used by the CPNRD to update their Groundwater Management Plan.

The study area was focused around the CPNRD, which includes parts of 10 counties in central Nebraska and a total area of 2,136,304 acres. The main hydrologic features are the Platte River, which flows from west to east for about 205 miles, and the High Plains aquifer, which underlies the entire study area with saturated thicknesses ranging from about 50 to 550 feet. There are about 1 million irrigated acres of cropland in the CPNRD and 936,000 acres are supplied by pumping groundwater from the underlying High Plains aquifer. An extensive network of canals diverts water from the Platte River to surface-water irrigators in Buffalo, Dawson, Kearney, and Phelps Counties. The geologic units in the study area consist of Quaternary-age valley-fill, dune sand, loess, and alluvium; and Tertiary-age Ogallala Formation silt and sandstone. The Ogallala Formation is the principal geologic unit that forms the Northern High Plains aquifer, which includes the hydrologically connected Quaternary-age alluvial aquifers. The contact between the Ogallala Formation and underlying Pierre Shale, which is not hydrologically connected to the Ogallala Formation, represents the base of the Northern High Plains aquifer. Regional groundwater-flow directions are generally from west to east but can vary locally. The groundwater-flow system is connected to streams where groundwater receives inflows from stream leakage or outflows as base flow to streams.

An integrated hydrologic model, called the Central Platte Integrated Hydrologic Model (CPIHM), was constructed using the MODFLOW–One-Water Hydrologic Model code and used the Newton solver. The MODFLOW–One-Water Hydrologic Model integrates climate, landscape, surface water, and groundwater-flow processes in a fully coupled approach to hydrologic modeling that simulates the natural feedbacks of a system. The CPIHM consisted of 163 rows and 327 columns with horizontal cell sides of 2,640 feet by 2,640 feet and was vertically discretized into three layers of varying spatial extents and thickness according to the hydrogeology and aquifer. Layers 1, 2, and 3 represented the Quaternary-age valley-fill, loess deposits, and alluvial aquifers; Quaternary-age loess deposits and Upper-Tertiary-age portions of the Ogallala Formation; and the Tertiary -age Ogallala Formation. The CPIHM included two models: a pre irrigation development model that represented a steady-state equilibrium prior to April 30, 1895, and a development period model that was temporally discretized into 610 stress periods to simulate transient conditions from May 1, 1895, to December 31, 2016. There were 212 water accounting units, called water-balance subregions, delineated for use in the Farm Process package, which were merged into the 24 GWMAs as "supergroups" to present results.

Calibration of the CPIHM involved two phases: a manual adjustment of parameters, followed by the automated calibration using BeoPEST. During the automated calibration phase, 435 parameters were adjusted to improve the fit between 40,711 streamflow and groundwater-level observations and their simulated equivalent values at 53 streamgages and 963 observation well locations. Additionally, the automated calibration was facilitated by the employment of the singular value decomposition-assist features of the Parameter Estimates (PEST) software that specified 50 super parameters and Tikhonov regularization. The average absolute groundwater-level residuals for model layers 1, 2, and 3 were 6.1, 12.4, and 7.4 feet, respectively, and after 1980 were 4.0, 10.7, and 7.5 feet, respectively, which indicated that the CPIHM adequately simulated the groundwater levels for each layer. Calibrated horizontal hydraulic conductivity values estimated at pilot points and interpolated to the model grid were about 70, 32, and 35 feet per day for layers 1, 2, and 3, respectively, which were similar to values from previous studies.

Simulated landscape water budgets for the calibrated development model maintained the general trends and magnitudes expected from the conceptual understanding of the landscape water subsystem. The largest inflow component was precipitation with an average development period (May 1, 1895, to December 31, 2016) annual volume of 9,978,276 acre-feet per year (acre-ft/yr) (24.3 inches if spread equally across the model domain). The largest outflow from the landscape was evapotranspiration of precipitation at an average annual flux of 7,935,263 acre-ft/yr (19.3 inches). In the last 5 years of the development model simulation (2011–16), the average annual volume of total evapotranspiration, which included evapotranspiration of precipitation and irrigation water sources, was 8,420,099 acre-ft/yr (20.5 inches). For the groundwater budget, the largest inflow component was recharge (analogous to deep percolation from the landscape), with an average development period annual volume of 1,122,257 acre-ft/yr (2.7 inches). The largest groundwater outflows were to irrigation wells at an average annual volume of 693,171 acre-ft/

yr (10.2 inches for the CPNRD). For the total development period, there was a net replenishment to groundwater storage of −122,393 acre-ft/yr (−0.3 inches per year). For the recent groundwater budget (2011–16), the average annual releases from groundwater storage were like those from recharge from deep percolation at about 2,326,871 acre-ft/yr (5.7 inches) and 2,056,936 acre-ft/yr (5.0 inches), respectively, because irrigation wells received most of their 2,132,994 acre-ft/yr of groundwater pumped from storage; however, recovery during the nonirrigation season included replenishment to storage of −2,045,430 acre-ft/yr. After 1980, average monthly recharge was the largest inflow from October to June. The largest volumes of recharge occurred in April, May, and October when evapotranspiration and groundwater pumping to irrigation wells was minimal or inactive and precipitation was relatively high.

The CPIHM simulated the effects of eight different potential future climate and irrigation pumping conditions that included one base scenario, three alternative irrigation scenarios, and four drought scenarios. The scenario simulation period included 396 monthly stress periods from January 1, 2017, to December 31, 2049. A base scenario simulated average climate conditions of precipitation and potential evapotranspiration, the four drought scenarios included the simulation of an intense 3-year drought, a moderate 10-year drought, a mid-growing season drought from June to September each year, and an early growing season drought from March to May each year. The three alternate irrigation scenarios included the simulation of an annual 7-inch depth limit on groundwater pumped, an annual 9-inch depth limit on groundwater pumped, and an annual 10-inch depth limit on groundwater pumped. The simulated groundwater levels for each scenario were compared to the baseline 1982 (April 30, 1982) average groundwater levels simulated by the development model, the groundwater levels simulated at the end of the development period (December 31, 2016), and the maximum acceptable decline groundwater-level elevation for each GWMA.

Base scenario average groundwater levels for the CPNRD were 0.2 foot below the baseline 1982 groundwater level and 0.3 foot below the prescenario (December 31, 2016) groundwater level by the end of the scenario period (December 31, 2049). Additionally, the average annual groundwater irrigation pumping depths were 9.3 inches for the CPNRD. Alternate irrigation pumping scenario average groundwater levels were 7.6, 6.1, and 5.4 feet above the baseline 1982 groundwater levels for the 7-inch, 9-inch, and 10-inch pumping scenarios, respectively, at the end of the scenario period for the CPNRD. Additionally, average CPNRD groundwater levels at the end of the scenario period (December 31, 2049) were 7.5, 6.0, and 5.3 feet above their prescenario (December 31, 2016) groundwater levels for the 7-inch, 9-inch, and 10-inch pumping scenarios, respectively. Across all three of these forecasts, the drier western region GWMAs that required the highest average outflows to irrigation for the FutBase scenario were also the regions that were most groundwater supply limited. In general, the amount of pumping varied by GWMA which indicated that a limit on irrigation pumping had a variable effect on the groundwater-flow system depending on the local stresses specific to each GWMA. GMWAs 19 and 23 exhibited the highest surplus irrigation state because their irrigation requirements were very small when compared to other GWMAs and they exhibited substantial net inflow from adjacent zones. Conversely, GMWA 6 exhibited the highest deficit irrigation state because it had one of the lowest rates of farm net recharge and lacked other sources of water such as net inflows from adjacent zones and limited net inflow from streams to offset outflows to irrigation wells.

The 3-year intense drought scenario average groundwater levels for the CPNRD were 1.7 feet below the baseline 1982 groundwater-level and 1.8 feet below the prescenario (December 31, 2016) groundwater level by the end of the scenario period (December 31, 2049). The average annual groundwater irrigation pumping depths were 10.2 inches for the CPNRD. The 10-year moderate drought scenario average groundwater levels for the CPNRD were 2.0 feet below the baseline 1982 groundwater-level and 2.1 feet below the prescenario (December 31, 2016) groundwater level by the end of the scenario period. Additionally, the average annual groundwater irrigation pumping depths were 10.0 inches for the CPNRD. GWMAs that exhibited more recharge and lower irrigation rates exhibited groundwater levels that generally recovered to predrought levels, whereas GWMAs with less recharge and higher irrigation rates exhibited groundwater levels that continued to decline postdrought.

The early growing season drought scenario average groundwater levels for the CPNRD were 11 feet below the baseline 1982 groundwater level and 11.1 feet below the prescenario (December 31, 2016) groundwater level by the end of the scenario period (December 31, 2049). Additionally, the average annual groundwater irrigation pumping depths were 9.7 inches for the CPNRD. The mid-growing season drought scenario average groundwater levels for the CPNRD were 13.8 feet below the baseline 1982 groundwater level and 13.9 feet below the prescenario (December 31, 2016) groundwater level by the end of the scenario period (December 31, 2049). Additionally, the average annual groundwater irrigation pumping depths were 11.7 inches for the CPNRD. Overall, there were two general trends in groundwater levels by the end of the scenario period: 16 GWMAs exhibited greater declines for the mid-growing season drought scenario and eight GWMAs exhibited greater declines for the early growing season drought scenario. The GWMAs that exhibited larger declines for the early growing season drought were affected by less net farm recharge, which indicated that less precipitation and recharge during spring (March to May) had a larger effect on net storage than irrigation well pumping. Conversely, the GWMAs that exhibited greater declines in groundwater levels for the mid-growing season drought were affected more by larger outflows to irrigation wells.

With respect to the maximum acceptable declines in groundwater-levels, in general, by the end of the scenario period (December 31, 2049) for the Base scenario, 7-inch, 9-inch, and 10-inch pumping scenarios, most GWMAs exhibited an increase in groundwater levels above their baseline 1982 groundwater levels with seasonal irrigation related drawdowns that never approached the maximum acceptable declines during any period of the scenario. In general, the 3-year drought scenario had a larger effect on groundwater levels compared to the 10-year drought scenario for some GWMAs, such as GWMA 2 where groundwater levels did not recover above their maximum acceptable declines even after 30 years of average climate and stream inflow conditions. In contrast, groundwater levels did not decline below the maximum acceptable declines in GWMA 2 for the 10-year drought scenario, although postdrought recovery was similar to the recovery from the 3-year drought scenario.

Forecast uncertainty was assessed for this study using the linear "first order second moment" uncertainty analysis techniques within the PEST++GLM code. Forecast uncertainty was evaluated for 24 theoretical future groundwater altitudes in the base scenario, corresponding to end of scenario (December 31, 2049) groundwater altitudes at the center of each of the 24 GWMAs. Uncertainty in the forecasted groundwater altitude at each location was reduced from an average of about 15.47 feet prior to the model calibration to 0.14 foot after the model calibration (posterior). The large reduction in forecast uncertainty for all regions in the CPIHM was primarily attributed to the fixed landscape parameters, particularly the reference evapotranspiration scale factors; local uncertainty differences between GWMAs were because of different amounts of observations that informed the calibration in those areas.

References Cited

Alexander, J.S., Schultze, D.M., and Zelt, R.B., 2013, Emergent sandbar dynamics in the lower Platte River in eastern Nebraska—Methods and results of pilot study, 2011: U.S. Geological Survey Scientific Investigations Report 2013–5031, 42 p. with appendixes., accessed September 1, 2020, at https://doi.org/10.3133/sir20135031.

Allen, R.G., Pereira, L.S., Raes, D., and Smith, M., 1998, Crop evapotranspiration—Guidelines for computing crop requirements: Rome, Italy, United Nations Food and Agriculture Organization, Irrigation and Drainage Paper no. 56, 300 p. [Also available at https://www.researchgate.net/publication/235704197_Crop_evapotranspiration-Guidelines_for_computing_crop_water_requirements-FAO_Irrigation_and_drainage_paper_56.]

Anderson, J.A., Morin, R.H., Cannia, J.C., and Williams, J.H., 2009, Geophysical log analysis of selected test holes and wells in the High Plains aquifer, Central Platte River basin, Nebraska: U.S. Geological Survey Scientific Investigations Report 2009–5033, 16 p. [Also available at https://doi.org/10.3133/sir20095033.]

Anderson, M.P., Woessner, W.W., and Hunt, R.J., 2015, Applied groundwater modeling (2nd ed.). Academic Press, 630 p.

Bakker, M., Post, V., Langevin, C.D., Hughes, J.D., White, J.T., Starn, J.J., and Fienen, M.N., 2016, Scripting MODFLOW model development using Python and FloPy: Ground Water, v. 54, no. 5, p. 733–739. [Also available at https://doi.org/10.1111/gwat.12413.

Barlow, P.M., Cunningham, W.L., Zhai, T., and Gray, M., 2014, U.S. Geological Survey Groundwater Toolbox, a graphical and mapping interface for analysis of hydrologic data (version 1.0)—User guide for estimation of base flow, runoff, and groundwater recharge from streamflow data: U.S. Geological Survey Techniques and Methods, book 3, chap. B10, 27 p. [Also available at https://doi.org/10.3133/tm3B10.]

Barlow, P.M., Cunningham, W.L., Zhai, T., and Gray, M., 2017, U.S. Geological Survey Groundwater Toolbox version 1.3.1, a graphical and mapping interface for analysis of hydrologic data: U.S. Geological Survey software release, accessed May 26, 2017, at https://doi.org/10.5066/F7R78C9G.

Boyce, S.E., Hanson, R.T., Ferguson, I., Schmid, W., Henson, W., Reimann, T., Mehl, S.M., and Earll, M.M., 2020, One-Water Hydrologic Flow Model—A MODFLOW based conjunctive-use simulation software: U.S. Geological Survey Techniques and Methods, book 6, chap. A60, 435 p., accessed September 2020 at https://doi.org/10.3133/tm6A60.

Cannia, J.C., Woodward, D.W., and Cast, L., 2006. Cooperative hydrology study hydrostratigraphic units and aquifer characterization report: Cooperative Hydrology Study, 91 p., accessed September 1, 2017, at http://cohyst.nebraska.gov/document/dc012hydro_aquifer_022406.pdf.

Cannia, J.C., Abraham, J.D., and Asch, T.H., 2017, Hydrogeologic framework of selected areas in the Twin Platte and Central Platte Natural Resources Districts: Aqua Geo Frameworks, accessed September 1, 2020, at https://www.dropbox.com/s/re4rzd96e7g8t55/TPNRD-CPNRD_AEM_Hydrogeologic_Report_AGF_28Dec2017_v1.pdf?dl=0.

Carney, C.P., 2008, Groundwater flow model of the eastern model unit of the Nebraska Cooperative Hydrology Study (COHYST) area: Cooperative Hydrology Study Technical Committee, 80 p., accessed September 1, 2017, at http://cohyst.nebraska.gov/adobe/dc012CMU_GFMR_081224.pdf.

Center for Advanced Land Management Information Technologies, 2010, 2005 Land use mapping: Lincoln, University of Nebraska-Lincoln Center for Advanced Land Management Information Technologies, accessed February 1, 2019, at http://www.calmit.unl.edu/2005landuse.

Central Nebraska Public Power and Irrigation District, 2019, Reservoir/river data: accessed March 15, 2019, at https://www.cnppid.com/wp-content/uploads/2016/06/lakeRiverData.html.

Central Platte Natural Resources District, 2019, Groundwater Quantity Management Program: accessed September 1, 2019, at http://cpnrd.org/groundwater-quantity/.

Central Platte Natural Resources District, 2020a, Groundwater management plan rules and regulations: Central Platte Natural Resources District, 68 p., accessed September 1, 2020, at http://cpnrd.org/wp-content/uploads/2018/10/GWMP-RR-September2018.pdf.

Central Platte Natural Resources District, 2020b, Integrated management plan jointly developed by the Central Platte Natural Resources District and the Nebraska Department of Natural Resources: Central Platte Natural Resources District, 102 p., accessed September 1, 2020, at http://cpnrd.org/wp-content/uploads/2019/12/CPNRD-IMP-final.pdf.

Condor Team, 2012, Condor version 7.6.6 manual: Madison, Wisc., University of Wisconsin, 1003 p.

Cooperative Hydrology Study, 2017, COHYST 2010—A total water budget approach to integrated water management in the Platte River Nebraska—2017 documentation of revised integrated model: Cooperative Hydrology Study, 1795 p., accessed June 2017 at https://cohyst.nebraska.gov/#md.

Conservation and Survey Division, 1998, The groundwater atlas of Nebraska: Institute of Agriculture and Natural Resources, University of Nebraska-Lincoln, Resource Atlas No. 4a/1998, 44 p.

Conservation and Survey Division, 2019, Topographic regions—Geology related GIS data: Institute of Agriculture and Natural Resources, University of Nebraska-Lincoln, , accessed February 15, 2019, at http://snr.unl.edu/data/geographygis/geology.aspx.

Dappen, P., Ratcliffe, I., and Robbins, C., 2007, Delineation of 2005 land use patterns for the State of Nebraska Department of Natural Resources: University of Nebraska-Lincoln Center for Advanced Land Management Information Technologies, 80 p., accessed February 1, 2018, at https://calmit.unl.edu/pdf/2005_Landuse_FinalReport.pdf.

Darton, N.H., 1898, Underground waters of a portion of southeastern Nebraska: U.S. Geological Survey Water Supply and Irrigation Paper 12, 56 p., accessed September 1, 2019, at https://doi.org/10.3133/wsp12.

Darton, N.H., 1905, Preliminary report on the geology and underground water resources of the central Great Plains. U.S. Geological Survey Professional Paper 32, 433 p., accessed September 1, 2019, at https://doi.org/10.3133/pp32.

Dieter, C.A., Maupin, M.A., Caldwell, R.R., Harris, M.A., Ivahnenko, T.I., Lovelace, J.K., Barber, N.L., and Linsey, K.S., 2018, Estimated use of water in the United States in 2015: U.S. Geological Survey Circular 1441, 65 p. [Supersedes USGS Open-File Report 2017–1131], accessed September 2019 at https://doi.org/10.3133/cir1441.

Doherty, J.E., 2005, PEST, model independent parameter estimation—User manual (5th ed.): Brisbane, Australia, Watermark Numerical Computing, accessed July 26, 2011, at https://pesthomepage.org/.

Doherty, J.E., Hunt, R.J., and Tonkin, M.J., 2010a, Approaches to highly parameterized inversion: A guide to using PEST for model-parameter and predictive-uncertainty analysis: U.S. Geological Survey Scientific Investigations Report 2010–5211, 71 p. [Also available at https://doi.org/10.3133/sir20105211.]

Doherty, J.E., 2018, PEST Programs—Groundwater utilities: accessed January 2018 at https://pesthomepage.org/programs.

Doherty, J.E., Fienen, M.N., and Hunt, R.J., 2010b, Approaches to highly parameterized inversion—Pilot-point theory, guidelines, and research directions: U.S. Geological Survey Scientific Investigations Report 2010–5168, 36 p.

Doherty, J., and Hunt, R.J., 2009, Two statistics for evaluating parameter identifiability and error reduction: Journal of Hydrology, v. 366, no. 1-4, p. 119–127. [Also available at https://doi.org/10.1016/j.jhydrol.2008.12.018.]

Doherty, J.E., and Hunt, R.J., 2010, Approaches to highly parameterized inversion—A guide to using PEST for groundwater-model calibration: U.S. Geological Survey Scientific Investigations Report 2010–5169, 59 p. [Also available at https://doi.org/10.3133/sir20105169.]

Doherty, J., 2015, Calibration and uncertainty analysis for complex environmental models: Brisbane, Australia, Watermark Numerical Computing, 227 p.

Domenico, P.A., and Schwartz, F.W., 1990, Physical and chemical hydrogeology: New York, John Wiley & Sons, 824 p.

Exner, M.E., Perea-Estrada, H., and Spalding, R.F., 2010, Long-term response of groundwater nitrate concentrations to management regulations in Nebraska's Central Platte Valley: The Scientific World Journal, v. 10, p. 286–297. [Also available at https://doi.org/10.1100/tsw.2010.25.]

Fetter, C.W., 2001, Applied hydrogeology (4th ed.): Upper Saddle River, N.J., Prentice Hall, 624 p.

Fenneman, N.M., 1931, Physiography of western United States: New York, Mcgraw-Hill, Inc., 11 p.

Fienen, M.N., Doherty, J.E., Hunt, R.J., and Reeves, H.W., 2010, Using prediction uncertainty analysis to design hydrologic monitoring networks—Example applications from the Great Lakes water availability pilot project: U.S. Geological Survey Scientific Investigations Report 2010–5159, 44 p. [Also available at https://doi.org/10.3133/sir20105159.]

Google, 2018, Imagery: Google Earth, April 19, 2017, accessed October 1, 2018

Gutentag, E.D., Heimes, F.J., Krothe, N.C., Luckey, R.R., and Weeks, J.B., 1984, Geohydrology of the High Plains aquifer in parts of Colorado, Kansas, Nebraska, New Mexico, Oklahoma, South Dakota, Texas, and Wyoming: U.S. Geological Survey Professional Paper 1400–B, 63 p. [Also available at https://doi.org/10.3133/pp1400B.]

Hall, B.M., and Rus, D.L., 2013, Comparison of water consumption in two riparian vegetation communities along the central Platte River, Nebraska, 2008–09 and 2011: U.S. Geological Survey Scientific Investigations Report 2013–5203, 28 p., accessed September 1, 2018, at https://doi.org/10.3133/sir20135203.

Hanson, R.T., Boyce, S.E., Schmid, W., Hughes, J.D., Mehl, S.M., and Leake, S.A., Maddock, T., III, and Niswonger, R.G., 2014a, One-Water Hydrologic Flow Model (MODFLOW–OWHM): U.S. Geological Survey Techniques and Methods, book 6, chap. A51, 120 p., accessed November 2016 at https://doi.org/10.3133/tm6A51.

Hanson, R.T., Schmid, W., Faunt, C.C., Lear, J., and Lockwood, B., 2014b, Integrated hydrologic model of Pajaro Valley, Santa Cruz and Monterey Counties, California: U.S. Geological Survey Scientific Investigations Report 2014–5111, 166 p., accessed November 2017 at https://doi.org/10.3133/sir20145111.

Hanson, R.T., Ritchie, A.B., Boyce, S.E., Ferguson, I., Galanter, A.E., Flint, L.E., and Henson, W.R., 2018, Rio Grande transboundary integrated hydrologic model and water-availability analysis, New Mexico and Texas, United States, and Northern Chihuahua, Mexico: U.S Geological Survey Open-File Report 2018–1091, 185 p., accessed September 2020 Year at https://doi.org/10.3133/ofr20181091.

Harbaugh, A.W., 2005, MODFLOW-2005—The U.S. Geological Survey modular ground-water model—The Ground-Water Flow Process: U.S. Geological Survey Techniques and Methods, book 6, chap. A16, [variously paged]. [Also available at https://doi.org/10.3133/tm6A16.]

Harbaugh, A.W., Banta, E.R., Hill, M.C., and McDonald, M.G., 2000, MODFLOW–2000, the U.S. Geological Survey modular ground-water model—User guide to modularization concepts and the ground-water flow process: U.S. Geological Survey Open-File Report 00–92, 121 p. [Also available at https://doi.org/10.3133/ofr200092.]

High Plains Regional Climate Center, 2018, National Weather Service surface observations and automated weather data network data: Lincoln, Nebr., University of Nebraska, digital data, accessed May 11, 2018, at http://www.hprcc.unl.edu.

Hill, M.C., and Tiedeman, C.R., 2007, Effective groundwater model calibration—With analysis of data, sensitivities, predictions, and uncertainty: New York, Wiley and Sons, 455 p. [Also available at https://doi.org/10.1002/0470041080.]

Hiller, T.L., Powell, J.A., McCoy, T.D., and Lusk, J.J., 2009, Long-term agricultural land-use trends in Nebraska, 1866–2007: Great Plains Research, v. 19, p. 225–237. [Also available at https://digitalcommons.unl.edu/cgi/viewcontent.cgi?article=1348&context=natrespapers.]

Houston, N.A., Gonzales-Bradford, S.L., Flynn, A.T., Qi, S.L., Peterson, S.M., Stanton, J.S., Ryter, D.W., Sohl, T.L., and Senay, G.B., 2013, Geodatabase compilation of hydrogeologic, remote sensing, and water-budget-component data for the High Plains aquifer, 2011: U.S. Geological Survey Data Series 777, 12 p. [Also available at https://doi.org/10.3133/ds777.]

Irmak, S., 2014, Potential reference and actual evapotranspiration trends across the U.S. High Plains in relation to irrigation development and climate change: University of Nebraska-Lincoln Extension, EC712, 12 p. [Also available at https://extensionpublications.unl.edu/assets/pdf/ec712.pdf.]

Irmak, S., Odhiambo, L.O., Krnaz, W.L., and Eisenhauer, D.E., 2011, Irrigation efficiency and uniformity, and crop water use efficiency: University of Nebraska-Lincoln Extension, EC732, 8 p. [Also available at https://digitalcommons.unl.edu/biosysengfacpub/451/.]

Irmak, S., and Rudnick, D.R., 2014, Corn soil-water extraction and effective rooting depth in a silt-loam soil: University of Nebraska-Lincoln Extension, NebGuide G2245, accessed September 1, 2019, at https://extensionpublications.unl.edu/assets/pdf/g2245.pdf.

Irmak, S. and Skaggs, K.E., 2011, Variability of reference evapotranspiration across Nebraska: University of Nebraska-Lincoln Extension, EC 733, 6 p. [Also available at https://extensionpublications.unl.edu/assets/pdf/ec733.pdf.]

Irmak, S., Sharma, V., and Koffi, D., 2016 Winter wheat (*Triticum aestivum* L.) evapotranspiration (crop water use) and crop coefficients: University of Nebraska-Lincoln-Extension, EC3005, accessed September 1, 2019, at https://extensionpublications.unl.edu/assets/pdf/ec3005.pdf.

Irons, T.P., Hobza, C.M., Steele, G.V., Abraham, J.D., Cannia, J.C., and Woodward, D.D., 2012, Quantification of aquifer properties with surface nuclear magnetic resonance in the Platte River valley, central Nebraska, using a novel inversion method: U.S. Geological Survey Scientific Investigations Report 2012–5189, 50 p. [Also available at https://doi.org/10.3133/sir20125189.]

Johnson, B., Thompson, C., Giri, A., and Van NewKirk, S., 2011, Nebraska irrigation fact sheet: University of Nebraska-Lincoln, Department of Agricultural Economics, Report no. 190, 6 p., accessed April 2021 at https://agecon.unl.edu/a9fcd902-4da9-4c3f-9e04-c8b56a9b22c7.pdf.

Kang, S., Gu, B., Du, T., and Zhang, J., 2003, Crop coefficient and ration of transpiration to evapotranspiration of winter wheat and maize in a semi-humid region: Agricultural Water Management, v. 59, no. 3, p. 239–254. [Also available at https://doi.org/10.1016/S0378-3774(02)00150-6.]

Kimball, B., Boote, K., Hatfield, J., Ahuja, L.R., Stockle, C., Archontoulis, S.V., Baron, C., Basso, B., Bertuzzi, P., Chen, M., Constantin, J., Derying, D., Dumont, B., Durand, J.-L., Ewert, F., Gaiser, T., Gayler, S., Griffis, T., Hoffmann, M., Jiang, Q., Kim, S.-H., Lizaso, J., Mouin, S., Nendel, C., Parker, P., Palosuo, T., Priesack, E., Zhiming Qi, Z., Srivastava, A., Stella, T., Tao, F., Thorp, K., Timlin, D., Twine, T., Webber, H., Willaume, M., and Williams, K., 2016, Prediction of evapotranspiration and yields of maize—An inter-comparison among 29 maize models: Phoenix, Arizona, ASA-CSSA-SSSA annual meeting, November 6–9, 2016, 4 p. [Also available at https://www.researchgate.net/publication/347439031_Prediction_of_Evapotranspiration_and_Yields_of_Maize_Phase_1_and_2_of_an_Inter-Comparison_Among_42_Maize_Models_and_Future_Plans.]

Kollet, S.F., and Zlotnik, V.A., 2003, Stream depletion predictions using pumping test data from a heterogeneous stream–aquifer system (a case study from the Great Plains, USA): Journal of Hydrology, v. 281, no. 1-2, p. 96–114, accessed September 1, 2020, at https://doi.org/10.1016/S0022-1694(03)00203-8.

Köppen, W., 1936, Das geographische System der Klimate, *in* Köppen, W., and Geiger, R., eds., Handbuch der Klimatologie: Berlin, Verlag von Gebrüder Borntraeger, v. 1, Part C, p. 1–44.

Kranz, W.L., Irmak, S., van Donk, S.J., Yonts, C.D., and Martin, D.L., 2008, Irrigation management for corn: University of Nebraska-Lincoln Extension, Institute of Agriculture and Natural Resources, NebGuide G1850, 4 p. [Also available at https://extensionpublications.unl.edu/assets/html/g1850/build/g1850.htm.]

Lappala, E.G., Emery, P.A., and Otradovsky, F.J., 1979. Simulated changes in ground-water levels and streamflow resulting from future development (1970 to 2020) in the Platte River basin: U.S. Geological Survey Water-Resources Investigations Report 79–26, 82 p., accessed September 1, 2018, at https://doi.org/10.3133/wri7926.

Lauffenburger, Z.H., Gurdak, J.J., Hobza, C., and Woodward, D., 2018, Irrigated agriculture and future climate change effects on groundwater recharge, northern High Plains aquifer, USA: Agricultural Water Management, v. 204, 69–80 p., accessed September 1, 2019, at https://digitalcommons.unl.edu/cgi/viewcontent.cgi?article=2094&context=usgsstaffpub.

Luckey, R.R., and Cannia, J.C., 2006, Groundwater flow model of the western model unit of the Nebraska Cooperative Hydrology Study (COHYST) area: Cooperative Hydrology Study Technical Committee, p. 63, accessed September 1, 2017, at http://cohyst.nebraska.gov/adobe/dc012WMU_GFMR_060519.pdf.

McKay, L., Bondelid, T., Dewald, T., Johnston, J., Moore, R., and Rea, A., 2012, NHDPlus Version 2—User guide: Horizon Systems Corporation Web page, accessed November 15, 2014, at http://www.horizon-systems.com/NHDPlus/NHDPlusV2_documentation.php.

McGuire, V.L., 2017, Water-level and recoverable water in storage changes, High Plains aquifer, predevelopment to 2015 and 2013–15: U.S. Geological Survey Scientific Investigations Report 2017–5040, 14 p., accessed February 2019 at https://doi.org/10.3133/sir20175040.

McGuire, V.L., Lund, K.D., and Densmore, B.K., 2012, Saturated thickness and water in storage in the High Plains aquifer, 2009, and water-level changes and changes in water in storage in the High Plains aquifer, 1980 to 1995, 1995 to 2000, 2000 to 2005, and 2005 to 2009: U.S. Geological Survey Scientific Investigations Report 2012–5177, 28 p., accessed February 1, 2019, at https://doi.org/10.3133/sir20125177.

Merritt, M.L., and Konikow, L.F., 2000, Documentation of a computer program to simulate lake-aquifer interaction using the MODFLOW Ground-Water Flow Model and the MOC3D Solute-Transport Model: U.S. Geological Survey Water-Resources Investigations Report 00–4167, 146 p.

National Climatic Data Center, 2019, Climate data online, weather observation station daily summaries: Asheville, N.C., National Climatic Data Center, digital data, accessed April 2, 2019, at https://www.ncdc.noaa.gov/cdo-web/.

Nebraska Association of Resources Districts, 2020, Natural Resources District information: accessed September 1, 2020, at https://www.nrdnet.org/nrds/about-nrds.

Nebraska Department of Natural Resources, 2017, Registered groundwater wells data retrieval: Nebraska Department of Natural Resources digital data, accessed May 1, 2017, at https://nednr.nebraska.gov/dynamic/Wells/Wells.

Nebraska Department of Natural Resources, 2018, Digital elevation model data retrieval: Nebraska Department of Natural Resources digital data, accessed September 1, 2018, at ftp://dnrftp.dnr.ne.gov/Pub/data/dems

Nebraska Department of Natural Resources, 2019, Stream gaging data retrieval: Nebraska Department of Natural Resources digital data, accessed March 15, 2019, at https://nednr.nebraska.gov/RealTime/.

Nebraska Department of Natural Resources, 2020, County Boundaries retrieval: Nebraska Department of Natural Resources digital data, accessed January 2, 2020, at https://www.nebraskamap.gov/datasets/county-boundaries/explore?location=41.467718%2C-99.634627%2C7.73

Nebraska Legislature, 1969, Legislative Bill 1357—Combine Nebraska's 154 special purpose entities into 24 Natural Resources Districts by July, 1972: accessed September 1, 2020, at https://www.nrdnet.org/news/01-04-2022/natural-resources-districts-reflect-50-years.

Nebraska Legislature, 2004, Legislative Bill 962—Ground water management plan; Nebraska Legislature, Statute 46-709, accessed September 1, 2020, at https://www.nebraskalegislature.gov/laws/statutes.php?statute=46-709.

Nebraska Legislature, 2014, Legislative Bill 513—Action to control or prevent runoff of water; natural resources district; rules and regulations; power to issue cease and desist orders; notice; hearing., Nebraska Legislature, Statute 46-708, accessed September 1, 2020, at https://www.nebraskalegislature.gov/laws/statutes.php?statute=46-708.

Nebraska Agricultural Water Management Network, 2018, Growth stage charts: University of Nebraska-Lincoln. [Also available at https://nawmn.unl.edu/GrowthStageData.]

Niswonger, R.G., Panday, S., and Ibaraki, M., 2011, MODFLOW–NWT, a Newton formulation for MODFLOW–2005: U.S. Geological Survey Techniques and Methods, book 6, chap. A37, 44 p. [Also available at https://doi.org/10.3133/tm6A37.]

Niswonger, R.G., and Prudic, D.E., 2005, Documentation of the Streamflow-Routing (SFR2) Package to include unsaturated flow beneath streams—A modification to SFR1: U.S. Geological Survey Techniques and Methods, book 6, chap. A13, 47 p. [Also available at https://doi.org/10.3133/tm6A13.]

Niswonger, R.G., Prudic, D.E., and Regan, R.S., 2006, Documentation of the Unsaturated-Zone Flow (UZF1) Package for modeling unsaturated flow between the land surface and the water table with MODFLOW-2005: U.S. Geological Survey Techniques and Methods, book 6, chap. A19, 62 p. [Also available at https://doi.org/10.3133/tm6A19.]

Peckenpaugh, J.M., and Dugan, J.T., 1983, Hydrology of parts of the Central Platte and Lower Loup Natural Resources Districts, Nebraska: U.S. Geological Survey Water-Resources Investigations Report 83–4219, 125 p. [Also available at https://pubs.usgs.gov/wri/1983/4219/report.pdf.]

Peckenpaugh, J.M., Dugan, J.T., Kern, R.A., and Schroeder, W.J., 1987, Hydrogeology of the Tri-Basin and parts of the Lower Republican and Central Platte Natural Resources Districts, Nebraska: U.S. Geological Survey Water-Resources Investigations Report 87–4176, 117 p. [Also available at https://pubs.usgs.gov/wri/1987/4176/report.pdf.]

Peterson, S.M., 2009, Groundwater flow model of the eastern model unit of the Nebraska Cooperative Hydrology Study (COHYST) area: Lincoln, Nebraska Department of Natural Resources, 80 p., accessed June 21, 2010, at http://cohyst.dnr.ne.gov/adobe/dc012EMU_GFMR_090507.pdf.

Peterson, S.M., and Carney, C.P., 2002, Estimated ground-water discharge to streams from the High Plains Aquifer in the Eastern Model Unit of the COHYST study area for the period prior to major groundwater irrigation: Cooperative Hydrology Study, 25 p., accessed September 1, 2018, at http://cohyst.nebraska.gov/adobe/dc012EMU_baseflw_02.pdf.

Peterson, S.M., Flynn, A.T., and Traylor, J.P., 2016, Groundwater-flow model of the northern High Plains aquifer in Colorado, Kansas, Nebraska, South Dakota, and Wyoming: U.S. Geological Survey Scientific Investigations Report 2016–5153, 88 p., accessed December 3, 2019, at https://doi.org/10.3133/sir20165153.

Peterson, S.M., Traylor, J.P., and Guira, M., 2020, MODFLOW–NWT groundwater flow model used to evaluate groundwater availability with five forecast scenarios in the Northern High Plains aquifer in Colorado, Kansas, Nebraska, South Dakota, and Wyoming: U.S. Geological Survey data release, accessed September 2020 at https://doi.org/10.5066/P92UNY4F.

Reitz, M., Sanford, W.E., Senay, G.B., and Cazenas, J., 2017, Annual estimates of recharge, quick-flow runoff, and evapotranspiration for the contiguous U.S. using empirical regression equations: Journal of the American Water Resources Association, v. 53, no. 4, p. 961–983, accessed April 2022 at https://onlinelibrary.wiley.com/doi/10.1111/1752-1688.12546.

Schmid, W., and Hanson, R.T., 2009, The farm process version 2 (FMP2) for MODFLOW-2005—Modifications and upgrades to FMP1: U.S. Geological Survey Techniques and Methods, book 6, chap. A32, 102 p. [Also available at http://doi.org/10.3133/tm6A32.]

Schreuder, W.A., 2009, BeoPEST programmer's documentation: Principia Mathematica, Inc., v. 1, 12 p., accessed September 2019 at https://www.prinmath.com/pest/BeoPESTprog.pdf

Steele, G.V., Gurdak, J.J., and Hobza, C.M., 2014, Water movement through the unsaturated zone of the High Plains Aquifer in the Central Platte Natural Resources District, Nebraska, 2008–12: U.S. Geological Survey Scientific Investigations Report 2014–5008, 51 p., plus tables and app., accessed September 2020 at https://doi.org/10.3133/sir20145008.

Summerside, S.E., Dreeszen, V.H., Hartung, S.L., Khisty, M.J., and Szilagyi, J., 2001, Update and revision of regional 1x2 degree water-table configuration maps for the state of Nebraska (OFR-73): University of Nebraska-Lincoln, 9 p.

Szilágyi, J., and Kovacs, A., 2010, Complementary-relationship-based evapotranspiration mapping (CREMAP) technique for Hungary: Periodica Polytechnica, Civil Engineering, v. 54, no. 2, p. 95–100. [Also available at https://doi.org/10.3311/pp.ci.2010-2.04.]

Traylor, J.P., 2023, MODFLOW-One-Water model used to support the Central Platte Natural Resources District Groundwater Management Plan, central Nebraska: U.S. Geological Survey data release, accessed March 2023 at https://doi.org/10.5066/P9G3Q5XK.

University of Nebraska-Lincoln, 2018, Soils of Nebraska: University of Nebraska-Lincoln School of Natural Resources Soil GIS Data, accessed September 1, 2018, at http://snr.unl.edu/data/geographygis/soil.aspx.

University of Nebraska-Lincoln, 2020, Regulations and policies: Natural Resources Districts, Institute of Agriculture and Natural Resources, UNL Water, 1 p., accessed September 1, 2020, at https://water.unl.edu/article/agricultural-irrigation/regulations-policies.

U.S. Census Bureau, 2012, Nebraska—2010—Summary population and housing characteristics: U.S. Census Bureau, access September 1, 2018, at https://www.census.gov/prod/cen2010/cph-1-29.pdf.

U.S. Department of Agriculture, 1997, Usual planting and harvesting dates for U.S. field crops—December 1997: National Agriculture Statistics Service Handbook 628, 51 p., accessed November 2018 at https://downloads.usda.library.cornell.edu/usda-esmis/files/vm40xr56k/9p290c614/kw52jb531/planting-12-05-1997.pdf.]

U.S. Department of Agriculture, 2016, Irrigation guide, Part 652: accessed November 2018 at https://www.nrcs.usda.gov/Internet/FSE_DOCUMENTS/nrcs141p2_017640.pdf.

U.S. Department of Agriculture, 2019, Quick stats: National Agricultural Statistics Service, accessed on February 1, 2019, at https://quickstats.nass.usda.gov/results/5F332E2C-25E0-3DF5-B0A1-76ECCC3B8660.

U.S. Geological Survey, 2017, USGS water data for the Nation: U.S. Geological Survey National Water Information System database, accessed January 2017 at https://doi.org/10.5066/F7P55KJN.

U.S. Geological Survey, 2018, National Elevation Dataset: U.S. Geological Survey, accessed September 1, 2018, at https://ned.usgs.gov/.

U.S. Geological Survey, 2020, Advanced research computing—USGS Denali Supercomputer: U.S. Geological Survey, accessed September 2020 at https://doi.org/10.5066/P9PSW367.

Weaver, J.E., and Bruner, W.E., 1948, Prairies and pastures of the Dissected Loess Plains of central Nebraska: Ecological Monographs, v. 18, no. 4, p. 507–549, accessed February 2019 at https://doi.org/10.2307/1948587.

White, J.T., Fienen, M.N., Doherty, J.E., 2016, pyEMU—A python framework for environmental model uncertainty analysis, version .07: U.S. Geological Survey software release, accessed October 2018 at https://doi.org/10.5066/F75D8Q01.

White, J.T., Welter, D., and Doherty, J.E., 2019, PEST++, ver. 4.2.1: 180 p., accessed March 1, 2020, at https://github.com/usgs/pestpp/tree/master/documentation.

Yang, L., Jin, S., Danielson, P., Homer, C., Gass, L., Bender, S.M., Case, A., Costello, C., Dewitz, J., Fry, J., Funk, M., Grannemann, B., Liknes, G.S., Rigge, M., and Xian, G., 2018, A new generation of the United States National Land Cover Database—Requirements, research priorities, design, and implementation strategies: ISPRS Journal of Photogrammetry and Remote Sensing, v. 146, p. 108–123, accessed September 1, 2018, at https://doi.org/10.1016/j.isprsjprs.2018.09.006.

Appendix 1. Canal Diversions, Final Farm Process Parameter Values, and Preliminary Parameter Sensitivities

Tables 1.1–1.3 are available for download at https://doi.org/10.3133/sir20235024 (Traylor, 2023).

References Cited

Traylor, J.P., 2023, MODFLOW-One-Water model used to support the Central Platte Natural Resources District Groundwater Management Plan, central Nebraska: U.S. Geological Survey data release, accessed March 2023 at https://doi.org/10.5066/P9G3Q5XK.

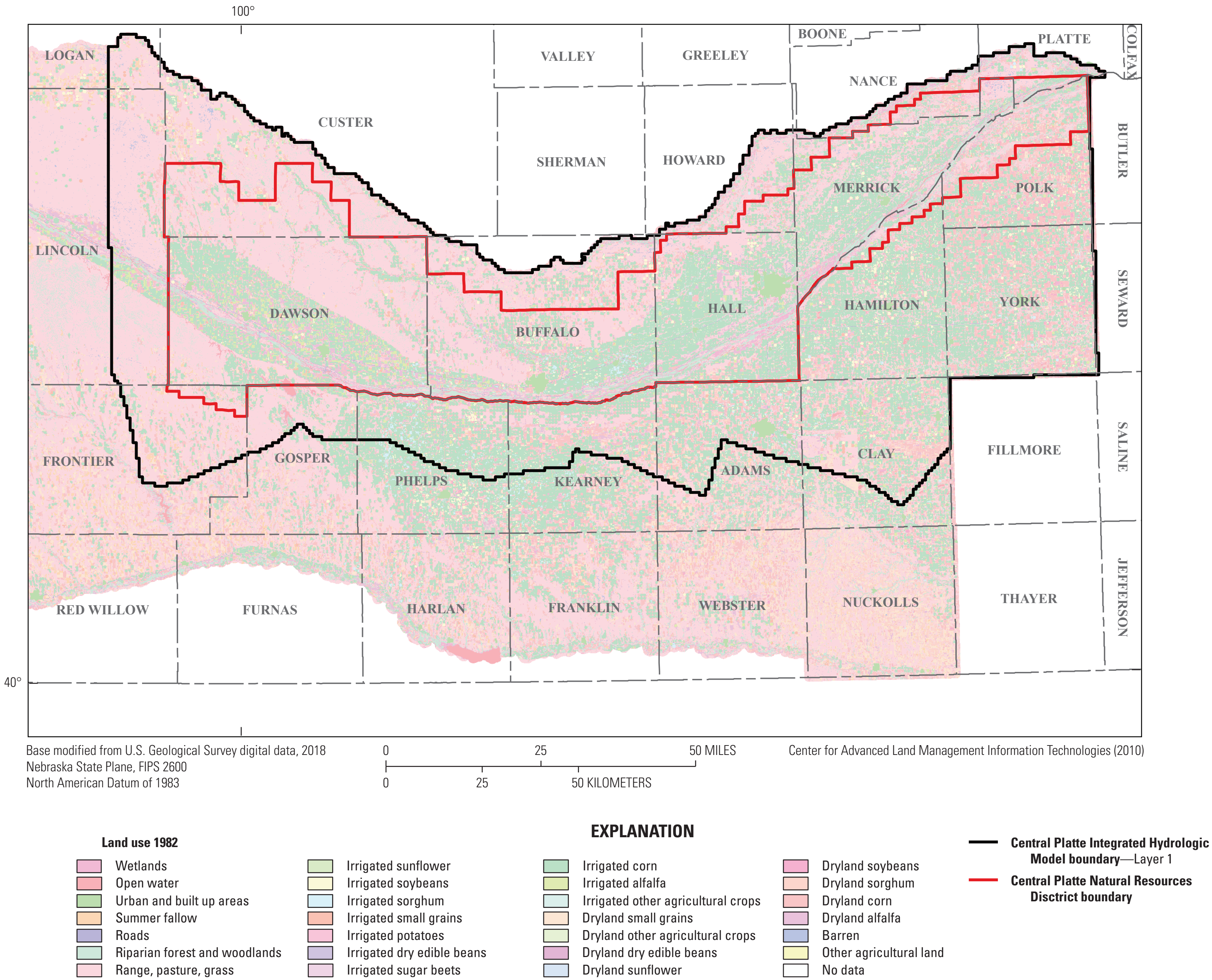

Figure 1.1. Distribution of land uses for 1982.

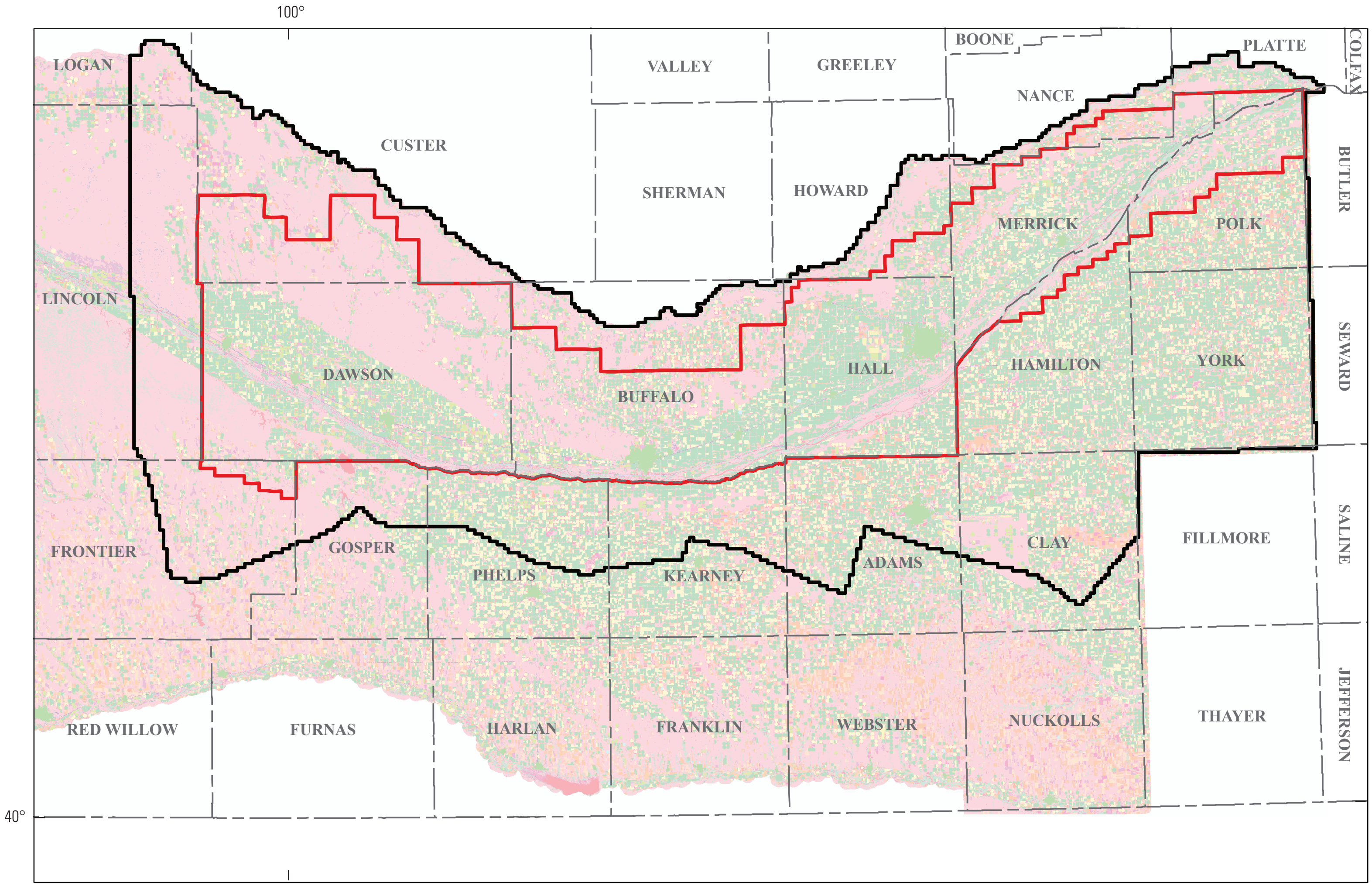

Base modified from U.S. Geological Survey digital data, 2018
Nebraska State Plane, FIPS 2600
North American Datum of 1983

0 25 50 MILES
0 25 50 KILOMETERS

Center for Advanced Land Management Information Technologies (2010)

EXPLANATION

Land use 2005

- Wetlands
- Open water
- Urban and built up areas
- Summer fallow
- Roads
- Riparian forest and woodlands
- Range, pasture, grass
- Irrigated sunflower
- Irrigated soybeans
- Irrigated sorghum
- Irrigated small grains
- Irrigated potatoes
- Irrigated dry edible beans
- Irrigated sugar beets
- Irrigated corn
- Irrigated alfalfa
- Irrigated other agricultural crops
- Dryland small grains
- Dryland other agricultural crops
- Dryland dry edible beans
- Dryland sunflower
- Dryland soybeans
- Dryland sorghum
- Dryland corn
- Dryland alfalfa
- Barren
- Other agricultural land
- No data

Central Platte Integrated Hydrologic Model boundary—Layer 1

Central Platte Natural Resources Dsictrict boundary

Figure 1.2. Distribution of land uses for 2005.

Appendix 2. Additional Calibration Statistics that Include Measured and Simulated Plots and Residual Value Distribution Histograms by Observation Group

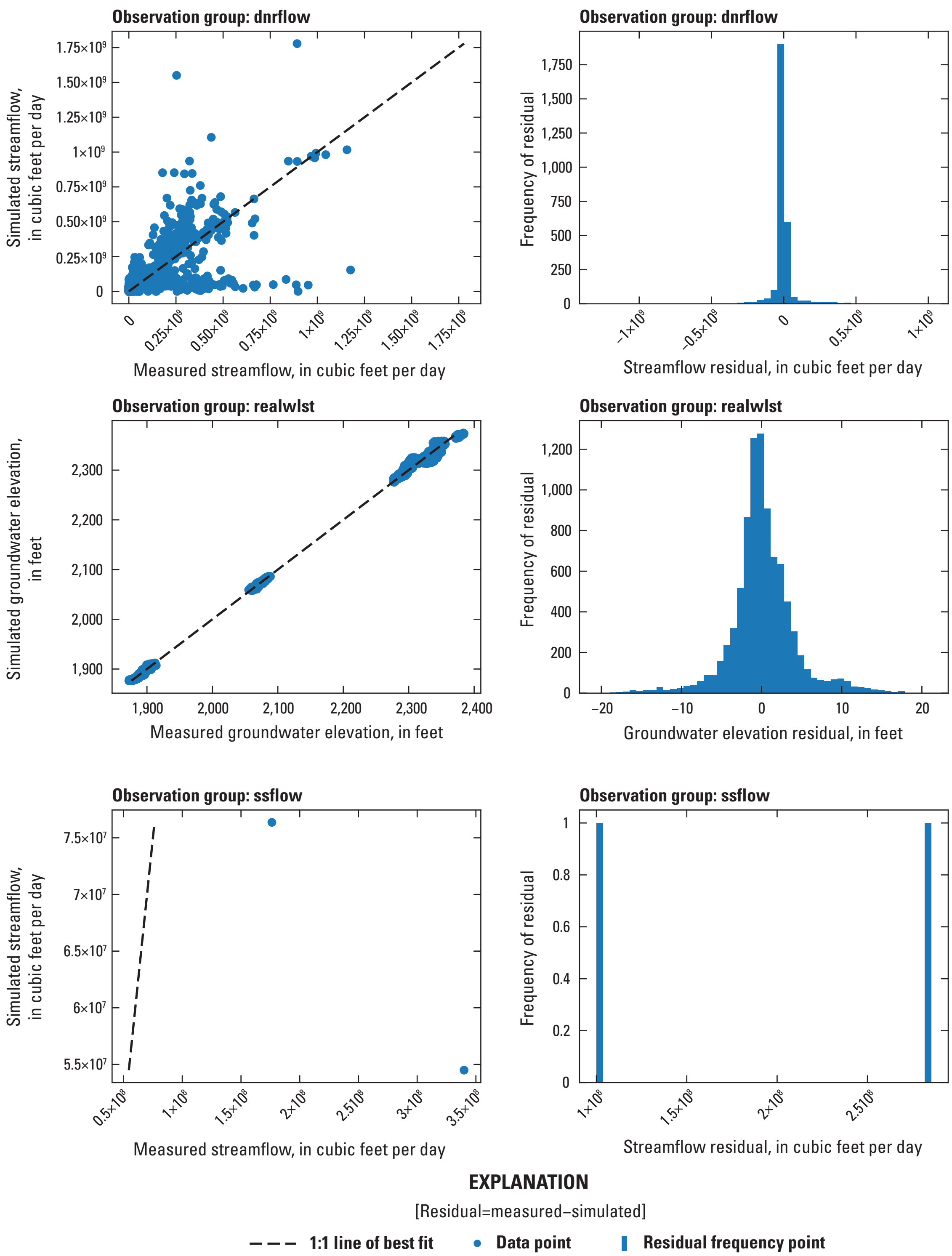

Figure 2.1. Plot of measured compared to simulated values and residual values distributions for observation groups (see table 9 for observation group definitions).

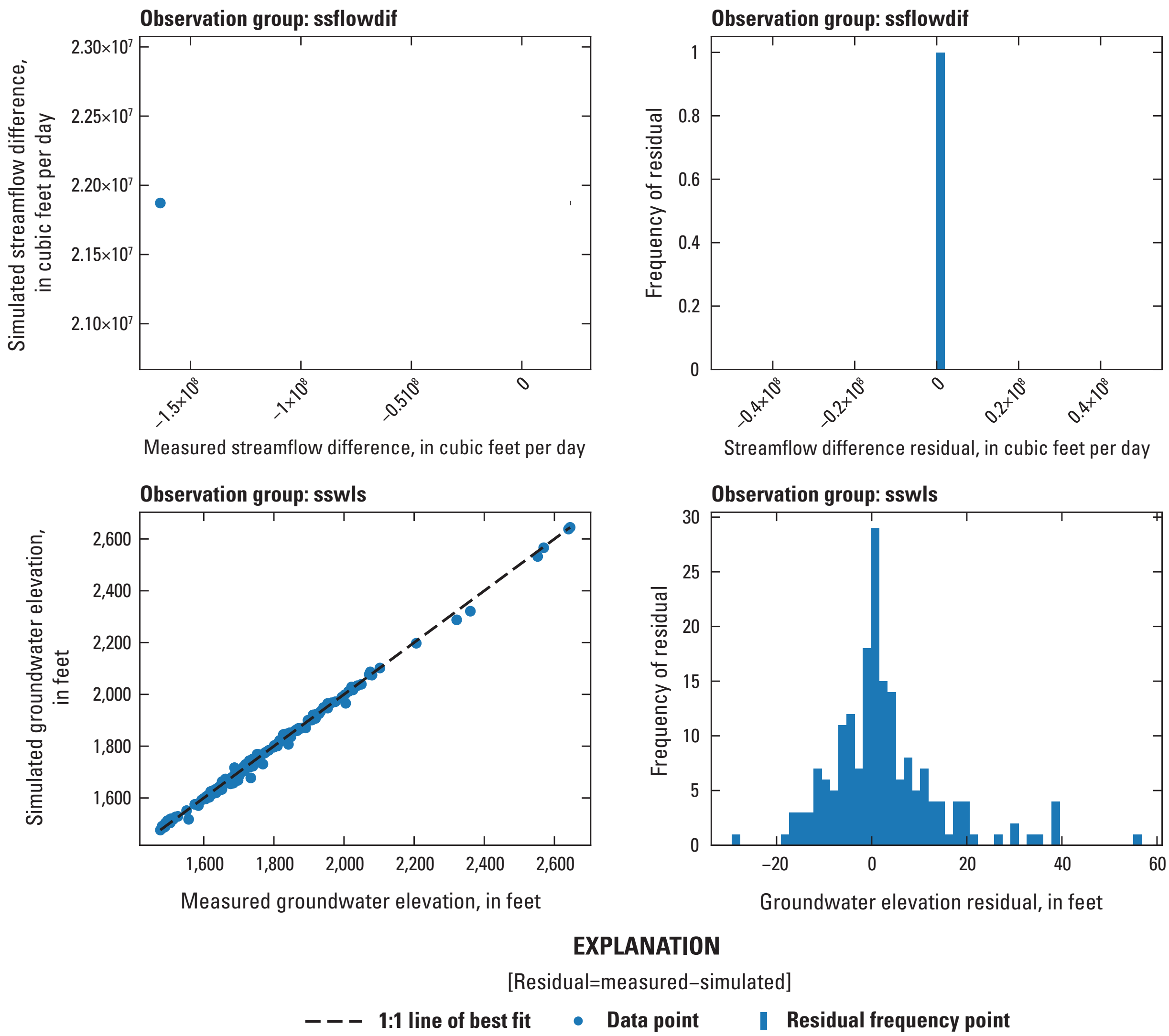

Figure 2.1.—Continued

Appendix 3. Additional Average Landscape Water and Groundwater-Flow Budget Tables for the Development Period Central Platte Integrated Hydrologic Model and Groundwater Management Areas as Volumetric Rates and Net Volumetric Rates

Tables 3.1–3.6 are available for download at https://doi.org/10.3133/sir20235024.

Appendix 4. Additional Average Landscape Water and Groundwater-Flow Budget Tables for Each Scenario of the Central Platte Integrated Hydrologic Model by Groundwater Management Area as Area Normalized Volumetric Rates and Net Volumetric Rates

Tables 4.1–4.24 are available for download at https://doi.org/10.3133/sir20235024.

Appendix 5. Additional Simulated Groundwater-Levels for Each Scenario and Groundwater Management Area

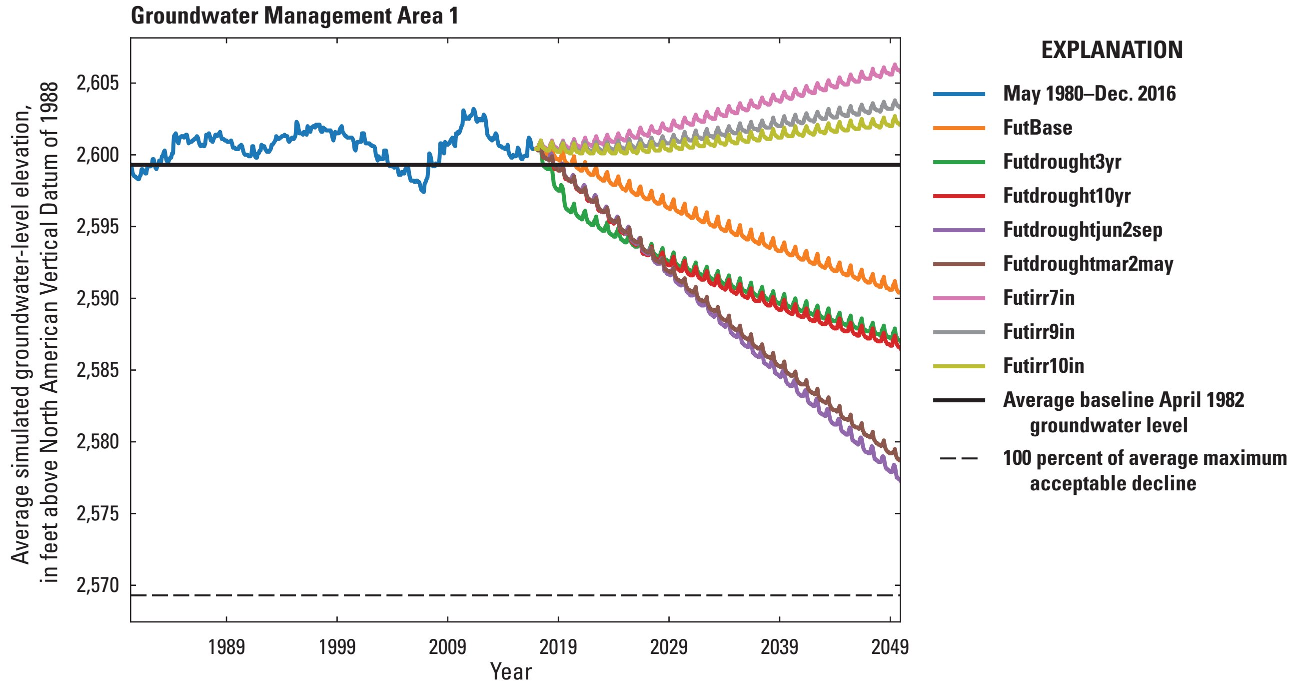

Figure 5.1. Simulated groundwater levels from May 1980 to December 2016 development period and January 2017 to December 2049 scenario period for the Central Platte Integrated Hydrologic Model in Groundwater Management Area 1.

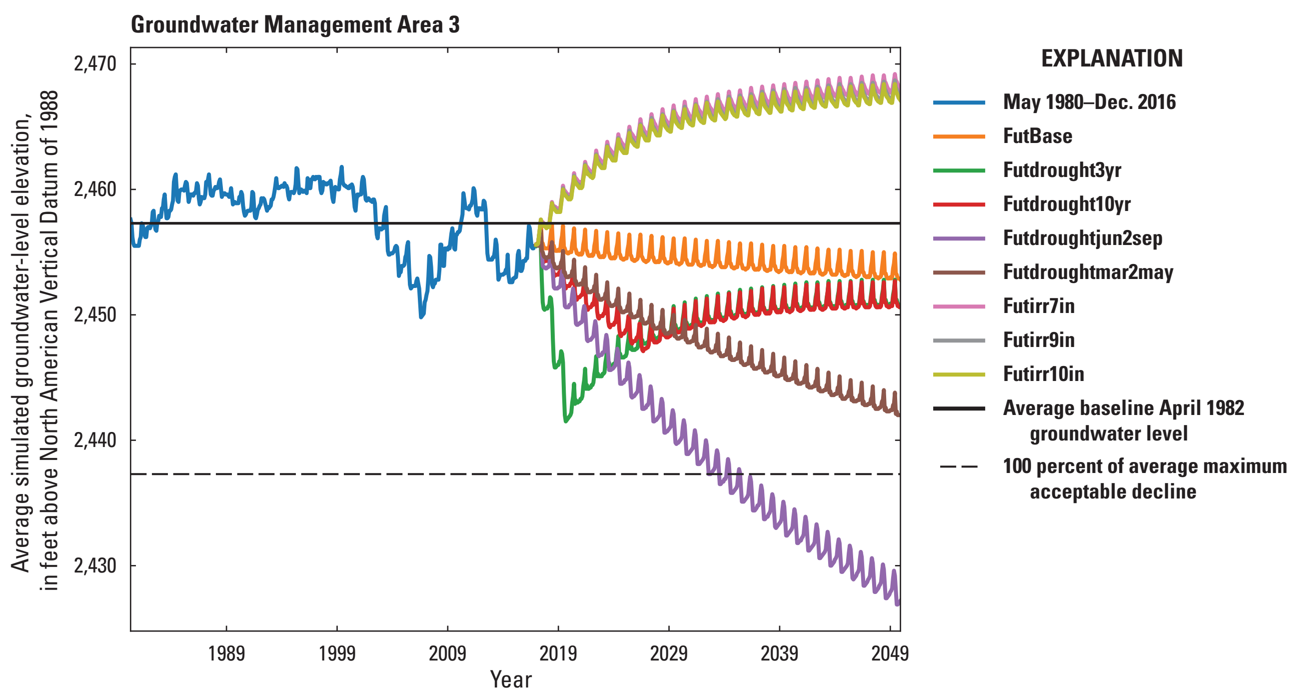

Figure 5.2. Simulated groundwater levels from May 1980 to December 2016 development period and January 2017 to December 2049 scenario period for the Central Platte Integrated Hydrologic Model in Groundwater Management Area 3.

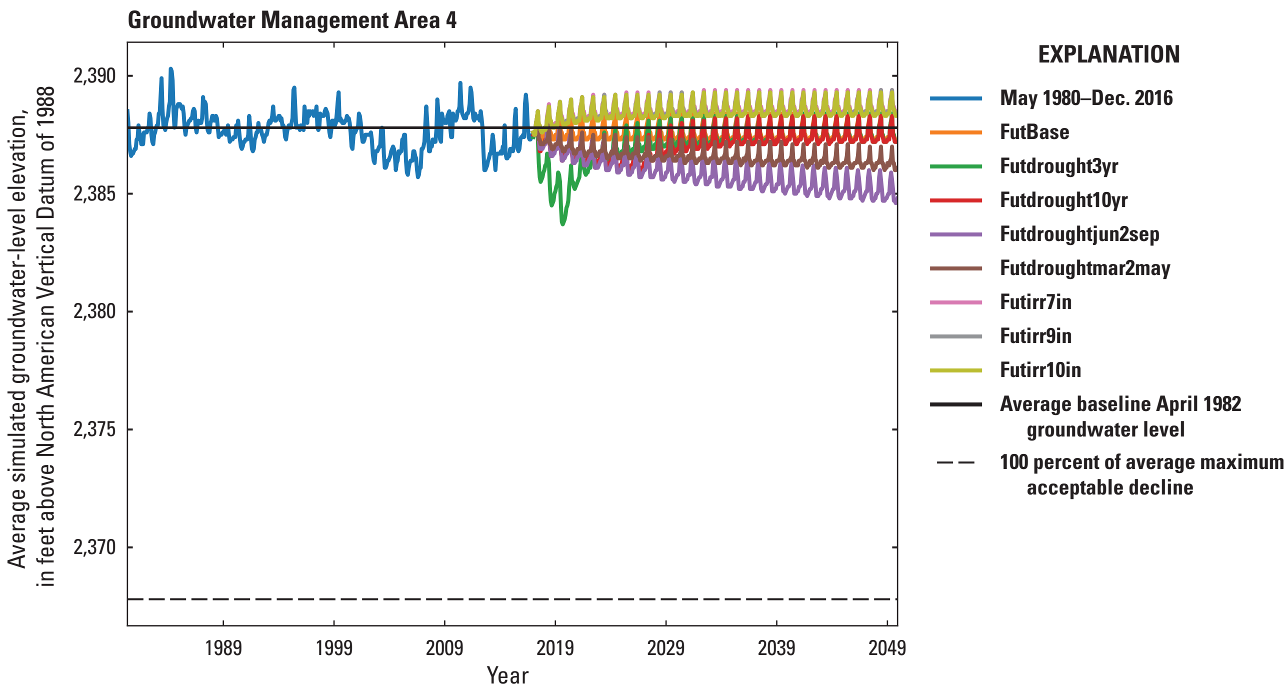

Figure 5.3. Simulated groundwater levels from May 1980 to December 2016 development period and January 2017 to December 2049 scenario period for the Central Platte Integrated Hydrologic Model in Groundwater Management Area 4.

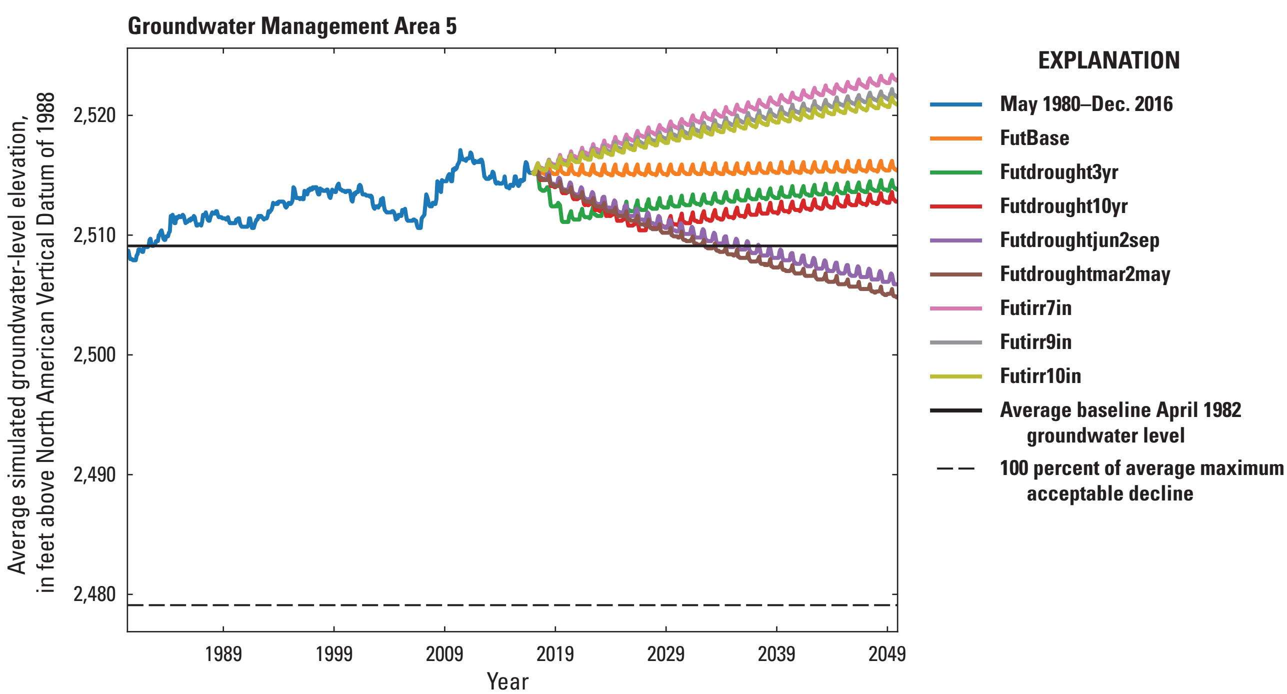

Figure 5.4. Simulated groundwater levels from May 1980 to December 2016 development period and January 2017 to December 2049 scenario period for the Central Platte Integrated Hydrologic Model in Groundwater Management Area 5.

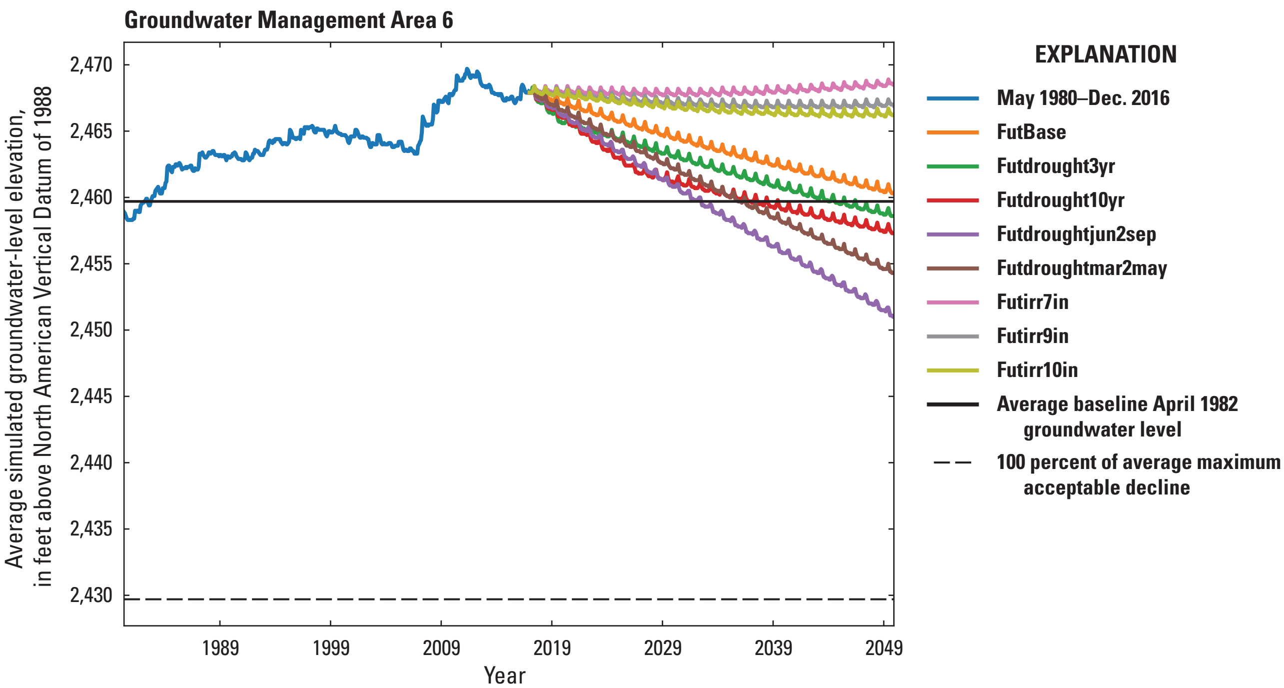

Figure 5.5. Simulated groundwater levels from May 1980 to December 2016 development period and January 2017 to December 2049 scenario period for the Central Platte Integrated Hydrologic Model in Groundwater Management Area 6.

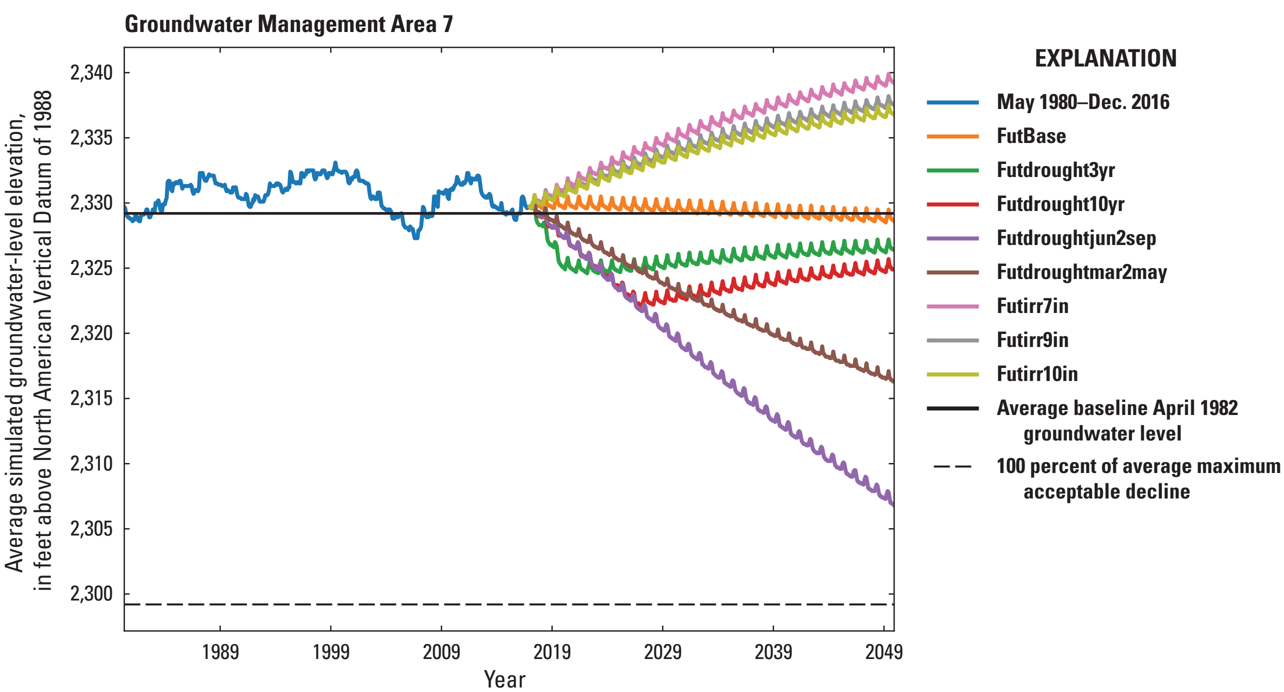

Figure 5.6. Simulated groundwater levels from May 1980 to December 2016 development period and January 2017 to December 2049 scenario period for the Central Platte Integrated Hydrologic Model in Groundwater Management Area 7.

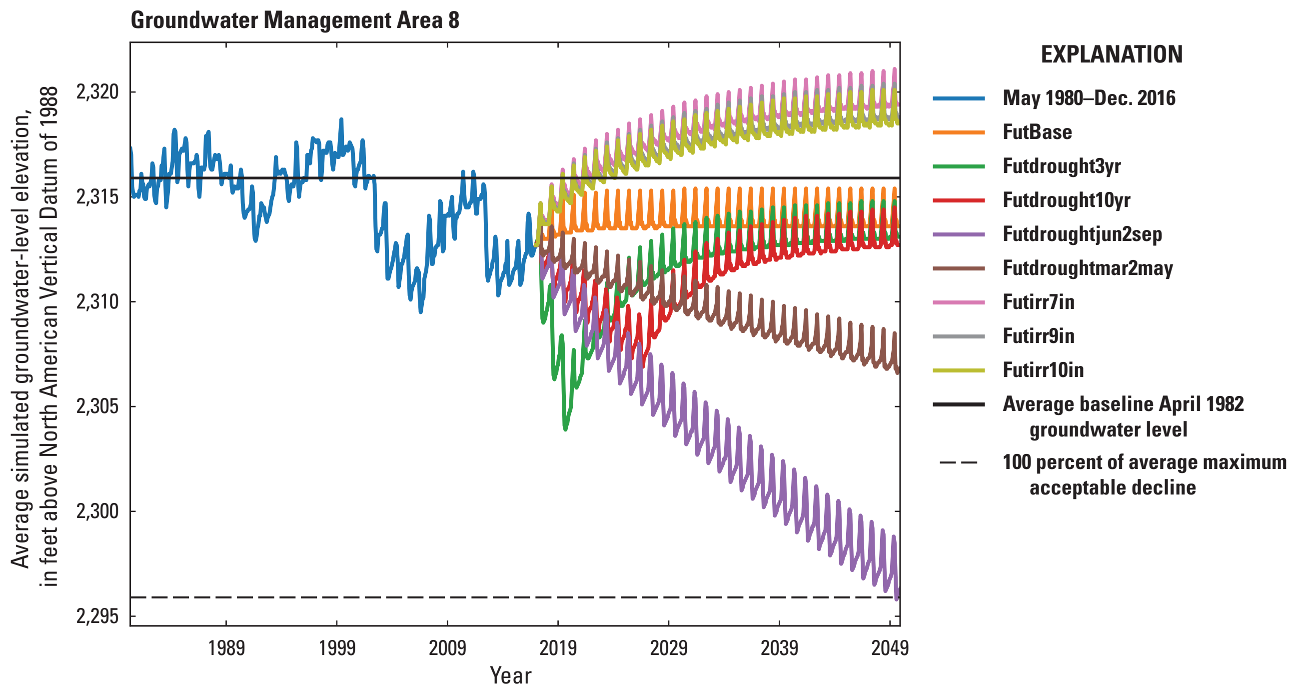

Figure 5.7. Simulated groundwater levels from May 1980 to December 2016 development period and January 2017 to December 2049 scenario period for the Central Platte Integrated Hydrologic Model in Groundwater Management Area 8.

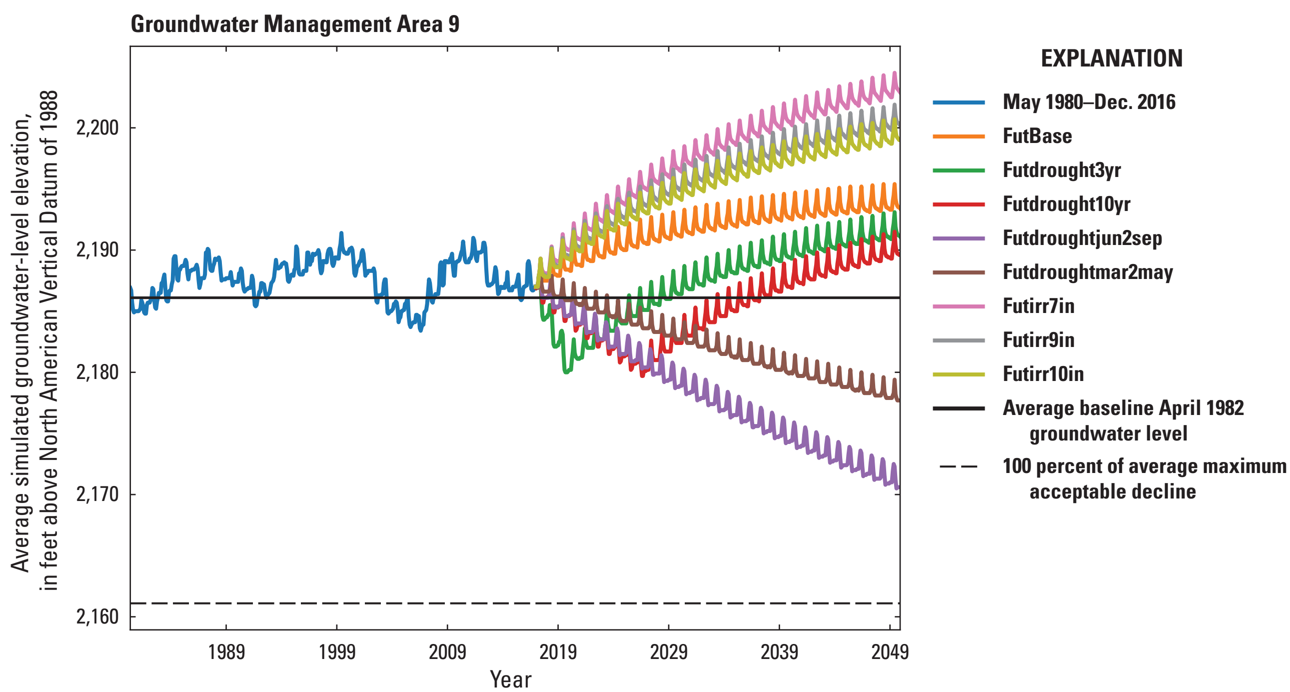

Figure 5.8. Simulated groundwater levels from May 1980 to December 2016 development period and January 2017 to December 2049 scenario period for the Central Platte Integrated Hydrologic Model in Groundwater Management Area 9.

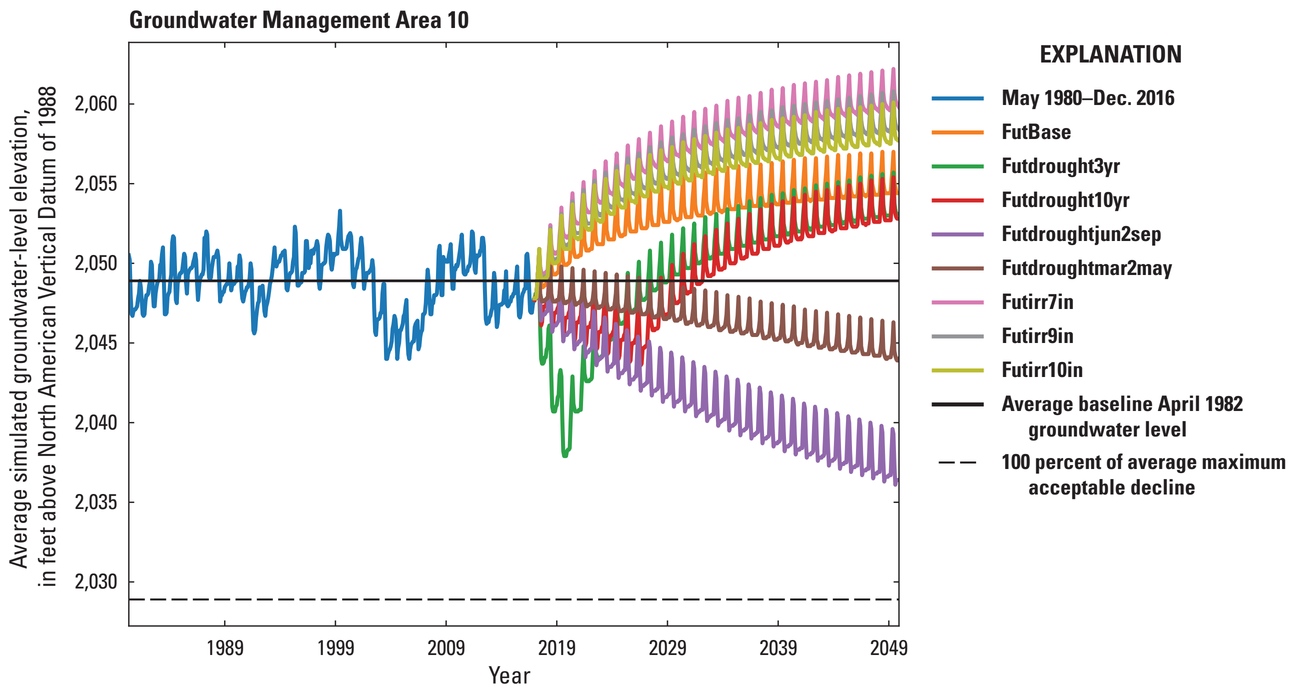

Figure 5.9. Simulated groundwater levels from May 1980 to December 2016 development period and January 2017 to December 2049 scenario period for the Central Platte Integrated Hydrologic Model in Groundwater Management Area 10.

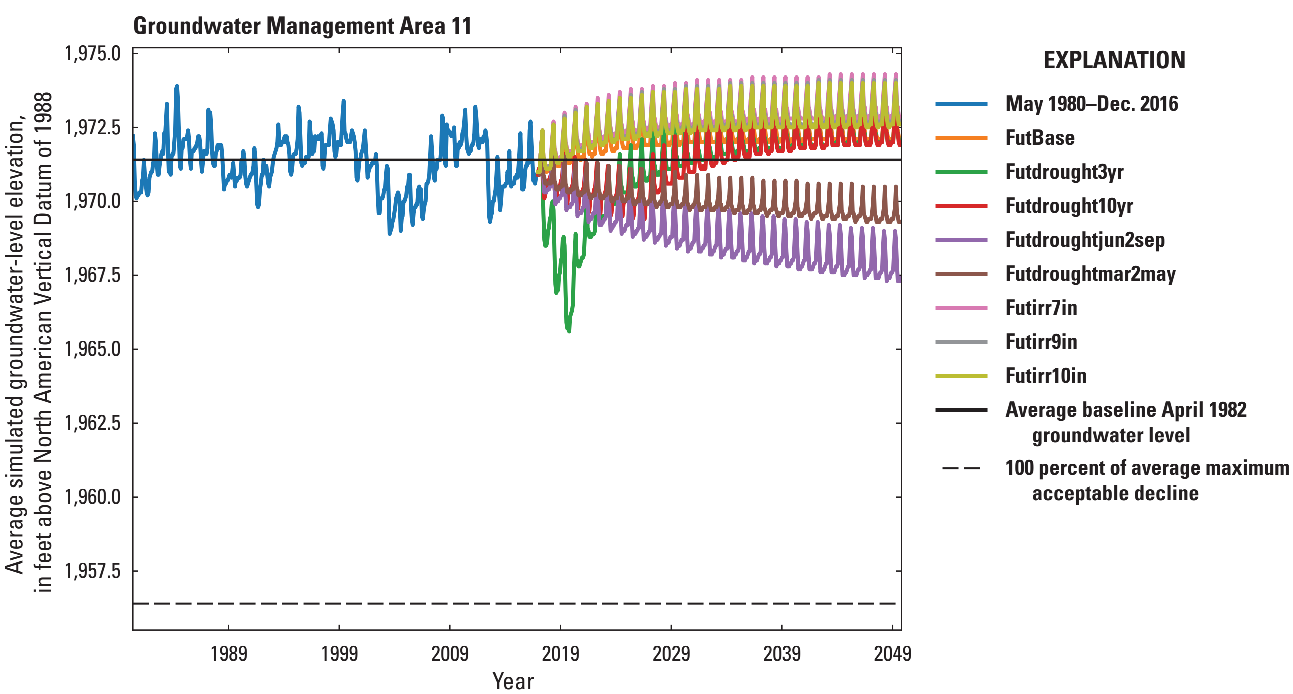

Figure 5.10. Simulated groundwater levels from May 1980 to December 2016 development period and January 2017 to December 2049 scenario period for the Central Platte Integrated Hydrologic Model in Groundwater Management Area 11.

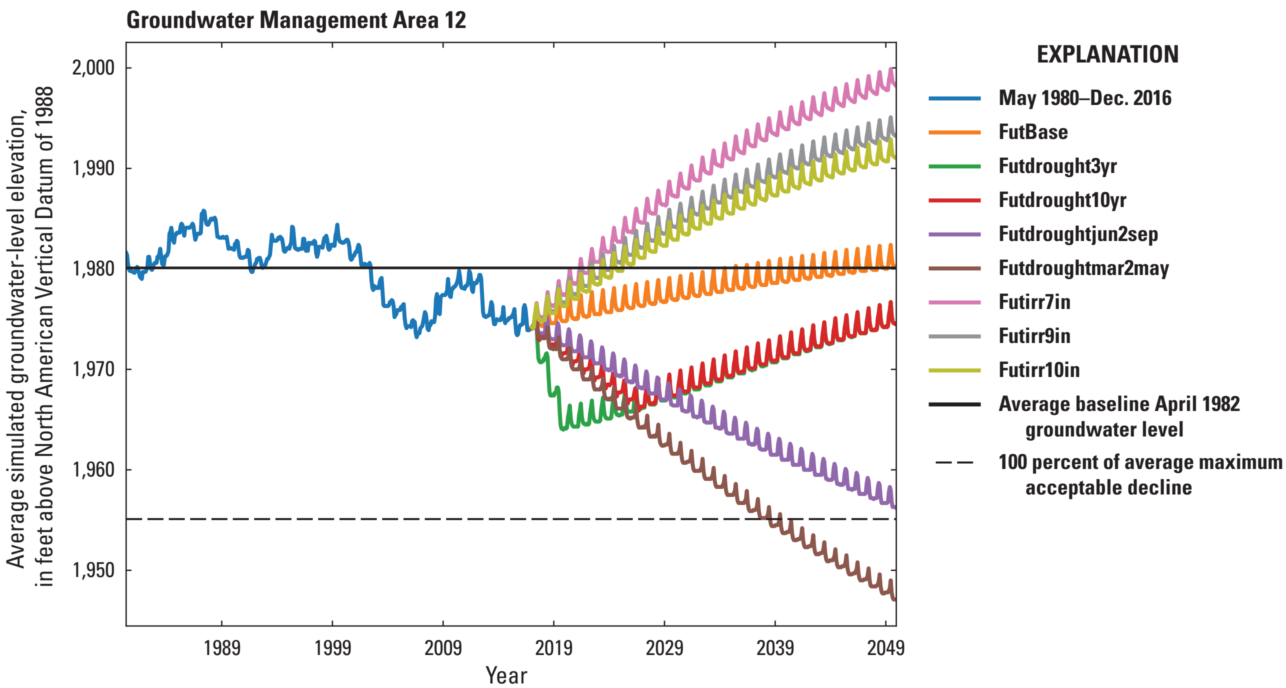

Figure 5.11. Simulated groundwater levels from May 1980 to December 2016 development period and January 2017 to December 2049 scenario period for the Central Platte Integrated Hydrologic Model in Groundwater Management Area 12.

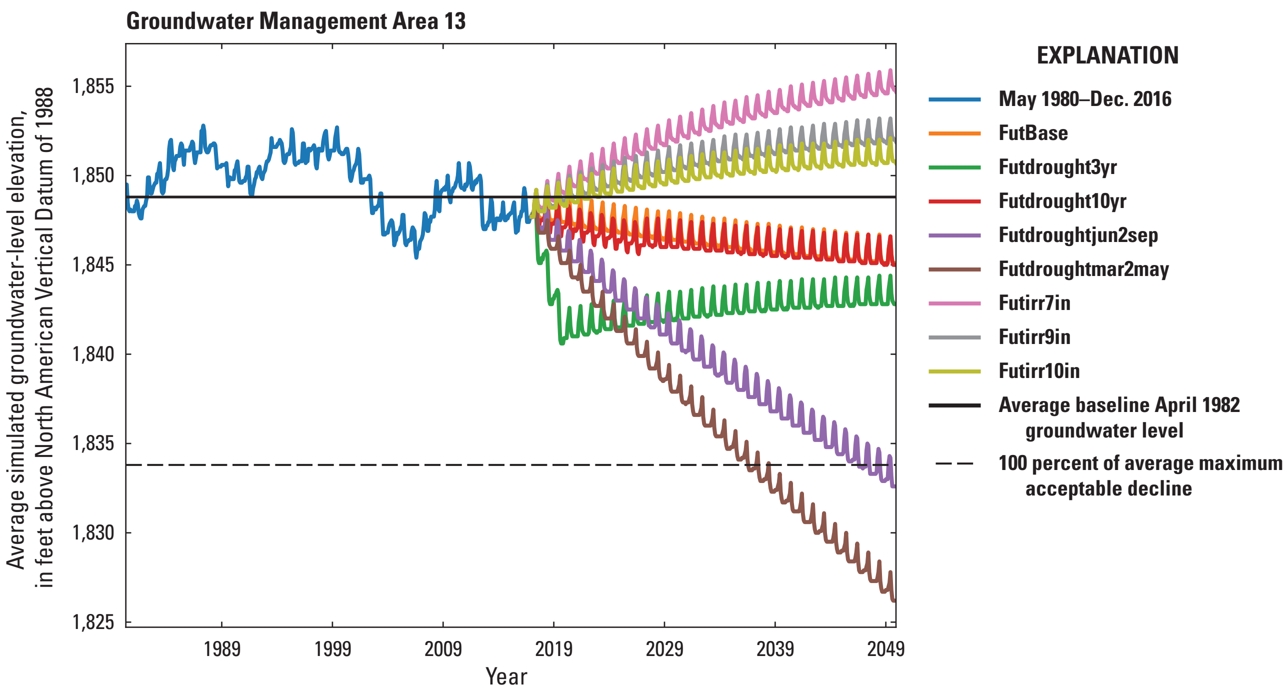

Figure 5.12. Simulated groundwater levels from May 1980 to December 2016 development period and January 2017 to December 2049 scenario period for the Central Platte Integrated Hydrologic Model in Groundwater Management Area 13.

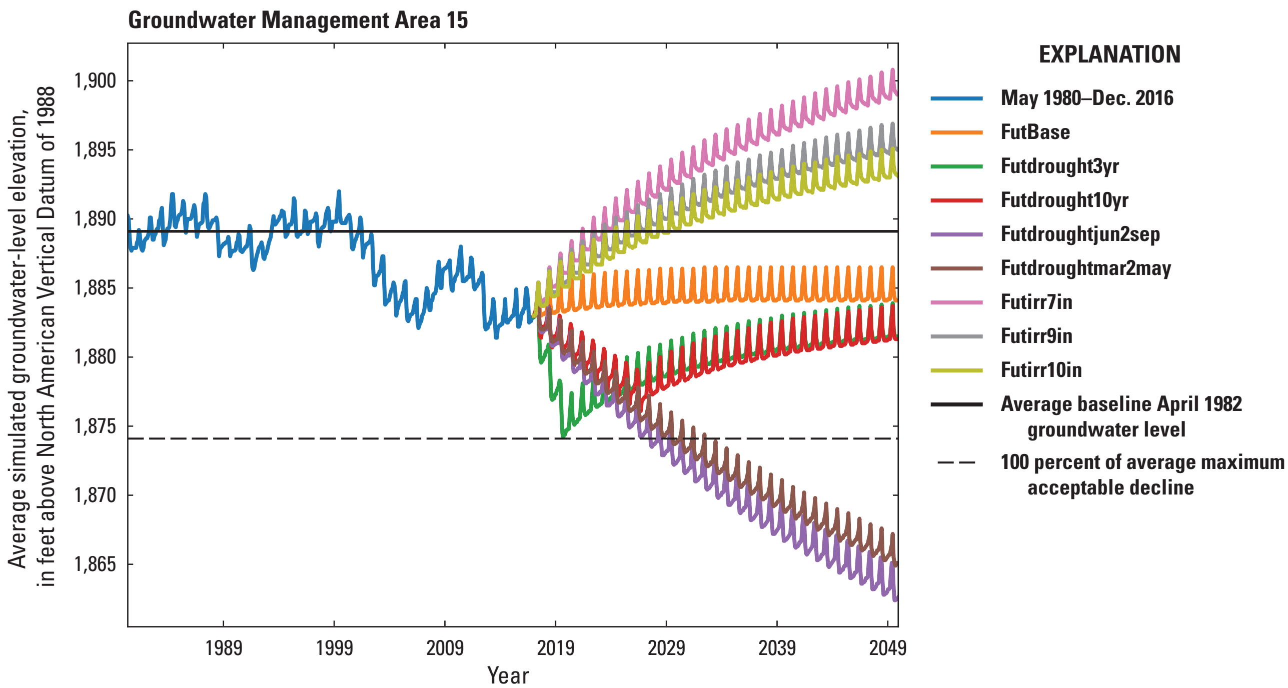

Figure 5.13. Simulated groundwater levels from May 1980 to December 2016 development period and January 2017 to December 2049 scenario period for the Central Platte Integrated Hydrologic Model in Groundwater Management Area 15.

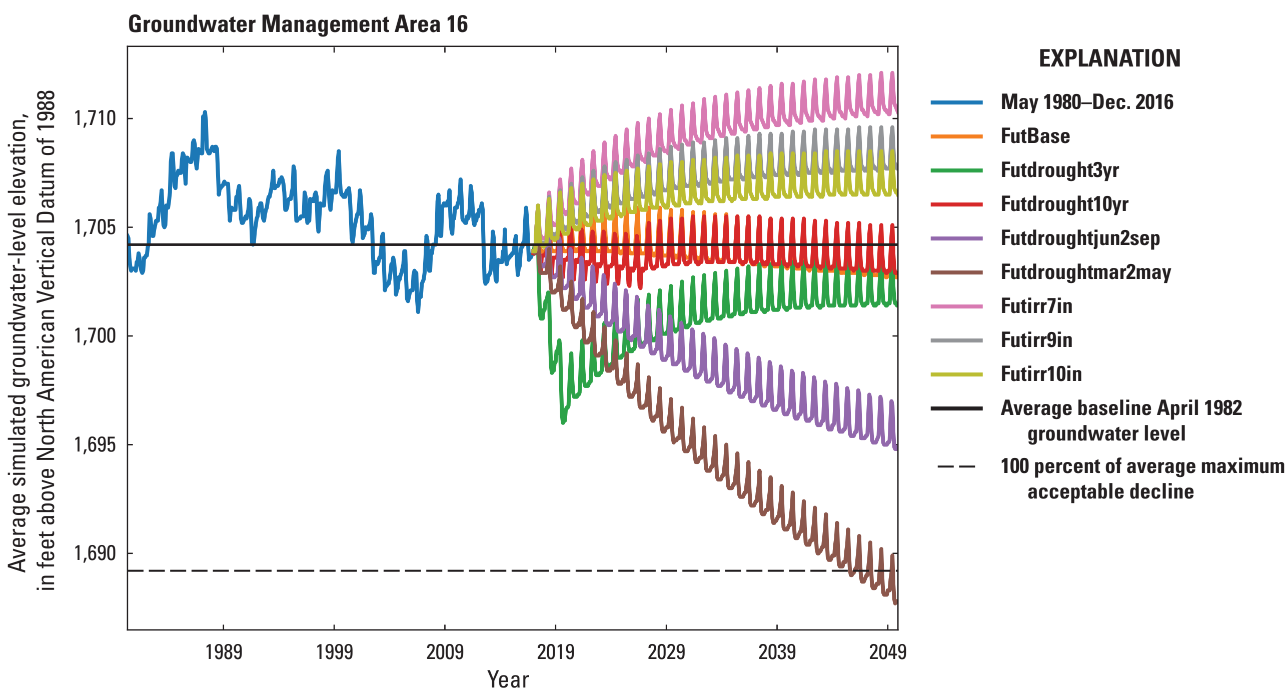

Figure 5.14. Simulated groundwater levels from May 1980 to December 2016 development period and January 2017 to December 2049 scenario period for the Central Platte Integrated Hydrologic Model in Groundwater Management Area 16.

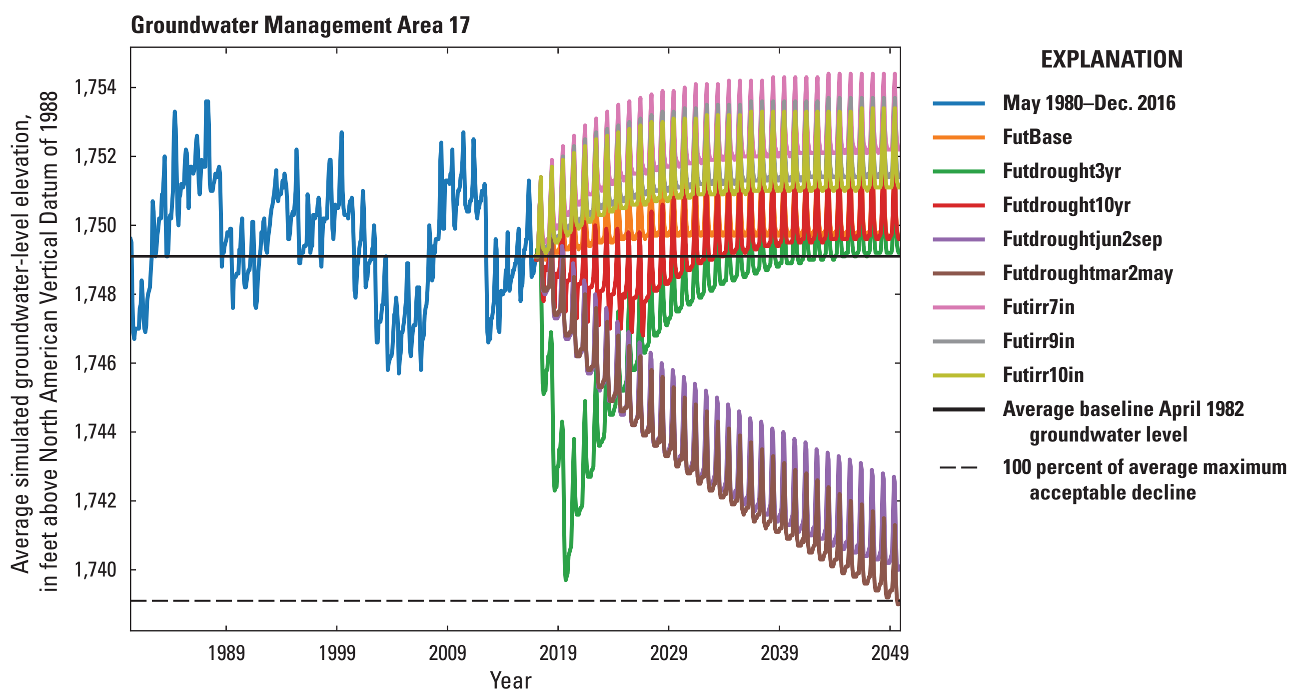

Figure 5.15. Simulated groundwater levels from May 1980 to December 2016 development period and January 2017 to December 2049 scenario period for the Central Platte Integrated Hydrologic Model in Groundwater Management Area 17.

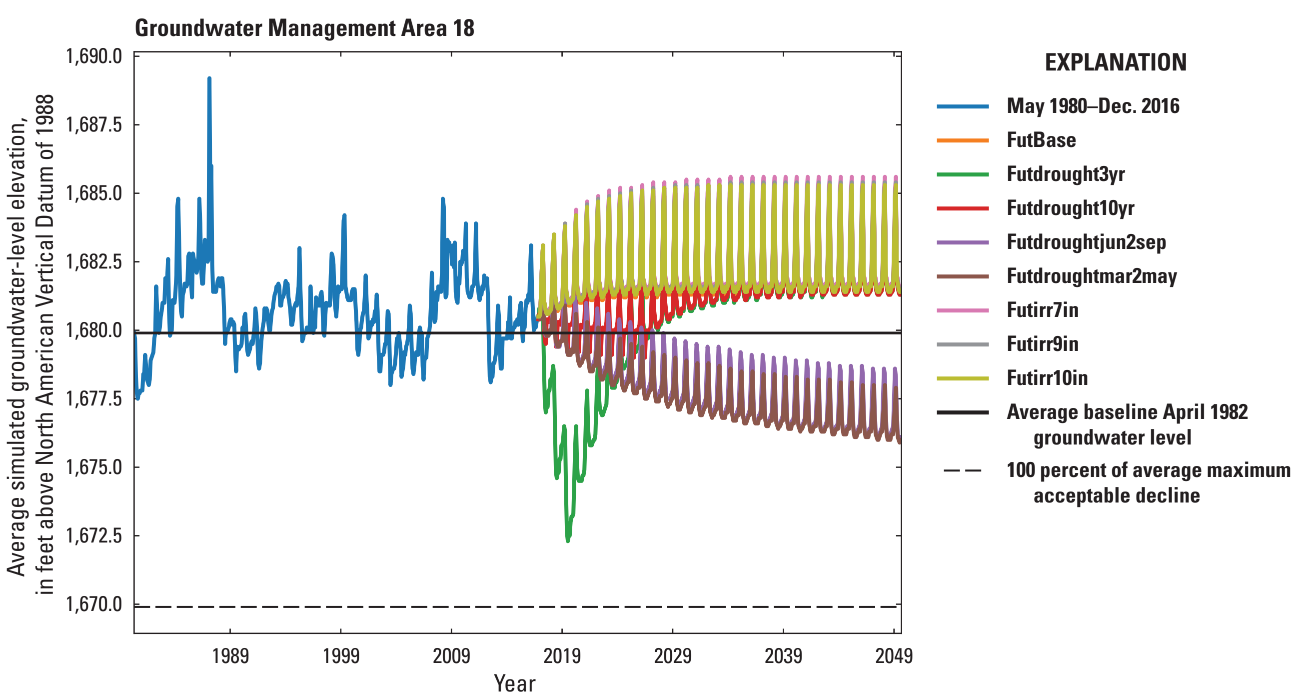

Figure 5.16. Simulated groundwater levels from May 1980 to December 2016 development period and January 2017 to December 2049 scenario period for the Central Platte Integrated Hydrologic Model in Groundwater Management Area 18.

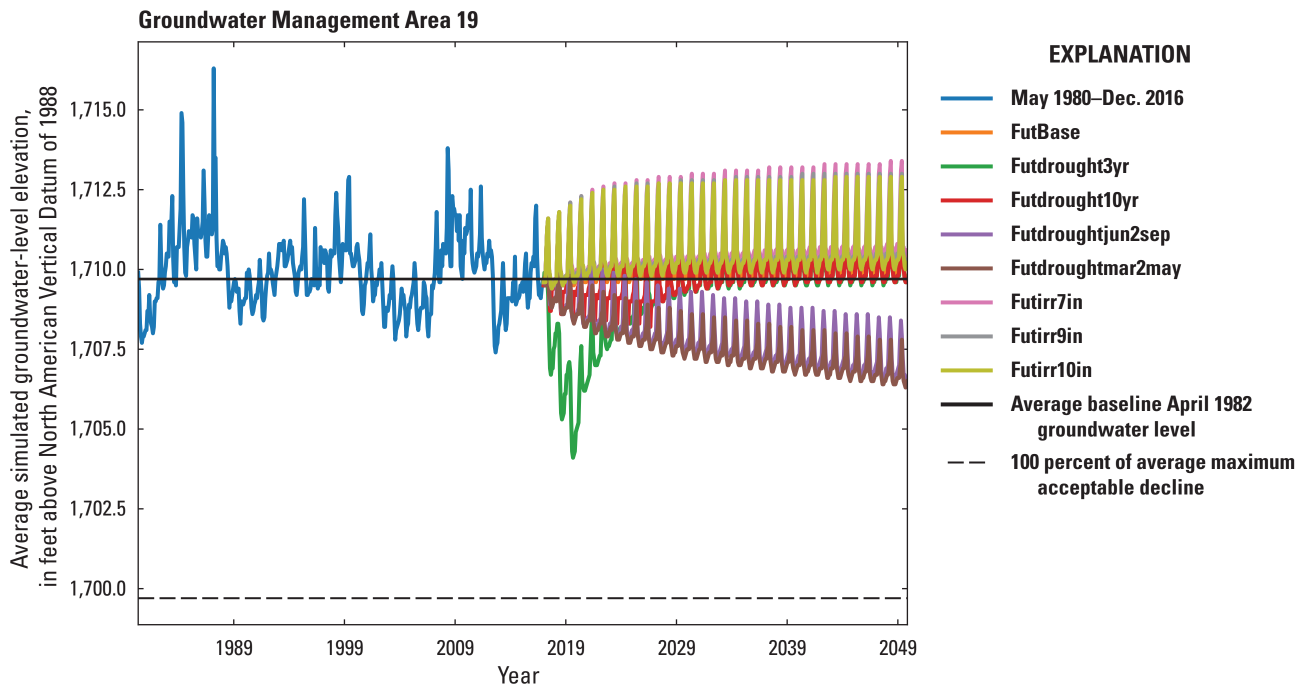

Figure 5.17. Simulated groundwater levels from May 1980 to December 2016 development period and January 2017 to December 2049 scenario period for the Central Platte Integrated Hydrologic Model in Groundwater Management Area 19.

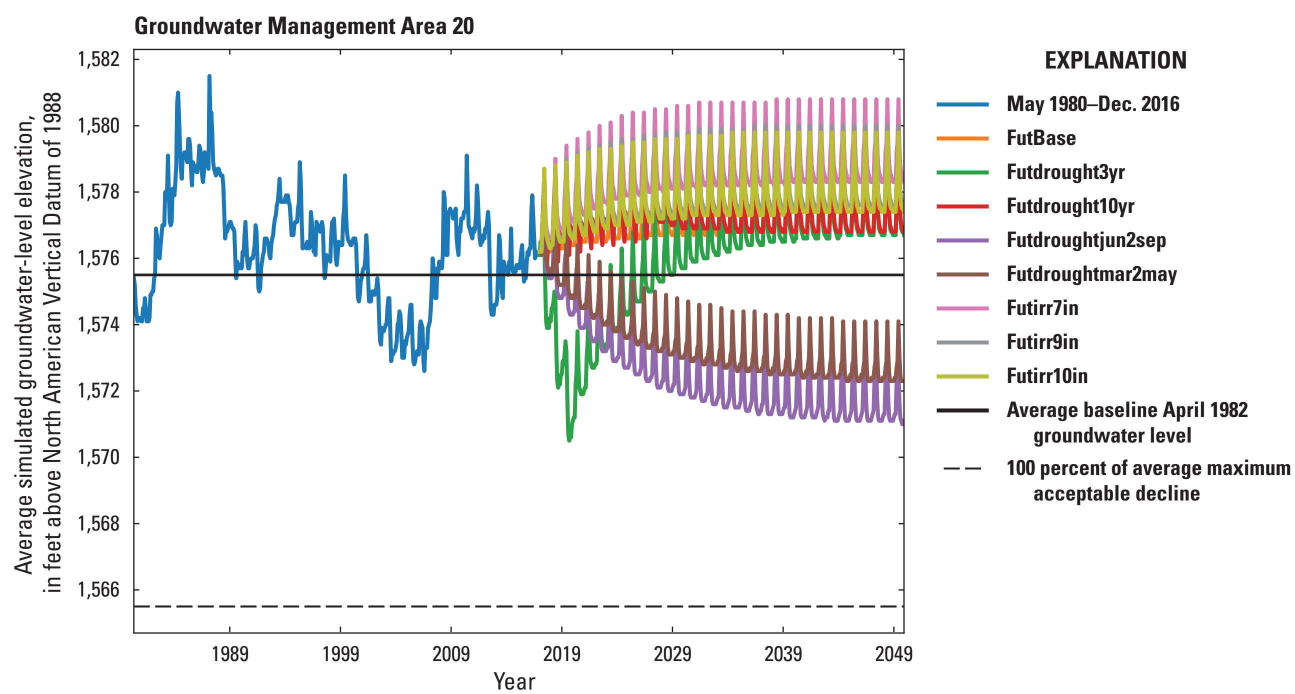

Figure 5.18. Simulated groundwater levels from May 1980 to December 2016 development period and January 2017 to December 2049 scenario period for the Central Platte Integrated Hydrologic Model in Groundwater Management Area 20.

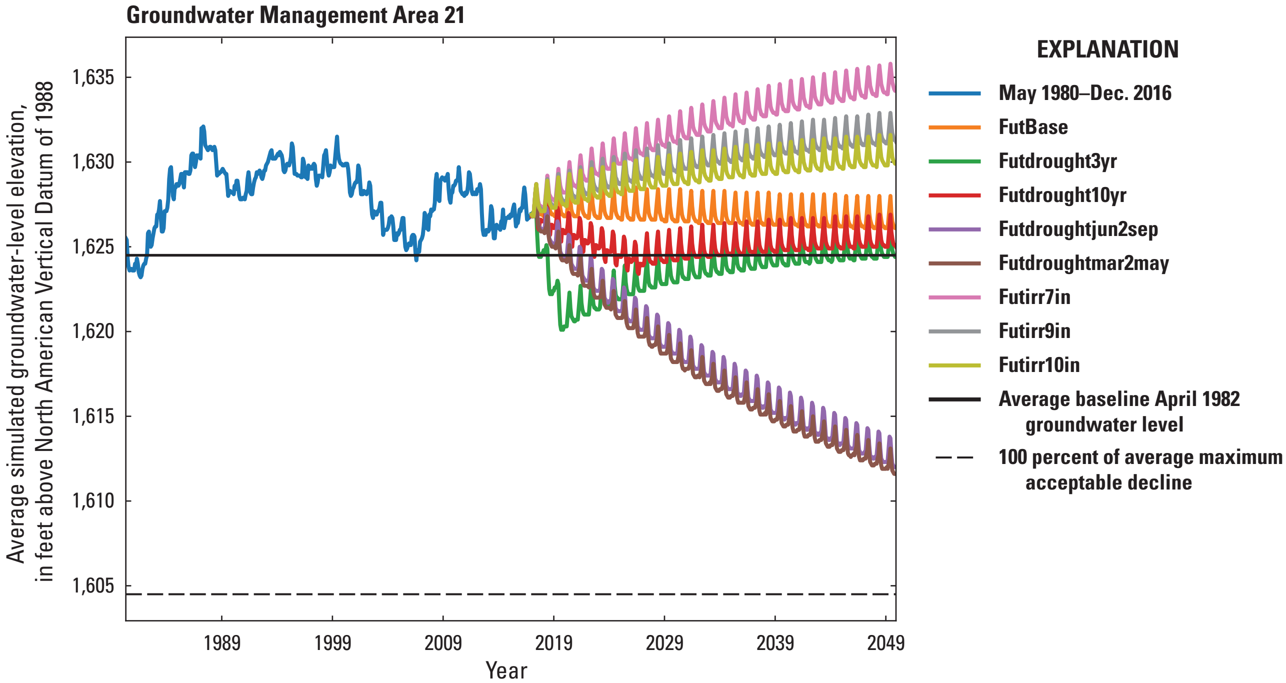

Figure 5.19. Simulated groundwater levels from May 1980 to December 2016 development period and January 2017 to December 2049 scenario period for the Central Platte Integrated Hydrologic Model in Groundwater Management Area 21.

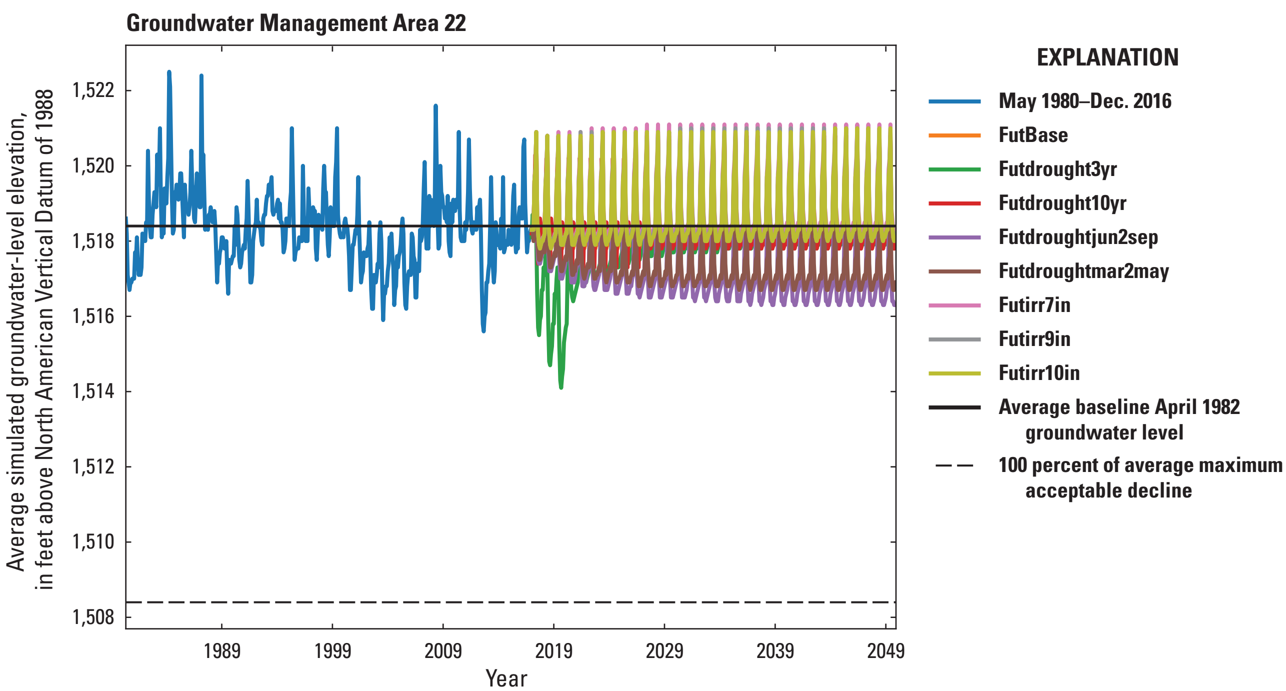

Figure 5.20. Simulated groundwater levels from May 1980 to December 2016 development period and January 2017 to December 2049 scenario period for the Central Platte Integrated Hydrologic Model in Groundwater Management Area 22.

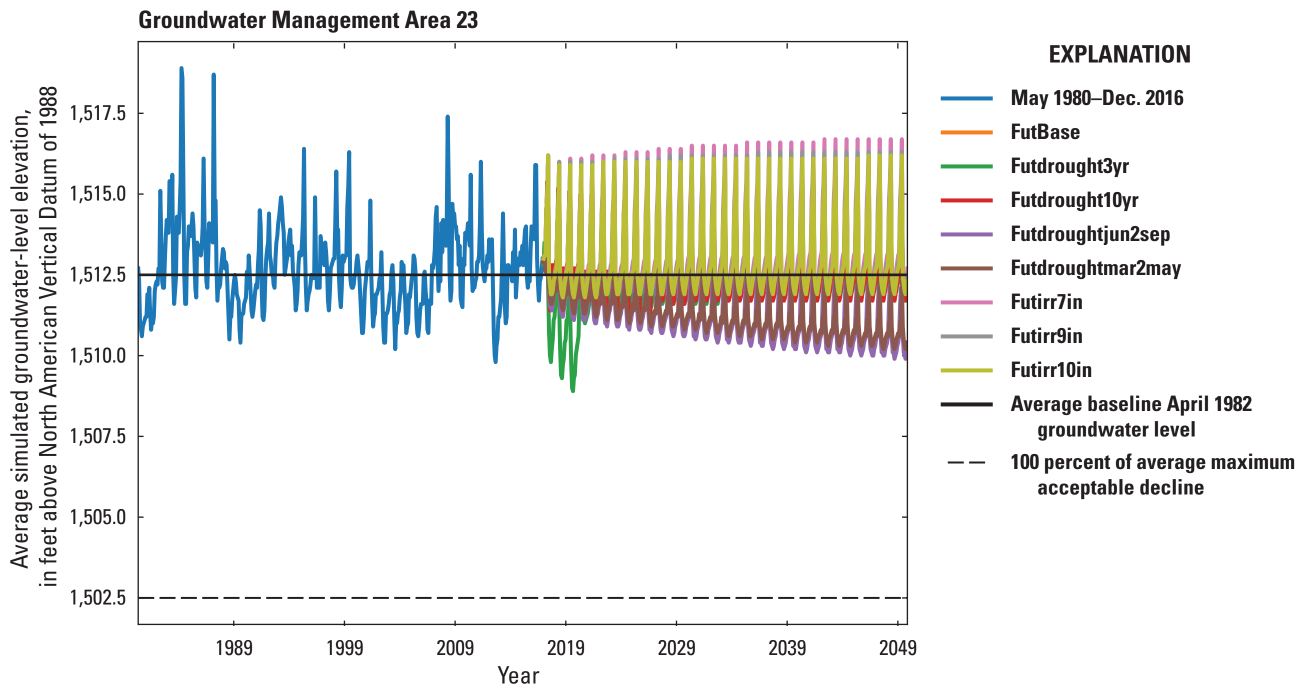

Figure 5.21. Simulated groundwater levels from May 1980 to December 2016 development period and January 2017 to December 2049 scenario period for the Central Platte Integrated Hydrologic Model in Groundwater Management Area 23.

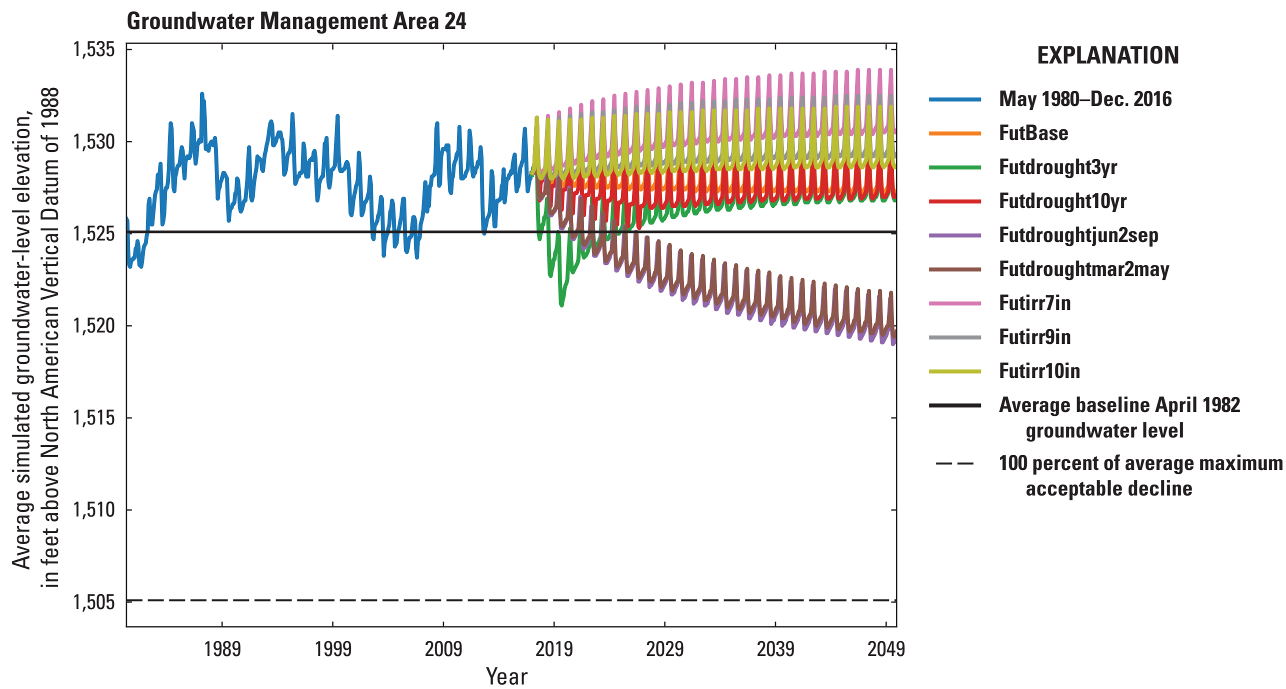

Figure 5.22. Simulated groundwater levels from May 1980 to December 2016 development period and January 2017 to December 2049 scenario period for the Central Platte Integrated Hydrologic Model in Groundwater Management Area 24.

For more information about this publication, contact:
Director, USGS Nebraska Water Science Center
5231 South 19th Street
Lincoln, NE 68512
402–328–4100

For additional information, visit: https://www.usgs.gov/centers/ne-water

Publishing support provided by the
Rolla Publishing Service Center

Traylor and others—**An Integrated Hydrologic Model to Support the Central Platte Natural Resources District Groundwater Management Plan**—SIR 2023–5024

ISSN 2328-0328 (online)
https://doi.org/10.3133/sir20235024